Preservation of Tissue Structures in Late Cretaceous Vertebrate Remains from Alberta, Canada

by

Aaron J. van der Reest

A thesis submitted in partial fulfillment of the requirements for the degree of

Master of Science

in

Systematics and Evolution

Department of Biological Sciences
University of Alberta

ABSTRACT

Here I investigate the rates of preserved original organic tissue and their quality within vertebrate bones that were preserved during the late Cretaceous of Alberta. Specimens recovered from the Dinosaur Park Formation provide a baseline for comparison to four other Alberta Formations (Brazeau, Foremost, Horseshoe Canyon, and Wapiti). Formations are all limited to approximately 13 MYA of one another, in order to eliminate excessive temporal variation in specimens. The formations studied were also chosen to cover a virtual transect of depositional settings from upland near source, to upper shoreface marine environments. This provides the opportunity to investigate if the general depositional environments play a major role in the preservation of original organic tissues in vertebrate remains from deep time. In addition to depositional environment, other previously proposed preservational factors are addressed, including the associated depositional matrix and amount of weathering before burial (degree of articulation). Findings reveal a general trend of greater tissue degradation across the terrestrial transect of depositional environments from upland to coastal plains. A marked increase in the preservation frequency and quality of tissues in upper shoreface facies reveals the potential of further investigations into tissues of extinct marine reptiles. Although groundwater quality during deposition of each of the formations has not been addressed in the literature, evidence addressed herein indicates that slight alkaline conditions were present in upland environments and slightly acidic conditions were present in those of coastal plains. Research done in an archaeological context has shown that groundwater pH plays the most significant role in the preservation of bone and its organic component. Findings made during

this research indicate that initial pH levels not only have short term effects on the mineral and organic phases of bone, but also play a major role in preserving them into deep time.

PREFACE

Chapter 2 of this thesis has been worked on as a collaborative effort among myself, A. Wolfe, W. Zheng, J. Lindgren, P. Currie, R. McKellar, and M. Schweitzer. Nevertheless, I am lead on the project, while W. Zheng, J. Lindgren, are conducting specialized laboratory experiments, A. Wolfe and R. McKellar are assisting with interpretation of microstructures, and P. Currie and M. Schweitzer are assisting in editing and laboratory access.

Chapter 3 of this thesis was published online January 8, 2020 as van der Reest, A.J. and P.J. Currie. Preservation frequency of tissue-like structures in vertebrate remains from the Late Campanian of Alberta: Dinosaur Park Formation. Cretaceous Research 109, 104370.

Chapter 9 of this thesis is a collaborative effort among myself, A. DuFrane, A. Reyes, and P. Currie. Nevertheless, I am lead on this project as well, while A. DuFrane has conducted radiometric dating on the tephra, A. Reyes has performed statistical analysis and assisted in editing with P. Currie.

This thesis is dedicated to those who have guided me in this direction, my parents, colleagues, and supervisors.

“It’s been a long time running,

It’s been a long time coming,

It’s well worth the wait.”

-Gordon Downie

ACKNOWLEDGEMENTS

I thank my supervisor, Philip Currie, for providing assistance through this research and for the appreciated guidance he provided. I also thank Eva Koppelhus for her support of my endless research ideas over the years.

Thanks goes to all those that have provided invaluable discussions. They include A. Dufrane, D. Eberth, R. Holmes, W. Langenburg, H. Larsson, J. Mallon, R. McKellar, K. Muehlenbachs, A. Reyes, M. Sander, M. Schweitzer, J. Scott, L. Schill, C. Sullivan, K. Wiersma, T. Wintrich, and A. Wolfe. I also send my immense gratitude to all those that assisted in the preparation of specimens studied, including A. Ito, C. Libke, K. Nguyen, and O. Vernygora. Thanks to both A. Reyes and F. Sperling for access to their lab areas.

Special thanks go to all those who have impacted my life to push me in this direction, and all my friends and family for embracing my love of dinosaurs since my childhood. I am grateful to my brother and sister for their support over the years. My Father, and the support he has provided for decades, cannot be thanked enough. For never wavering in the support she gave, I am eternally grateful to my late Mother.

Funding was provided by the Dinosaur Research Institute and University of Alberta Department of Biological Sciences. The Mountainous Alberta Dinosaur Project fieldwork team was outfitted by Arc'teryx (Vancouver, British Columbia).

TABLE OF CONTENTS

LIST OF TABLES

Chapter 2

Chapter 3

Chapter 4

Chapter 5

Chapter 6

Chapter 7

LIST OF FIGURES

Chapter 1

Chapter 3

Chapter 4

Chapter 5

Chapter 6

Chapter 7

Chapter 8

Chapter 9

Appendix 2-1

Figure A2-5. UALVP unaccessioned specimen, unknown sex, *Rhea pennata* (Darwin's Rhea).

INSTITUTIONAL ABBREVIATIONS

CMN – Canadian Museum of Nature, Ottawa, Ontario, Canada

MNHN ARC - Muséum National d'Histoire Naturelle, Paris, France

TMP – Royal Tyrrell Museum of Palaeontology, Drumheller, Alberta, Canada

ROM – Royal Ontario Museum, Toronto, Ontario, Canada

RSM – Royal Saskatchewan Museum, Regina, Saskatchewan, Canada

UALVP – University of Alberta Laboratory for Vertebrate Palaeontology, Edmonton, Alberta, Canada

UAMZ – University of Alberta Museum of Zoology, Edmonton, Alberta, Canada

OTHER ABBREVIATIONS

BADP – Boreal Alberta Dinosaur Project

BF – Brazeau Formation

DMT – Drumheller Marine Tongue

DPF – Dinosaur Park Formation

EDTA – (ethylenedinitrilo)tetraacetic acid, disodium salt, dihydrate

EOM – extracellular organic matrix

ETOH – ethanol

FESEM – field emission scanning electron microscopy

FF – Foremost Formation

HCF – Horseshoe Canyon Formation

IHC – Immunohistochemistry

Ma – Mega-annum

MADP – Mountainous Alberta Dinosaur Project

Mya – Million years ago

NaOH – sodium hydroxide

NDS – normal donkey serum

PBS – phosphate buffer solution

TEM – transmission electron microscopy

ToF-SIMS – Time of Flight Secondary Ionizing Mass Spectrometry

U/Pb – Uranium/Lead

WF – Wapiti Formation

Chapter 1: INTRODUCTION

1.1 Identification of soft tissues

Methods in palaeontology changed little over the first 150 or so years since the first dinosaur fossils were described (Buckland 1824), with most of the research focussing on basic anatomical description of bones and the analysis of relationships. Description of anatomy and classification of different species are fundamental steps towards more complex, derived studies, such as rates of evolution or speciation. Studies of extant taxa through the use of molecular data from species genomes have started to dominate phylogenetic research for modern clades (Jarvis et al. 2014). Although modern molecular data have been questioned in the past due to the age of fossils studied, recent work has improved the resolution of evolutionary rates and divergence dates (Morlon et al. 2011). Palaeontology, which was slow to adopt new methodologies until the last few decades, is now adopting more sophisticated methods of study from other scientific fields. Many of these developments have benefited from statistical analyses using computer programs such as “R” (Benson et al. 2014, Campione et al. 2014).

Prior to 2000, six reports were made of evidence of tissues or proteins being preserved in fossil vertebrates from deep time (Pawlicki et al. 1966, Miller and Wyckoff 1968, Gurley et al. 1991, Muyzer et al. 1992, Schweitzer et al. 1997, 1999). Reports of cellular preservation by Pawlicki et al. (1966) were the first suggestion that original organic structures had the potential to survive in deep time. Two years later, Miller and Wyckoff (1968) provided evidence that bone could also preserve polypeptide fragments. In 1999, a theropod dinosaur from Mongolia,

Shuvuuia, was shown to have small white filamentous fragments preserved in the matrix surrounding the specimen. Ensuing IHC trials indicated positive reactivity to antibodies in fibres preserved around *Shuvuuia* were in fact fragments of unaltered feathers with protein still intact (Schweitzer et al. 1999). Following the discoveries with *Shuvuuia,* pliable tissues were reported from dissolved bone of a *Tyrannosaurus rex* (Schweitzer et al. 2005b). These microscopic tissues consisted of fibrous, flexible, collagen like structures, as well as anastomosing vessel-like structures containing red, spherical objects with darker cores. It was proposed these structures represented unaltered soft tissues – including collagen-1, blood vessels, and red blood cells – preserved within the bone matrix. Further investigation into the preservation of soft tissues in vertebrate fossil and sub-fossil elements from around the world (Schweitzer et al. 2007b) indicates these structures are not uncommon. Taxa with soft tissue structures published by Schweitzer et al. (2007b) included *Brachylophosaurus canadensis, Mammuthus, Megoeodon*, *Triceratops horridus,* an indeterminate trichechid, *Tyrannosaurus rex,* a dicynodont, and two unidentified theropods (one from Madagascar and the other from the Santana Formation of Brazil). Although, in this study, most specimens sampled contained preserved soft tissue, many specimens were discovered to possess some form of vessel-like structures, collagen, or osteocytes (Schweitzer et al. 2007b). Subsequent to the release of Schweitzer et al. (2007*b*), the analysis of unaltered preserved soft tissue was taken to the next level. Immunohistochemistry was again employed to investigate collagen-like bundles that were observed within the bone matrix of *Tyrannosaurus rex* (Schweitzer et al. 2007a). By using several anti-body treatments, it was shown that collagen-1 (the primary collagen type within bone) was still present, although degraded, within the bone matrix. This was the first instance where collagen-1 was found to be

present within bone matrix of a dinosaur and was the first bone older than 66 Mya. Unsurprisingly, the finding that protein fragments could survive through deep time was contentious. It was claimed that the more likely interpretation of these structures would be biofilms formed by bacterial colonies during decomposition (Kaye et al. 2008). On the other hand, it has also been suggested that if original protein is in fact present, then bacterial biofilms must play a role in preserving it (Peterson et al. 2010). Following the identification and confirmation of the presence of unaltered proteins in dinosaur bone using immunohistochemistry, sequences of collagen-1 and -2 were sequenced using mass spectrometry (Schweitzer et al. 2009a). This work was duplicated several years later using more precise measurements and sequencing technology, confirming that the results were repeatable, and showing that original results were accurate (Schroeter et al. 2017).

Extraction of soft tissues from fossilised vertebrate bone has raised the potential for studies once thought to be impossible for taxa from deep time. Studies could potentially produce molecular phylogenies, evolutionary rate estimates, divergence events, molecular evidence of cladogenesis and/or anagenesis, and genetic diversity within populations, to name a few. To facilitate these studies however, bone dissolution is the primary, and most successful procedure currently known to extract preserved soft tissues from fossil bone.

1.2 Hypotheses on modes of tissue preservation

Because investigation of preserved original organics is a new field of palaeontology, research into the primary mechanism for preservation of unaltered tissues has only produced a few hypotheses. Schweitzer et al. (2007a) performed an in-depth investigation into tissue

preservation trends related to the provenance of specimens studied. Factors that this work investigated were geochemical, geographical, taxonomic, and temporal. Not unexpectedly, the best tissues preserved were from those specimens with youngest ages (i.e. <20 Ka): however, it is suggested that if time was a major factor, tissue would not have been observed as commonly from the Triassic. No other trends were observed except for most samples having originated from sandstones, as a result, it was proposed that the higher porosity within a sandstone matrix would facilitate the drainage of water and decay enzymes away from remaining tissues within bone. Schweitzer (2011) also proposed that cells and tissues undergo a natural fixation process through crosslinking with other surrounding tissues, free radical reactions, of the Maillard reaction (a reaction between amino acids and reducing sugars), arresting the degradation of tissues. Haemoglobin iron binding to proteins to form crosslinking (Schweitzer et al., 2013) has also been proposed. Investigations into the preservation of collagen and osteocytes recovered from *Lufengosaurus* (Early Jurassic, 190-197 Ma) proposed that hematite cementation may play a role in preventing the degradation of soft tissue within bone (Lee et al. 2017). The authors suggest that the iron used to form the hematite may come from erythrocytes (red blood cells). However, they also point out that it would require approximately 20,000 cells to form a single 10 µm hematite sphere. The most recent proposal for the preservation of tissues in the fossil record suggests that the proteins form N-heterocyclic polymer chains by oxidation reactions, and that organics should not be recovered from chemically reducing sediments like those in deep marine environments (Wiemann et al. 2018). Shortly after the proposal that reducing environment chemistry could be destroying tissues, a specimen of the Jurassic ichthyosaur *Stenopterygius* was recovered from deep marine sediments of Holzmaden, Germany,

preserving original blubber, melanocytes, and skin cells were also found preserved intact (Lindgren et al., 2018). This suggests that N-heterocyclic polymerization due to oxidative environments requires further research, and that reducing environments can preserve original tissues as well. Due to the disagreements regarding the mode of preservation of original tissues in deep time, a proper in-depth investigation utilizing a large sample size of specimens is required to test several of the hypothesized modes of preservation.

1.3 Objectives

In this thesis, preservation of original organic tissues from the Late Cretaceous of Alberta is investigated. This includes specimen selection, bone sample dissolution, tissue recovery, imaging, description, and analysis. Also, feathers preserved on an *Ornithomimus* (an ornithomimid theropod dinosaur) are described in detail with evidence of original proteins being preserved. The first description of vertebrate remains from the Brazeau Formation is also presented, indicating that the formation is a valuable source of fossil resources. This work is broken into three main components.

1. The first portion of the thesis describes the macro- and microscopic morphology of primitive feathers preserved on an *Ornithomimus*. Multiple types of analysis provide evidence showing that the original β-keratin proteins are intact and retain their original three-dimensional structure.
2. The second portion involves investigating the frequency and quality of preserved original organic tissues recovered from vertebrate remains from five different formations that span a virtual transect of the different depositional environments

from the paleo Rocky Mountains east to the Western Interior Seaway. Based on data collected, an environmentally controlled factor for tissue preservation in deep time is hypothesised.

3. The last portion of this project is the first description of vertebrate remains from the Brazeau Formation. This was done because bone used in the dissolution portion of the research originated from the Brazeau Formation, as such it was decided to provide readers with some background on the vertebrate fauna from the formation.

1.4 Materials and Methods for dissolution of bone fragments

In order to not repeat the same procedures multiple times in chapters 3-7, portions of the Materials and Methods are provided here.

1.4.1 Preparation of samples

Because several specimens that were used had been collected, prepared, and stored in non-sterile environments for up to a century, the following protocols were used to remove as much previous contamination as possible. To reduce the potential of personnel contamination within the laboratory environment, all lab work was performed while wearing a lab coat, hair net, medical face mask, safety glasses, and nitrile gloves to prevent contamination from persons involved.

To clean specimens of any potential contaminating debris, the following steps were taken:

1. All samples were sonicated using de-ionized water to remove surface contaminants.

2. All samples were then sonicated in 50% ETOH solution to remove any unknown consolidants, to sterilize bacteria, and to further remove any debris from the surfaces. The low viscosity of ETOH allows penetration into the specimen.
3. All samples were then sonicated one further time in de-ionized water to flush ETOH.

Once cleaned, samples were taken from the final sonication directly into individual wells in 6-well, non-tissue-culture treated sterile culture plates.

1.4.2 Chemical Laboratory Protocols

All solutions used within the study were mixed by hand in the Earth and Atmospheric Sciences radiocarbon dating wet lab in the Centennial Centre for Interdisciplinary Sciences at the University of Alberta, Edmonton. Fifty percent ETOH solution for the sterilization sonic bath was made by mixing equal parts of 100% ETOH and deionized water. Dissolution of bone used a 0.5 mol solution of EDTA (molecular weight = 372.240 g/mol). To create a 2 litre solution, approximately 372.240 g of solid EDTA was weighed into a 4 litre beaker and then deionized water was added until a volume of 2 litres was reached. Due to the low solubility at low pH of EDTA, NaOH was slowly added until both EDTA and NaOH was dissolved. The final pH was tested using pH indicator strips with a target of 8.0. This solution was then filtered through a 2 μm filter to remove all undissolved crystals and other debris that may have entered the solution by air.

1.4.3 Dissolution of samples

Samples (three samples from each specimen) of bone were each placed into a single well in a sterile 6-well non-TC treated microculture plate (two specimens per each 6-well plate).

Approximately 9 mL of 0.5 M EDTA was then added to each sample well by sterile transfer pipette. Each well was inspected daily for evidence of tissue-like structures as the bone fragment samples dissolved. EDTA is a chelating agent, binding to metal ions (*i.e.* calcium, magnesium, etc.) in bone, slowly dissolving the samples. Samples that contained identifiable soft tissue-like structures had organics removed and were placed into microfuge tubes containing 0.1 mol/L EDTA to prevent further dissolution and damage. Transfers of soft tissue-like structures were performed using sterile glass Pasteur pipettes with manual bulbs. Specimen treatment log sheets were kept as each sample was dissolved or other treatments were performed (Appendix 3-1).

1.4.4 Mounting and imaging of tissues

Selected tissue samples were transferred to single depression slides using sterile glass Pasteur pipettes and manual bulbs. Depression slides were chosen to prevent three dimensional structures such as vascular networks from being crushed and/or distorted during imaging. Cover slips for microscope slides were held in place using nail-polish.

Imaging was conducted in the Department of Biological Sciences Microscopy Laboratory using a Leica compound microscope with attached camera. Scale bars were calibrated using a stage micrometre.

Chapter 2: Early evolutionary origins of feather micro architectural elements facilitated properties for flight.

2.1 INTRODUCTION

The identification of complex feathers in *Archaeopteryx* led to its identification as the first bird more than a century ago (Owen 1862). Until the discovery of feathers in non-avian theropods (Ji and Ji 1996, Chen et al. 1998), these integumentary structures were the defining features of birds. Feathers in extant birds are comprised primarily of β-keratin, a sauropsid-specific protein distinct from the more basal α-keratins found in all tetrapods. The former are characterized by a higher concentration of sulfur-containing amino acids that facilitate a greater number of intra- and inter-specific crosslinks, a β-pleated sheet conformation, and smaller filaments (3nm vs 8-10 nm in α-keratin proteins) (Wang et al. 2016). A feather is also characterized by a dense but lightweight cortex, strut-like pith filling the medullary region of a rachis, and barbs (Wang et al. 2016), and a hierarchical branching structure resulting in a tightly organized vane required for flight.

Although it had been predicted for at least thirty years that some theropod dinosaurs may have possessed feathers, the first specimen to show such integument-derived structures was *Sinosauropteryx prima*, recovered in 1995 and described in 1996 (Ji and Ji 1996, Chen et al. 1998). Many examples of feathered non-avian and avian dinosaurs have since been reported, primarily on the basis of specimens from China (Ji et al., 1998; Xu et al., 2004, 2001; Zheng et al., 2009). These specimens have been described as exemplifying various stages of a simplified

five-stage hypothesis of feather evolution (Prum 1999, Brush 2000, Xu and Guo 2009). Stage I feathers have a cylindrical invagination of the epidermis to form the base of the feather papilla, and a collar, which is a hollow cylinder resembling the calamus of a modern feather. At Stage II, longitudinal ridges develop within the collar, and unbranched filament bundles (rami)originate from a central calamus. Pairs of rami in Stage IIIa fuse to the elongate rachis to form a branching structure, whereas a Stage IIIb, barbules formed prior to fusion of rami. Stages IIIa+b, characterized by the combination of the two Stage III forms, culminate in a rachis, paired rami, and barbules to form an open-vaned (plumaceous) feather. Stage IV is characterized by a rachis, paired rami, and barbules with hooklets that together form a closed vaned (pennaceous) feather. Finally, Stage V is represented of specialized feathers, including asymmetrical flight feathers, afterfeathers, down, and other derivatives. Unfortunately, taphonomic alteration or compression makes it difficult to accurately trace these features in fossils (Xu et al. 1999, Currie and Chen 2001).

One juvenile (TMP 2009.110.0001) and one adult specimen (TMP 2008.070.0001) of *Ornithomimus edmontonicus* from the Late Cretaceous that preserve feathers, housed at the Royal Tyrrell Museum of Palaeontology, Alberta, Canada, have been described from North America. These two specimens were described as preserving Stage I or II integumentary filaments (Zelenitsky et al. 2012). Here, both the macro- and microstructure of the first well-defined individual Stage IIIa feathers from a non-avian dinosaur are described. This revises the evolutionary stage of feathers possessed by Ornithomimosauria. UALVP 52531 was recovered 2009 from the lower Dinosaur Park Formation (Upper Campanian) of southern Alberta and is only the third dinosaur recovered from North America on which feathers are preserved,

providing further information on ptilosis evolution in birds. UALVP 52531 preserves feathers over the body, tail, and upper femur (van der Reest et al. 2016) (Fig. 2-1).

Although similar in overall morphology to previously described theropod feathers (Xu et al. 1999, Zhang et al. 2006, Li et al. 2012), it is hypothesized that these structures would also share microstructural and chemical/molecular features with feathers of extant birds. This can be confirmed with analytical methods. Various microscopy techniques, together with time-of-flight secondary ion mass spectrometry (ToF-SIMS), Fourier transform infrared spectroscopy (FTIR), and immunohistochemistry (IHC) are employed to test this hypothesis.

2.2 MATERIALS AND METHODS

2.2.1 Specimen preparation

Feather preparation was conducted by hand with the aid of a table boom binocular microscope with adjustable magnification, using carbide needles with a diameter of 0.25 and 0.5 mm. No cyanoacrylates or other forms of stabilizers were used to consolidate surfaces of preserved feathers because of the risk of washing the preserved integument off the sedimentary matrix. Once prepared into view, the macro-structure of the feathers was studied using both a boom binocular microscope and high magnification photographs. Modern feathers used in this study were all collected from specimens in the collections of the UAMZ (Appendix 2-1), although the black-billed magpie feather has no collection number or associated information. Select modern feathers were cut with scalpel blades.

2.2.2 Photography

Photographic images were produced using a Canon 7D and 7D Mark II. A Canon 50 mm, f/2.5 macro lens was used for figures 2-1a,b. A MP-E 65mm lens set to f/6.8 at 5x magnification

was used for figures 2-1d,f. Because the MP-E 65 mm lens has an effective depth of field of approximately 0.1 mm, the camera was mounted to a Kiwi brand FC-1 macro focusing rail on a tripod. Photos of the same area were then taken with progressively changing focal points and stacked for processing in Adobe Photoshop CS6 Extended. Using the automated option, photos were blended together to produce a final image that was completely in focus. Images were then imported into Adobe Illustrator CS6, in which line drawings were created by tracing outlines using a Wacom Intuos 5 Touch tablet.

2.2.3 Field emission scanning electron microscopy

Rachis, rami, and barbules of modern feathers were cut using a razor blade at an oblique angle. FESEM images were created by attaching specimens of fossil and modern feathers onto conductive SEM stubs using carbon tape. Studs and specimens were sputter-coated with gold to minimize the charging on specimens during imaging procedures. Specimens were then viewed with a JEOL 6301F FESEM. To capture FESEM images, scan times were set to 30 seconds. Images were then enhanced in Adobe Photoshop CS6 Extended. FESEM work was conducted at the University of Alberta, Earth and Atmospheric Sciences, FESEM laboratory.

2.2.4 Transmission electron microscopy

After embedding (see 2.2.5 for embedding procedure), 90 nm sections were taken on a Leica EM UC6 Ultramicrotome and collected on carbon-coated nickel grids (EMS Cat CFT200-NI) and were observed using the FEI Talos F200X electron microscope in the Analytical Instrumentation Facility of North Carolina State University.

2.2.5 Immunohistochemistry

A feather from UAULP 52531 still attached to sediment was put into 50% Hydrogen fluoride (HF) for 5 hrs to remove the silicon minerals of the matrix. It was then washed with PBS. The feather fragments were collected and embedded in LR White resin (hard grade, Electron Microscopy Services) after partial dehydration in 70% ethanol and thorough penetration with pure LE white. The modern black chicken feather (collected from the Poultry Teaching Unit at North Carolina State University) and the goose feather that were used for comparison were cut into 1-2 mm sections and fixed in Neutral Buffered 10% Formalin 1h at RT before following the same embedding protocol. 200nm sections were taken on a Leica EM UC6 Ultramicrotome and dried overnight at 45^{o}C to each well of a six-well, Teflon-coated slide (Electron Microscopy Sciences Cat #63424-06). As digestion negative control, sections were incubated in 2mg/ml Keratinase (Creative Enzymes Cat # Feed-0001) in PBS pH 7.0 with 0.1% SDS enzyme activator for 1 hour at 65^{o}C.

All sections were etched with 25ug/ml proteinse K, 0.5MEDTA for epitope retrieval, followed by 1mg/ml sodium borohydride incubation for quenching autofluorescence. Unspecific binding was blocked with 4% Goat normal serum. Sections were immunolabelled with primary antibodies (Rabbit anti-feather (Biosynthesis BYSN6733) 1:200; Rabbit anti-keratin peptide B1 (Genscript A317090089) 1:100; Rabbit anti-Chicken Collagen Type I (USBiological C7510-13B) 1:75; Mouse anti-pan Cytokeratin AE1/AE3 (abcam 80826) 1:75; Mouse anti-peptidoglycan (BioRad 7263-1006) 1:75) diluted to final concentration in primary dilution buffer (1% Bovine Serum Albumin (BSA) (Fisher, BP1660-100), 0.1 % Cold Fish Skin Gelatine (Sigma G7765), 0.05% Sodium Azide (sigma S-8032), 0.01M PBS pH 7.2) or in primary dilution buffer only, without primary antibody added to control for non-specific secondary

antibody binding. All sections (control, fossil and modern) were washed thoroughly to remove unbound antibodies, then incubated with secondary antibodies (Biotinylated goat anti-rabbit IgG(H+L) (Vector BA-1000) diluted 1:500 for rabbit primary antibody, Biotinylated Goat anti-mouse IgG(H+L) (Vector Laboratories BA-6000) diluted 1:500 for mouse primary antibody) for 2 hours at room temperature or overnight at 4°C or dilution buffer alone to control for non-specific secondary antibody binding. Afterwards they were incubated with the secondary antibodies (biotinylated goat anti-rabbit IgG(H+L) (Vector BA-1000) diluted 1:500 for 2 h at room temperature. Fluorescein Avidin D (Vector Laboratories A-2001) was applied for 1hr. All incubations were separated by sequential washes, Finally, the sections were mounted with Anti-Fade mounting medium (Vector H-1000), and coverslips were applied. The sections were examined with a Zeiss Axioskop 2 Plus biological microscope.

2.2.6 Immunogold

The 90nm sections were made using a Leica EM UC6 Ultramicrotome and collected on carbon-coated nickel grids (EMS Cat CFT200-NI). Grids were incubated in PBS-Tween 20 for 10 minutes. Four percent NDS in PBS was applied to occupy non-specific binding sites for 1 hour at room temperature. Grids were incubated in primary antibody (Polyclonal Rabbit anti-feather 1:10) in primary dilution buffer for 3 hours at room temperature. Grids were rinsed with PBS-Tween20 for 10 x2 minutes. All Grids were then incubated with secondary antibody (12 nm Colloidal Gold AffiniPure Donkey Anti-Rabbit IgG (H+L) 1:20 (Jackson Immuno Research Inc Cat 711-205-152) for rabbit primary antibody; 12 nm Colloidal Gold AffiniPure Donkey Anti-Mouse IgG (H+L) 1:20 (Jackson Immuno Research Inc Cat 715-205-150) for mouse primary antibody) 1 hour. The grids were rinsed with PBS-Tween 20 for 10x2 minute, in E-pure water 3x30 dips, and

dried with filter paper. The sections were observed using the FEI Talos F200X electron microscope in AIF of North Carolina State University.

2.2.7 Time of flight secondary ionizing mass spectrometry

The molecular composition of the fossil feather (UALVP 52531) was examined by time-of-flight secondary ion mass spectrometry (ToF-SIMS). In ToF-SIMS, a focused, high-energy (primary) ion beam is rastered over a selected analysis area on the sample surface. Emitted (secondary) ions are detected in a ToF analyser to produce spatially-resolved mass-spectrometric data. The data can be presented as ion images, which display the signal intensity of specific ions over the analysis area, or as mass spectra from the total analysis area or from selected regions of interest (ROIs) (Thiel and Sjövall 2011).

2.3 DESCRIPTION

2.3.1 Extant Feathers

2.3.1.1 Macromorphology

Feathers from extant aves come in a vast variety of morphologies (Lucas and Stettenheim 1972), many of which are for sexual display purposes. For all the diversity observed in micromorphology, however, the general structure of each feather is the same in possessing a main shaft called the rachis, the primary branching structures called rami, and the secondary branching structures called barbules. Many species of Aves possess hooklets that project from the barbules, allowing the vane of the feather (the series of rami along the side of the feather) to stay locked together into a stable flat aerodynamic surface (Lucas and Stettenheim 1972). Contour feathers, those that cover and produce the outline of the body, are smaller than feathers that are used for flight and steering. Contours possess an open vane at

the base of the feather, whereas the distal half of the feather possesses a closed vane (Lucas and Stettenheim, 1972; Fig. 158). Down feathers, the insulative feathers closest to the skin, are lightly built, but come in a variety of forms. Although each down form always possesses a calamus, the general structure varies significantly between taxa, and no phylogenetic signal is recognised. The general structure varies from a short sharply tapering rachis with long wispy rami, to a long thin rachis with long wispy rami that randomly branch towards their tips (Lucas and Stettenheim 1972). Bristles are a unique class of derived feather that typically serve sensory functions on the head, or to act as lashes to prevent dust from entering the eye. Each of these feathers is characterized by a stiff rachis with rami only at the proximal end around the base of the feather (Lucas and Stettenheim 1972). Filoplumes, another sensory feather found throughout the body (not restricted to the head like bristles) possess a similar morphology; however, instead of rami at the base, rami are only found at the distal end (Lucas and Stettenheim 1972). Remiges and rectrices are the feathers primarily used in flight and are generally stiffer and stronger and possess enlarged rachises and rami. Remiges, the main flight feathers on the wings, typically have asymmetrical vanes, which aid in lift generation during takeoff. Rectrices, the main tail flight feathers, are more symmetrical, although the lateral feathers are slightly asymmetrical. Rectrices possess rachises that are enlarged and stiff, like those seen in remiges (Lucas and Stettenheim 1972). In many birds, rectrices are modified to perform display functions, taken to an extreme in peacocks for example.

2.3.1.2 Scanning Electron Microscopy (SEM)

Although microstructures relating to structural colouration (Prum 2006) of feathers have been researched extensively (>160 taxa according to Prum, 2006)) and cortical keratin

fibre weaving has also been investigated (Lingham-Soliar and Murugan 2013), little work has been done on describing the specifics of medulloid pith. Although research into the variation of medulloid pith is ongoing, it should be noted that not only is pith structure variable between taxa, it also varies between feather types within a single taxon as well.

The microstructure of feathers is poorly researched, especially variation within the internal components. Lucas and Stettenheim (1972) described in detail the internal structural components. These components include the cortex, a thick layer of β-keratin sheets that form the main walls of the rachis and rami, and the medulloid pith, a foam-like structure that fills the interior of the rachis and rami (Fig. 2-2). Medulloid pith is formed of keratinized epithelial cells that die as the feather grows (Lucas and Stettenheim 1972) and is only found in the rachis and ramus. The barbules, on the other hand, are solid structures. When pith cells die and decay, the β-keratin that was deposited around them remains, creating the foam like texture (Fig. 2-2). Pith walls comprise layers of keratin fibres can form loosely or densely woven webs, or in some cases a solid wall. If these fibres do not form a solid wall, the mesh will possess gaps between fibres, which will be referred to in this chapter as pith pores (Fig. 2-2). Modern taxa appear to have a variety of shapes and sizes of pores controlled by the density of keratin fibrils. Pith cells appear to grow at random, although a three-dimensional study of this structure has never been conducted.

Because no description of the variety of keratin fibres has ever been published, the following definitions and nomenclature are proposed for the structures observed in feather medulloid pith. Individual keratin fibres are common in several different forms in extant aves. The simplest (Type 1 k-fibrils) are single fibres with no bifurcations at either end. This singular

form of fibre is found randomly throughout the medulloid pith of all feathers (Fig. 2-3). The second form of keratin fibril is long and bifurcate at least once on one, or both ends (Type 2 k-fibrils) (Fig. 2-4). This form of fibril is often associated with clusters of melanosomes positioned on the pith wall or where pith walls are anchored to the cortex (Fig. 2-4c). Some extant bird taxa possess this form of bifurcating fibres spanning the entire pith cell (Fig. 2-4d). The third form of keratin fibril is a web-like structure with multiple branches originating from a central node (type 3 k-fibril) (Fig. 2-5). These are most often observed as a web of keratin present within the pith cell (Fig. 2-5c,d). Some extant birds possess pith walls formed by very loosely woven β-keratin fibrils that produce larger pith pores. Consequently, it can be difficult to determine what is pith wall and what is a type 3 k-fibril (Fig. 2-6). The possibility that 3 k-fibrils become incorporated within the pith wall unfortunately requires imaging techniques not available for this study.

Where multiple pith cells merge, a hollow void is present that extends the length of the junction. In cross section, it is circular (Fig. 2-7). These tube-like structures have never been described previously and are herein referred to as inter-pith canals. The inter-pith canals are much larger than the pith pores observed in pith walls, are more regular in shape, and always possess round cross sections. When inter-pith canals are exposed longitudinally, small keratinous fibres are observed across the top, and are referred to as keratinous bridges. These keratinous bridges narrow at their mid-points and expand where they attach to the pith wall (Fig. 2-7c).

2.3.1.3 Transmission electron microscopy (TEM)

Using TEM on extant feathers reveals the same general surface structures observed in SEM. However, it provides more information on how keratin layers are deposited during feather growth. In extant goose feathers, the inter-pith canals are observed as circular (although deformed from crushing) voids at the junction of pith walls (Fig. 2-8a). It is evident that the pith cell wall that is in contact with the cortex of the feather is an independent deposit of keratin, and that the cortex does not make up the pith cell in this region (Fig. 2-8a) Interestingly, however, the region where adjacent pith cells meet along the cortex appears to be reinforced by additional keratin fibrils. This may be a structure that ensures the cortex does not separate from the medulloid pith, which would drastically change the mechanical properties of the feather. The contact boundary between pith walls and the cortex keratin is observed as a prominent thin line of higher density keratin (Fig. 2-8). The cortex consists of alternating layers of at least two different densities of keratin. These layers have not been previously described in detail, and the following nomenclature will be used (from internal to external layers). The first layer, referred to as the melanosome bearing layer (MBL) is subdivided into two zones. The inner zone is very thin but formed by dense keratin. The outer zone is a moderately dense keratin layer, possessing approximately the same density as pith walls. The surfaces of more external MBLs are where melanosomes are deposited (Fig. 2-8), which is why it is referred to as the "melanosome bearing" layer. The second layer, referred to as the capping keratin layer (CKL), is a less dense keratin layer that is approximately the same thickness as the BKL (Fig. 2-8). It is referred to as the CKL because it caps the melanosomes that have been deposited on the surface of the BKL. The most external layer observed in an extant goose feather, appears to be a slightly thicker layer of BKL. Melanosomes are embedded

directly within the keratin, but there is no CKL. This may be because the higher density of the BKL provides greater resistance to environmental wear and tear on the feather surface. Within the outer cortex layers, "S" shaped structures are visible within the keratinous matrix (Fig. 2-9d).

2.3.1.4 Immunohistochemistry

Immunohistochemistry provided three different proteins visually identified using immunofluorescence within the feather structure. These included, β-keratin, cytokeratin AE1/AE3 (α-keratin), and whole feather proteins (all proteins from within a feather). When observed with a fluorescence microscope, the positions of each of these proteins are visible. Whole feather reactivity, as expected, is strongly visible throughout the entire keratinous structure (Fig. 2-9). β-keratin, also as expected, is visible throughout the entire keratinous region of the feather. However, the fluorescence is not as strong as whole feather proteins (Fig. 2-9). Also as expected, due to the lack of α-keratin within adult bird feathers, no fluorescence was observed for modern feathers.

2.3.1.5 Immunogold

Immunogold techniques produce similar results to those obtained using immunofluorescence. Immunogold, however, is used on the nanoscale, and shows exactly where antibodies are binding to protein epitopes. The density of visible gold beads in both the anti feather treatment and the anti β-keratin antibody treatment is high, as expected because feathers are composed nearly completely of these proteins. The anti cytokeratin (α-keratin) binding was considerably less (Fig. 2-9).

2.3.2 UALVP 52531 Feathers

2.3.2.1 Macromorphology

The feathers found with UALVP 52531 with greatest definition are those over the left ilium (Fig. 2-1), and are preserved in a loose, multi-layered mat (Fig. 2-1b). Towards the dorsal margin of the iliac crest, feather density decreases, allowing individual feathers to be differentiated (Fig. 2-1d-g). Feather rachises have an average diameter of 250 µm and the maximum length of the average body feather is estimated to be about 5 cm, based on the most complete feathers observed throughout the specimen. They remain a uniform width through most of their length, tapering only towards the terminus. The rachises possess parallel lines of dark carbonaceous material bordering the lateral margins.

Rami are laterally paired and spaced equally along the length of the rachis approximately every 1.5 mm (Fig. 2-1d-g). In all cases, rami branch from the rachis at shallow angles, and are sub-parallel with other rami along the lateral edges. The most complete individual ramus (Fig. 2-1d) is 700 µm in length, and the mean width of rami is 50 µm. The diameters of the rami are statistically distinct from those of the rachises (Fig. 2-1c, Table 2-1, $p<0.001$). In most feathers of UALVP 52531, the rachises are slightly curved along their shafts (Fig. 2-1d,f). The rami, however, appear to be highly flexible. A ramus visible in one feather can be observed folded underneath the rachis and emerging on the opposite side (Fig. 2-1d, e).

2.3.2.2 Field emission scanning electron microscopy

FESEM images of UALVP 52531 feathers and extant bird feathers were used to investigate the microstructural features of both rachises and rami. Size and morphology of structures observed using FESEM imaging revealed that several UALVP 52531 feathers still preserve structures in detail that were almost certainly originally keratinous (Fig. 2-2a,d,g,j).

The best-preserved pith wall (Fig. 2-2j, Fig. 2-4a) is approximately 0.3 µm thick and is fastened to the cortex at approximately 90 degrees. Although the base of the pith wall is mostly obscured by keratinous debris, enough detail remains to indicate that the pith wall is anchored to the cortex by multiple individual keratin fibres that branch at both ends (Type 2 k-fibres). Other portions of the cortex in the adjacent area have fragments of branching fibres that abruptly terminate or are covered by keratinous debris (Fig. 2-4a). Several pith pores have been observed in samples from UALVP 52531 (Fig. 2-2d, arrows), and are clearly associated with small ridges and fibre-like structures identified as the keratin of pith walls, although due to slight diagenesis morphology is slightly altered. Inter-pith pores are arranged linearly, separated by thin keratin fibres of varying widths. Adjacent to these inter-pith canals, several different layers of crushed keratin are visible.

FESEM images reveal some information regarding the distribution of melanosomes, which will be discussed further in the section on TEM. Melanosomes are primarily deposited in a dense layer within the cortex of both the rachis and ramus (Fig. 2-3a,b). Melanosomes are occasionally observed deposited on the surfaces of pith walls in association with keratin strands (Fig. 2-3). FESEM confirms a semi-solid medulloid pith was present in *Ornithomimus*.

2.3.2.3 Transmission electron microscopy

Fragments of a feather rachis of UALVP 52531 were observed using TEM, and show exceptional detail for preserved feathers of such a basal coelurosaur. A portion of the rachis can be seen with fine keratinous layers containing small voids, similar to those observed in the outer regions of modern feathers (Fig. 2-10a). Small filamentous portions of keratin are also observed in this same specimen and are interpreted as pith wall keratinous fibres that have

pulled away from the cortex. Pith is also observed as a web-like series of fibres surrounding a void within the TEM image (Fig. 2-10b). Individual fibrils are observed projecting into the voids of the pith pores. By using a tiltable TEM, several samples could be visualized three-dimensionally. These reveal the presence of a complete network of keratinous fibres forming a loose web, similar to those that hold pith walls to the cortex in extant bird feathers (Fig. 2-10b). TEM conducted on immunogold-labeled feather fragments also revealed well preserved keratin layers with well preserved melanosomes *in situ* (Fig. 2-11), and small sinusoidal structures thought to be some form of keratin fibre or fibre bundle (Fig. 2-10c)(Schweitzer, pers com). However, future research is planned to identify these as they are equally abundant in feather cortices of extant birds.

2.3.2.4 Immunohistochemistry

Immunofluorescence tests for cytokeratin (AE1/AE3, α-keratin), β-keratin, and whole feather protein were done on feather fragments from UALVP 52531 and the feathers of extant birds. Due to the exquisite preservation of the feathers on UALVP 52531, antibody reactivity had positive results. Immunofluorescence occurred throughout all of the preserved fragments of keratin of both fossilized and modern feathers, and β-keratin and whole feather protein fluoresced strongly. Interestingly, reactivity for cytokeratin (AE1/AE3, α-keratin) was also very strong in UALVP 52531, although not as strong with the other two antibodies (Fig. 2-11a-c). Although extant feathers show virtually no reaction to cytokeratin, a feathered specimen of *Anchiornis* has also had α-keratin binding in feather samples (Lindgren et al. 2015).

2.3.2.5 Immunogold

TEM images of immunogold treatments to UALVP 52531 feather fragments support the immunofluorescence results. Both the β-keratin and whole feather protein results indicate that a significant amount of preserved protein remains (Fig. 2-11d-f). However, reduced amounts of visible gold beads suggest that either a "primitive" epitope for antibodies is present within the *Ornithomimus* feathers, or protein has degraded in most of the feather. Until further work is conducted on the polypeptide sequence it is uncertain why the resultant reactivity is lower than in extant feathers. Similar to the results for immunofluorescence, immunogold results for α-keratin show a significant increase in antibody binding, showing there is a significant amount of α-keratin throughout the feathers of the *Ornithomimus*.

2.3.2.6 Time of Flight Secondary Ionizing Mass Spectrometry

Negative ion ToF-SIMS data acquired from a small piece of the fossilized feathers of UALVP 52531 reveal clear signals from the characteristic ions of eumelanin (Lindgren et al. 2012). These have a complementary spatial distribution compared to that of sediment-specific ions (Fig. 2-12a-f), suggesting the presence of eumelanin in the fossil feather. Furthermore, spectra generated from ROIs with strong signals from the eumelanin-characteristic ions in the ion images of UALVP 52531 agree in detail with spectra acquired from a natural eumelanin reference sample (*Sepia officinalis*). These include the detection of all major eumelanin-related peaks, with the same m/z positions and similar signal intensity distributions as in the *Sepia* reference spectrum (Fig. 2-12g-h). In addition to the eumelanin-related peaks, the spectra of UALVP 52531 include peaks related to the sediment and an unidentified O-containing organic contaminant (marked "*" and "+"in Fig. 2-12g). Similarly, peaks related to contaminants in the Sepia reference were also identified (marked "°" in Fig. 2-12h). A detailed comparison between

UALVP 52531 and the *Sepia* reference with regards to the distribution of the signal intensities of the eumelanin-characteristic peaks (Fig. 2-12i) shows overall agreement. This confirms the identification of eumelanin in UALVP 52531. However, there are some deviations, including lower signal intensities of peaks at m/z 50, 66, 74, 98 and higher intensities at m/z 49, 73, 97 in the UALVP 52531 spectra compared to the *Sepia* reference spectrum. Ion identification reveals that the peaks with lower signals in the fossil spectra correspond to N-containing ions (C_nN^- and C_nNO^-) and those with higher signals in the fossil correspond to C_nH^- ions. These patterns suggest a loss of nitrogen in the eumelanin molecular structure during diagenetic maturation.

2.4 COMPARISONS

2.4.1 Extinct taxa

Sinosauropteryx prima possesses filamentous integumentary structures described as soft, pliable, and semi-independent of each other (Chen et al. 1998, Currie and Chen 2001). These filaments vary in thickness from 0.1 mm to 0.2 mm, with occasional filaments being reported as exceeding 0.3 mm in diameter. The filaments on *Sinosauropteryx* fall within the range of rachis diameter found on UALVP 52531. However, the "rami" on *Sinosauropteryx* are double the size. These large filaments of *Sinosauropteryx* are reported as being dark portions along the margins and light medially (Currie and Chen 2001), which suggests that some filaments may have been tubular (Chen et al. 1998, Currie and Chen 2001, Prum and Brush 2002). This same characteristic is also observed in UALVP 52531, in which an essentially solid medulloid pith is known to exist. Although it was suggested that the integument may be composed of branching structures, the matting of the filaments makes it difficult to interpret with certainty (Currie and Chen 2001). If *Sinosauropteryx* integumentary structures are

branching, the filaments are too large to match the rami found in UALVP 52531, indicating a different morphology. Without clearer representations of the filamentous integument on *Sinosauropteryx prima,* it is difficult to make direct comparisons. However, it can be concluded that they likely possess different morphologies due to the difference in filament sizes. It is possible that the 'hollow' filament in *Sinosauropteryx* represents an early stage in feather evolution in which medulloid pith had already evolved. This has major implications for understanding the origin of proto-feathers, in that pith may lead to better understanding the original function of these integumentary structures.

Sinornithosaurus millenii, a Lower Cretaceous dromaeosaur from the Yixian Formation of China, possesses an integument formed by compound structures containing multiple filaments (Xu et al. 2001). Two types of feathers are reported, the first resembles that suggested for Prum Model Stage 2. The second, which is more difficult to interpret, appears to be a branching filament, closer to those suggested for Prum Model Stage 3a. The mode of preservation with overlapping layers of filaments is similar to that of *Sinosauropteryx*, which makes interpretation difficult (Currie and Chen 2001). However, phylogenetics suggest that *Sinornithosaurus* likely possessed Stage 3a feathers, which supports the hypothesis that the branched structures are interpreted correctly. Filamentous integumentary clusters in *Sinornithosaurus* are significantly wider (1-3 mm, Xu et al., 2001) than those measured in UALVP 52531 (~0.25 mm), which suggests a different morphotype of branching feather, possibly due to different ecological adaptations.

Dilong paradoxus, an Early Cretaceous basal tyrannosauroid from the Yixian Formation of China, has an integument that consists of simple branching structures (Xu et al. 2004). Two

types of feather-like integumentary structures were briefly described. Rauhut et al. (2012) and Xu et al. (2004) both recognized at least some filamentous integumentary structures on *Dilong* Stage 1 feathers, but the latter also recognized Stage 3a structures. Those reported to be Stage 3a are represented by what appears to be a rachis with several small rami branching off on the distal portion of the feather. Because the description of these feathers does not give any measurements or scale bars, size comparisons with UALVP 52531 is not possible. However, the general morphology is similar in the two taxa. The feathers in *Dilong* appear to be slightly more rigid than those observed in UALVP 52531, but this may be due to the vagaries of preservation.

Two *Ornithomimus edmontonicus* specimens from the Upper Cretaceous Horseshoe Canyon Formation of Alberta, Canada, possess preserved filamentous integumentary structures (Zelenitsky et al. 2012). An adult specimen (TMP 2008.070.0001) has black carbonaceous traces preserved in sandstone surrounding the cervical and dorsal vertebral series, as well as anterior to the scapula on the chest region. These appear to be individual filaments similar to those of basal Liaoning theropods, and measure up to 50 mm in length and 0.5 mm in diameter (Zelenitsky et al. 2012). This adult has a similar overall size to UALVP 52531 and possesses feather structures of the same size. The second specimen, a juvenile (TMP 2009.110.0001) has an almost complete covering of plumage preserved in a ferruginous layer (Zelenitsky et al. 2012). These feathers were originally described as Stage 1 single filaments possessing hollow cores (supplementary information (Zelenitsky et al. 2012)). Personal observations of these specimens suggest the central streaks of calcite reported as hollow cores are actually the spaces between the rachis and ramus. The pattern observed in TMP 2009.110.0001 matches that seen in all feathers throughout the plumage of UALVP 52531.

2.4.2 Amber specimens

UALVP 52581 represents a Stage 1 filamentous integument in amber from the Late Cretaceous of Alberta, Canada (McKellar et al. 2011). Filaments are individual tubular structures that are an average of 16.4 µm in diameter. These are significantly smaller than the 50 µm measured for the average ramus on feathers of UALVP 52531. The fibres of UALVP 52581 are a true tubular structure, containing no obvious medulloid pith. This matches the suggested characteristics of Stage 1 filaments proposed by Prum (1999).

UALVP 52822 represents a Stage 2 filamentous integumentary structure from the Late Cretaceous of Alberta, Canada (McKellar et al. 2011). They are tightly adpressed to form a cluster (McKellar et al. 2011). Individual filaments measure approximately 0.2 mm in diameter and resemble those of UALVP 52581. They are similar in average width to the rachises seen in UALVP 52531, but only half as wide as the largest measured rachis. The rami in UALVP 52531 are significantly larger than individual filaments of UALVP 52822.

MNHN ARC 115.6 represents seven feathers in a single piece of amber collected from the Early Cretaceous of western France (Perrichot et al. 2008). They are exceptionally small branching structures, and the largest is only 2.3 mm long, and has a rachis diameter of 0.01 mm. Structures suggested to be rami are not paired and do not completely fuse to the rachis as in modern feathers (Perrichot et al. 2008). Although the general appearance is similar to feathers of UALVP 52531, the sizes are significantly smaller in MNHN ARC 115.6. The ramus is one fifth the diameter of a rachis in UALVP 52531, which suggests the French specimens may actually represent subcomponents of larger feathers, such as basal rami with barbules (McKellar et al. 2011), suggesting these originated from more derived feathers.

2.4.3 Extant taxa

The feathers preserved on UALVP 52531 are macromorphologically similar to those of a modern rhea, which is covered by long, narrow, and delicate open vane feathers. Unlike the feathers of a rhea and all other extant birds, however, those of UALVP 52531 do not show any evidence of barbules. This long, wispy, feather morphology shows that, as in large ratites, the feathers were for camouflage and insulation, and certainly not flight. Both extant and *Ornithomimus* feathers have rami that are paired and spaced approximately equidistant along the entire length of the rachis.

In both the feathers of extant birds and *Ornithomimus*, the cortex of a feather is formed by multiple layers of keratin with small voids between the external layers. Additionally, melanosomes are deposited within the same regions of cortical keratin and are approximately the same size. Nano scale, "S" shaped fibre bundles are found in feathers of both extant birds and *Ornithomimus*, and in similar quantities. Unfortunately, due to the crushing of keratinous structures in most of the UALVP 52531 feathers, it is difficult to get a detailed picture of its cortex. Immunofluorescence and immunogold techniques show that ornithomimids incorporated a significant amount of α-keratin into the keratinous matrix of their developed feathers, unlike in modern Aves.

Presence of pith walls in both sizes of feather structures of UALVP 52531 indicate that the interpretation of a rachis/ramus branching structure that lacks barbules is correct (Fig. 2-13) because feathers of extant birds do not contain pith within barbules. The pith wall density resembles that found in the remex ramus of *Pica hudsonia*, where few pith pores are observed. A section of ramus from UALVP 52531 possesses a portion of free-standing pith wall that

remains anchored to the cortex by long branching fibres (Fig. 2-2j). This is regularly observed in feathers of extant birds (Fig. 2-2c,d). Pith pores observed in UALVP 52531 appear as holes between crushed pith wall keratin fibres. Several pores penetrate deeper through the pith wall than others, thus appearing as small, well-defined, depressions. This indicates that diameter and depth varied in *Ornithomimus* feathers, as in modern taxa that show a wide variety of shapes and sizes of pores (Fig. 2-14c,d). Inter-pith pores of similar morphology are visible in both UALVP 52531 and extant feathers.

2.5 DISCUSSION

2.5.1 Morphology

Zelenitsky et al. (2012) proposed that ornithomimid feathers were at Stage I or II in feather evolution. However, the feathers they examined were preserved in either an ironstone layer surrounding the skeleton, or in a coarse sandstone, and neither permitted detailed observations. The feathers of UALVP 52531 are preserved in three different matrices across the specimen, including iron-rich sandstone, coarse sandstone, and mudstone. Those preserved in mudstone provide spectacular details of rachises and paired rami in branching structures that lack barbules. Ornithomimids therefore have feathers that represent Model IIIa of Prum (1999).

Most feathers of UALVP 52531 have rachises that are slightly bent along their length (Fig. 2-1d,f), which suggests that these structures were somewhat flexible. In size and flexibility, the rachises and rami resembled down feathers of extant taxa. This observation supports the hypothesis that these feathers were used for insulation, as suggested for other non-avian theropods (Chen et al. 1998, Qiang et al. 1998, Xu et al. 2004, Zhang et al. 2006, Xu and Guo 2009). However, the possible presence of semi-rigid rachises in other non-avian theropods (Xu

et al. 2001) suggests they were not down-like. These feathers were perhaps serving functions similar to the semiplumes or contour feathers found in extant large bodied palaeognaths.

Previous assessments of proto-feathers with lighter cores have concluded that filaments of non-avian theropods were hollow (Currie and Chen 2001, Zelenitsky et al. 2012). Based on the anatomy of extant feathers, however, it is proposed that this feature may rather be attributed to the overall thicker vertical accumulation of keratin on the lateral faces compared to the dorsal and ventral surfaces combined. It is therefore proposed that proto-feathers were likely also filled with pith.

2.5.2 Micromorphology

The feathers of extant avians have several architectural components: the cortex (herein includes the cortex and epicortex, as these are not distinguishable in fossil specimens), cortical ridges, ventral ridges, a ventral groove, and the medulloid pith (Lucas and Stettenheim 1972, Lingham-Soliar and Murugan 2013). Pith has a foam-like texture formed by the keratinized walls of epithelial cells that infill the centres of the rachises and rami, making these structures functionally more solid than tubular (Lucas and Stettenheim 1972) (Fig. 2b,c,e,f). This weighs against previous interpretations of theropod feathers as hollow (Currie and Chen 2001, Zelenitsky et al. 2012), and instead suggests that observed density differences reflect the presence of pith within a solid cortex.

Microbodies proposed to represent intracellular, pigment-containing organelles called melanosomes have been identified in multiple fossilized feathers (Li et al. 2010, 2012, Knight et al. 2011, Field et al. 2013, Moyer et al. 2014, Thomas et al. 2014), and similar structures are observed in UALVP 52531. Because melanosomes and microbes overlap completely in size,

shape and overall morphology (Moyer et al. 2014), these cannot be definitively identified as one or the other in these feathers based upon morphology alone. ToF-SIMS results, however, provide a positive identification of these microbodies as melanosomes. Melanosome research has previously attempted to reconstruct the colours of fossil feathers (Li et al. 2010, 2012), although the complexity of colouration in extant avian feathers suggests that identifying accurate colours in dinosaur feathers is unlikely (McGraw 2006a, 2006b, 2006c, Prum 2006, Moyer et al. 2014). The melanosomes observed within the dense matrix of UALVP 52531 feathers are represented by three shapes – circular, ovoid, and bacilliform. They are also within the size ranges of both extant avian melanosomes and bacteria (Fig. 2-15). These microbodies in UALVP 52531 are primarily found as tightly associated mats and are commonly associated with fragments of rachises and rami. There is cortical keratin moulded around them (Fig. 2-15a) and they are rarely observed in isolation. This is the first record of melanosomes being identified within Ornithomimosauria.

The early evolutionary advantages of feathers progressing from Stage I into Stage III (Prum 1999) are still being debated, but UALVP 52531 provides invaluable macro- and microscopic information on how these early branching feathers were structured. Although cortical and ventral ridges, and a ventral groove were not observed with certainty in these specimens, the positive identification of the phylogenetically basal-most known medulloid pith in dinosaur feathers represents a major leap in understanding the evolution of feathers and their role in the origin of flight. The Prum (1999) model of feather evolution suggests that Stage IIIa feathers result from the fusion of rami bases to form the rachis. If this is correct, then the

filaments found in bundles of Stage II should also possess medulloid pith cells, and further investigation should reveal at what stage medulloid pith arose.

Dinosaur taxa basal to *Ornithomimus* that were reported to have hollow integumentary structures (Currie and Chen 2001) may also have possessed pith within the core of the filaments, which would suggest that pith was a plesiomorphic structural feature in feathers. If dinosaur specimens possessing Stage II feathers that show indications of pith are discovered in the future, this will help verify that the origin of Stage III feathers was indeed the fusion of rami bases to form the rachis. Therefore, it is suggested that true feathers should be defined as "an integumentary β-keratin, branching structure consisting of a minimum of a rachis and multiple rami with medulloid pith interiors, and their evolutionary derivatives".

TABLES

Table 2-1. UALVP 52531 Feather Specimen Width Measurements

Location of Measured Filament			
Lateral Ilium (left)		Base of Tail	
Rachis Width	Ramus Width	Rachis Width	Ramus Width
0.22	0.06	0.26	0.05
0.29	0.03	0.31	0.05
0.12	0.06	0.27	0.05
0.24	0.04	0.25	0.05
0.23	0.04	0.33	0.06
0.20	0.06	0.17	0.05
0.23	0.04	0.45	0.05
0.21	0.04	0.13	0.05
0.20	0.05	0.17	0.05
0.27	0.04	0.19	0.06
0.16	0.03	0.24	0.06
0.11	0.04	0.28	0.06
0.22	0.05	0.30	0.05
0.29	0.06	0.14	0.04
0.18	0.06	0.32	0.04
0.24	0.06	0.30	0.06
0.30	0.06	0.27	0.05
0.19	0.05	0.16	0.05
0.17	0.06	0.28	0.05
0.29	0.05	0.25	0.05
0.28	0.04	0.25	0.06
0.27	0.05	0.29	0.03
0.28	0.06	0.29	0.04
0.24	0.06	0.22	0.03
0.25	0.06	0.20	0.05
0.17		0.41	0.05
0.31		0.39	0.05
		0.37	0.05
		0.32	0.03
		0.17	0.04
		0.24	0.05
		0.22	0.05
		0.35	0.05
		0.21	0.05
		0.38	0.06

			0.19	0.04
			0.21	0.05
			0.35	0.05
			0.29	0.06
			0.23	0.06
			0.22	0.06
			0.29	0.03
			0.35	0.04
			0.31	0.05
			0.25	0.06
			0.30	0.05
			0.30	0.04
			0.25	0.06
			0.21	0.04
			0.26	0.05
			0.25	0.03
			0.20	0.05
			0.25	0.03
			0.28	0.05
	Rachis Width Mean	Ramus Width Mean	Rachis Width Median	Ramus Width Median
	0.25	0.05	0.25	0.05
standard deviation	0.06633552	0.009418331		
number of specimens	81	79		

Figures

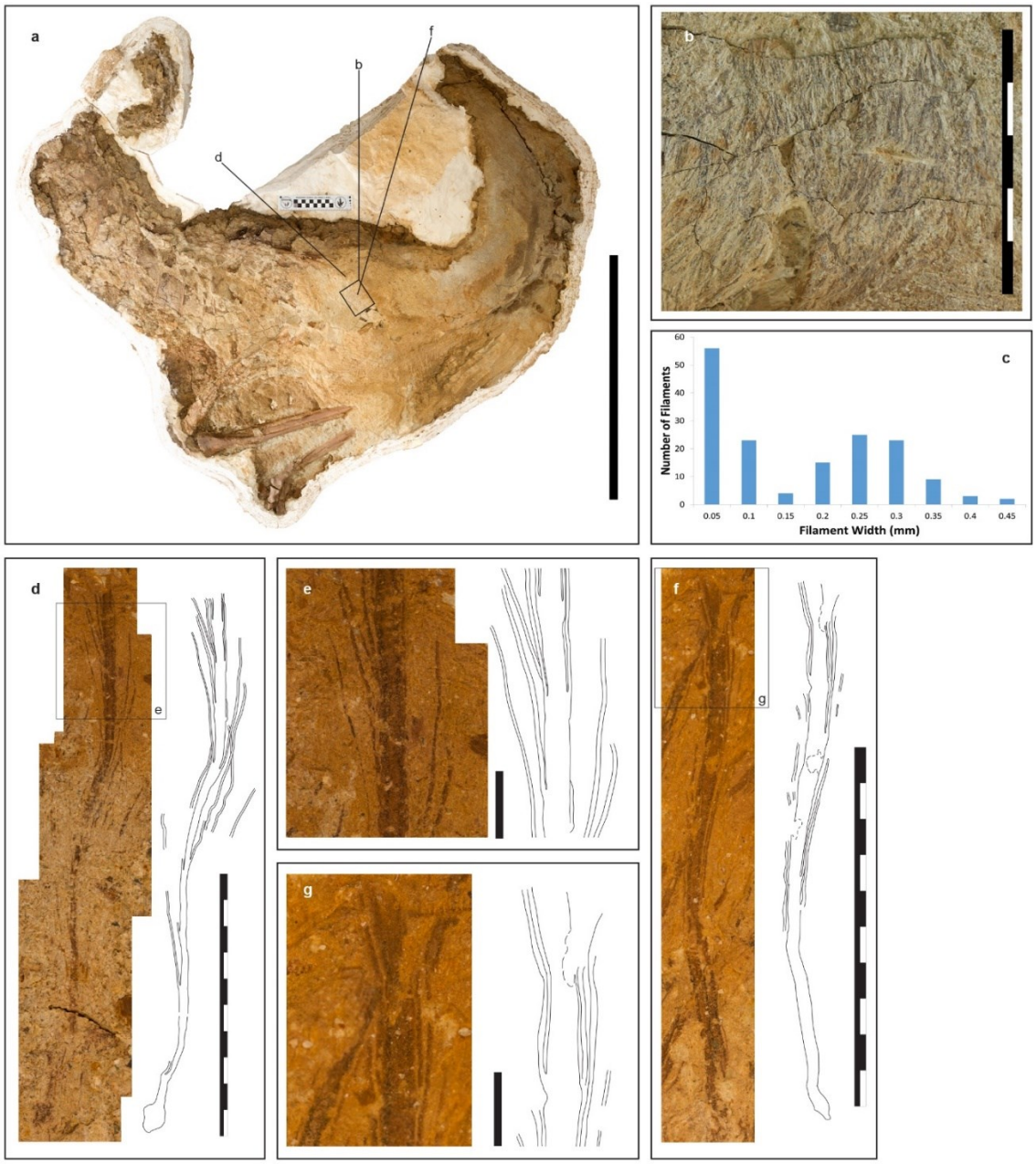

Figure 2-1. UALVP 52531 specimen indicating location of feather images (**a**). Scale bar, 50 cm. **b**, feather patch over left ilium. Scale bar, 5 cm. **c**, histogram of filament widths showing a bimodal distribution, indicating two distinct filament sizes, rachis and ramus. **d**, **f**, composite photo and line drawing of a single feather showing rami branching from rachis. **e**, enlarged area outlined in (**d**). **g**, enlarged area outlined in (**f**).

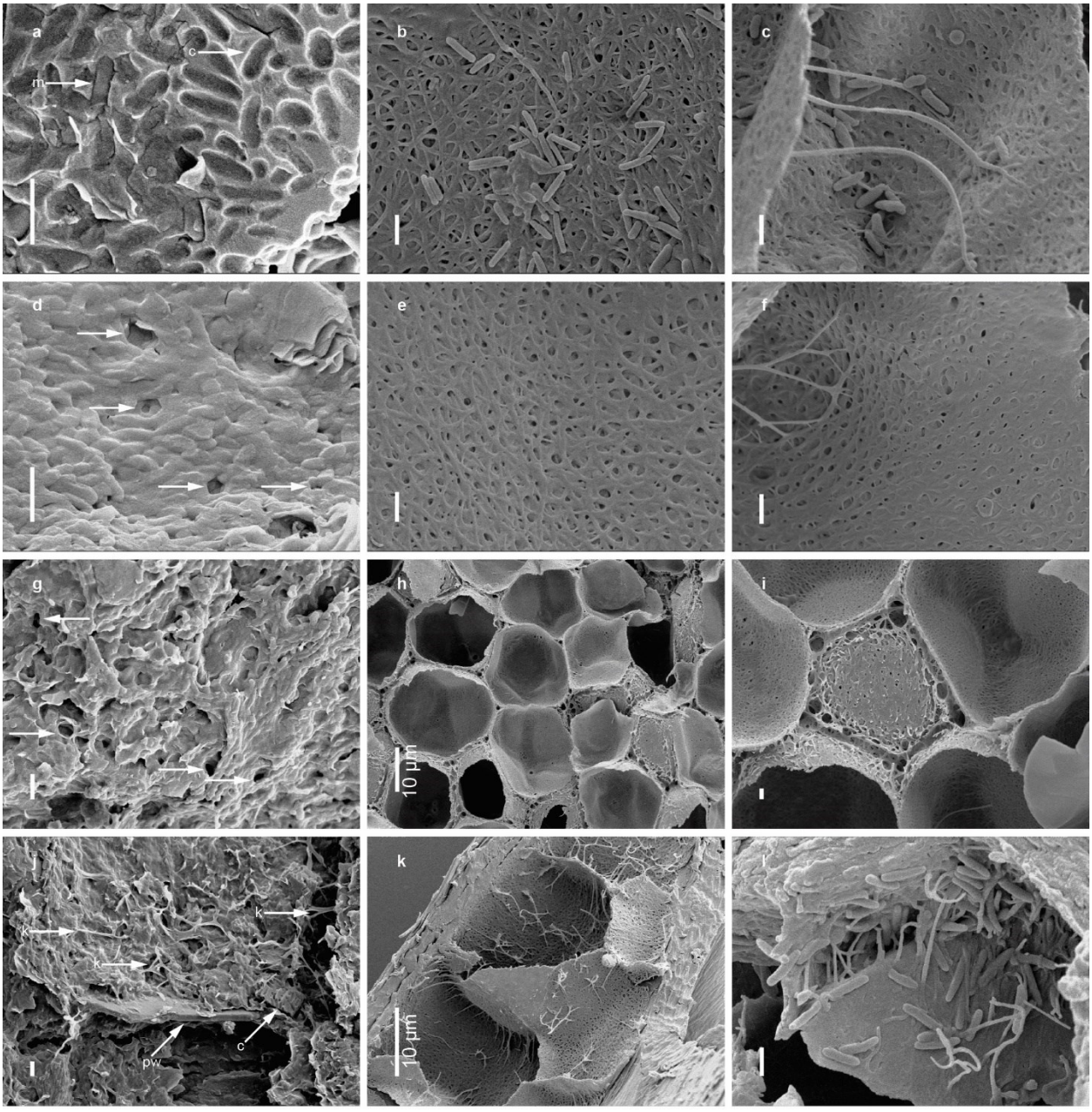

Figure 2-2. Electron micrographs of UALVP 52531 feathers (**a**, **d**, **g**, **j**) with modern feather comparisons. **a**, melanosomes (m) embedded within amorphous matrix; lost melanosomes are represented by casts (c). **b** (Great Northern Loon), **c** (Canada Goose), pith with melanosomes. **d**, potential pith pores (arrows) within presumed keratin sheets. **e** (Canada Goose), **f** (Red Tailed Hawk), pith pores are more abundant. **g**, inter-pith pores (arrows) with thin keratin bridges. **h** (Common Quail), cut pith showing inter-pith pores at cell intersections (please mark with

arrows). **i** (Common Quail), interior surface of pith wall, adjoining cell ripped away revealing inter-pith pores and keratin bridges. **j**, pith wall (pw) with presumed keratin fibres (k) adhering it to the ramus cortex. Sections of cortex keratin have fallen away revealing melanosome casts (c). **k** (Canada Goose) ramus with pith walls adhered to the cortex with keratin fibers. **l** (Black-billed Magpie), ramus pith wall adhered to the cortex by keratin fibres, melanosomes can be seen adhered to the surface of the pith wall and cortex. Scale bars, 1 μm, unless otherwise specified in image. See supplemental information for further information on specimens.

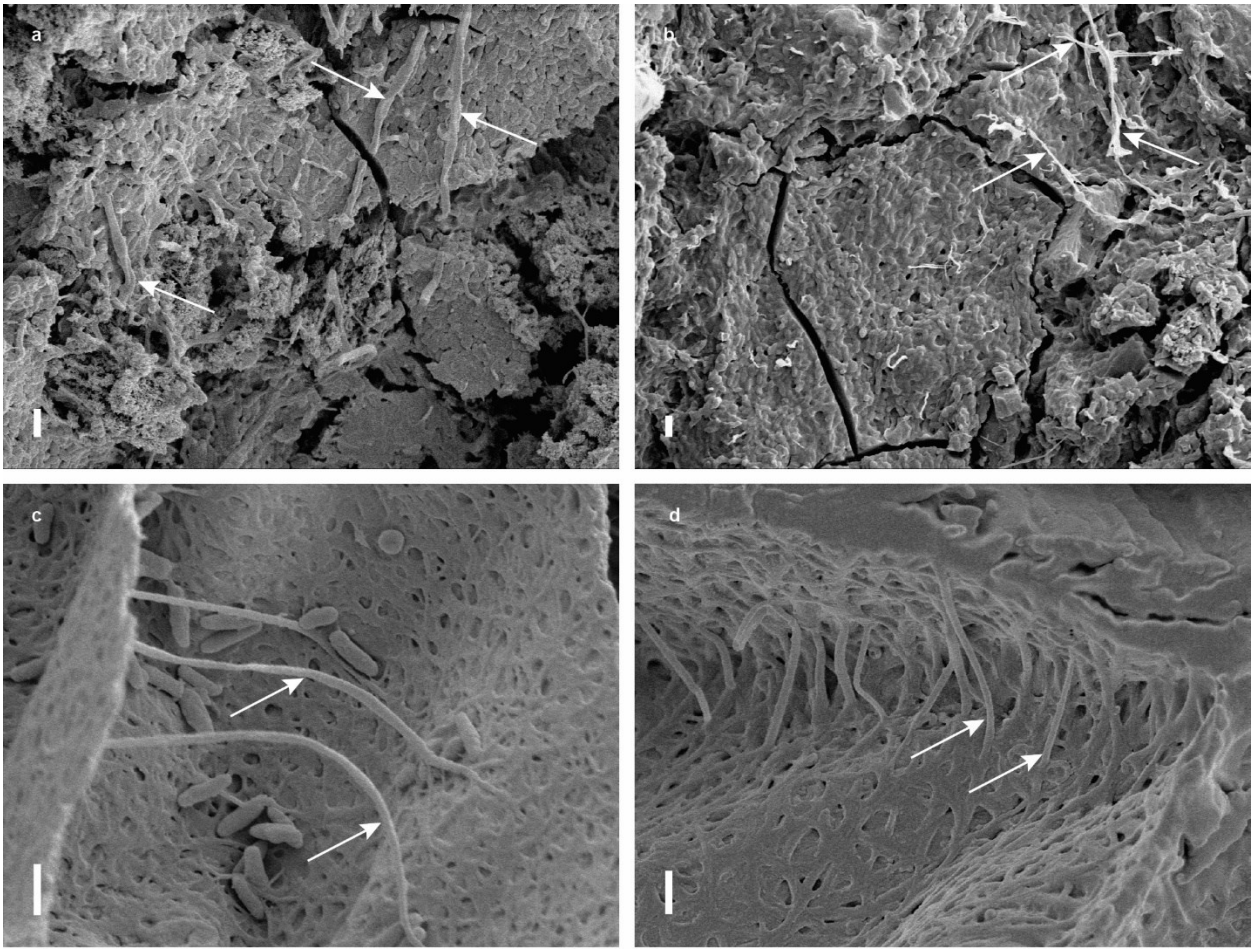

Figure 2-3. Non-branching Type 1 k-fibres. a, UALVP 52531 keratin fibers overlying melanosome cluster and cortex keratin. b, UALVP 52531 keratin fibres associated with pith wall. c, Canada Goose remex ramus. d, Great Northern Loon rectrix ramus pith with non-branching keratin. Scale bar 1 µm.

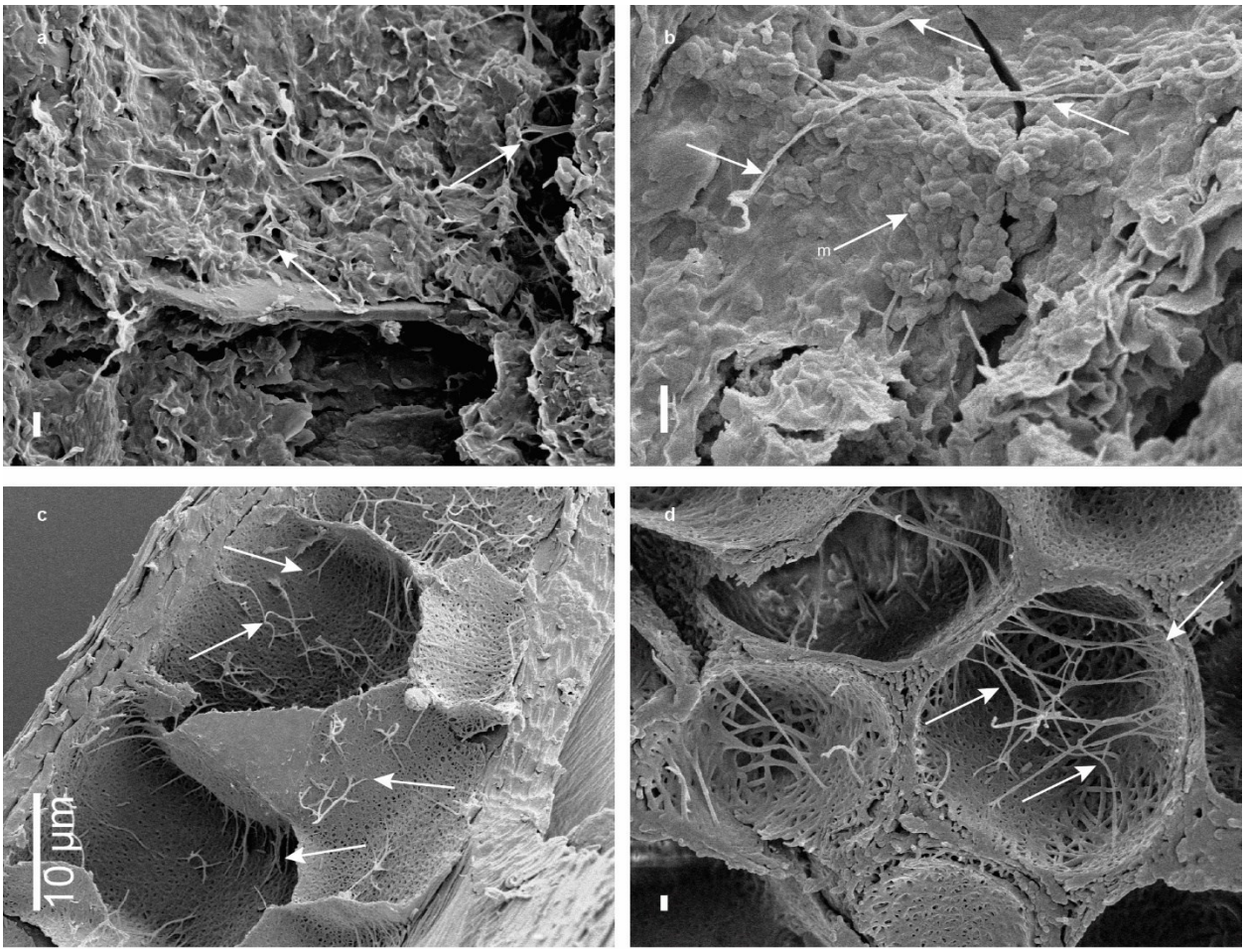

Figure 2-4. Bifurcating Type 2 k-fibres. a, UALVP 52531 ramus. b, UALVP 52531 melanosome cluster with associated keratin fibres. c, Canada Goose contour ramus. d, Great Northern Loon rectrix rachis. Scale bar 1 µm unless otherwise stated.

.

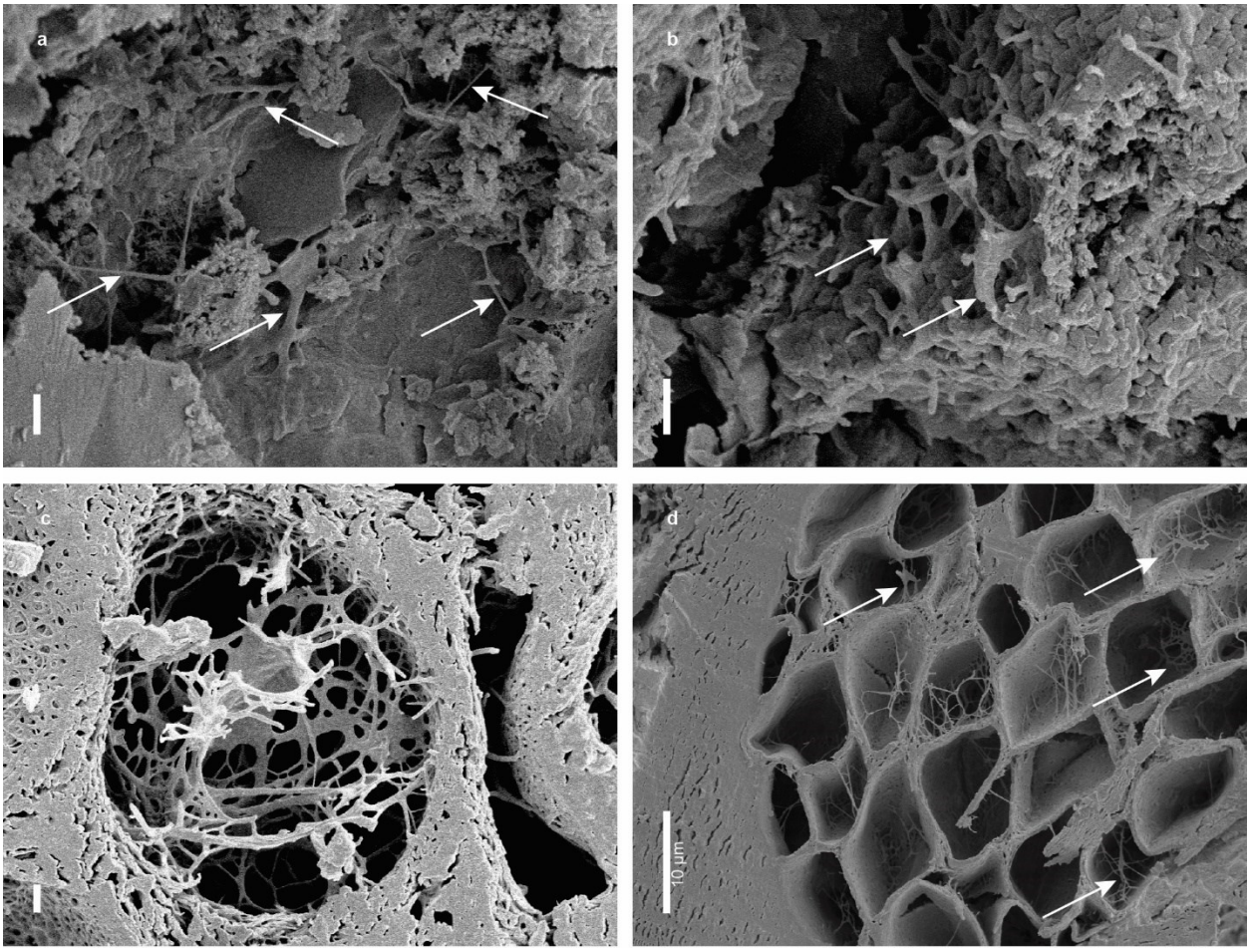

Figure 2-5. Web-like Type 3 k-fibres. a, UALVP 52531 rachis. b, UALVP 52531 rachis. c, Darwin's Rhea contour rachis. d, Red-tailed Hawk down rachis. Scale bar 1 µm unless otherwise stated.

Scale bar 1 µm unless otherwise stated.

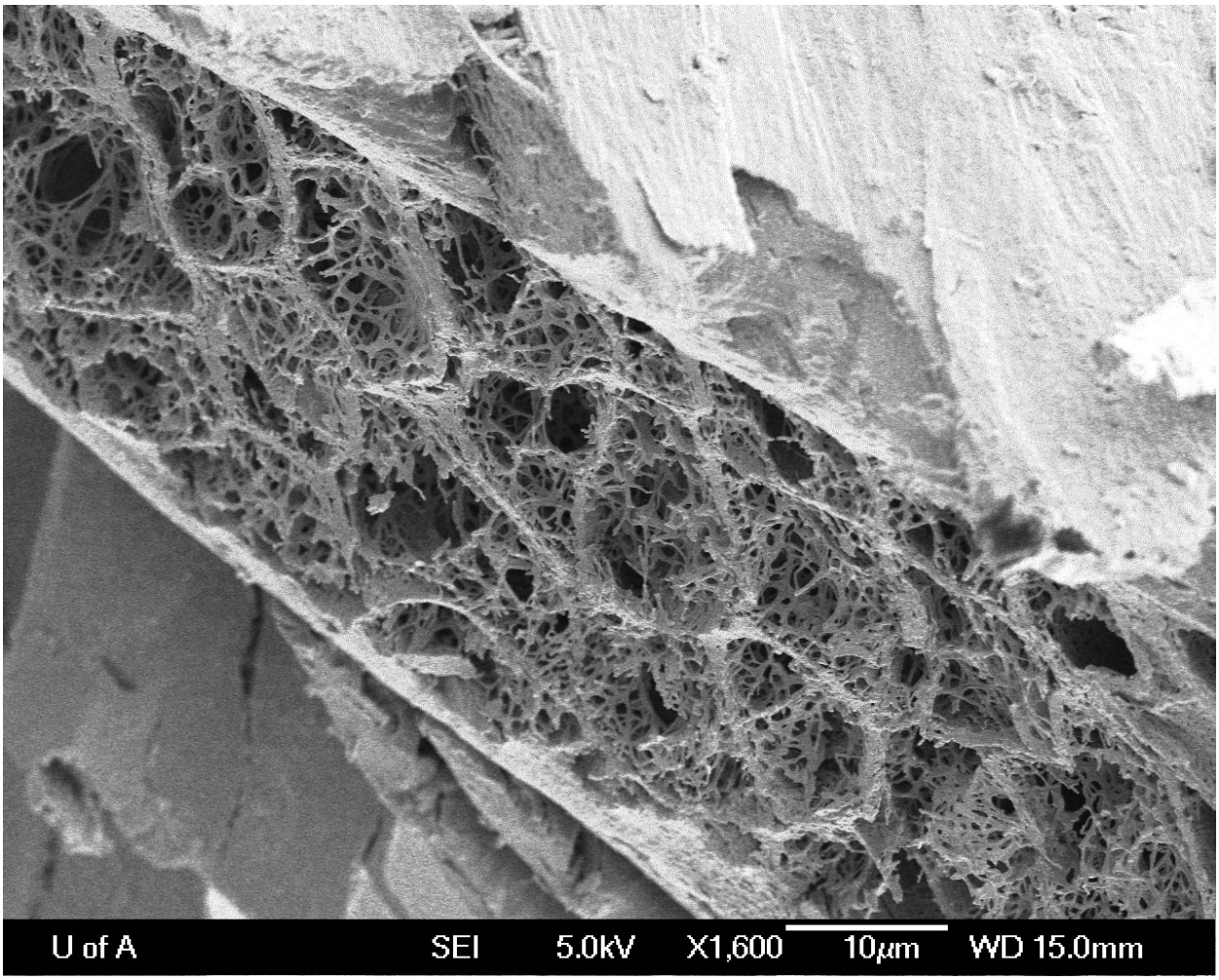

Figure 2-6. Pith structure within a ramus of Darwin's Rhea. Not the extremely loose weaving in the pith walls, and the type 3-k fibrils.

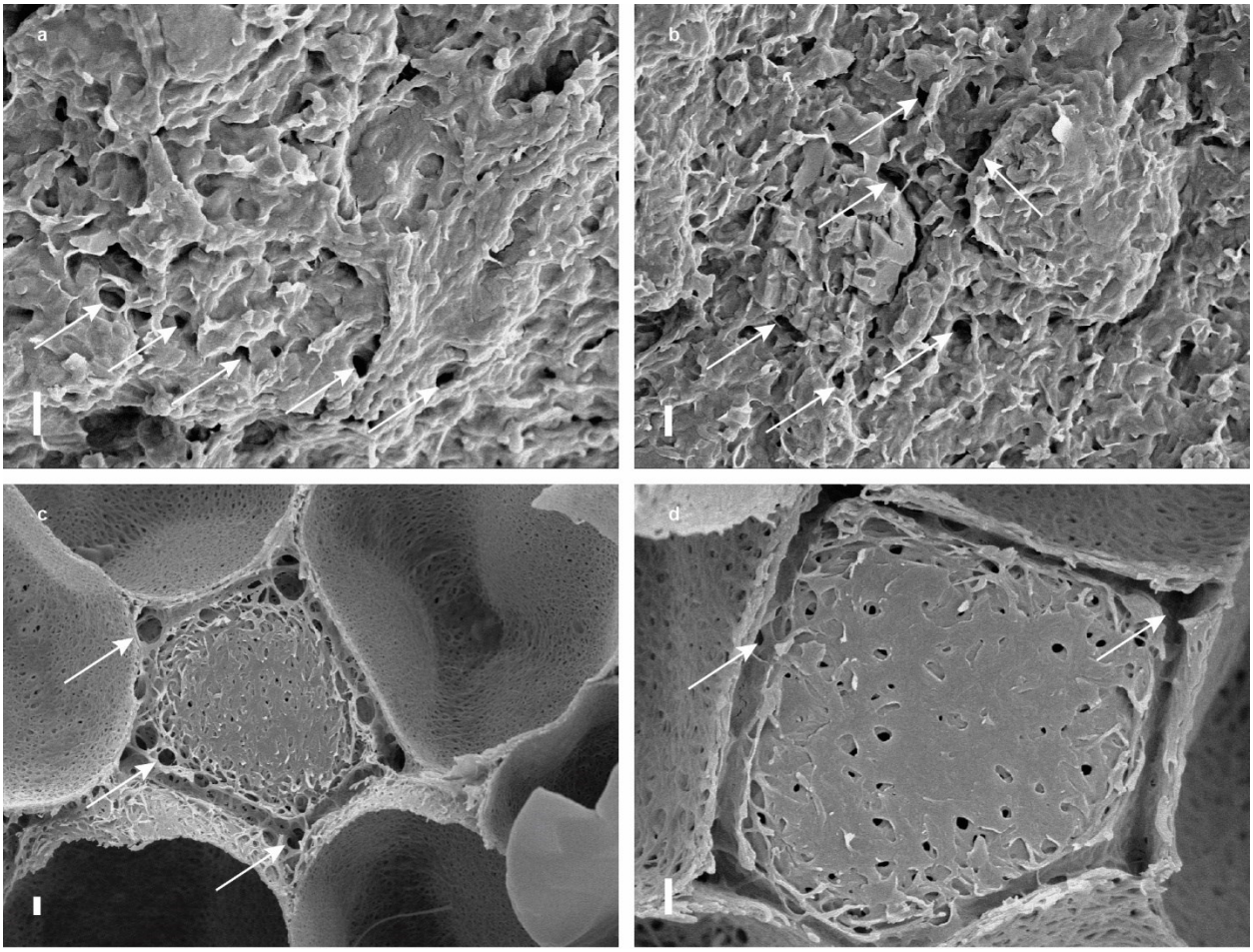

Figure 2-7. Inter-pith pores. a, UALVP 52531 rachis with a line of inter-pith pores. b, UALVP 52531 rachis showing several inter-pith pores. c, Common Quail rectrix rachis with inter-pith pores at junctions between three pith cells. d, Great Northern Loon contour rachis showing small inter-pith pores along junctions between multiple pith cells. Scale bar 1 µm.

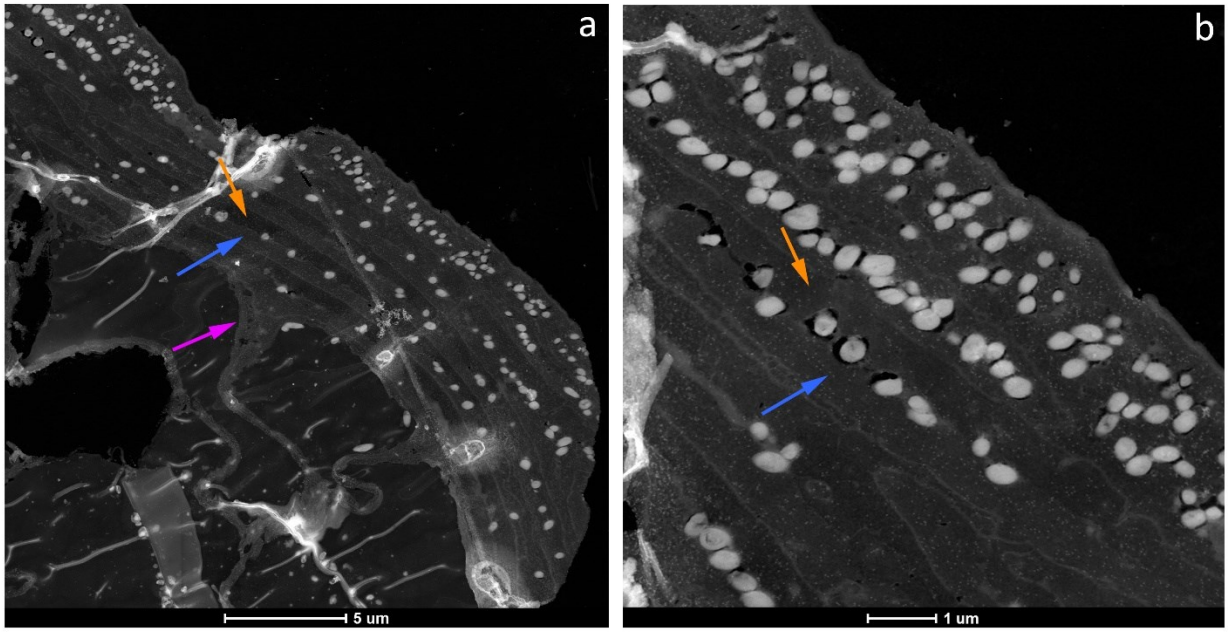

Figure 2-8. Reversed contrast TEM images of modern Goose feather. a) Overview of where a pith wall attaches to the cortex by means of a web like mass of keratin fibres (pink arrow). Base keratin layers (BKL, blue arrow) appear as lighter bands within the cortex due to their higher density, whereas capping keratin layers (CKL, gold arrow), are less dense and so appear slightly darker. b) Enlarged area of cortex showing a region where the BKL and CKL contain melanosomes between them (large white circular structures).

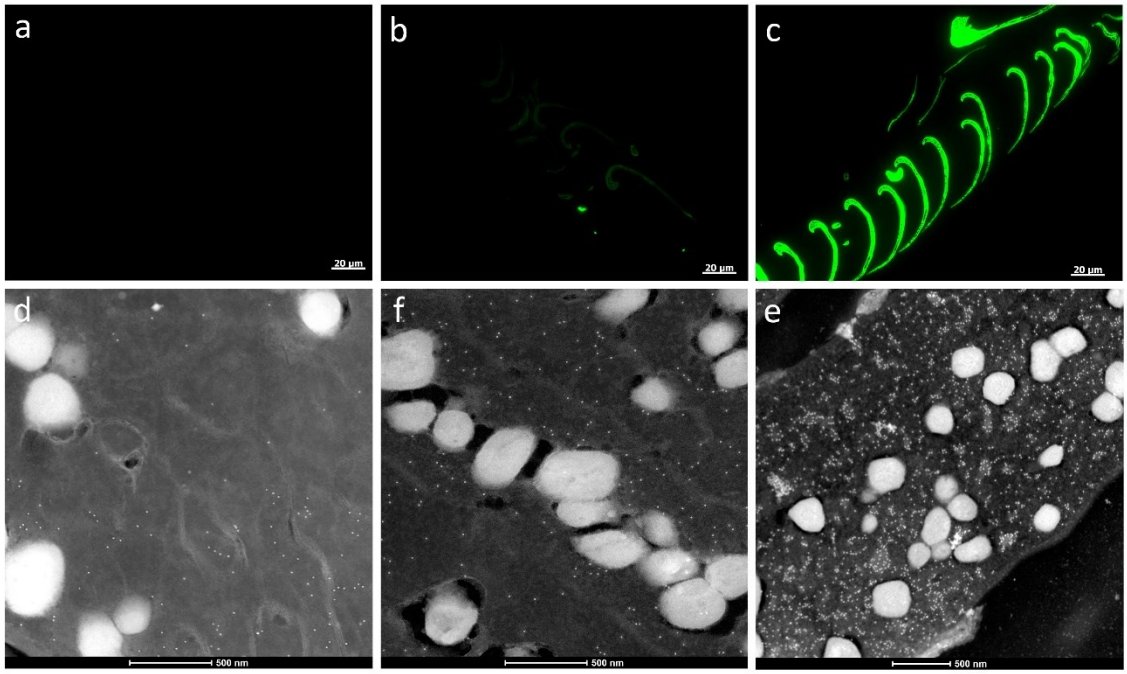

Figure 2-9. Immunohistochemistry of extant feathers. a-c, immunofluorescence. d-f, reverse contrast immunogold TEM. a) Reactivity to AE1/AE2 (α-keratin). b) Reactivity to β-keratin. c) Reactivity to whole feather. All immunofluorescence specimens imaged at 63x and exposed for 100 ms. d) binding to AE1/AE2 (α-keratin). e) binding to β-keratin. c) binding to whole feather. (small white dots are gold bead heads on marker antibodies, large white structures are melanosomes.

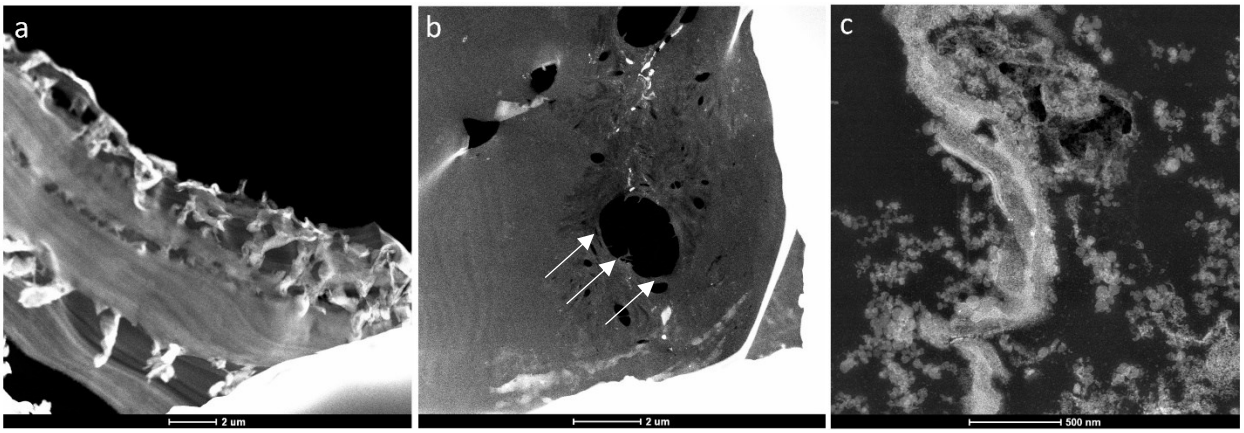

Figure 2-10. TEM of UALVP 52531 feather keratin structures. a) Cortex of rachis with visible keratin layering and voids between layers. b) portion of pith cell with individual keratin fibres. c) “S” shaped structures like those observed in extant feathers, hypothesised to be a form of keratin bundle.

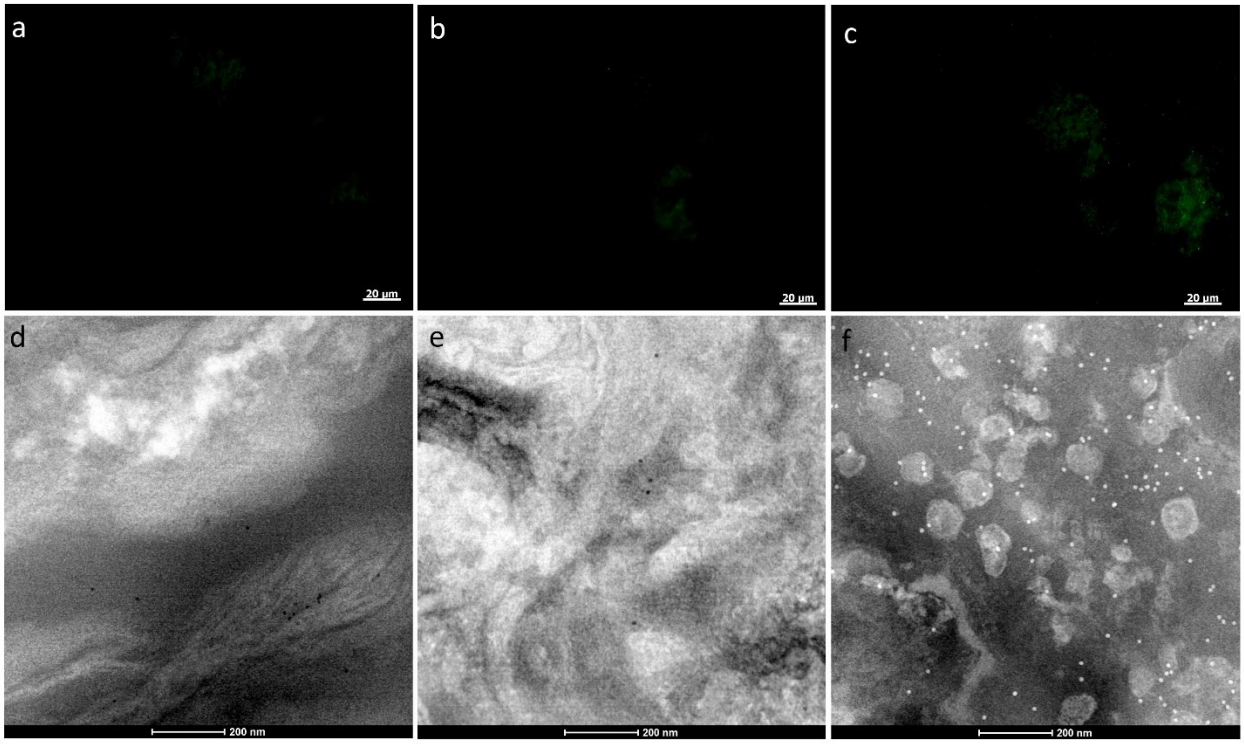

Figure 2-11. Immunohistochemistry of UALVP 52531 *Ornithomimus* feathers. a-c, immunofluorescence. d-f, reverse contrast immunogold TEM. a) Reactivity to AE1/AE2 (α-keratin). b) Reactivity to β-keratin. c) Reactivity to whole feather. All immunofluorescence specimens imaged at 63x and exposed for 100 ms. d) binding to AE1/AE2 (α-keratin). e) binding to β-keratin. c) binding to whole feather. (small black/white dots are gold bead heads on marker antibodies, large white structures are melanosomes).

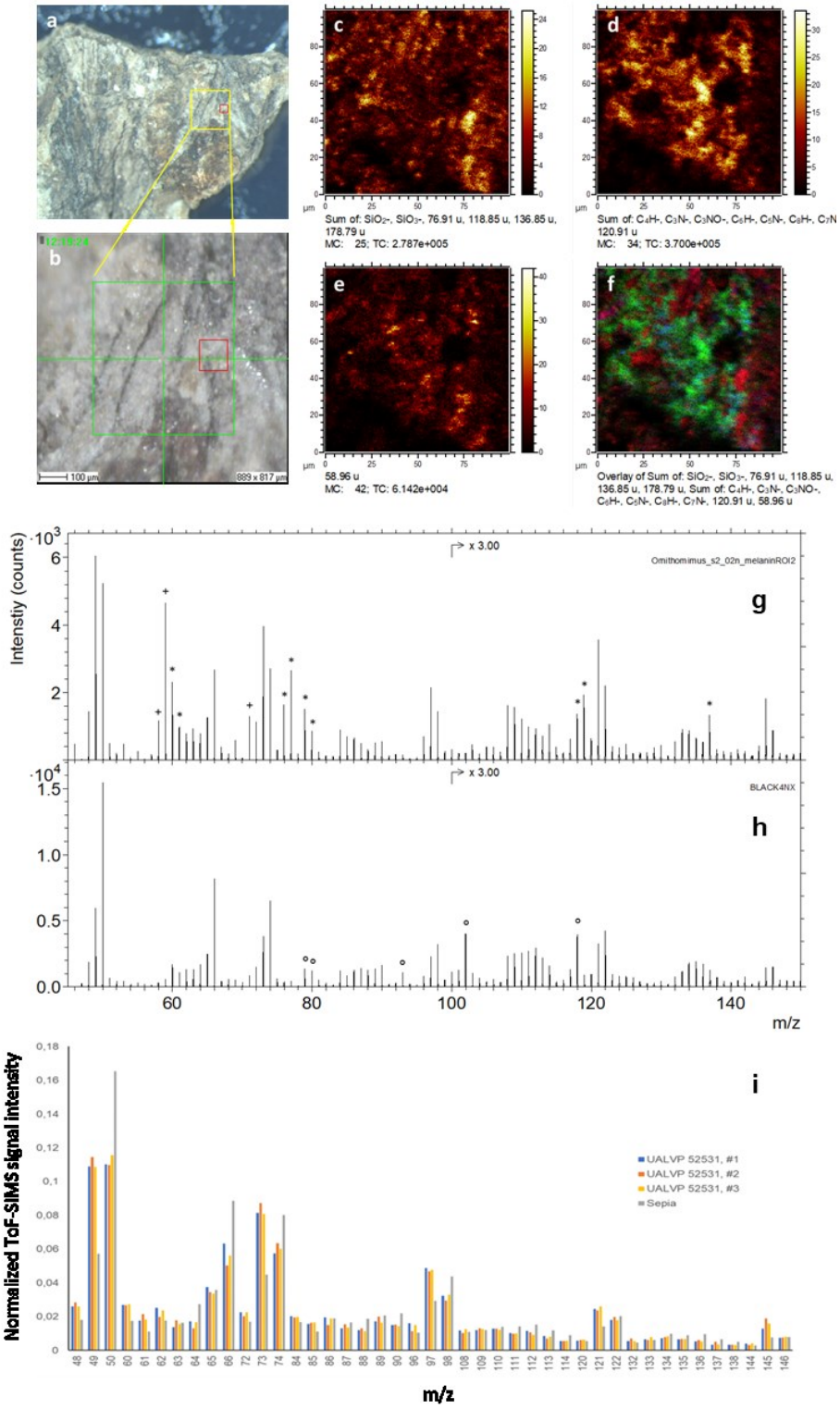

Figure 2-12. ToF-SIMS analysis of UALVP 52531. (a-b) Optical micrographs of sample surface with analysis area indicated by the red squares. (c-f) Negative ion images representing (c)

sediment, (d) eumelanin, (e) m/z 59 organic contaminant and (f) overlay image showing the signal from sediment in red, eumelanin in green and the m/z 59 contaminant in blue. Negative ion spectra of (g) UALVP 52531 and (h) eumelanin from *Sepia officinalis*. Labelled peaks represent sediment (*) and O-containing organic contaminant (+) in UALVP 52531 and contaminants in *Sepia officinalis* reference (°). (i) Signal intensities of characteristic eumelanin peaks in three spectra of UALVP 52531 and one spectra of eumelanin from *Sepia officinalis*.

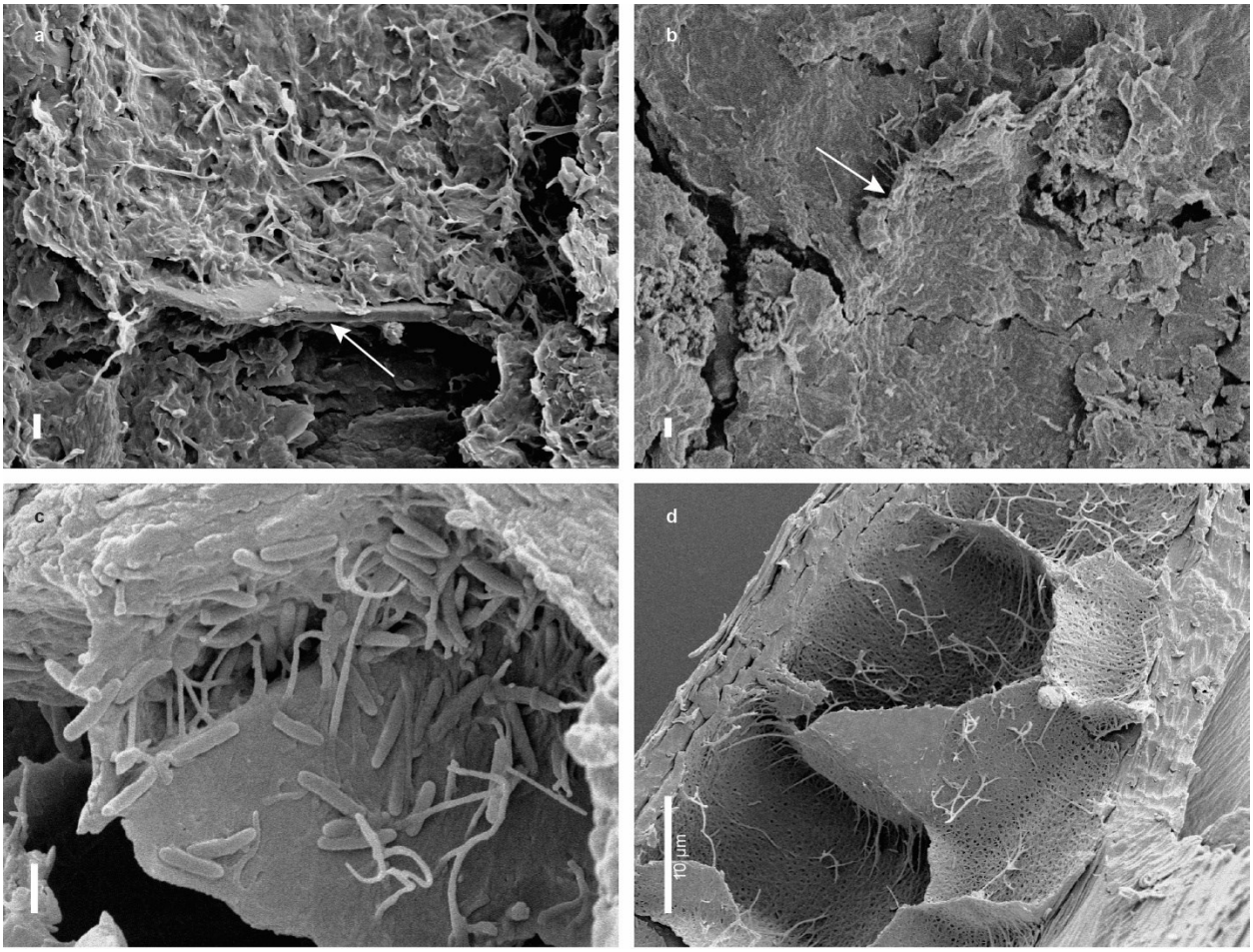

Figure 2-13. Pith walls. a, UALVP 52531 ramus with pith wall adhered to cortex. b, UALVP 52531 rachis with pith wall. c, Black-billed Magpie remex ramus with pith wall adhered to cortex. d, Canada Goose contour ramus showing orientation of multiple pith walls. Scale bar 1 µm unless otherwise stated.

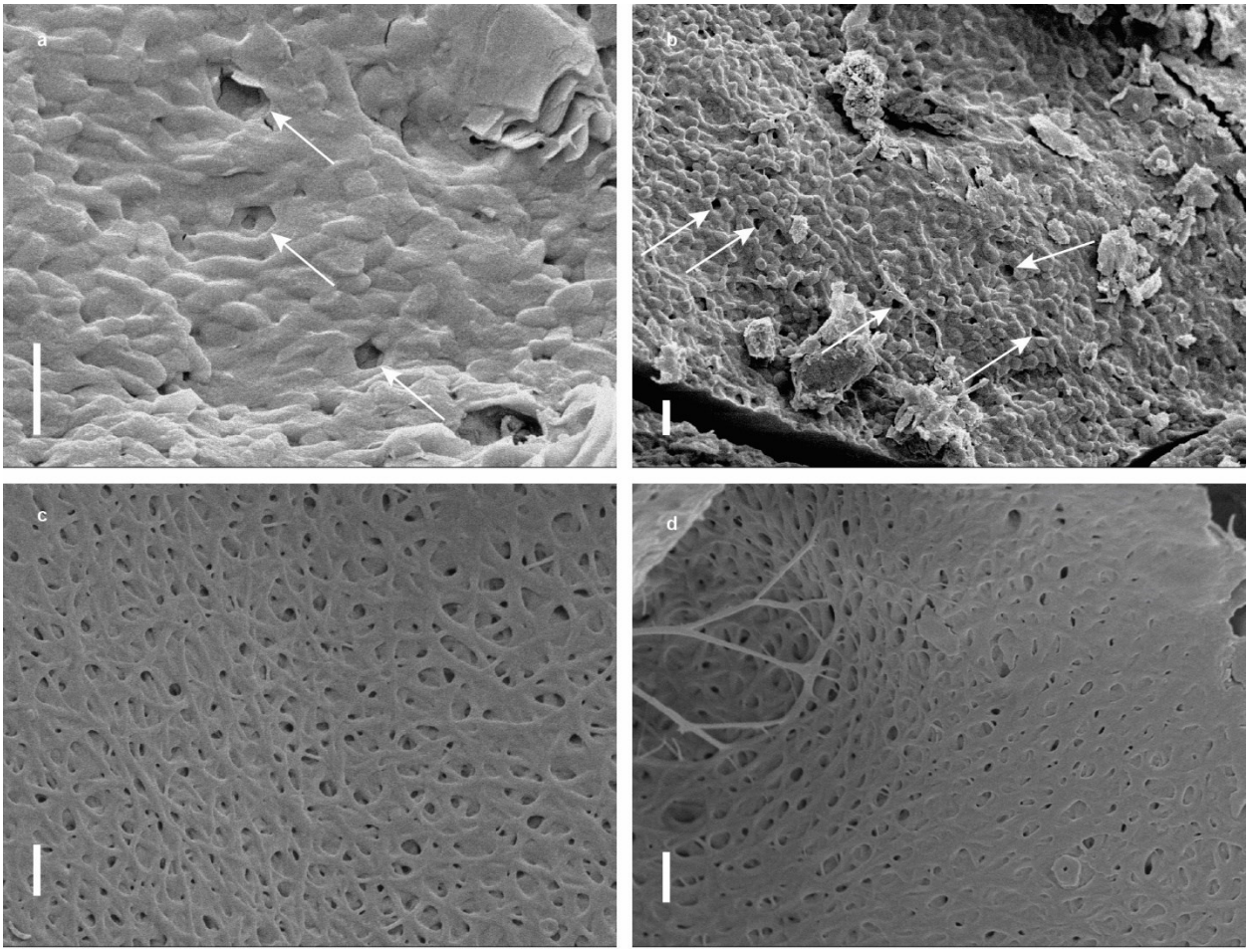

Figure 2-14. Pith pores. a, UALVP 52531 rachis. b, UALVP 52531 rachis. c, Canada Goose rectrix ramus. Scale bar 1 µm.

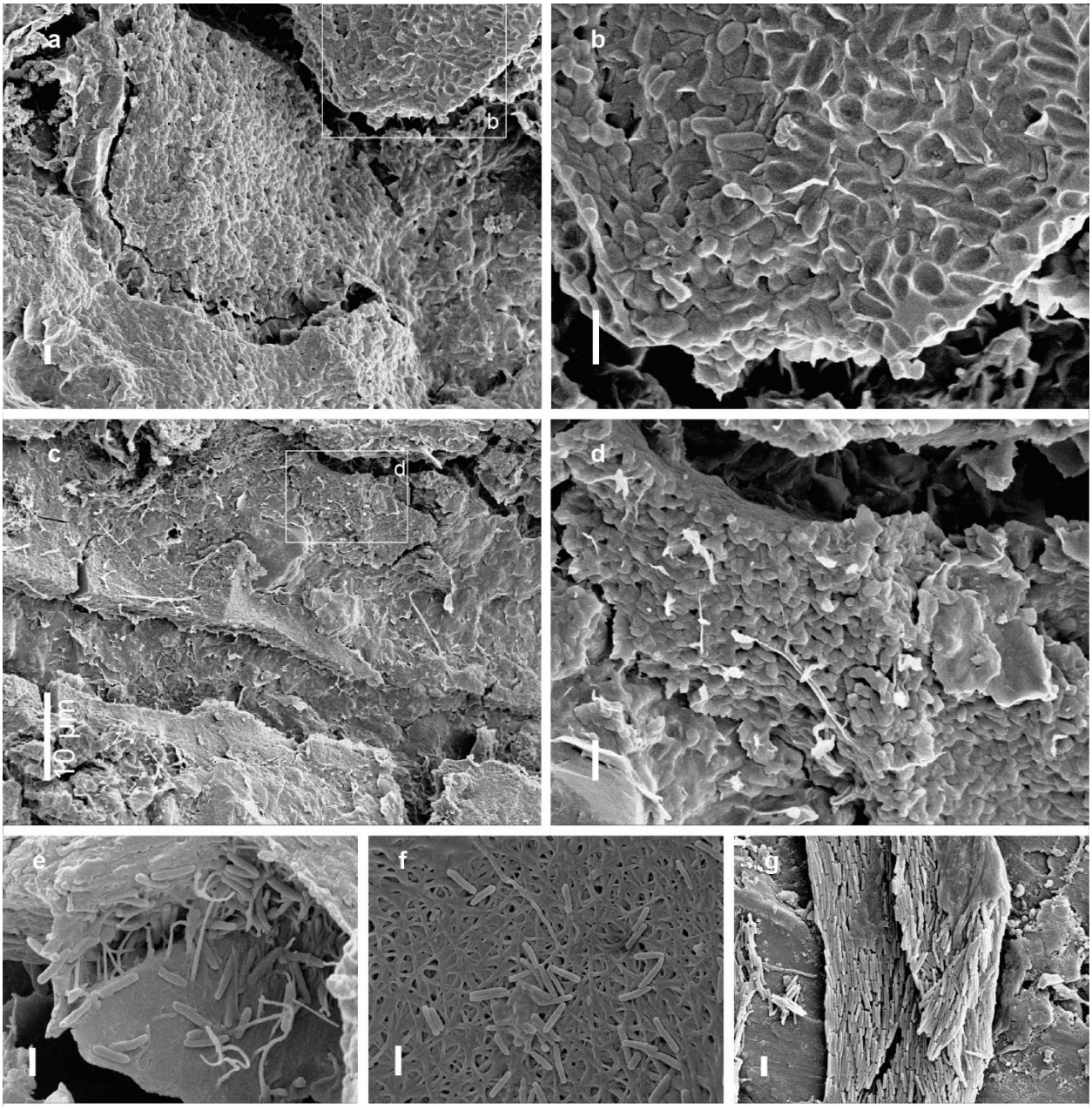

Figure 2-15. Comparisons of melanosome deposits within UALVP 52531 and modern birds. a, portion of *Ornithomimus* rachis where keratin has been broken away revealing melanosome layer in the cortex. b, enlarged portion outlined in (a), melanosomes seen embedded in within

cortex keratin, melanosome casts are seen they have been removed from the keratin. c, lateral edge of *Ornithomimus* rachis. d, enlarged portion outlined in (c), melanosome layer exposed after keratin was removed. e, Black-billed Magpie remex ramus with melanosomes deposited on pith wall. f, Great Northern Loon rectrix rachis with small cluster of melanosomes on pith wall. Peacock rectrix barbule showing the density of melanosomes embedded in keratin. Scale bar 1 µm unless otherwise stated.

Chapter 3: Preservation frequency of tissue-like structures in vertebrate remains from the Upper Campanian of Alberta: Dinosaur Park Formation.

3.1 INTRODUCTION

Methods in palaeontology changed little over the first 150 or so years since the first dinosaur fossils were described (Buckland 1824), with most of the research focussing on basic anatomical description of bones and the analysis of relationships. Description of anatomy and classification of different species are fundamental steps towards more complex, analytical studies, such as those concerning rates of evolution or speciation. Studies of extant taxa using genomic data have started to dominate phylogenetic research on modern clades (Jarvis et al. 2014). Although modern molecular data has been questioned in the past, recent work has improved the resolution of evolutionary rates and divergence dates (Morlon et al. 2011). Palaeontology, which was slow to adopt new methodologies until the last few decades, is now adopting more sophisticated methods of study from other scientific fields. Many of these developments have benefited from statistical analyses using computer programs such as "R" (Benson et al. 2014, Campione et al. 2014).

In 1999, a theropod dinosaur from Mongolia, *Shuvuuia*, was shown to have small white filamentous fragments preserved in the matrix surrounding the specimen. Resulting IHC trials indicated the fibres preserved around *Shuvuuia* were in fact fragments of unaltered feathers with protein still intact (Schweitzer et al. 1999). Following the discoveries with *Shuvuuia,* pliable tissues were reported from dissolved bone of a *Tyrannosaurus rex* (Schweitzer et al. 2005b). These tissues consisted of fibrous, flexible, collagen like structures, as well as anastomosing

vessel-like structures containing red, spherical objects with darker cores. It was proposed that these structures represented unaltered soft tissues – including collagen-I, blood vessels, and red blood cells – preserved within the bone matrix. Further investigation into the preservation of soft tissues in vertebrate fossil and sub-fossil elements from around the world (Schweitzer et al. 2007b) indicates these structures are not uncommon. Taxa with soft tissue structures published by Schweitzer et al. (2007b) included *Brachylophosaurus canadensis, Mammuthus, Megoeodon*, *Triceratops horridus,* an indeterminate Trichechidae sp*, Tyrannosaurus rex,* a dicynodont and two unidentified theropods (one from Madagascar and the other from the Santana Formation of Brazil). Although, in this previous study, not all specimens sampled contained preserved soft tissue, many specimens were discovered to possess some form of vessel-like structures, collagen, or osteocytes (Schweitzer et al. 2007b). Subsequent to the release of Schweitzer et al. (2007*b*), the analysis of unaltered preserved soft tissue was taken to the next level. Immunohistochemistry was again employed to investigate collagen-like bundles that were observed within the bone matrix of *Tyrannosaurus rex* (Schweitzer et al. 2007a). By using several anti-body treatments, it was shown that collagen-I was still present, although degraded, within the bone matrix. This was the first instance in which collagen-I was found to be present within bone matrix of a dinosaur, and the first in which it was found in bone older than 66 Mya. Unsurprisingly, the thought that protein fragments could survive through deep time was contentious. It was claimed that the structures would be more plausibly interpreted as biofilms formed by bacterial colonies during decomposition (Kaye et al. 2008). On the other hand, it has also been suggested that if original protein is in fact present, then bacterial biofilms must play a role in preserving it (Peterson et al. 2010). Following the identification and

confirmation of the presence of unaltered proteins in dinosaur bone using immunohistochemistry, samples of the collagen-I and -II were sequenced using mass spectrometry (Schweitzer et al. 2009a). This work was duplicated several years later using more precise measurements and sequencing technology, confirming that the results were accurate and replicable (Schroeter et al. 2017).

Research into the primary mechanism for preservation of unaltered tissues has investigated several potential factors. Originally, it was proposed that the higher porosity within a sandstone matrix would facilitate the drainage of water and decay enzymes away from remaining tissues within bone (Schweitzer et al. 2007a). Further research into chemical influences on preservation of unaltered proteins suggested that molecular cross-linking in collagen fibrils stabilizes the molecule (San Antonio et al. 2011). Most recently, investigations into the preservation of collagen and osteocytes recovered from *Lufengosaurus* (Early Jurassic, 190-197 Ma) proposed that hematite cementation may play a role in preventing the degradation of soft tissue within bone (Lee et al. 2017). The authors suggest that the iron used to form the hematite may come from erythrocytes (red blood cells). However, they also point out that it would require approximately 20,000 cells to form a single 10 µm hematite sphere.

Extraction of soft tissues from fossilised vertebrate bone has raised the potential for studies once thought to be impossible for taxa from deep time. Studies could potentially produce molecular phylogenies, evolutionary rate estimates, time estimates for divergence events, molecular evidence of cladogenesis and/or anagenesis, and measures of genetic diversity within populations to name a few. To facilitate these studies, however, bone

dissolution is essential as the primary and most effective procedure currently known for extracting preserved soft tissues from fossil bone.

Select bones were dissolved to extract tissue-like structures from a multitude of vertebrate taxa from the Dinosaur Park Formation, primarily within Dinosaur Provincial Park in southern Alberta (Fig. 3-1). The primary goal of this project was to obtain a better understanding of the required environmental and sedimentological conditions during burial of vertebrate remains to preserve possible soft tissue-like structures. Two potential preservational criteria were tested: 1) Sedimentological association (sandstone or mudstone) was considered, to determine if soft tissue-like structures are in fact limited to sandstones; and 2) Degree of articulation of a specimen (articulated/associated skeletons or isolated elements/microvertebrate sites) was considered, to test if the length of time exposed to environmental conditions prior to final burial decreases the likelihood of soft tissue-like structure preservation. Structures that were most commonly recovered and identified in this study are vessel-like (Fig. 3-2), EOM-like (Fig, 3-3), or osteocyte-like (Fig. 3-4). Because this study is not intended to determine if these structures are unaltered original tissues, structures are referred to as “tissue-like”, “vessel-like”, etc., although for simplicity the terms “vessel(s)”, “osteocyte(s)”, etc. are sometimes used.

3.2 MATERIALS AND METHODS

3.2.1 Specimen Selection

Specimens used within the study were selected based on three main criteria. First, specimens were chosen to ensure that as many different taxa as possible were represented in

the sample. This provides future opportunities to expand the work to encompass potential protein sequencing and thus molecular phylogenetic studies. Of the nineteen specimens sampled, there are fifteen dinosaurs, two crocodilians, one fish, and one turtle. All specimens were collected from the Dinosaur Park Formation to reduce stratigraphic variation that may influence preservation. Secondly, specimens were chosen on the basis of the depositional matrix composition – sandstone or mudstone – that they were found in. This was investigated to determine if preservation potential differs between depositional environments as proposed by Schweitzer at al. (2007a). Thirdly, specimens were chosen based on whether they were articulated or associated with more complete skeletons, or were isolated or recovered from bonebeds (including microvertebrate sites). This was done to determine whether the length of time a specimen was exposed to environmental conditions prior to burial influences soft tissue-like preservation. It is assumed that in most cases better articulated specimens were buried more rapidly than disarticulated and isolated bones. However, it is recognized that this approach is simplistic as processes and timing of disarticulation between the death of an animal and its final burial are highly variable. Nevertheless, degree of articulation was used as a rough proxy for rapidity of burial, to see if differences exist.

All samples were taken from specimens from the collections of the University of Alberta Laboratory for Vertebrate Palaeontology. Specimens from microsites were generally small enough to be placed directly into dissolution dishes without needing to be broken up. Samples from larger articulated or isolated specimens were typically fractured off by using a hammer and awl, or wire cutters. The work surface was clean, and fragments were usually taken from the insides of the specimens, rather than the exposed surfaces. This method was employed

instead of using any type of sawblade to reduce the number of potential contaminants introduced into the bone matrix by cutting pieces off with saws. All samples were collected while wearing nitrile gloves to prevent contamination with proteins from human skin. Once removed from the original specimen, samples were placed into clean plastic baggies during transport to further protect them from contamination.

3.3 RESULTS

Although all specimens had at least one type of soft tissue recovered post dissolution, the amount recovered varied dramatically. Several specimens produced such large quantities that some samples were removed from the EDTA for other analyses. Results herein are reported phylogenetically, followed by specimen numbers if multiple specimens of the same genus and species were sampled.

3.3.1 Anchiacipenser acanthaspis (Actinopterygii, UALVP 56596 from Q266, articulated, river sandstone, Fig. 3-1-"1")

UALVP 56596, the holotype of *Anchiacipenser acanthaspis* (Sato et al. 2018), had three samples taken from a dorsal osteoderm. In all three samples, small fragments of blood vessels (Fig. 3-2f) were recovered as well as an unidentified white mesh-like structure. In one of the three samples, a tightly bound fibrous mat was found. This mat originated from the bottom-most layer of the osteoderm and was oriented anteroposteriorly along the midline. Currently, the morphology of the mat most closely resembles that of dermal collagen, which is not unexpected because osteoderms derive from dermal tissues during ontogeny. Small clumps of EOM-like material were recovered.

3.3.2 Basilemys sp. (Testudines, UALVP 59613, disarticulated ungual from a microsite in mudstone Fig. 3-1-"2")

UALVP 59613, a *Basilemys* ungual, was broken into three portions. From each sample, large quantities of degraded vessels were recovered. Visually, they appeared to be crystalline in structure, suggesting that there had been some form of alteration to the original cellular matrix. Until further work can be done, the true nature of these organics cannot be positively determined. However, they are considered as tissue-like structures in this study. Small clusters of EOM-like material were visible, although rare.

3.3.3 Crocodylia indet. (Archosauria, UALVP 59615, isolated osteoderm within a mudstone microsite, Fig. 3-1-"3")

UALVP 59615, a single, unfragmented, small crocodylian osteoderm was placed into one dish well. This specimen produced a large number of vessel structures and EOM-like fibrous matrix. Although vessels are abundant, most appear to have undergone some form of alteration and now appear as crystalline-like structures. Some vessel structures, however, do appear to contain structures resembling endothelial nuclei (Fig. 3-2), suggesting there is the possibility of some residual organics remaining.

3.3.4 Leidyosuchus canadensis (Alligatoroidea, UALVP 59616, articulated skull, mudstone, Fig. 3-1-"4")

UALVP 59616, an articulated skull and mandibles of *Leidyosuchus*, had fragments from the left parasphenoid and left dentary removed because of fractures within the specimen. Vinac consolidant had been applied to the specimen when it was in the field, but was removed

by soaking samples in acetone for 10 minutes with agitation. Although few vessels were recovered, those that were (Fig. 3-2e), contained large numbers of hematite spheres. Large bundles of EOM-like fibres were also recovered (Fig. 3-3a), and several osteocyte-like structures were observed (Fig. 3-4d). Osteocyte-like structures are poorly preserved and have badly damaged 'filipodia'.

3.3.5 cf. *Euoplocephalus tutus* (Ankylosauridae, UALVP 56607, isolated partial skull found in a well cemented sandstone, Fig. 3-1-"5")

UALVP 56607, a partial *Euoplocephalus* skull from Q265, had a small fragment and a larger fragment (subsequently broken into two) of the posterior part of the skull sampled for dissolution. The initial small fragment was recovered from a piece that had been weathered off the main specimen in the field. Although vessels are common, most of these are heavily infilled with solid hematite or crystalline hematite spheres (Fig. 3-2d). In areas where the original pliable vessel tissues are visible, structures resembling endothelial nuclei can be discerned. Interestingly, regions of vessel structures are consistently capped on either end by large amounts of hematite. Although EOM-material was not uncommon, no osteocytes were observed.

3.3.6 Panoplosaurus mirus (Nodosauridae, UALVP 12, partial cranium with isolated osteoderms, no other skeletal elements, sandstone concretion with high iron, no locality data so not figured in Fig. 3-1)

UALVP 12 is a partial cranium of *Panoplosaurus* associated with osteoderms collected in 1920 by G. Sternberg. A fragment of dermal armour with original ironstone matrix still attached

was sampled. After nearly three months of dissolution in EDTA, virtually no possible soft anatomical material was recovered. A few small, and heavily stained EOM-like clumps were visible, and only a couple of osteocyte-like structures were observed (Fig. 3-4c). Similar to other osteocyte-like structures, these are poorly preserved with limited extensions of 'filipodia'.

3.3.7 Mercuriceratops gemini (Ceratopsidae, UALVP 54559, squamosal with associated cranial fragments (Ryan et al. 2014), sandstone, Fig. 3-1-"6")

UALVP 54559 had a fragment of associated cranial bone of *Mercuriceratops* divided into two smaller samples and a third small fragment of surface collected bone from the main specimen was used as the third sample. Two of the three fragments released high amounts of iron staining upon dissolution. These two samples also produced high numbers of flexible vessel and EOM-like fibres after dissolution. EOM-like matrix is abundant around vessels and throughout the bone. Interestingly no osteocyte-like structures were recovered. Nearly all vessels observed are three-dimensional anastomosing structures. Within the vessel walls, endothelial nuclei-like structures can be discerned, although large pyrite crystals are also present within the lumina of vessels. The third sample produced organic-like structures, although in significantly fewer amounts.

3.3.8 Chasmosaurus belli (Ceratopsidae, UALVP 52613, articulated skeleton of juvenile in sandstone Fig. 3-1-"7")

UALVP 52613, an articulated juvenile *Chasmosaurus belli* from Q255, had fragments of surface collected cranial bone sampled from a complete skull (Currie et al. 2016). Of all the specimens sampled, UALVP 52613 produced the highest number of vessels and collagen. During

dissolution of the specimens, three dimensional anastomosing vessels could be seen protruding from every surface. Vessels were surrounded by a fibrous matrix of EOM-like filaments after the dissolution of bone matrix. EOM-like fibres are more common and densely intertwined but can easily be pulled apart. Although vessels remain intact throughout all three fragments, they appear to have been altered significantly. Large amounts of small clear crystals resembling calcite and or silicates are found throughout most of the vessels. Fractured, orange organic-like structures are visible on the inner surfaces of the vessel walls. One osteocyte-like structure was observed (Fig. 3-4b), but was poorly preserved.

3.3.9 Chasmosaurus sp. (Ceratopsidae, UALVP 55926, partially articulated skeleton from Q263, mud filled channel mudstone, Fig. 3-1-"8")

Three fragments of the tibia of a *Chasmosaurus* (UALVP 55926) were removed as samples. Each sample contained significant numbers of vessels and EOM-like fibrous filaments. The vessels are well-preserved and appear to frequently contain endothelial nuclei-like structures. Most vessels appear slightly pitted with depressions (Fig. 3-2c), possibly due to damage from EDTA. Vessels are three-dimensional anastomosing structures, and several have EOM-like matrix surrounding them. Minerals such as hematite and calcite are observed throughout most vessels. Because of the quantity of vessel-like structures recovered, one bone sample was removed from the EDTA and scanned at 2.3 µm per pixel, allowing observation of vessels within the Haversian canals of the bone. Nearly all Haversian canal spaces contained visible traces of vessels, including those spaces that opened to the exterior of the bone surface.

3.3.10 Centrosaurus apertus (Ceratopsidae, UALVP 55794, isolated eroded skull in sandstone, and because there is no locality data, the specimen is not included in Fig. 3-1)

Samples were removed from a fragment of cranial bone (UALVP 55794) recovered as an eroded portion of a *Centrosaurus* skull. Although only three fragments of vessels were recovered from one sample and no osteocyte-like structures were observed, several loosely woven EOM-like fragments were observed in this specimen.

3.3.11 Styracosaurus albertensis (Ceratopsidae, UALVP 52612, partially articulated skeleton from Q256 from very fine sand, Fig. 3-1-"9")

Samples were removed from a fragment of unidentified cranial bone found eroding out along with the skull of a *Styracosaurus* (UALVP 52612). Few tissue structures were recovered from any of the three samples. Only a few small fragments of vessels were recovered, and only small portions of collagen-like fibres were observed. No osteocyte-structures were observed.

3.3.12 Styracosaurus albertensis (Ceratopsidae, UALVP 55900, articulated skeleton from a channel lag sandstone in Q262, Fig. 3-1-"10")

Two skeletal elements from UALVP 55900 (*Styracosaurus*) were sampled. Three samples were removed from the left scapula and another three from the left humerus. Interestingly few vessels were recovered from the scapula. However, all three samples from the humerus produced high numbers of vessels (Fig. 3-2a) and EOM-like structures. Vessels are fully three-dimensional structures connecting through multiple levels of the cortex. Regardless of the number of these structures, no osteocyte-like material was observed. Small, red, spherical objects are present within a few vessels, although many precipitated minerals are also present.

3.3.13 Hadrosauridae indet. (UALVP 59614, isolated caudal vertebra centrum, mudstone, Fig. 3-1-“11”)

UALVP 59614 represents a young hadrosaur that had an unfused neural arch. Three samples, two from the lower half (mainly internal spongy bone) and one from the top half (mainly cortical bone from the attachment point for neural arch), were removed. Of the three samples, the only one to produce structures of interest was one that came from the attachment point of the neural arch. This one sample produced a high number of vessels and EOM-like material. Vessels are highly flexible with few minerals within the lumen. Osteocyte-like structures were not observed.

3.3.14 Prosaurolophus maximus (UALVP 55880, articulated specimen from a fluvial sandstone in Q264, Fig. 3-1-”12”)

Six samples in total were removed from UALVP 55880 – three from the right radius and the rest from an ossified tendon. The tendon was sampled to determine if tendons produce anything that looks like it might be soft tissue-like structures, because if they do then there will be less need for sampling of more diagnostic skeletal elements. After dissolution of the tendon, small fragments of vessel were observed (Fig. 3-2b), as well as EOM-like bundles; however, no osteocytes were recovered. The amount of material of interest in the tendon fragments was not significant. Unlike the tendons, fragments from the radius produced significant amounts of soft tissue-like material. Vessels are three dimensionally anastomosing flexible structures like those seen in other specimens. EOM-like material is fibrous and is observed in some cases

surrounding vessel-like structures. Several osteocytes were recovered from the radius, although these were poorly preserved with little of the 'filipodia' remaining.

3.3.15 Gorgosaurus libratus (UALVP 10, closely associated skeleton found in sandstone with highly cemented nodules, Fig. 3-1-"13")

UALVP 10 was collected from Q048 by G. Sternberg in 1921, and as a result, it was not expected to produce much soft tissue-like structures, as it may be expected that degradation of tissue occurs upon exposure to atmosphere. Samples were removed from the pubic shaft where the bone was still encased within the sandstone. Of the three samples, all produced EOM-like structures and two produced vessels. Several poorly preserved osteocyte-like structures were also recovered. One vessel recovered appears to possess five small spherical red objects that morphologically appear similar to modern and other preserved red blood cells.

3.3.16 Gorgosaurus libratus (UALVP 49500, partially articulated, mud with traces of sand and concretions, Fig. 3-1-"14")

Three samples were taken from a larger unidentified long bone fragment collected in the quarry (Q253) from which UALVP 49500, a sub-adult *Gorgosaurus*, was excavated. All three samples had significant quantities of anastomosing vessels surrounded by EOM-like matrix. Most vessels contain large amounts of hematite spheres. However, several well-preserved vessels contain spherical red structures that resemble red blood cells (Fig. 3-5). No osteocyte-like structures were recovered.

3.3.17 Ornithomimus edmontonicus (UALVP 52531, articulated skeleton from Q254, sample removed from mud with traces of sand, Fig. 3-1-"15")

Samples were removed from the right femur of *Ornithomimus edmontonicus*, UALVP 52531. This specimen is important because of the presence of preserved feathers across nearly the entire body (van der Reest et al., 2015). UALVP 52531 was chosen to be sampled it was believed that because feathers were preserved it would have the best chance of preserving tissue-like structures. All three samples produced vessels and EOM-like structures. However, osteocyte-like structures were not recovered.

3.3.18 Saurornitholestes langstoni (UALVP 55700, articulated skeleton from Q260, iron rich sandstone, Fig. 3-1-"16")

Samples were taken from small portions of a caudal vertebrae of the *Saurornitholestes*, UALVP 55700. Despite well preserved keratin sheaths on manual and pedal claws, very few soft tissue-like structures were recovered. Three small fragments of vessels and small portions of EOM-like structures were identified. Interestingly, although there were few vessels and EOM-like structures present, osteocyte-like material was recovered (Fig. 3-4a). Because of keratinous sheaths on claws, the potential for soft tissue-like structures in the bone is still high, and a long bone should be sampled for further vessel structures and collagen-like material.

3.3.19 Latenivenatrix mcmasterae (UALVP 55804, isolated articulated pelvis, channel sandstone, Fig. 3-1-"17")

Samples were taken from fragments of the left ilium of *Latenivenatrix* (UALVP 55804) (van der Reest and Currie, 2017). Each sample produced small numbers of vessels but higher amounts of EOM-like fibrous material (Fig. 3-3b). One vessel in particular is preserved exceptionally well (Fig. 3-6). The fragment possesses several endothelial nuclei-like structures

bulging into the lumen. Most of these possess what appears to be a secondary internal membrane-like structure resembling the morphology of a nucleus (Fig. 3-6b,d). The surface texture of each nuclear membrane-like structure is textured with small bumps. Also, within a branching portion of the vessel a single red blood cell-like object is present. Within this structure, a central darker spherical region, resembling a nucleus, is observed. A second organic-like structure is also observed within the lumen of the vessel. This structure is orange in colour and appears to be bilobed (Fig. 3-6d). Surrounding this structure are several granules. All the granules and the main lobed structures are contained within thin membrane like structures. If this structure is organic in origin, its morphology most closely resembles that of a basophil, which would be expected to possess a two lobed internal structure with many small granules-like structures on the nuclear membrane (Vellis 2011). This vessel is the best-preserved structure with the highest definition of all samples within the study. This quality of preservation suggests that, if this is original organic material, proteins may persist.

3.4 DISCUSSION

The number of specimens examined that produced soft tissue-like structures in this study was significantly higher than anticipated. All samples produced soft tissue-like structures. A previous study performed at Imperial College London (London, U.K), using specimens from the Natural History Museum (London, UK) collected by Cutler and Sternberg also recovered similar organic-like structures (Bertazzo et al. 2015). Their study of material from the Dinosaur Park Formation produced similar results to this study, although they did not report the rock type in which each specimen was preserved. In the current study, only UALVP 12, *Panoplosaurus* (Nodosauridae) did not produce any sign of vessel-like structures. There are two

possible reasons why this specimen did not preserve soft tissue-like structures. First, UALVP 12 was one of the first specimens ever collected for the University of Alberta vertebrate paleontology collections (1920). If length of time exposed to modern atmospheric conditions affects preserved soft tissues, nearly a century of exposure could have destroyed any recognizable tissue structures. However, one would then expect to see similar effects in UALVP 10 (*Gorgosaurus*), which was collected only a year later. Secondly, the major difference between UALVP 12 and other specimens examined is the significant amount of ironstone that encased the specimen. The sample was taken from an osteoderm enclosed in a hard, dense layer of concreted ironstone several millimetres thick. It is possible that as the ironstone precipitated out in the vascular and Haversian canals of the cortical bone, tissue-structures were destroyed. Although nearly all other specimens that possessed vessel structures contained some form of precipitated crystalline mineral, the most common precipitates are hematite spheres. This has been suggested in previous studies as having originated from hemoglobin within red blood cells (McGowan, 1983; Lee et al., 2017). The amount of iron in concretions around the bone of UALVP 12, however, likely originates from another source. Further investigation into the fractionation of stable isotopes may reveal the origin of this iron. The second most common crystalline mineral precipitate found in vessel lumina is calcite. It is hypothesised that this mineral is deposited within the lumina as $CaCO_3$ as saturated ground water enters the bone through nutrient canals, allowing dissolved minerals to begin to nucleate on the lumen wall and continue forming a centre for growth. The third most common mineral observed within vessels is pyrite. Pyrite is identified by its cubic crystalline structure that is

impermeable to light. Only three specimens were observed to possess pyrite, two of which had hard sandstone nodules associated with them.

Although the original hypothesis proposed by Schweitzer et al. (2007a) that sedimentology affects the preservation of tissue structures in general does not extend to the Dinosaur Park Formation of southern Alberta because tissue structures were recovered from both mudstone and sandstone (Table 3-1), it does appear to be related to osteocyte-like structures from articulated/associated specimens from sandstone deposits (Table 3-2). All specimens that were sampled from mudstone produced some form of tissue-like structures, suggesting that high porosity in the surrounding sediment is not required to facilitate the drainage of the enzymes responsible for decay. The hypothesis proposing that degree of articulation may play a role in tissue-like structure preservation was tested by sampling specimens that were either articulated/associated or isolated in origin. For tissues in general, there was no difference in either category that could be determined for preservation of tissue. Osteocyte-like tissues specifically, however, do appear to be more readily preserved in specimens that were recovered as articulated/associated skeletons. It must be noted, however, that all osteocyte-like structures that were recovered were poorly preserved with none possessing complete, or even partial, 'filipodia'. Osteocyte-like structures are identified in these specimens by size, morphology, and the presence of numerous 'filipodia' bases that are visible as raised protrusions from the body of the structure. Most tissue-like material recovered was brown-orange in colour, which has been suggested to be the result of diagenetic alteration of proteins into N-heterocyclic polymers (Wiemann et al. 2018). This suggests that the structures

that were recovered in this study are potentially altered original organics, although further chemical analyses are required for confirmation.

3.5 CONCLUSIONS

This study suggests that neither sediment type nor degree of articulation have any influence on the preservation of tissue-like structures in vertebrate remains from the Dinosaur Park Formation. Nevertheless, the preservation of osteocyte-like structures appears to be correlated with articulated/associated skeletons from sandstone deposits. These findings support, for osteocytes but not any other tissue-like structures, the hypothesis proposed by Schweitzer et al. (2007a) that depositional and/or taphonomic differences between geological formations play a role in tissue preservation. This is further supported by the association of osteocytes with articulated specimens. The underlying cause behind the lower preservational rates of osteocyte-like structures is currently unknown. However, the smaller filipodia found to have been destroyed on virtually all those observed suggests that if these are indeed original cells, the phospholipid bilayer has been compromised and thus the cells are destroyed. Endothelial cells and extracellular organic matrix that contain collagen-I and elastin may be more resilient and thus survive longer in the geological record.

A possible explanation for the high amount of preserved tissue-like structures could be the precipitated minerals within vascular and Haversian canals. Once canals are sealed and chemical reactions are neutralized, vessel structures remain stable and persist until geological and taphonomic conditions become unfavourable and the tissues are destroyed. These

conditions may include the increase in subterranean temperatures, pressures, radioactivity, or exposure to current atmospheric conditions.

TABLES

Table 3-1. List of samples derived from specimens and types of soft-tissue preservations noted for each. Sediment: M, Mudstone; S, Sandstone. Association: AR, Articulated skeleton; AS, Associated skeleton; I, Isolated bones; M, Micro vertebrate site. Paired grey rows indicate specimens that originated from the same UALVP specimen. Abundance of tissue-like structures, X, rare; XX, common; XXX, abundant. Precise numbers are exact numbers found in 40 µL of dissolution fluid.

Taxon	Element	Specimen number	Vessels	EOM	Osteocytes	Sediment	Association
Actinopterygii							
Anchiacipenser	osteoderm	56592	X	XX		S	AR
Testudines							
Basilemys sp.	ungual	59613	XXX	XX		M	M
Archosauria							
Crocodylia indet.	osteoderm	59615	XXX	XXX		M	M
Leidyosuchus	parasphenoid, dentary	59616	XXX	XX	2	M	AS
Ankylosauridae							
cf. Euoplocephalus	cranium	56607	XXX	X		S	I
Nodosauridae							
Panoplosaurus	osteoderm	12		X	2	S	I
Ceratopsidae							
Mercuriceratops	squamosal	54559	XXX	XX		S	AS
Chasmosaurus	cranium	52613	XXX	XX	1	S	AR
cf. Chasmosaurus	tibia	55926	XXX	XXX		M	AR
Centrosaurus	cranium	55794	XX	XX		S	I
Styracosaurus	cranium	52612	XX	XX		S	AR
Styracosaurus	humerus	55900	XXX		1	S	AR
	scapula	55900	XX		3	S	AR
Hadrosauridae							
Hadrosauridae indet.	caudal centrum	59614	XX	XX		M	I
Prosaurolophus	tendon	55880	X	X		S	AR
	radius	55880	XXX	XX	1	S	AR
Tyrannosauridae							
Gorgosaurus	pubis	10	X	X	1	S	AS
Gorgosaurus	femur	49500	XX	XX		M	AS
Ornithomimidae							
Ornithomimus	femur, pedal phalanx	52531	XX	XX		M	AR
Dromaeosauridae							
Saurornitholestes	caudal centrum	55700	X	X	1	S	AR
Troodontidae							
Latenivenatrix	ilium	55804	XX	XX		S	I

Table 3-2. Relationship between sediment type and degree of articulation for preservation rates of osteocyte-like structures.

		Sediment type	
		Sandstone	Mudstone
Degree of articulation	Articulated	5	1
	Isolated	1	0

FIGURES

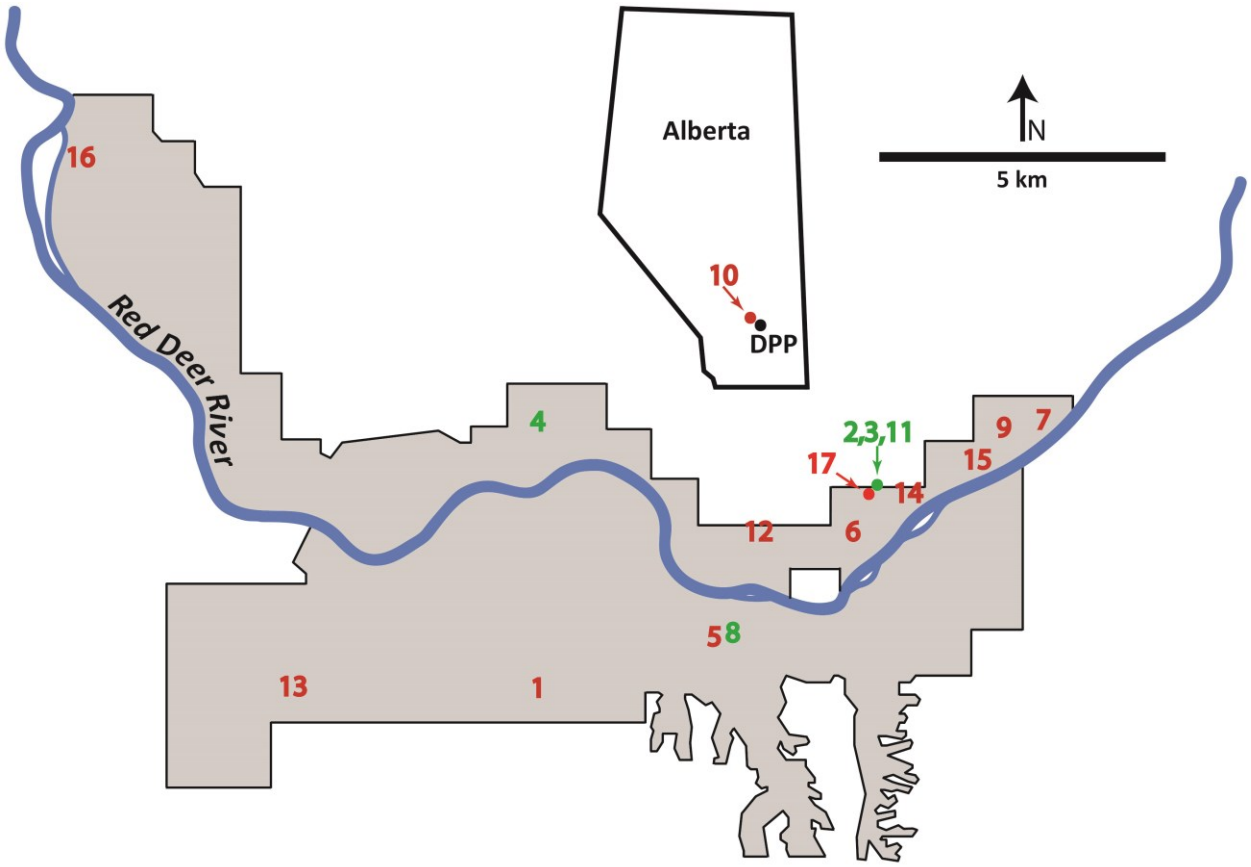

Figure 3-1. Map of Alberta and Dinosaur Provincial Park indicating where specimens were recovered. See specimen descriptions for corresponding numbers. Red numbers indicate specimens recovered from sandstone and green from mudstone.

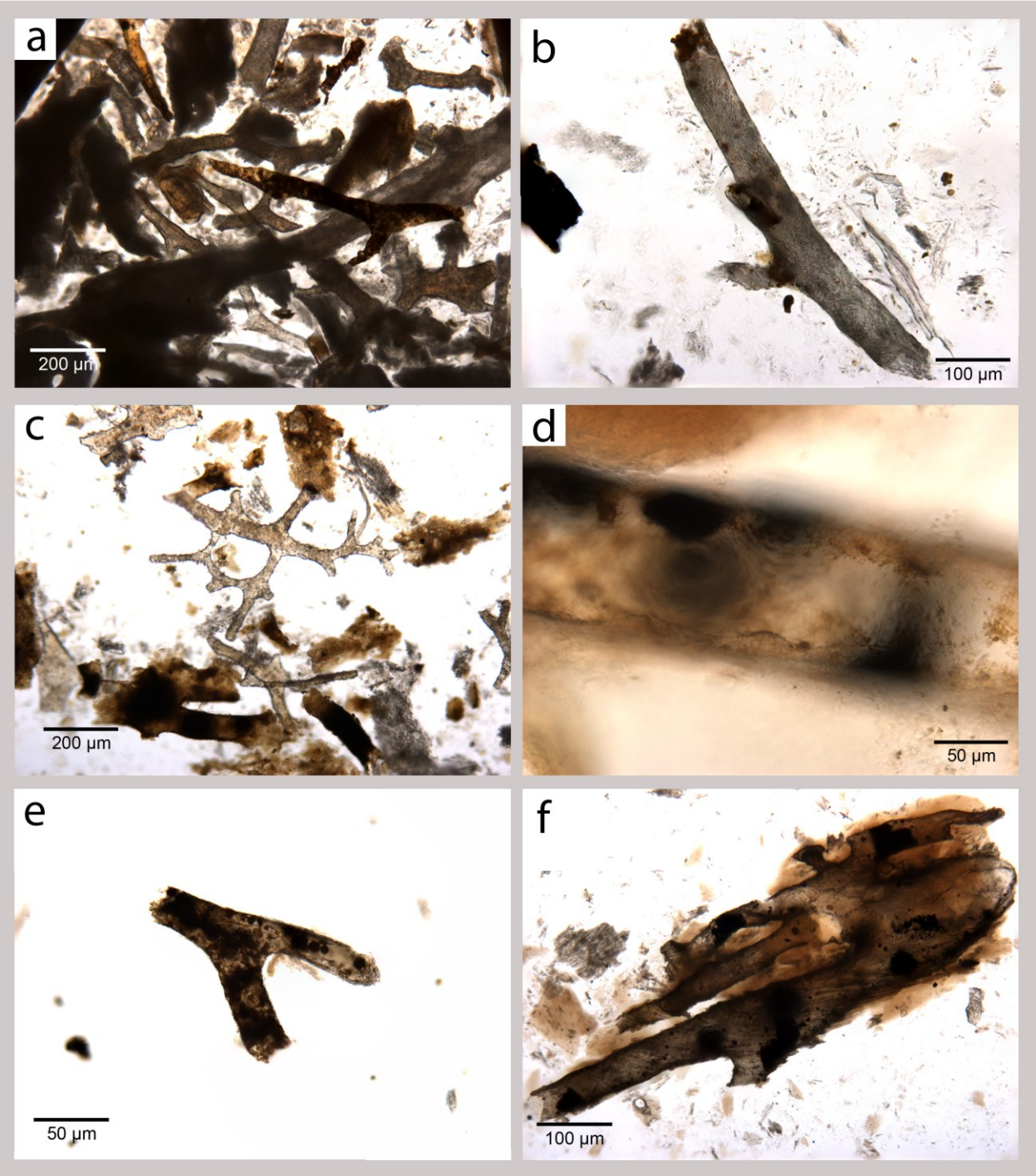

Figure 3-2. Select blood vessel-like structures. a) UALVP 55900, *Styracosaurus*. b) UALVP 55880, *Prosaurolophus*. c) UALVP 55926, *cf. Chasmosaurus sp*. d) UALVP 56607, *cf. Euoplocephalus*. e) UALVP 59616, *Leidyosuchus*. f) UALVP 56596, *Anchiacipenser acanthaspis*.

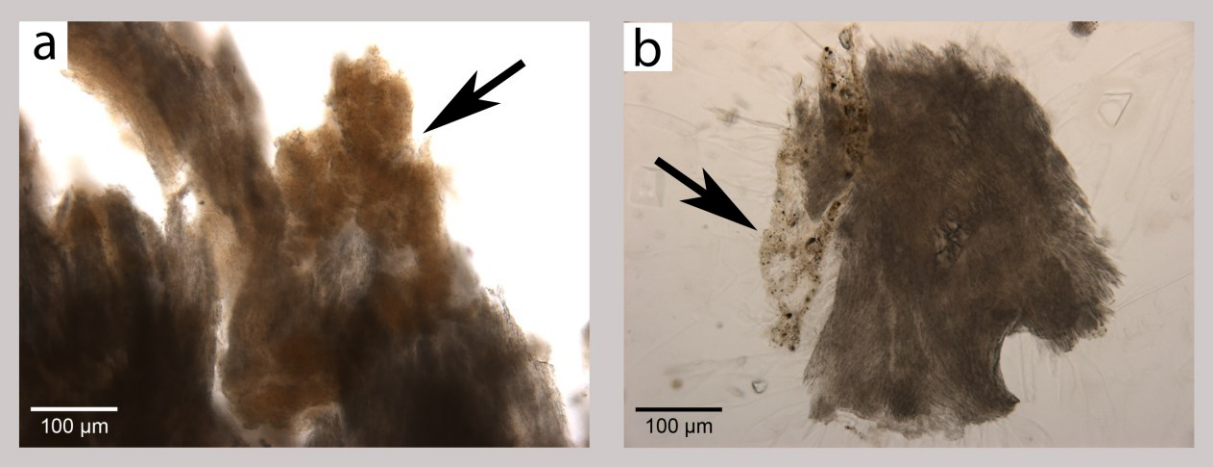

Figure 3-3. Extracellular organic matrix-like structures. a) UALVP 59616, *Leidyosuchus*. b) UALVP 55804, *Latenivenatrix*. Arrows identify EOM-like structures, grey fibrous material is undissolved bioapatite.

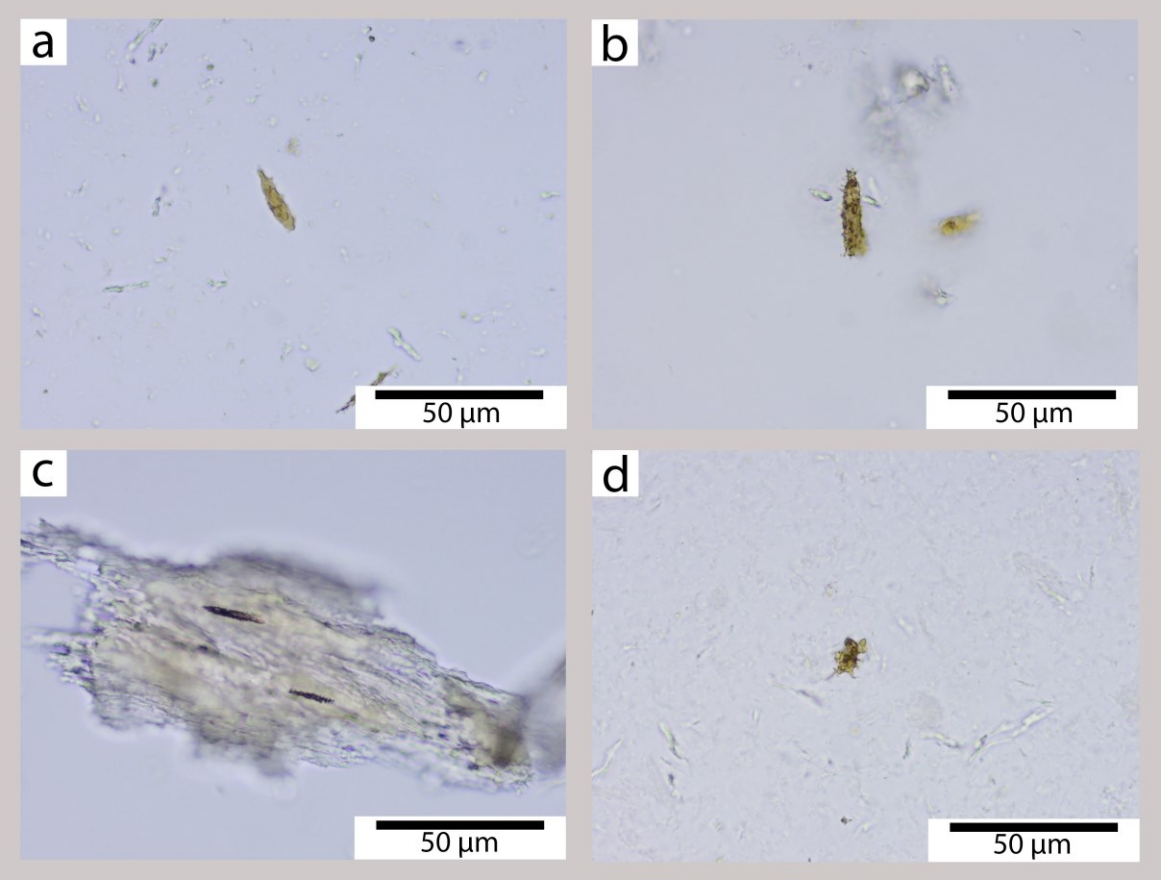

Figure 3-4. Select osteocyte-like structures. a) UALVP 55700, *Saurornitholestes*. b) UALVP 52613, *Chasmosaurus belli* (juvenile). c) UALVP 10, *Panoplosaurus*. Note that two osteocyte-like structures remain *in situ* within the bioapatite bone matrix. d) UALVP 59616, *Leidyosuchus*.

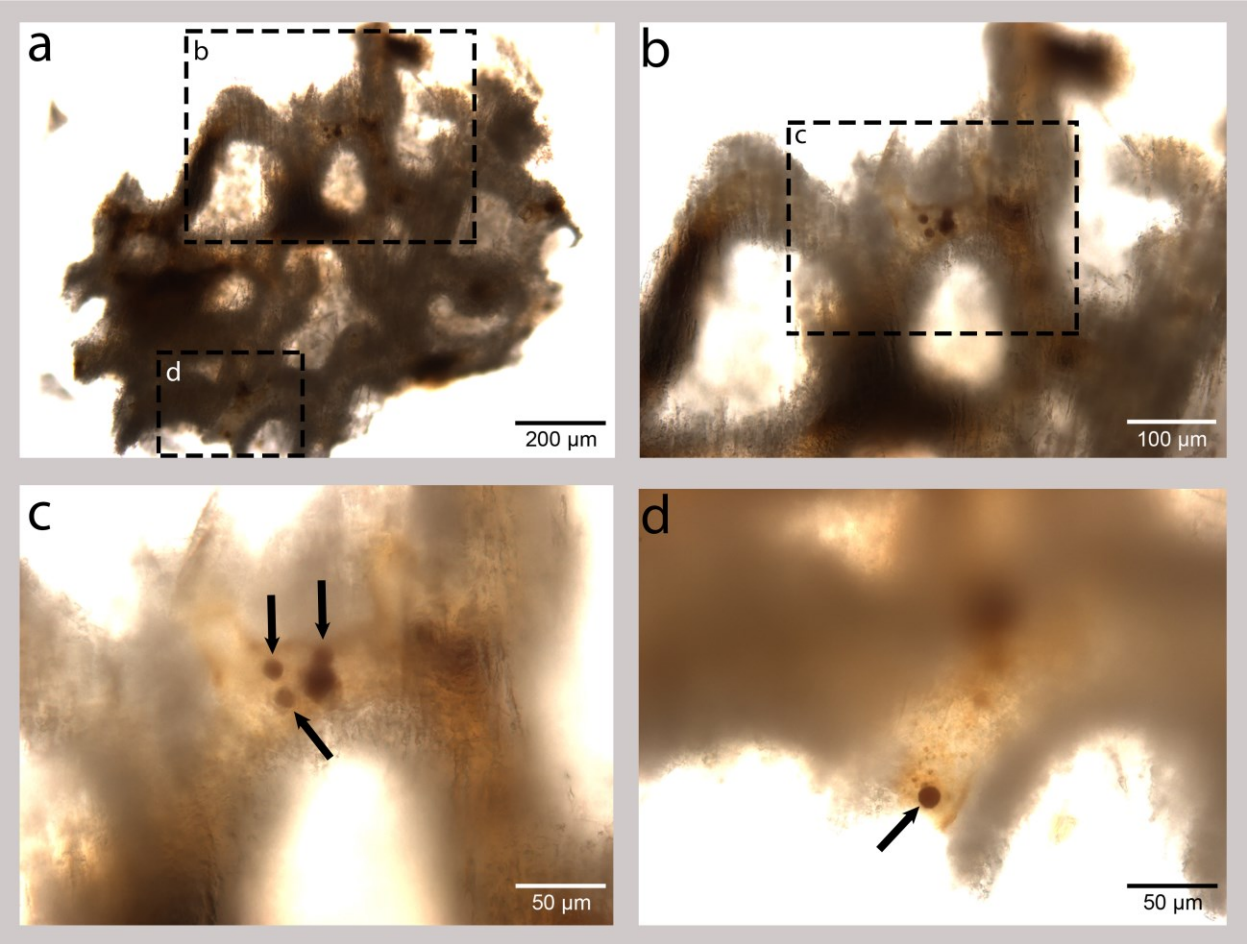

Figure 3-5. Anastomosing vessel-like network in UALVP 49500, *Gorgosaurus* subadult. Grey fibrous material is remaining bioapatite bone matrix. a) Overview of structure indicating enlarged images in b and d. b) enlarged area indicated in a. c) Enlarged portion outlined in b, black arrows point to red blood cell-like structures within the lumen of the vessel structure. d) Enlarged area as indicated in a, black arrow points to red blood cell-like structure.

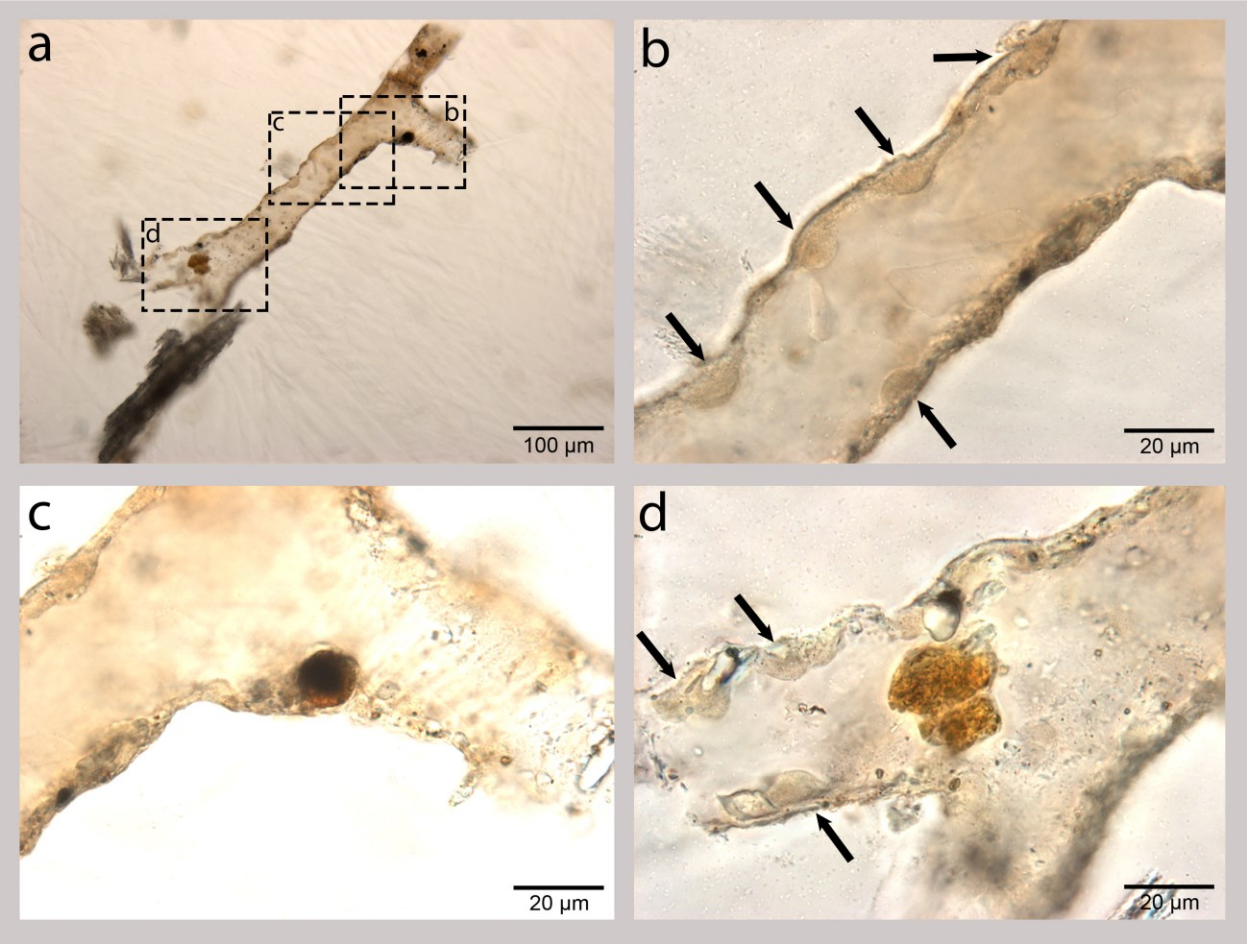

Figure 3-6. Portion of vessel-like structure from the ilium of *Latenivenatrix*. a) Overview of vessel indicating where enlarged areas in a-c are from. b) Portion of main length of the vessel structure. Black arrows indicate the nucleus-like structures bulging into the lumen of the vessel. c) Red blood cell-like structure remaining within the vessel. Note dark centre, suggesting possible nucleus-like structure. d) Large bilobed object possessing similar morphology to a basophil. Black arrows indicate endothelial nuclei-like structures.

Chapter 4: Preservation rates of tissue-like structures in vertebrate remains from the upper Campanian of Alberta: Horseshoe Canyon Formation.

4.1 INTRODUCTION

Original tissue research in the geological record has been a recent development in vertebrate palaeontology (Muyzer et al. 1992, Schweitzer et al. 2016b, 1997, 2005a, 2009b, 2013, 2014, Embery et al. 2000, Asara et al. 2007, Smith and Hayward 2010, Cleland et al. 2015, Wiemann et al. 2018, Saitta et al. 2018). Previous work conducted on a variety of bone from the Dinosaur Park Formation suggested that original tissues are far more common than initially anticipated (Chapter 3). Although EOM and vessels are found in nearly 100% of DPF remains tested, osteocytes are rarely found and those observed are poorly preserved and lacking all filipodia.

The Horseshoe Canyon Formation is a fluvial coastal floodplain sequence dominated by floodplain muds, major river sands, swamp coals, and rare paleosols. The lower HCF represents a regression of the Western Interior Seaway while the upper HCF records the Fox Hills transgressive-regressive cycle as the Drumheller Marine Tongue (Eberth et al. 2013). The DMT occurs during a period cool and dry climate at the top of the Morrin Member and the bottom of the Tolman Member. Although much of the lower HCF contains extensive coals, the Tolman Member (~70.5-68.5 Mya) has no major coals (Eberth et al. 2013), suggesting a similarity in palaeoenvironmental conditions to the Dinosaur Park Formation.

Ten dinosaur bone specimens were collected from the Tolman Member of the Horseshoe Canyon Formation in and around Dry Island Buffalo Jump Provincial Park, and

samples were removed from each bone for dissolution (Fig. 4-1). Specimens from the Tolman Member of the Horseshoe Canyon Formation were chosen to investigate the preservation frequency of tissue structures in a similar environment to that represented in the Dinosaur Park Formation. Although no correlation has been found between preservation rate and degree of articulation or sedimentology, the Horseshoe Canyon Formation is being investigated to reveal further information relating to these factors and/or to confirm that osteocyte preservation is rare as in the DPF. Investigated factors included: 1) Sedimentological association (sandstone or mudstone). 2) Degree of articulation of a specimen. 3) Depositional environment, to investigate if different environmental conditions may influence preservation of original tissues. Structures that were most commonly recovered and identified in this study are vessel-like (Fig. 4-2), EOM-like (Fig, 4-3), or osteocyte-like (Fig. 4-4).

4.2 MATERIALS AND METHODS

4.2.1 Specimen Selection

Specimens used within the study were selected based on four main criteria. First, specimens were collected specifically for this study to ensure that they were not contaminated with glue or bacterial contamination from storage. Secondly, specimens were from a variety of taxa for future investigations into proteomics. Of the ten specimens sampled, seven are hadrosaurid, one ceratopsid, one champsosaur, and one ornithomimid. All specimens were collected from the Tolman Member of the Horseshoe Canyon Formation, to reduce stratigraphic variation that may influence preservation. Thirdly, specimens were chosen based on depositional matrix composition – sandstone or mudstone – from which they were recovered. Lastly, specimens were chosen based on their degree of articulation.

4.2.2 Dissolution of samples

Specimen treatment log sheets were kept as each sample was dissolved or other treatments were performed (Appendix 4-1).

4.3 RESULTS

At least one type of tissue-like structure was recovered from nine of the ten specimens post dissolution, but the amount recovered varied dramatically between samples. Specimens that produced significant amounts of tissue-like structures had samples removed for $\delta^{13}C$ and $\delta^{15}N$ isotope analysis. Results herein are reported phylogenetically, followed by specimen numbers if multiple specimens of the same genus and species were sampled. Findings are summarized in Table 4-1.

4.3.1 Champsosauridae indet. (Choristodera, UALVP 59699, isolated femur, mudstone, Fig. 4-1 ”1”)

UALVP 59699, an isolated femur recovered from mudstone, preserved no tissue-like structures, however, several fragments of fungal hyphae were also recovered (Fig. 5). Unfortunately, due to the poor quality of these hyphae, it is unlikely that they are identifiable. The hyphae are identified due to their significantly minute size (~10 µm in diameter) and coenocytic nature (i.e. they lack cell septa). The hyphae are identified as original, having grown within the bone prior to burial of the element because of the presence of small calcite crystals within them. If these were modern hyphae, they would be more likely to remain intact, and would not contain calcite crystals.

4.3.2 Ceratopsidae indet**.** (Ornithischia, UALVP 60152, isolated pedal phalanx, sandstone, Fig. 4-1 “2”)

UALVP 60152, an isolated juvenile ceratopsid pedal phalanx, had three small fragments removed. Each sample produced vessel-like (Fig. 4-2) and EOM-like structures. Vessel structures appear slightly degraded, possessing a fibrous appearance, and are slightly flexible, although they fracture if not handled carefully. One vessel fragment was observed to possess a small reddish spherical object resembling that of a red blood cell (Fig. 4-2). EOM-like material was recovered, although in low quantities.

4.3.3 Hadrosauridae indet**.** (Ornithischia, UALVP 60153, isolated manual phalanx, mudstone, Fig. 4-1 “3”)

UALVP 60153, a hadrosaurid manual phalanx recovered from mudstone, was fractured and had three fragments dissolved. This specimen had no tissue-like structures preserved in the fragments tested. Observations made during dissolution and subsequent microscopy imaging revealed that the bioapatite appears to have been significantly altered, suggesting that an unknown taphonomic process can recrystallize bone such that it becomes vitrified. Small dark objects are visible within bone fragments, and may represent original tissues (Fig. 4-6), but do not survive dissolution of the surrounding bone.

4.3.4 Hadrosauridae indet**.** (Ornithischia, UALVP 60154, associated ilium from sandstone, mudstone, Fig. 4-1 “4”)

UALVP 60154, a juvenile hadrosaur ilium associated with several other bones, including a complete caudal vertebra, had small fragments removed from a region previously damaged

due to in situ cracking. This specimen unexpectedly preserved no vessels nor EOM-like structures but did preserve osteocyte-like structures in low quantities. The osteocyte-like structures are moderately well preserved, although the filipodia are missing, their bases are usually preserved.

4.3.5 Hadrosauridae indet**.** (Ornithischia, UALVP 60156, associated humerus from mudstone, Fig. 4-1 “5”)

UALVP 60156, a complete juvenile humerus, found in association with a tibia and other unidentified elements, had three small bone fragments removed by hammer and awl. This specimen was found to contain no original tissue-like structures, similar to DI-2018-003. Also like UALVP60153, the bioapatite had been altered into a vitrified form during taphonomic processes.

4.3.6 Hadrosauridae indet**.** (Ornithischia, UALVP 60157, distal end of metatarsal III from mudstone, Fig. 4-1 “6”)

UALVP 60157 is the distal end of an adult metatarsal III. A fragment of bone was fractured off and subsequently broken into three smaller pieces. This specimen produced tissue-like structures of all three types after dissolution. Vessel-like structures were found preserved in large three-dimensional anastomosing vascular networks (Fig. 4-7), most sections of which were surrounded by portions of preserved EOM-like material. Portions of vascular network were common enough to provide sampling for $\delta^{13}C$ and $\delta^{15}N$ isotope analysis. Although osteocyte-like structures were also found in low numbers in UALVP 60157, the quality

of preservation is significantly better than those in other specimens from the Horseshoe Canyon Formation, with many possessing partial filipodia (Fig. 4-4).

4.3.7 Hadrosauridae indet. (Ornithischia, UALVP 60159, isolated maxilla from sandstone, Fig. 4-1 “7”)

UALVP 60159, a partial juvenile hadrosaur maxilla with teeth, had three small fragments of weathered bone dissolved. Vessel-like structures were numerous and slightly flexible, similar to those from specimens from the Dinosaur Park Formation (Chapter 3). Interestingly, fungal hyphae were also recovered from UALVP 60159 (Fig. 5). Recovered hyphae appear to be like those from UALVP 59699, but are straight and appear to branch. Hyphae are coenocytic and contain small elongated black objects.

4.3.8 Hadrosauridae indet**.** (Ornithischia, UALVP 60161, isolated pathologic rib from sandstone Fig. 4-1 “8”)

UALVP 60161, a heavily weathered pathological rib found in poor condition, was sampled by taking fragments from the best-preserved area that could be altered without disturbing the lesion. Although osteocyte-like structures were not recovered, several vessel-like structures and EOM-like structures were.

4.3.9 Hypacrosaurus altispinus (Hadrosauridae, UALVP 60160, dorsal vertebra neural spine, associated skeleton from sandstone, Fig. 4-1 “9”)

UALVP 60160 is a dorsal vertebra from an associated skeleton of *Hypacrosaurus altispinus*, identified by elongated neural spines and stratigraphic position of the skeleton

within the Horseshoe Canyon Formation. Fragments of the neural spine were removed using large clippers. Vessel-like structures were common and appeared to be slightly altered, although they were still slightly flexible. UALVP 60160 yielded the highest number of osteocyte-like structures, a total of 5 being recovered in 40 µL of dissolution fluid from below the first bone fragment. These osteocyte-like structures no longer possess complete filipodia (Fig. 4-4), however, the bases are preserved like those observed in specimens from the Dinosaur Park Formation (Chapter 3).

4.3.10 Ornithomimidae indet**.** (Theropoda, UALVP 60158, rib in bonebed from sandstone Fig. 4-1 "10")

UALVP 60158 is a partial ornithomimid rib (rib head and proximal quarter of rib shaft) recovered from a moderately dense multitaxic bonebed. Three samples from the rib shaft were removed for dissolution. The preservation of the vascular network of vessel-like structures is exceptional (Fig. 4-7). Nearly the entire network remains as an intact three-dimensional anastomosing structure surrounded by the EOM-like material. Due to the quantity and quality of preservation of the vascular network, one of the bone fragments had a portion removed for $\delta^{13}C$ and $\delta^{15}N$ isotope analysis. Despite the high quality of preservation for vessel and EOM-like structures, no osteocyte-like structures were recovered.

4.4 DISCUSSION

Field work in and around Dry Island Buffalo Jump Provincial Park during the summer of 2018 was conducted with the specific intention of recovering vertebrate remains within a restricted stratigraphic zone to reduce variables that may influence preservation of original

tissues. Tissue preservation rates within the Tolman Member of the Horseshoe Canyon Formation is moderate for vessels (60%) and EOM (40%), but low for osteocytes (30%). Interestingly, fungal hyphae were recovered from two specimens (UALVP 59699 and UALVP 60159). Although this suggests that 20% of the specimens from the Horseshoe Canyon Formation may contain fungal remains, the sample size is small, and sampling targeted isolated and easily collected specimens that were especially likely to have been exposed to environmental elements for longer durations prior to burial.

Tissue-like structures are more commonly preserved in sandstone than in mudstone, with 67% of specimens from sandstone preserving vessel-like structures, 50% preserving EOM-like ones, and 33% preserving osteocyte-like ones. Only a single specimen from mudstone (25%) contained tissues (UALVP 60157), although this specimen preserved EOM, osteocytes, and vessels. Interestingly, UALVP 60157 is the only specimen that preserved all three tissue-like structures. Higher rates of tissue preservation in specimens from sandstone have been observed previously and suggested to be the result of a higher porosity within the surrounding sediment, facilitating the drainage of decay enzymes within carcasses (Schweitzer et al. 2007a). The results herein suggest that this factor may indeed affect the preservation of original tissues in both the Tolman Member of the Horseshoe Canyon Formation and the Hell Creek Formation of Montana. The hypothesis that the degree of articulation influences preservational rates of tissue-like structures is not supported because rates for both associated skeletons and isolated elements were roughly equal at approximately 70%. The preservation of fungal hyphae provides interesting insight into the taphonomy of the two specimens from which they were recovered. Saprophytic fungi feed on dead organic matter, receiving nutrients as decay

proceeds. Lichen, a composite organism formed by the symbiotic relationship of fungal and algal species, is commonly observed growing on modern bone surfaces throughout the world, taking advantage of a stable substrate that can be rich in nutrients. Further research into the type of hyphae recovered from the Tolman Member samples may provide insights into the environmental conditions the bone was exposed to, the length of time it was exposed for, and – given enough specimens – fungal diversity in the setting in which the Tolman Member of the Horseshoe Canyon Formation was deposited.

Taphonomic processes on a molecular level are not currently well understood, but have recently been investigated to address soft tissue preservation in deep time (Reisz et al. 2013, Schweitzer et al. 2014, 2016a). Two samples in this study (UALVP 60153 and UALVP 60156) show significant alteration to the bioapatite, resulting in a vitreous appearance under high magnification. Vitrification of bone may result in EOM being destroyed, as bioapatite is restructured and invades collagen spaces. If recrystallization continues, the phospholipid bilayer of osteocyte filipodia may become compromised, causing the cell to undergo lysis and ultimately destruction. If vitrification continues, lysis of the vessel endothelial cells may occur, resulting in destruction of the last original organics remaining. Vitrification of bone is observed regularly in the Horsethief Member of the Horseshoe Canyon Formation and marine-influenced portions of the Dinosaur Park Formation, and is most often found in relation to a white concreted rind on the surface (personal observations). This rind may be an indicator as to the nature of the taphonomic processes that cause the recrystallization of bioapatite in these two stratigraphic intervals, and the subsequent destruction of original organic tissue structures. Taphonomic processes on a molecular level are not currently well understood, but have

recently been investigated to address soft tissue preservation in deep time (Reisz et al. 2013, Schweitzer et al. 2014, 2016a). Two samples in this study (UALVP 60153 and UALVP 60156), show significant alteration to the bioapatite, resulting in a vitreous appearance under high magnification. Vitrification of bone may result in EOM being destroyed as bioapatite is restructured and invades collagen spaces. If recrystallization continues, the phospholipid bilayer of osteocyte filipodia may become compromised, leading to the lysis of the cell, and ultimate destruction of the entire cell. If vitrification continues further, lysis of the vessel endothelial cells may occur, resulting in the destruction of the last original organics remaining. Vitrification of bone is observed regularly in the Horsethief Member of the Horseshoe Canyon Formation and marine influenced portions of the Dinosaur Park Formation and is most often found in relation to a white concreted rind on the surface (personal observations). This rind may be an indicator as to the nature of the taphonomic processes that cause the recrystallization of bioapatite in these two stratigraphic regions, and the subsequent destruction of original organic tissue structures.

The Tolman Member of the Horseshoe Canyon Formation spans ~70.4 - ~68.3 Mya, is underlain by the maximum flooding surface of the Drumheller Marine Tongue deposits of the Western Interior Seaway, and is overlain by coarser-grained palaeochannel sandstones, carbonaceous shales, and coals of the Carbon Member (Eberth and Braman 2012). The Tolman Member is non-coaly, indicating a well drained environment, and has been proposed to have been deposited during a cool and dry interval (Eberth and Braman 2012, Eberth et al. 2013). Low numbers of precipitated mineral crystals within the lumen of vessels may be the result of the well drained Tolman Member environment. Further investigation into other stratigraphic

members within the Horseshoe Canyon Formation [in ascending order; Strathmore, Drumheller, Horsethief, Morrin, Carbon, and Whitemud Members (Eberth et al. 2013)], could provide further information on variation in preservation may change in different climates.

4.5 CONCLUSIONS

Results herein suggest sandstone may favour the preservation of tissue-like structures in vertebrate remains from the Tolman Member of the Horseshoe Canyon Formation, although a larger sample size would be required to achieve more accurate numbers. This supports the hypothesis proposed by Schweitzer et al. (2007) that high porosity facilitates the drainage of digestive enzymes from decaying carcasses. The degree of association of skeletal elements does not appear to have a clear influence on the likelihood of tissue preservation in the Tolman Member of the Horseshoe Canyon Formation. Additionally, investigation into the remaining stratigraphic Members of the Horseshoe Canyon Formation could provide insight into whether climate may influence tissue preservation.

The low numbers of preserved osteocyte-like structures in specimens suggests a bias against their preservation in bone from the Tolman Member. Although the underlying cause of the lower preservation rates of osteocyte-like structures is unknown, it is suggested that the phospholipid bilayer becomes compromised through recrystallization and the cell succumbs to lysis. If vitrification continues, even endothelial cells and extracellular organic matrix that contain collagen-2 and elastin may be destroyed. Given how common tissue-like structures are in the fossil record, it suggests that perhaps research into what ultimately destroys tissues may be more important that what preserves it.

Table 4-1. List of samples derived from specimens and types of soft-tissue preservations noted for each. Sediment: M, Mudstone; S, Sandstone. Association: AS, Associated skeleton; I, Isolated bones. Abundance of tissue-like structures, X, rare; XX, common; XXX, abundant. Precise numbers are exact numbers found in 40 µL of dissolution fluid.

Taxon	Element	Specimen number	Vessels	EOM	Osteocytes	Fungal Hyphae	Sediment	Association
Choristodera								
Champsosaur	Femur	UALVP 59699	-	-	-	X	M	I
Ornithischia								
Ceratopsidae indet.	Phalanx	UALVP 60152	XX	X	-	-	S	I
Ornithischia								
Hadrosauridae indet.	Phalanx	UALVP 60153	-	-	-	-	M	I
Hadrosauridae indet.	Ilium	UALVP 60154	-	-	2	-	S	AS
Hadrosauridae indet.	Humerus	UALVP 60156	-	-	-	-	M	AS
Hadrosauridae indet.	Metatarsal III	UALVP 60157	XXX	XX	2	-	M	I
Hadrosauridae indet.	Maxilla	UALVP 60159	-	-	-	X	S	I
Hadrosauridae indet.	Rib	UALVP 60161	X	X	-	-	S	I
Hypacrosaurus	Vertebra	UALVP 60160	XX	-	5	-	S	AS
Theropoda								
Ornithomimidae indet	Rib	UALVP 60158	XXX	XXX	-	-	S	I

FIGURES

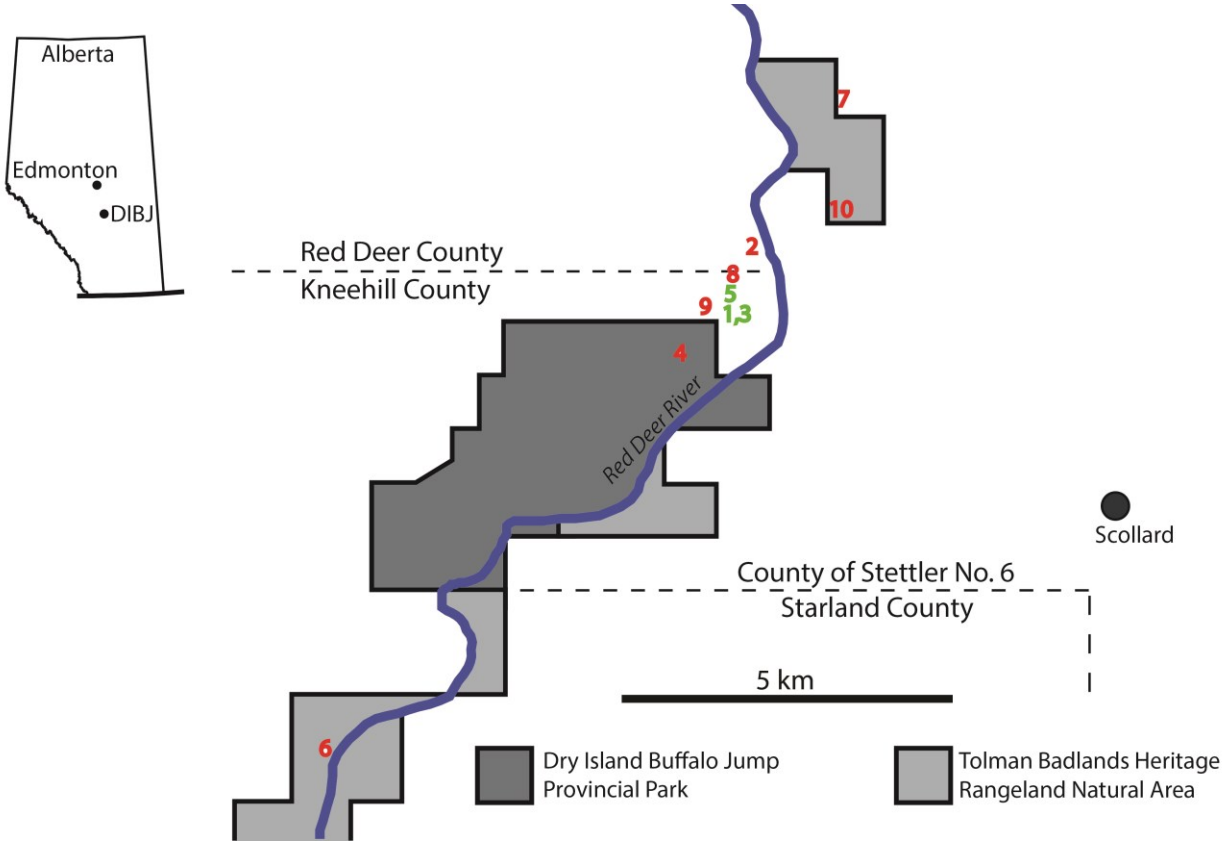

Figure 4-1. Map of Alberta and Dry Island Buffalo Jump Provincial Park (DIBJ) and area indicating where specimens were recovered. See specimen descriptions for corresponding numbers. Red numbers indicate specimens recovered from sandstone and green from mudstone.

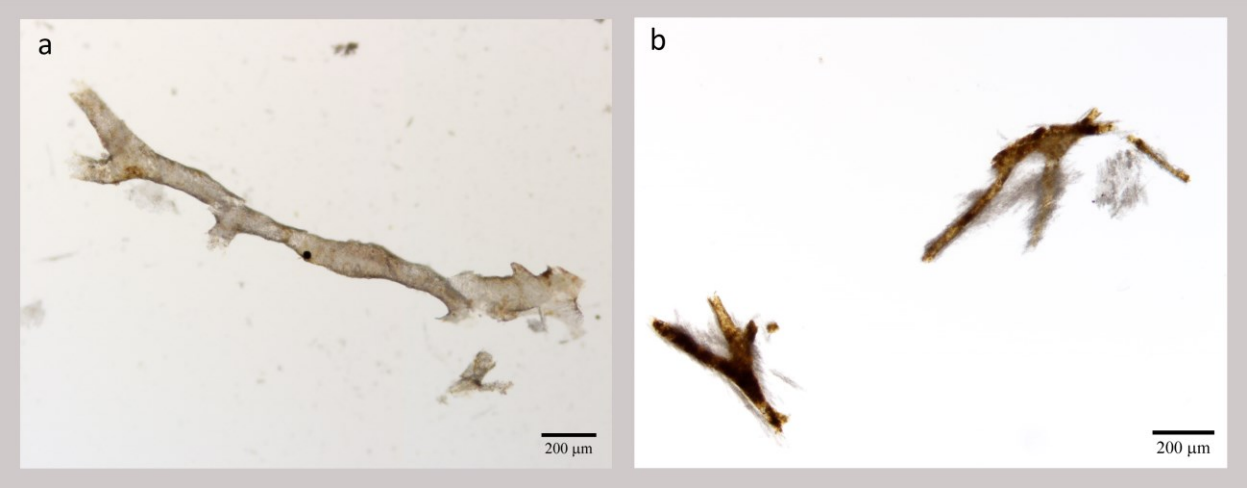

Figure 4-2. Select blood vessel-like structures from a) UALVP 60152, from a Ceratopsidae indet. pedal phalanx. and b) UALVP 60158, from a rib of an indeterminate Ornithomimidae.

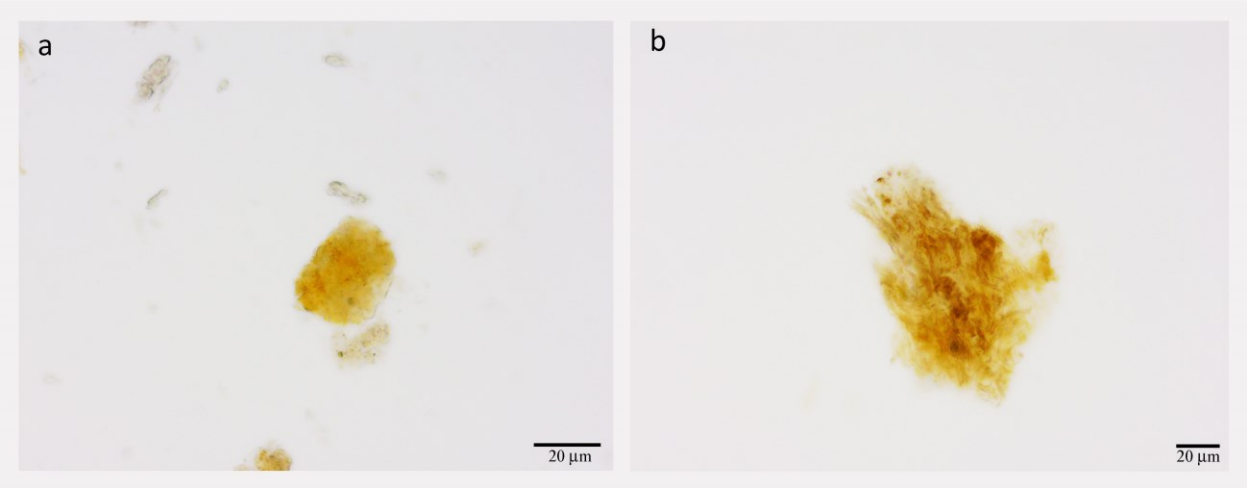

Figure 4-3. Extracellular organic matrix-like structures from. a) UALVP 60161, Hadrosauridae indet., from a rib, grey structures are undissolved bioapatite fragments. b) UALVP 60157, from a Hadrosauridae indet., metatarsal III.

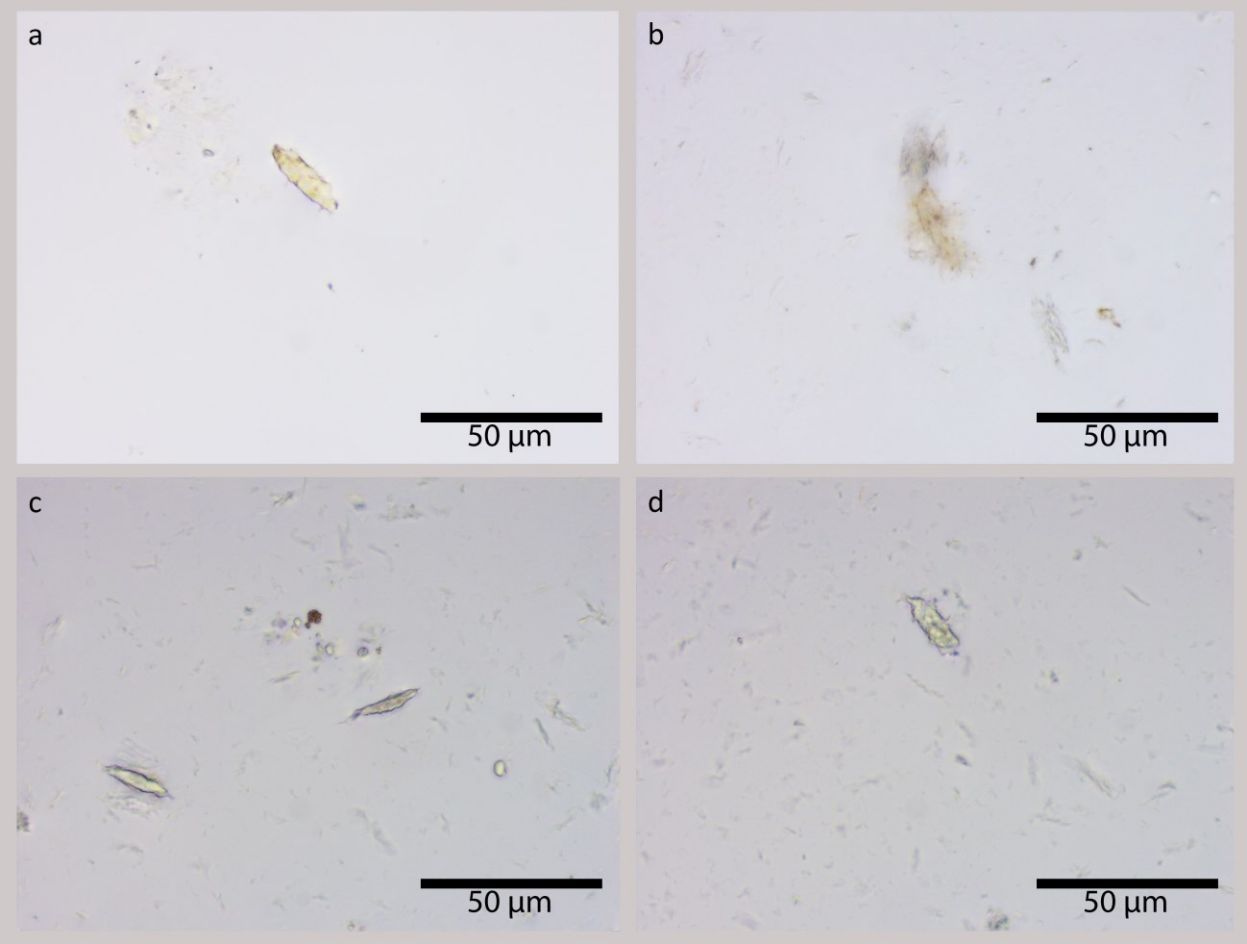

Figure 4-4. Select osteocyte-like structures. a) UALVP 60154, Hadrosauridae indet., from a juvenile ilium. b) UALVP 60157, from a Hadrosauridae indet., Metatarsal III. c and d) UALVP 60160, from an Ornithomimidae indet., rib.

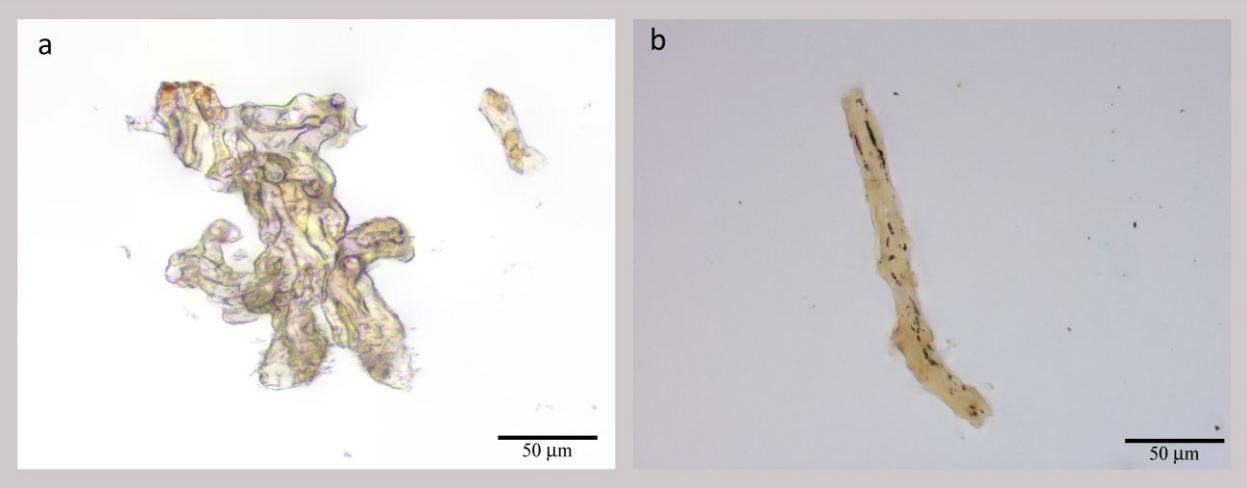

Figure 4-5. Preserved coenocytic fungal hyphae from, a) UALVP 59699, bundle of intertwined hyphae and fragment in upper right. b) UALVP 60159, single hyphae with bases of branching evident. Black objects are observed within the cellular space.

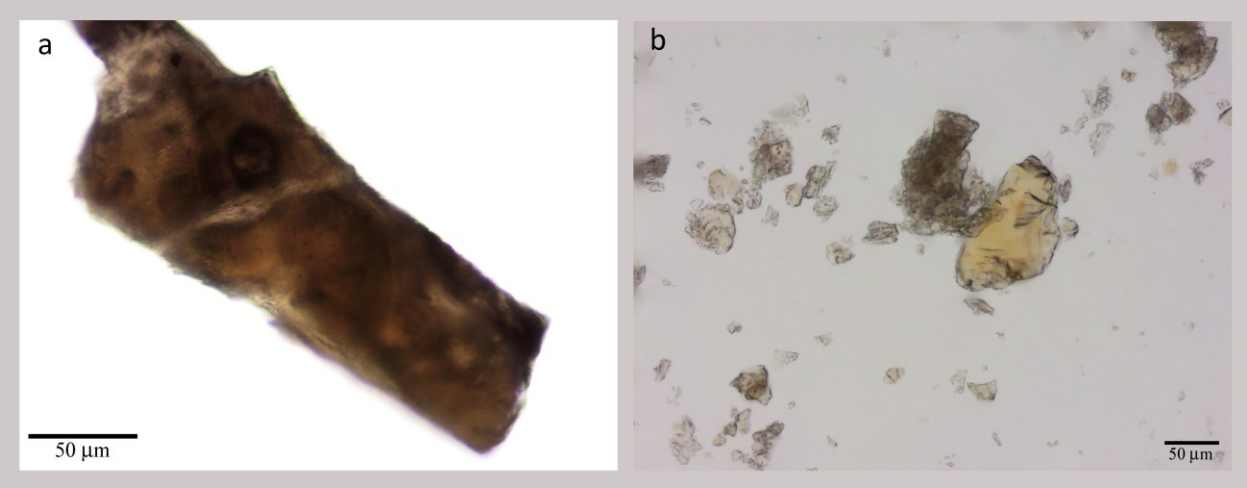

Figure 4-6. Vitrified bone fragments under compound light microscope from, a) UALVP 60153 from a Hadrosauridae indet. phalanx. Black objects inside may be altered organics that do not survive dissolution. b) UALVP 60156 Hadrosauridae indet. from a humerus. Small shard of bone showing significant vitrification.

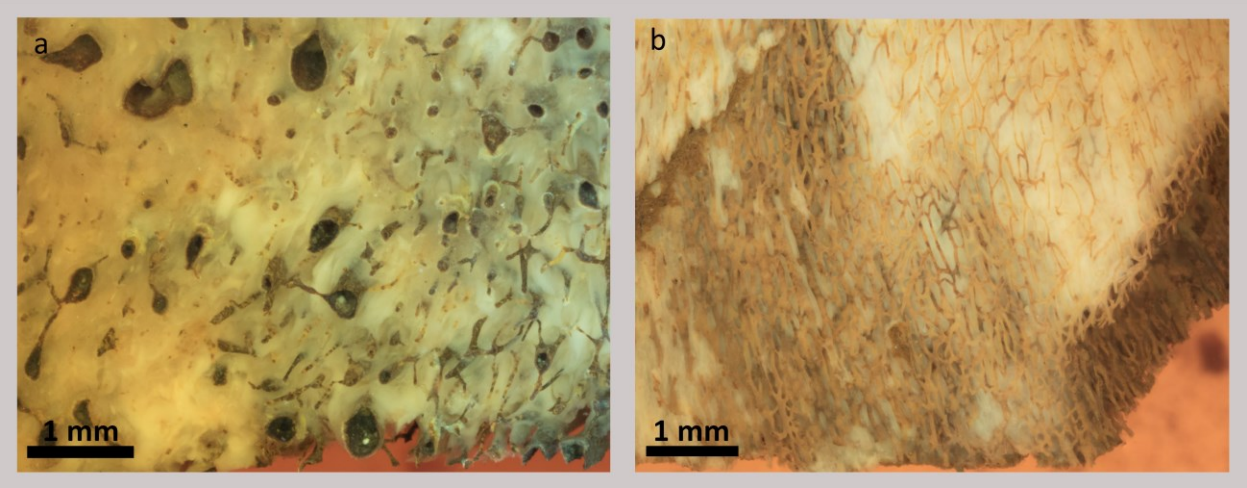

Figure 4-7. Macroscopic image of vascular networks in situ in bone from, a) UALVP 60157, from a Hadrosauridae indet. Metatarsal III. b) UALVP 60158, from an Ornithomimidae indet. rib.

Chapter 5: Preservation rates of tissue-like structures in vertebrate remains from the Upper Campanian of Alberta: Wapiti Formation.

5.1 INTRODUCTION

Original tissue research in the geological record has been a recent development in vertebrate palaeontology (Muyzer et al. 1992, Schweitzer et al. 2016b, 1997, 2005a, 2009b, 2013, 2014, Embery et al. 2000, Asara et al. 2007, Smith and Hayward 2010, Cleland et al. 2015, Wiemann et al. 2018, Saitta et al. 2018). Previous work conducted on a variety of bone from the Dinosaur Park Formation suggested that original tissues are far more common than initially anticipated (Chapter 3). Dissolution of bone from the Horseshoe Canyon Formation indicates that alteration of the bioapatite into a vitrified form destroys tissue-like structures (Chapter 4).

The Wapiti Formation represents the fluvial alluvium sequence of the northernmost section of the Alberta Late Cretaceous foreland basin, and is separated into five distinct stratigraphic units (Fanti and Catuneanu 2009). Unit 1, the transition between marine facies and fluvial facies, consists of progradational and aggradational deposits. Units 2 and 3 are similar in that they consist of massive channel-fill deposits at the base, fining upwards into floodplain dominated deposits. Unit 3 specifically has been interpreted as equivalent to the maximum transgression of the Western Interior Seaway during the deposition of the Bearpaw Formation in the central plains of Alberta. Unit 4 consists of major channel and floodplain deposits and is capped by the Red Willow Coal Zone and is equivalent to the Drumheller Marine Tongue (Horseshoe Canyon Formation, Tolman Member base). Unit 5 consists of small channel,

crevasse, and overbank deposits and is capped by the Cutbank Coal Zone (Fanti and Catuneanu 2009).

Vertebrate remains have been recovered from four major stratigraphic horizons within the Wapiti Formation including; the middle of Unit 1; the top of Unit 3 and bottom of Unit 4; the middle of Unit 4; and the bottom of Unit 5. Of these intervals, only the middle of unit 4 was not deposited at a time when the shoreline was relatively close (Fanti et al. 2013). The Pipestone Creek *Pachyrhinosaurus* bonebed and an *Edmontosaurus regalis* specimen possessing the preserved impression of a fleshy comb were both recovered from Unit 4, showing just how important this stratigraphic zone is (Fanti et al. 2013, Bell et al. 2014). Although vertebrate remains are more common during times of closer coastline proximity, the specimens sampled were deposited a distance from the shoreline. Therefore, the Wapiti Formation is herein considered a transitional depositional environment between a coastal floodplain environment like that observed in the middle Horseshoe Canyon Formation (Eberth and Braman 2012, Eberth et al. 2013), and a topographically elevated, more proximal fluvial dominant environment like that seen in the Brazeau Formation (Chapter 6).

Ten dinosaur bone specimens were collected from Unit 4 of the Wapiti Formation throughout the Grande Prairie Region and sampled for dissolution (Fig. 5-1). Specimens from the Wapiti Formation were chosen to investigate the preservation rate of tissue-like structures in a transitional environment between a near shore coastal floodplain and a topographically elevated, more proximal fluvial dominant environment. Although no correlation has been found between preservation rate and degree of articulation or sedimentology within the Dinosaur Park Formation (Chapter 3), the Horseshoe Canyon Formation appears to preserve vessels more

readily in sandstones (Chapter 4). Investigated factors herein included the degree of articulation of a specimen, and the environment in which the specimen was buried. Structures that were most commonly recovered and identified in this study are vessel-like (Fig. 5-2), extracellular organic matrix-like (EOM)(Fig, 5-3), or osteocyte-like (Fig. 5-4). One specimen produced preserved fungal hyphae (Fig. 5-5).

5.2 MATERIALS AND METHODS

5.2.1 Specimen Selection

Specimens were selected from among a collection of fossils recently recovered by members of the BADP, to ensure that they were not contaminated with glue or bacteria accumulated during long term storage. Due to the restricted number of specimens that have so far been recovered from the region, the only specimens available for dissolution that were not contaminated by glues had been recovered from sandstone, with no specimens from mudstone deposits available for comparison. Additionally, due to the scarcity of specimens identified to species, samples dissolved are generally bone fragments from bonebeds, with only one sample being identifiable as Hadrosauridae indet.

5.2.2 Dissolution of samples

Specimen treatment log sheets were kept as each sample was dissolved or other treatments were performed (Appendix 5-1).

5.3 RESULTS

Nine of ten specimens had at least one type of tissue-like structure recovered post dissolution, with two having all three structures (vessels, EOM, and osteocytes). However, the

amount recovered varied dramatically between samples. Specimens that produced significant amounts of tissue-like structures had samples removed for $\delta^{13}C$ and $\delta^{15}N$ isotope analysis. A single specimen contained high amounts of fungal hyphae, suggesting a longer amount of time of exposure to the environment prior to burial. Results herein are reported phylogenetically, followed by specimen numbers if multiple specimens of the same genus and species were sampled. Findings are summarized in Table 5-1.

5.3.1 Ornithischia indet**.** (Dinosauria, UALVP 57466-1, bone fragment, sandstone, Fig. 5-1 ”1”)

UALVP 57466, a bone fragment collected from a bonebed, produced significant amounts of all three tissue-like structures. Vessel-like structures are numerous, although do not retain the full three-dimensional vascular network structure such as that seen in other specimens from the Dinosaur Park Formation (Chapter 3) and Horseshoe Canyon Formation (Chapter 4). Extracellular organic matrix is common and still retains a fibrous appearance (Fig. 5-6). Osteocytes are abundant, with hundreds being recovered in 40 µm of dissolution fluid. Many clumps of preserved EOM-like structures contain osteocyte-like structures oriented and spaced similarly to that of modern bone (Fig. 5-6). Osteocyte-like structures do appear to be well preserved, and are generally unstained to only slightly stained, although very few still possess intact filipodia. A single cluster of well-preserved osteocyte-like structures with fully intact filipodia does show significant staining, and is bound tightly with fibrous EOM-like material (Fig. 5-6)

5.3.2 Ornithischia indet**.** (Dinosauria, UALVP 57478, possible rib fragment, sandstone, Fig. 5-1 “2”)

UALVP 57478, a possible rib fragment, preserved all tissues being investigated in this study plus significant quantities of fungal hyphae. Vessels are typically moderately to heavily stained and semi-flexible, but will fracture if manipulated aggressively (Fig. 5-7). EOM is moderately abundant and still retains a slightly fibrous texture (Fig. 5-3). Osteocytes are uncommon, but present, and most retain partial filipodia; some are preserved within collagen-like mats (Fig. 5-3). Fungal remains are common, with many of the hyphae containing microcrystals of clear minerals presumed to be calcite (Fig. 5-7). Hyphae are identified based on their minute diameters, ~10 µm, and possess septa (Fig. 5-5). The ends of each hypha end in a structure that resembles a modern hyphal perithecium, the structure in which spores develop and are released (Fig. 5-7). This interpretation is supported by several 'perithecia' possessing black objects in the region where spores are produced.

5.3.3 Ornithischia indet**.** (Dinosauria, UALVP 57428, possible rib fragment, sandstone, Fig. 5-1 "3")

UALVP 57428, a possible rib fragment, contained all three tissue structures of interest. Most organic structures are moderately stained, with the vessels preserving minerals within the lumina. Vessels are common but fragmentary. EOM and osteocyte structures are also common, and are regularly found associated, with osteocytes primarily found *in situ* within the fibrous extracellular organic matrix (Fig. 5-8). Preservational quality of osteocytes varies, with those that are isolated possessing few filipodia and those remaining in EOM being better preserved.

5.3.4 Ornithischia? indet**.** (Dinosauria, UALVP 57506, unidentifiable bone fragment, Sandstone, Fig. 5-1 "4")

UALVP 57506, a bone fragment surface collected from a bonebed, preserved only vessels, with no identified EOM not osteocytes. Vessels appeared highly altered, presenting a near crystalline appearance. Vessels were extremely brittle and may be heavily mineralized.

5.3.5 Ornithischia indet**.** (Dinosauria, UALVP 57523, unidentifiable fragment, sandstone, Fig. 5-1 "5")

UALVP 57523, an unidentifiable fragment of surface-collected bone, preserved only vessel structures, similarly to UALVP 57506. Vessel quality is moderate, some staining having occurred. Microcrystalline hematite and possible pyrite is visible in several vessels (Fig. 5-2). The preservation quality is similar to that observed in much of the Dinosaur Park and Horseshoe Canyon Formations (Chapters 3 and 4). Vessel surfaces appear to have altered into a semi-crystalline compound that appears globular in sections but still retains flexibility.

5.3.6 Ornithischia indet**.** (Dinosauria, UALVP 57449, unidentifiable fragment, sandstone, Fig. 5-1 "6")

UALVP 57523, an unidentifiable surface collected fragment, produced all three tissue structures of interest. Vessels are fragmentary and appear slightly crystalline in structure. EOM is present, although uncommon, and lacks a well-defined fibrous structure. Osteocytes are uncommon, but appear to be moderately well preserved with little to no staining. Filipodia on the osteocytes are incomplete, but often retain their bases (Fig. 5-4).

4.3.7 Ornithischia indet**.** (Dinosauria, UALVP 57466-2, unidentifiable fragment, sandstone, Fig. 4-1 "7")

UALVP 57466, an unidentified surface-collected bone fragment from a bonebed, produced both vessels and EOM, but no osteocytes were observed. Vessels are fragmentary, but well preserved, with little to moderate staining. Small portions of the vessel walls are altered with an orange-brown globular texture (Fig. 5-2). Micro-crystals of calcite are present in low concentrations within the lumen.

5.3.8 cf. Edmontosaurus sp. (Hadrosauridae, UALVP 59554, bone fragment from associated skeleton, sandstone, Fig. 5-1 "8")

UALVP 59554, a fragment of unidentified bone from a partial *cf. Edmontosaurus* skeleton recovered from a rockslide, was sampled for dissolution. This was the only specimen to not produce any tissue structures. Micro-fragments of partly dissolved bone under compound microscope show a vitrified appearance to the bone (Fig. 5-9), indicating that the bioapatite has been altered into a highly modified crystalline structure similar to that seen in specimens from the Horseshoe Canyon Formation (Chapter 4).

5.4 DISCUSSION

Specimens discussed herein were collected as part of the Boreal Alberta Dinosaur Project and sampled for dissolution because they were taxonomically unimportant. Specimens were chosen to reduce the stratigraphic distribution to minimize variables for tissue preservation. The middle Wapiti Formation appears to preserve tissue structures to a moderate quality. Vessels are the most common structure to be preserved (~90% of specimens), EOM being very common (75%), and osteocytes being common (50%). Vessels in general are moderately well preserved, showing slight flexibility, but often have a crystalline texture,

suggesting some alteration or mineralization of the tissue. This crystalline-like appearance has been reported previously in *Mammut americanum, Mammuthus columbi, Megoeodon grandis,* and *Tyrannosaurus rex* (Schweitzer et al. 2007b). Staining is commonly reported (Asara et al. 2007, Bertazzo et al. 2015, Wiemann et al. 2018), and has been suggested to be due to the crosslinking of proteins, suggesting that these structures are in fact original organics, although potentially altered (Wiemann et al. 2018). Extracellular organic matrix is commonly seen as fibrous material, suggesting a potential for future proteomics research when methods become more reliable. Most EOM is preserved like that described by Schweitzer et al. (2007b). Osteocytes are found in half of the specimens sampled, and in general are well preserved, with most cells still retaining portions of filipodia.

Unexpectedly, a single specimen, UALVP 57478, preserved a significant amount of septate fungal hyphae. These hyphae possessed small branches terminating in structures that morphologically resemble the spore producing structure, the perithecia. Additionally, these perithecia like structures contain multiple black objects that resemble developing spores. Saprophytic fungi feed on dead material, receiving the nutrients from decaying organic matter. Lichen, a composite organism formed by the symbiotic relationship of fungal and algal species, is commonly observed growing on modern bone surfaces throughout the world due to the nutrient levels and the stability of it as a substrate. The presence of 'stalked' perithecia, however, suggests that these hyphae are not lichenous in origin because perithecia in lichen are housed within a secondary structure on the surface of the ascocarp. Further research into the type of hyphae may provide information into the environmental conditions the bone was exposed to, and the length of time it was exposed for.

Taphonomic processes on a molecular level are not currently well understood, but have recently been investigated to address soft tissue preservation in deep time (Reisz et al. 2013, Schweitzer et al. 2014, 2016a). One sample herein (UALVP 57478), shows significant alteration to the bioapatite, resulting in a vitrified form when viewed under high magnification. This specimen is also the only specimen from which no tissue structures were recovered. Vitrification of bone appears to destroy EOM by means of bioapatite restructuring and invading collagen spaces. If recrystallization continues, the phospholipid bilayer of osteocyte filipodia may become compromised, leading to the lysis of the cell, damage to filipodia, or ultimate destruction of the entire cell. If vitrification continues further, lysis of the vessel endothelial cells may occur, resulting in the destruction of the last original organics remaining. Vitrification of bone is observed regularly in the Horsethief Member of the Horseshoe Canyon Formation and marine influenced portions of the Dinosaur Park Formation and is most often found in relation to a white concreted rind on the surface (personal observations). This rind may be an indicator as to the nature of the taphonomic processes that cause the recrystallization of bioapatite in these two stratigraphic regions, and the subsequent destruction of original organic tissue structures.

The Wapiti Formation represents an overall regressive sequence, with no exposure of the Bearpaw Formation in the Grande Prairie Region (Fanti and Catuneanu 2009). Although the exact distance from the Western Interior Seaway to the sites from which studied specimens were recovered is unknown, the sequence stratigraphy in the Grande Prairie Region suggests the coast line was further than equivalent beds in the Horseshoe Canyon Formation (Fanti and Catuneanu 2009, Eberth and Braman 2012). Although a simplistic view, this study considers the

regions in which the samples originated as a mid-fluvial system, where proximal fluvial systems are represented by deposits within 100 km of the palaeo-source/palaeo Rocky Mountains like that of the Brazeau Formation. Distal fluvial systems and coastal floodplains herein are considered those seen in the Tolman Member of the Horseshoe Canyon Formation, where the sequence stratigraphy includes marine sediments (Eberth and Braman 2012). The higher number of, and higher quality of, preserved osteocytes in the Wapiti Formation compared to the Horseshoe Canyon and Dinosaur Park Formations appear to correspond to both distance from a coastal floodplain environment, and the lower rates of precipitated minerals observed within cells and vessel lumina. Further work is required to determine if this trend continues.

5.5 CONCLUSIONS

The relatively high numbers of preserved osteocyte structures in specimens suggests the environmental conditions responsible for tissue preservation must have been nearly ideal. Although those specific conditions have not been identified, continued investigation into the Wapiti Formation may shed more light. Alteration of bone into a vitrified form suggests a potential candidate for the ultimate destruction of organic tissues by lysis of cells after the phospholipid bilayer is compromised. If vitrification continues, even endothelial cells and extracellular organic matrix that contain collagen-2 and elastin may be destroyed. Given how common tissue-like structures are in the fossil record, answers to the preservation of them may be discovered by investigating destructive factors instead of those that preserve them.

Table 5-1. List of samples derived from specimens and types of soft-tissue preservations noted for each. AS, Associated skeleton; BB, Bonebed, Isolated bones. Abundance of tissue-like structures, X, rare; XX, common; XXX, abundant.

Taxon	Element	Specimen number	Vessels	EOM	Osteocytes	Fungal Hyphae	Association
Dinosauria							
Ornithischia indet.	Fragment	UALVP 57466-1	XX	XX	XX		BB
Ornithischia indet.	Fragment	UALVP 57466-2	XXX	XX	-	-	BB
Ornithischia indet.	Rib	UALVP 57478	XX	XX	XX	XXX	BB
Ornithischia indet.	Rib	UALVP 57428	XX	XX	XX		BB
Ornithischia indet.	Fragment	UALVP 57506	XXX	-	-	-	BB
Ornithischia indet.	Fragment	UALVP 57523	XXX	-	-	-	I
Ornithischia indet.	Fragment	UALVP 57449	XXX	XX	XXX	-	BB
Ornithischia							
Hadrosauridae indet.	Fragment	UALVP 59554	-	-	-	-	As

FIGURES

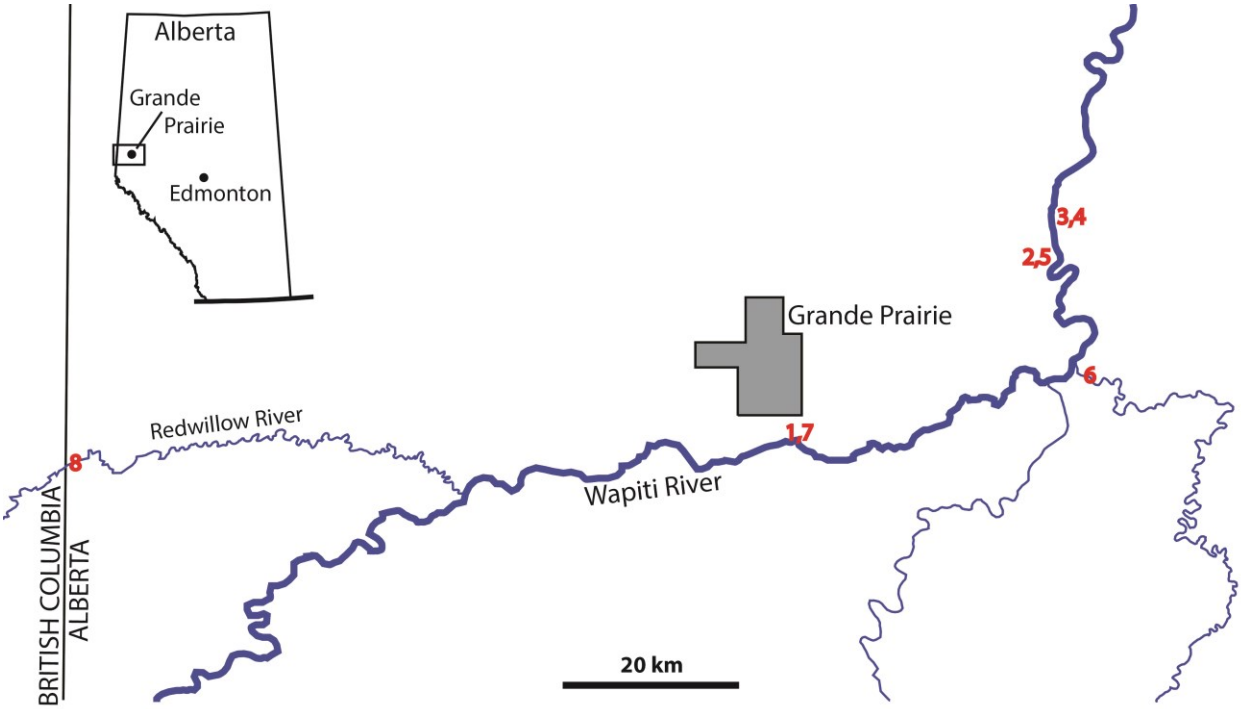

Figure 5-1. Map of Alberta and the Grand Prairie Region indicating where specimens were recovered. See specimen descriptions for corresponding numbers.

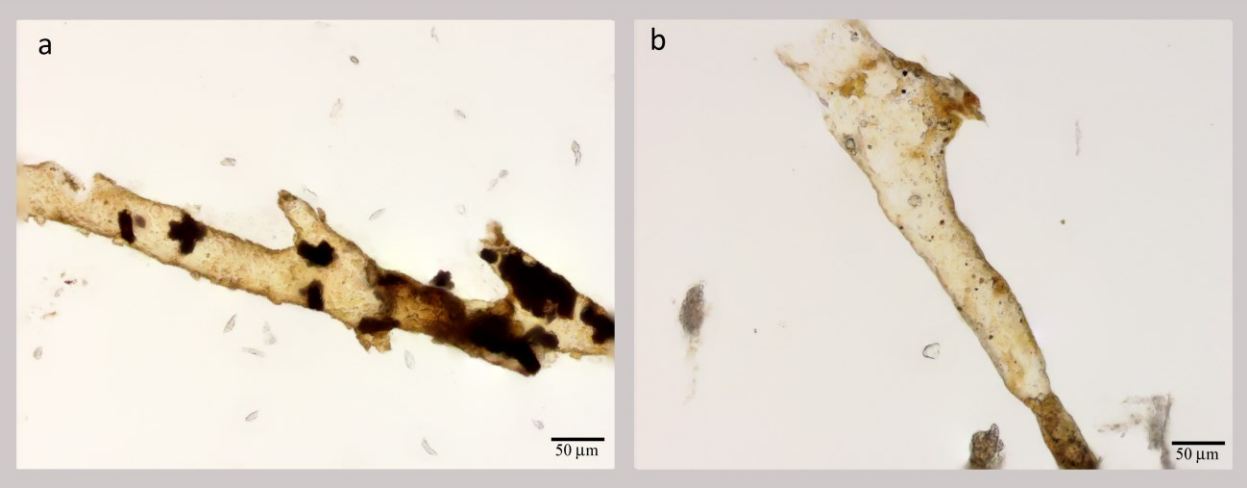

Figure 5-2. Select blood vessel-like structures. a) UALVP 57523, Ornithischia indet. from a possible rib fragment. b) UALVP 57466, Ornithischia indet. from a surface collected bone fragment.

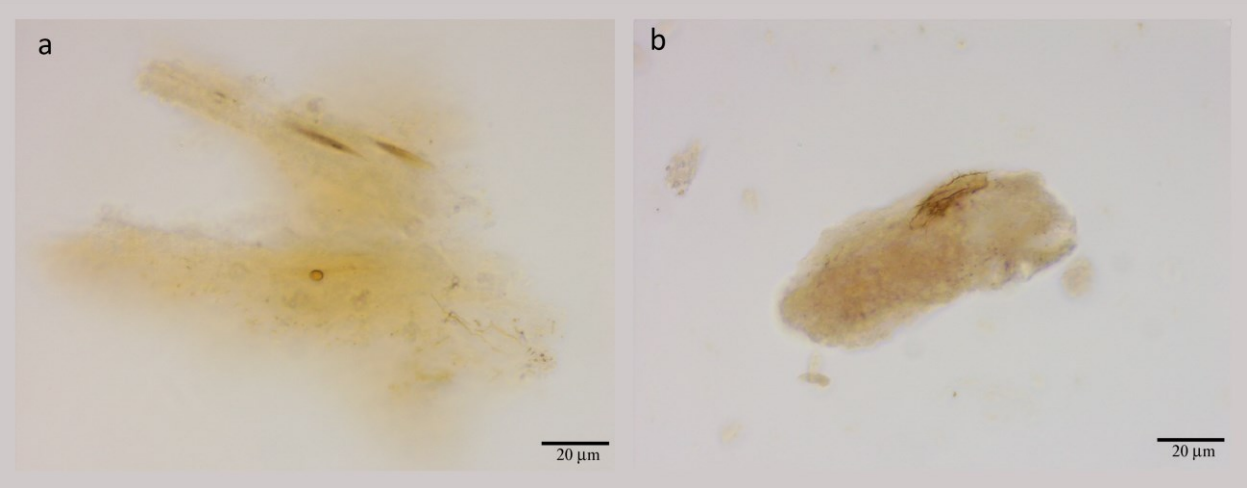

Figure 5-3. Extracellular organic matrix-like structures with osteocytes preserved within. a) UALVP 57428, Ornithischia indet. from a rib fragment. b) UALVP 57478, Ornithischia indet. from a rib fragment.

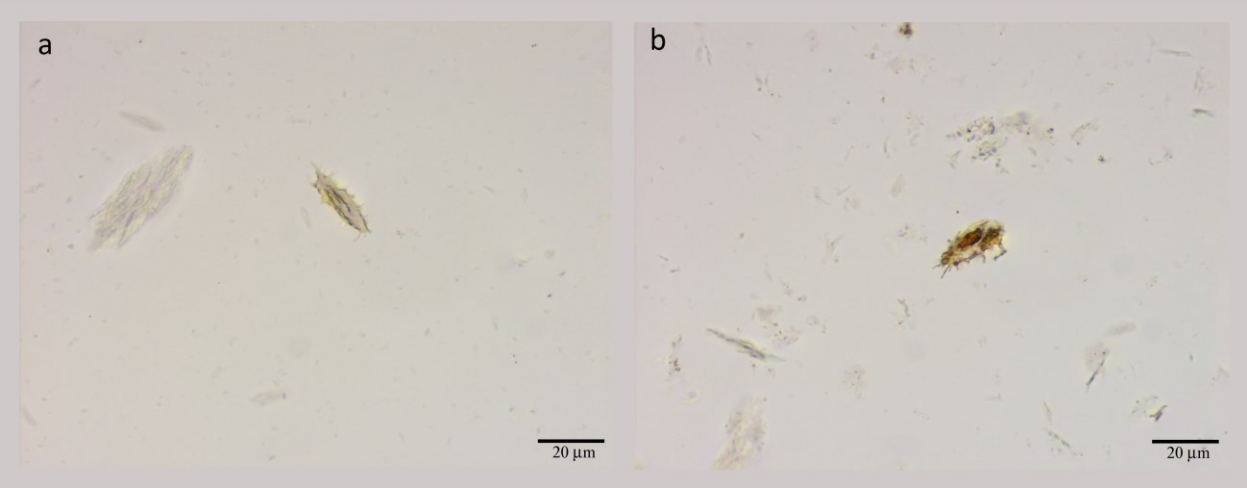

Figure 5-4. Select osteocyte-like structures. a) UALVP 57449, Ornithischia indet. from surface collected bone fragment b) UALVP 57428, Ornithischia indet. from a possible rib fragment. Filipodia are observed are numerous and moderately well preserved.

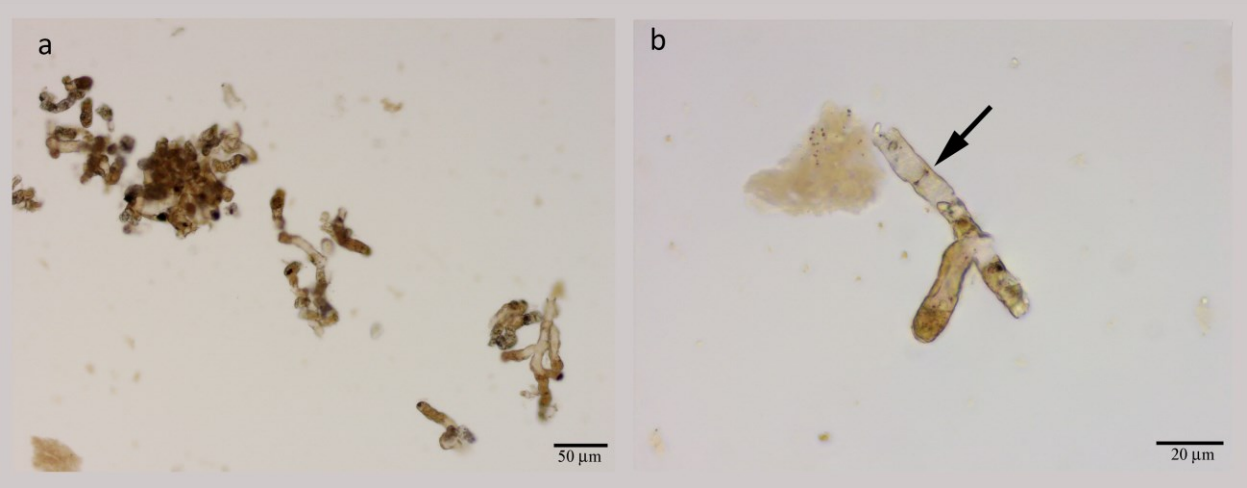

Figure 5-5. Preserved septate fungal hyphae recovered from UALVP 57478 after dissolution. a) Cluster of hyphal fragments. b) Single hyphal fragment with marked septum.

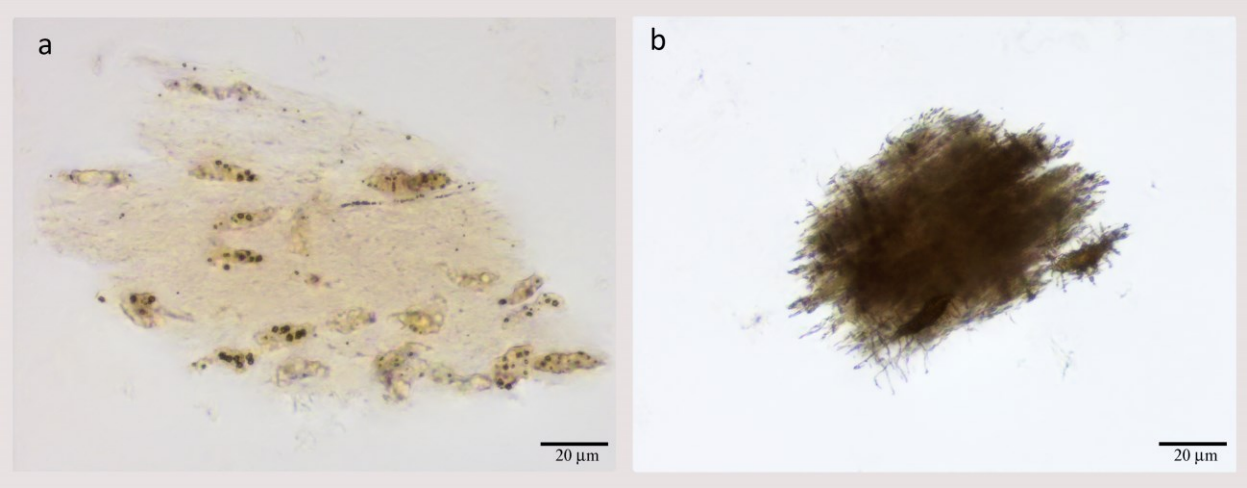

Figure 5-6. Osteocyte clusters preserved within fibrous organic matrix of UALVP 57466. a) lightly stained osteocytes possess a crystalline like appearance. b) heavily stained osteocytes are well preserved with intact filipodia.

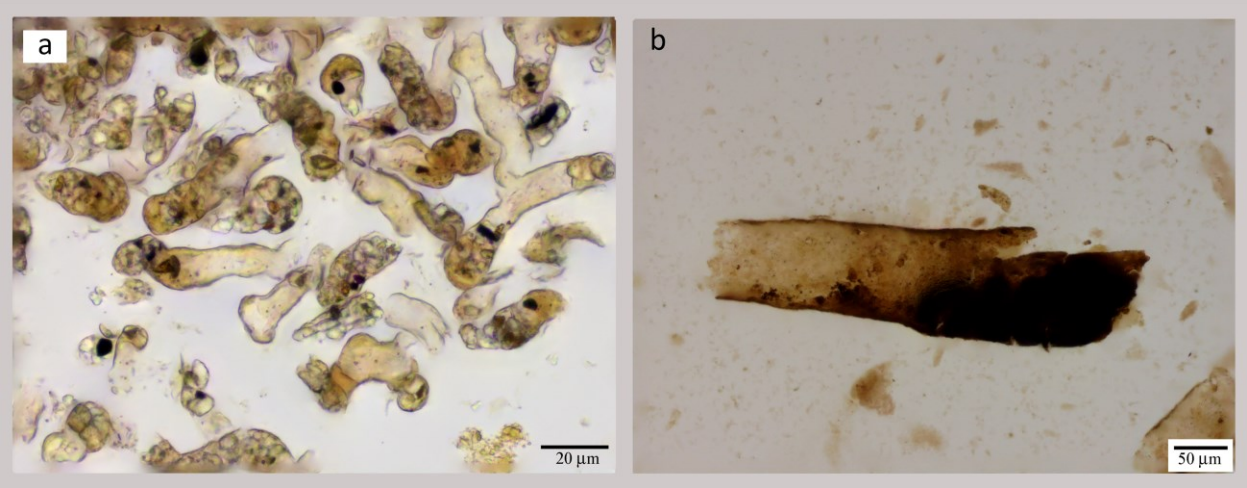

Figure 5-7. Organic material recovered from UALVP 57478. a) Fungal hyphae fragments with perithecium-like structures containing black objects that resemble spores. Note crystalline mineral precipitates within cellular spaces. b) Fragment of stained vessel.

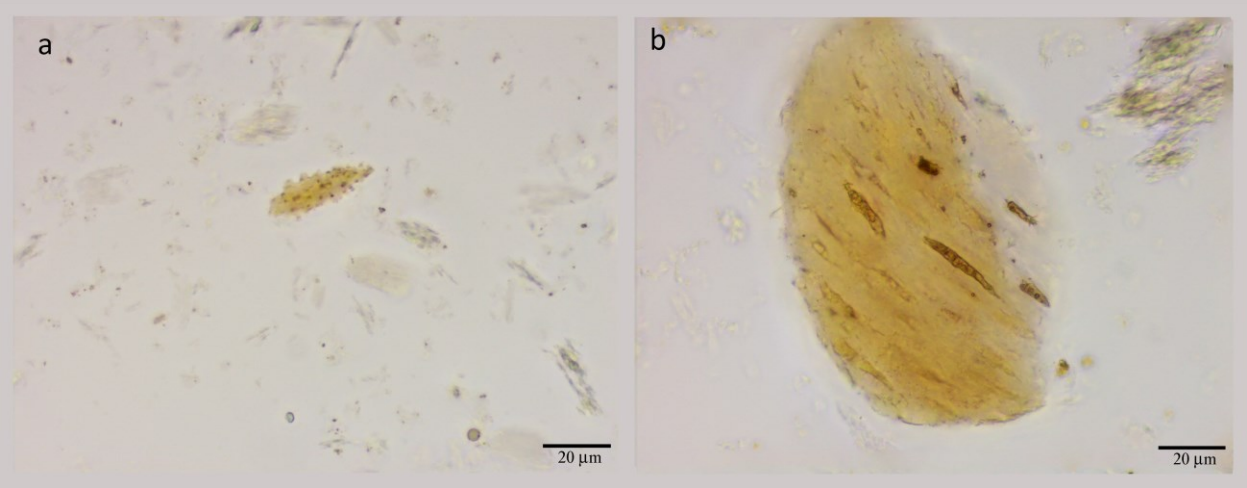

Figure 5-8. Osteocytes recovered from UALVP 57428. a) isolated osteocyte with filipodia bases projecting from the surface. b) cluster of osteocytes within an organic fibrous matrix.

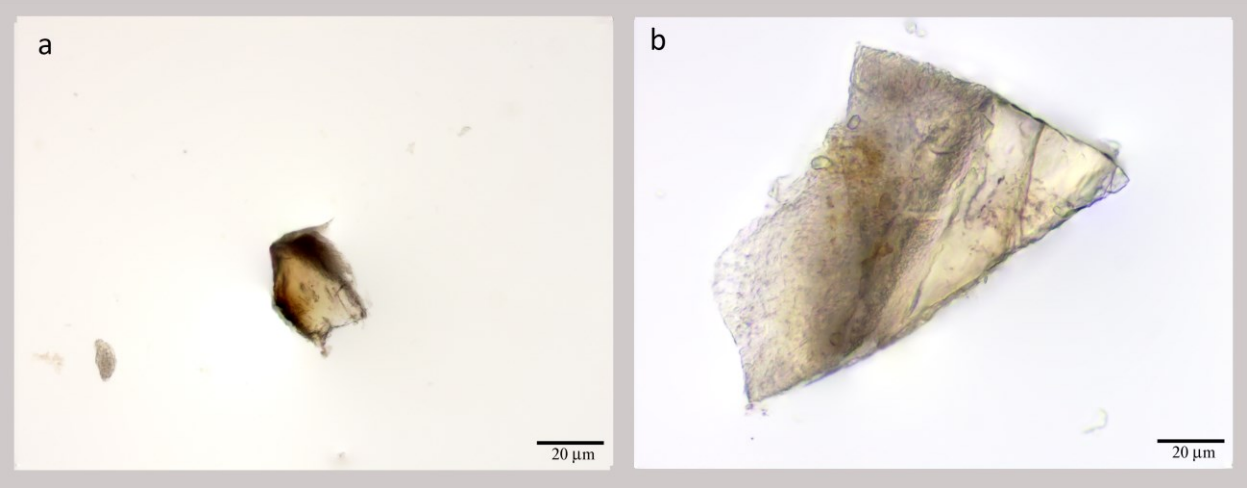

Figure 5-9. Vitrified bone fragments from UALVP 59554. No organics were recovered from this specimen.

Chapter 6: Preservation frequency of tissue-like structures in vertebrate remains from the Upper Campanian of Alberta: Brazeau Formation

6.1 INTRODUCTION

Original tissue research in the geological record has been a recent development in vertebrate palaeontology (Asara et al., 2016; Cleland et al., 2015; Embery et al., 2000; Muyzer et al., 1992; Saitta et al., 2018, 2017; San Antonio et al., 2011; Schweitzer et al., 2016a, 2013a, 2013b, 2009b, 2005b, 1997; Smith and Hayward, 2010; Wiemann et al., 2018). Previous work (Chapter 3) conducted on a variety of bone from the Dinosaur Park Formation suggested that original tissues are far more common than initially anticipated. Dissolution of bone from the Horseshoe Canyon and Wapiti Formations indicates that alteration of the bioapatite into a vitrified form destroys tissue-like structures (Chapter 4).

The Brazeau Formation is a near-source proximal fluvial alluvium sequence exposed along the eastern Rocky Mountain Front Ranges, Ram Range, and Foothills (Fig. 6-1). Unfortunately, little detailed work has been conducted on the stratigraphy of the Brazeau Formation (Chapter 8). Due to the lack of radiometric dating of volcanogenic deposits from the Brazeau Formation (Chapter 8), stratigraphic positions of specimens were determined using geological maps and local lithology compared to that described by Jerzykiewicz, (1997). Although the Brazeau Formation spans a variety of depositional environments and regions, specimens collected for this study primarily originate from proximal fluvial systems. Two specimens have been linked to lacustrine deposits based on their association with freshwater stromatolites. These stromatolites are primarily reported from the middle Brazeau and have

been suggested to indicate lakes that are time equivalent to the Bearpaw Formation in central and eastern Alberta (Jerzykiewicz 1997).

Vertebrate remains from the Brazeau Formation are significantly under-sampled. The only specimens officially reported in scientific literature were briefly mentioned in a geology report from the Canadian Department of Mines and Resources (Lang 1947). These specimens were collected by R.C. Sibley, a local train station attendant in Entrance, Alberta. He sent them to the America Museum of Natural History, where they were identified as *"*Corythosaur*"* bones and *"Gorgosaurus"* teeth by Dr. Barnum Brown (Chapter 9, Lang, 1947) based on similarities with specimens in the area that is now Dinosaur Provincial Park in southern Alberta. Langston (1959), published a conference field guide article briefly discussing fossil vertebrates from Alberta. In this article, he states that a fauna from the Saunders formation – which in its upper parts contains Paleocene mammals – in the Foothills has a strong Foremost and Oldman flavour with *Aspideretes, Basilemys, Compsemys, Lepisosteus, Myledaphus*, a crocodile and various dinosaurs. Unfortunately, the Saunders is not, and was not considered a formation during the time of the publication of the field guide; instead it was, and still is, the Saunders Group. The Saunders Group is subdivided into three formations, namely (from bottom to top) the Brazeau, Coalspur, and Paskapoo Formations (Jerzykiewicz 1985a). Because of this, it is difficult to know from which formation these specimens would have originated. The taxa that Langston (1959) claimed are known from the Saunders Group are all known from other Campanian and Maastrichtian formations of Alberta. A thorough investigation into vertebrate palaeontological collections throughout Canada (CMN, Redpath, ROM, RSM, TMP, and UALVP), the American Museum of Natural History (location of material collected by R.C. Sibley), and the Museum of

Natural History London (as many collections from Alberta were sold to this museum) have revealed no evidence of any specimens from the Brazeau or Coalspur formations representing the taxa listed by Langston. Lithologically and structurally, the Brazeau Formation and the time equivalent St. Mary River Formation (southern Alberta Foothills and Plains) are very similar and can be difficult to distinguish, which suggests there is a gradational boundary between the two formations (Jerzykiewicz 1997). Because each of the taxa reported by Langston (1959) is found in the St. Mary River Formation, and no museum records of these taxa in the Brazeau Formation are known, it is possible that the list provided in the field guide resulted from a misinterpretation of formational boundaries. Therefore, there is no existing proof that any of these taxa originated from the Saunders Group, or the Brazeau Formation.

For the present study, eight dinosaur bone fragments were collected from the lower, middle, and upper units of the Brazeau Formation throughout the central Alberta Foothills and sampled for dissolution (Fig. 6-1). Specimens from the Brazeau Formation were chosen to investigate the preservation rate of original organic structures in an (overall) near-source topographically elevated upland fluvial depositional environment. Although the majority of the Brazeau Formation represents fluvial environments, it must be noted that when the Western Interior Seaway (represented by the most western extent of the Bearpaw Formation) was at its highest levels, the region had extensive fresh water lakes, now reflected in shale, lake margin, lake delta, and fresh water stromatolites (Jerzykiewicz 1985a, 1997, Jerzykiewicz and Sweet 1988). Although no correlation has been found between preservation rates, degree of articulation, or sedimentation rates within the Dinosaur Park Formation (Chapter 3), the Horseshoe Canyon Formation appears to preserve vessels more readily in sandstones (Chapter

4). Three different factors that may influence organic tissue preservation are investigated: sediment type, the degree of articulation of a specimen, and depositional environment. Original organic structures that were most commonly recovered and identified from the Brazeau Formation are vessels (Fig. 6-2), EOM (Fig, 6-3), and osteocytes (Fig. 6-4). One specimen produced preserved fungal hyphae (See 6.3.4).

6.2 MATERIALS AND METHODS

6.2.1 Specimen Selection

Samples for analysis were selected from among recently collected specimens from the Rocky Mountain Foothills in Alberta, Canada, found along the James River in Clearwater County and along the Athabasca River in Yellowhead County. Specimens were never exposed to glues or consolidants. Bone fragments were collected by members of MADP to ensure that they were not contaminated with glue, or with bacteria accumulated during long term storage. Because relatively few specimens were recovered from the Brazeau Formation for this study, only eight specimens were sampled. Of these eight, only one was recovered from subsurface sediments, whereas all others were bones that were found on rockslides or along the edges of riverbanks. Specimens that were clearly exposed for extended periods of time were prepared to expose unweathered surfaces. Once fresh bone was exposed, samples were removed.

6.2.2 Dissolution of samples

Specimen treatment log sheets were kept as each sample was dissolved or other treatments were performed (Appendix 6-2).

6.3 RESULTS

On average, at least one type of tissue-like structure was recovered post-dissolution in six of every eight specimens, and four specimens produced all three structures (vessels, EOM, and osteocytes). However, the amount recovered varied between samples (Table 6-1). Specimens that produced a sufficient number of tissue-like structures had samples removed for $\delta^{13}C$ and $\delta^{15}N$ isotope analysis. All specimens sampled herein are hadrosaurid due to the rarity of other taxa in the Brazeau Formation. .

6.3.1 Hadrosauridae indet**.** (Ornithischia, UALVP 60166, fragment, sandstone, Fig. 6-1 "A")

UALVP 60166 is an associated hadrosaurid skeleton that was discovered in a large cobble conglomerate from a rockslide. The skeleton has not yet been collected due to the difficulty of removing it from a cliff face, but bone fragments were sampled for dissolution. The specimen preserves all tissues of interest in this investigation. Vessels are typically moderately to heavily stained and are brittle, fracturing easily (Fig. 6-5). EOM is moderately abundant and still retains a slightly fibrous texture (Fig. 6-3). Osteocytes are common (100s-1000s per 40 µL of spent EDTA), and regularly retain complete filipodia; some are preserved within collagen-like mats (Fig. 6-3).

6.3.2 Hadrosauridae indet**.** (Ornithischia, UALVP 60165 (JR.2017.001), femur recovered in a sandstone, Fig. 6-1 "A")

UALVP 60165 is a large hadrosaur femur that was preserved at the bottom of a channel sandstone. Fragments were removed but the specimen was not collected because of the unstable nature of the rockface. The dissolved samples contained all three tissue structures of interest. Most organic structures are moderately stained, with the vessels preserving minerals

within the lumina. Vessels are common but are fragmentary and unstained. They appear to have a crystalline-like appearance and contain multiple red, spherical, blood cell-like objects with darkened centres that resemble nuclei (Fig. 6-6). EOM and osteocyte structures are also common and are regularly found associated. Osteocytes are primarily found *in situ* within the fibrous extracellular organic matrix (Fig. 6-4). Preservation quality of the osteocytes is good, with most retaining filipodia and nucleus-like structures.

6.3.3 Hadrosauridae indet**.** (Ornithischia, UALVP 60164, dorsal vertebra, from a sandstone with stromatolite-like structures, Fig. 6-1 “A”)

UALVP 60164, an isolated hadrosaurid dorsal vertebra preserved within a stromatolitic concretion of sandstone contained no tissue like structures. Although the bone appears to be well preserved, with a moderate level of mineralization of porous spaces, the bone appears under high magnification to have been altered into a vitrified form. Lacunae are visible, but no osteocytes remain (Fig. 6-7).

6.3.4 Hadrosauridae indet. (Ornithischia, UALVP 60167, unidentifiable fragment in sandstone, Fig. 6-1 “B”)

UALVP 60167 is a poorly preserved, unidentifiable bone fragment recovered from the base of a sandstone unit. The surface has a powdery consistency, whereas there is a crumbly interior white texture. Samples were removed from the best-preserved part of the cortex in the hope that tissue preservation would be better in this region. Vessels are numerous, although not well preserved. EOM is uncommon, but present with staining. Osteocytes were not recovered. Fungal hyphae are also found and appear to be non-septate (Fig. 6-8), unlike the

septate forms described from the Wapiti Formation (Fig. 5-5). Staining of hyphae suggests that these are Cretaceous in origin, and not modern.

6.3.5 Hadrosauridae indet**.** (Ornithischia, UALVP 60163, caudal vertebra in sandstone, Fig. 6-1 "A")

UALVP 60163, an isolated caudal vertebral centrum that was collected from an organic rich sandstone. It produced EOM-like structures in low quantities but no other soft tissue structures. Based on the powdery bone quality, it is thought that the vertebra was exposed for an extended period prior to final burial.

6.3.6 Hadrosauridae indet**.** (Ornithischia, UALVP 58024, bone fragment from associated skeleton found in mudstone, Fig. 6-1 "C")

UALVP 58024 is a fragment of unidentified bone from a partial hadrosaurid skeleton that was sampled for dissolution. It was recovered from a rubble pile produced during construction. The specimen produced all three tissue structures of interest. Vessels are numerous, although they have a crystalline appearance and fracture easily. EOM-like structures are common and have a yellow-brown colouration and a fibrous texture. Well preserved osteocytes are common and are mostly intact, with filipodia that are missing only the finest ends (Fig. 6-9)

*6.3.7 Edmontosaurus regalis***.** (Hadrosauridae, UALVP 60178, bone fragment from a bonebed in mudstone, Fig. 6-1 "C")

UALVP 60178, a bone fragment surface collected from mudstone in the Bennett Bonebed (upper Brazeau Formation, lower Maastrichtian, Chapter 8), preserved all tissue structures of interest in abundance. All tissue structures are heavily stained, with vessels appearing globular on their surfaces (Fig. 6-2). EOM structures are stained yellow-brown and retain fibrous textures (Fig. 6-10). Osteocytes, although darkly stained, are exceptionally well preserved, and still possess the finest tips of their filipodia (Fig. 6-4).

6.3.8 Lambeosaurinae indet**.** (Hadrosauridae, UALVP 60162, associated skeleton in mudstone, Fig. 6-1 ”A”)

UALVP 60162 is a partial lambeosaurine skeleton identified by a presence of an ischial boot recovered from lacustrine deposit. The lacustrine environment was identified based on an abundant of clams, high amounts of organics, and stromatolite-like structures encasing several elements. A fragment of bone collected as surface float was sampled for tissue recovery. No soft tissue was recovered from the specimen; however, bone preservation has caused the bioapatite to have been altered into a vitrified form. Empty lacunae are visible within the altered bone matrix.

6.4 DISCUSSION

Specimens sampled for this research were collected during a preliminary investigation into vertebrates of the Brazeau Formation. Because no previous description of vertebrate material from the Brazeau Formation has ever been published, material from the Bennett Bonebed in Entrance, AB, was described (Chapter 8). Although *Edmontosaurus regalis* has been identified in the Upper Brazeau Formation in the Entrance area, unidentified hadrosaurids from

much lower in section, such as the associated skeleton from the lower Brazeau Formation (Oldman Formation equivalent), is not anticipated to be the same taxon. Because the Brazeau Formation spans ~13 million years, it provides an excellent opportunity to sample a wide variety of taxa, from a variety of different depositional environments. For this study, six of the eight specimens sampled originated from proximal fluvial, near source environments. Each of these six specimens produced at least one type of tissue-like structure. The two specimens that were not from proximal environments were recovered from lacustrine deposits from coastal floodplains and did not produce any tissue structures.

In general, the preservation of tissues is similar to that seen in specimens from other regions studied in Alberta (Chapters 3,4,5,7), and elsewhere around the world (Schweitzer et al. 2007b). All tissues appear to be semi-flexible, with only a few specimens possessing vessels that appear crystalline. These types of crystalline vessels also appear regularly in Alberta (Chapters 3,4,5) and have been reported by Schweitzer et al., (2007) from a variety of taxa throughout the past 67 million years of geological history. Staining seen in many of the tissues from the Brazeau Formation is like that observed in all other formations from Alberta, as well as formations from other geographic regions (Asara et al. 2007, Bertazzo et al. 2015, Wiemann et al. 2018). Wiemann et al. (2018) proposed that this staining is due to crosslinking of proteins that form an N-heterocyclic polymer. This supports the idea that these tissues are at least in some form “original” organic compounds. The degree of differential staining and the partial crystallization of tissue structures, however, may contradict this interpretation. Further research into the true nature of the staining is required. One specimen (UALVP 60165) preserved a large quantity of red blood cell-like objects that match the morphology of other

structures interpreted as blood cells (Schweitzer et al. 2005b, 2007b). These were preserved in fossil vertebrates from Montana, as well as specimens from the Dinosaur Park Formation (Chapter 3).

EOM represents the most commonly preserved type of soft tissue structure, occurring in 75% of specimens. About 63% of specimens preserve vessels, 50% preserve osteocytes, and around 13% preserve red blood cells. An unidentifiable bone fragment with a powdery surface consistency preserved fungal or lichen non-septate hyphae similar to those observed from the Horseshoe Canyon (Chapter 4) and Wapiti (Chapter 5) formations. Although rigorous study of the hyphae is outside the scope of this research, it is possible that those recovered could lead to better understanding of the environmental conditions to which specimens were exposed prior to final burial. The frequency with which fungal hyphae are recovered from bone with a powdery consistency (Chapters 4 and 5) suggests that this type of preservation reflects an extended period of time exposed to environmental conditions prior to final burial. The bone may have been damaged through bacterial, floral, saprophytic fungal, solar, or scavenging-related factors, among many others. Additional damage may be subsequently caused by partial mineralization of the bone as crystals precipitate within the voids, expanding and fracturing the bioapatite.

The depositional history of the Brazeau Formation is complex; the lowest portion represents a shallow nearshore marine environment that passed through a regressive sequence to become an upland near-source environment dominated by a braided river plain (Jerzykiewicz 1997). This was followed by the transgressive sequence that represents the maximum flooding surface of the Western Interior Seaway, which culminated in a coastal floodplain environment

with lacustrine deposits. The Upper Brazeau Formation represents a regressive sequence associated with the final regression of the Western Interior Seaway, beginning with a coastal floodplain environment with lacustrine deposits through to a proximal fluvial, near source, environment with sporadic lacustrine and overbank deposits. Because of this regression/transgression/regression cycle, it is possible to investigate the potential of soft tissue preservation to determine if it is controlled by the proximity to coastal floodplain environments. Although this study relied on a small sample size, there does appear to be a direct indication that lacustrine environments may have an influence on altering bioapatite into a crystalline form that has a vitrified appearance. Although the processes behind the vitrification of bone preserved in lacustrine deposits are currently unknown, the process involved in the alteration of the bioapatite appears to always destroy all organics within the bone (Chapters 4 and 5). Experiments performed on modern *Alligator* bone suggests that microbial action after burial in wetland environments alter the hydroxyapatite into a more thermodynamically stable fluorine-rich apatite (Keenan and Engel 2017). This suggests a similar or more long-term alteration process occurs in specimens from deep time, ultimately destroying all original organics. The recrystallization of bioapatite into a new form of large-crystal apatite is speculated to cause the rupture of the phospholipid bilayer causing the lysis of cellular tissue structures.

6.5 CONCLUSIONS

The high numbers of well-preserved osteocyte structures in specimens collected from the Brazeau Formation for this study suggests the environmental conditions responsible for soft tissue preservation were near-ideal, at least for a terrestrial setting. Although those specific

conditions have not been specifically addressed herein, continued investigation into other formations should provide further evidence of what geological factors influence the preservation of original tissues. Alteration of bone into a vitrified form appears to be linked to lacustrine deposits, providing some insight into one factor of preservation. Vitrified bone in the Brazeau Formation appears nearly identical to that observed in the Horseshoe Canyon and Wapiti Formations. In all three formations, the specimens lack any soft tissue structures. This suggests that the process that results in this form of preservation may be more important to investigate than the factors of preservation. Furthermore, specimens recovered from proximal, near-source, fluvial environments appear to preserve delicate structures more readily and with finer details than do coastal floodplain environments.

Table 6-1. List of samples derived from specimens and types of soft-tissue preservations noted for each. AS, Associated skeleton; BB, Bonebed; I, Isolated bones. Abundance of tissue-like structures, X, rare; XX, common; XXX, abundant. Change numbers to catalogue numbers.

Taxon	Element	Specimen number	Vessels	EOM	Osteocytes	Fungal Hyphae	Association
Ornithischia							
Hadrosauridae indet.	Fragment	UALVP 60166	XX	XX	XXX		As
Hadrosauridae indet.	Femur	UALVP 60165	XX	X	X	-	I
Hadrosauridae indet.	Dorsal Vertebra	UALVP 60164	-	-	-	-	I
Hadrosauridae indet.	Fragment	UALVP 60167	XX	X	-	X	I
Hadrosauridae indet.	Caudal Vertebra	UALVP 60163	-	X	-	-	I
Hadrosauridae indet.	Fragment	UALVP 58024	XX	XX	XX	-	AS
Edmontosaurus regalis	Fragment	UALVP 60178	XXX	XXX	XXX	-	BB
Lambeosaurinae indet.	Fragment	UALVP 60162	-	-	-	-	As

FIGURES

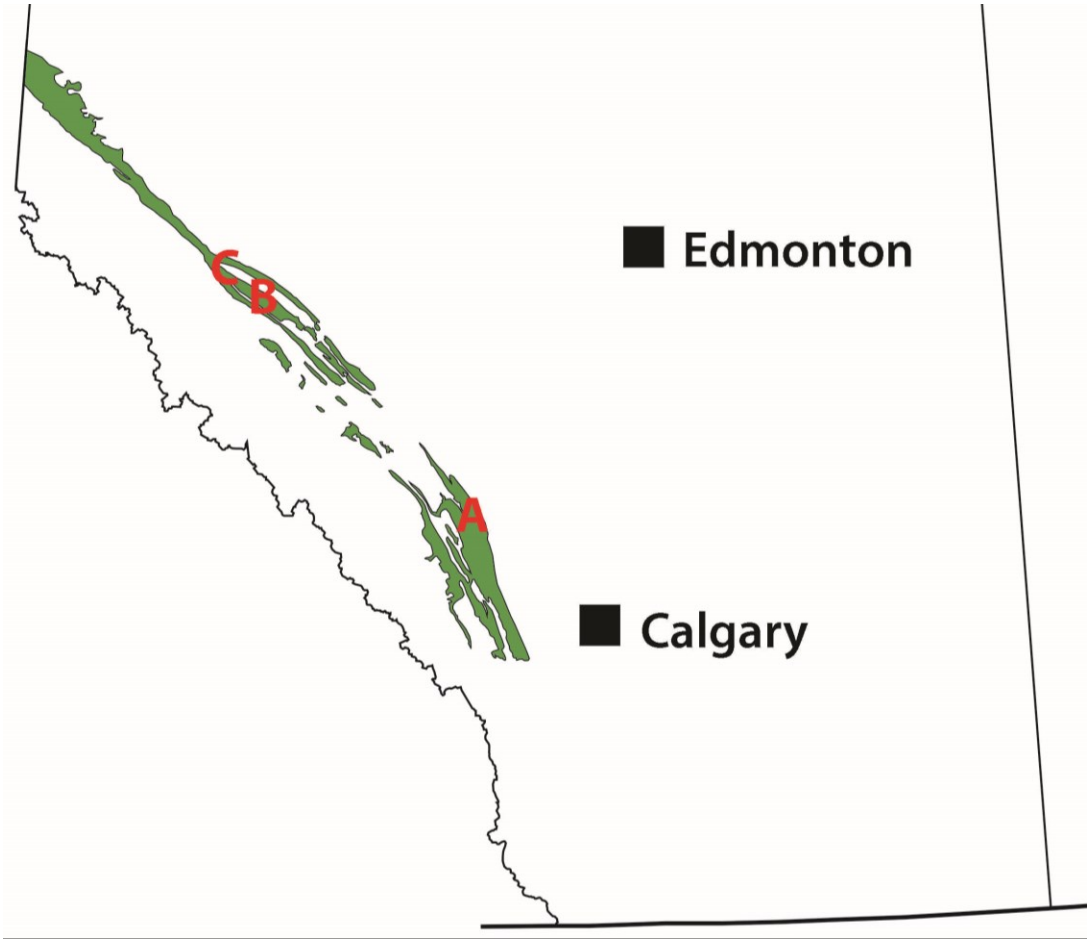

Figure 6-1. Map of southern Alberta showing the surface distribution of the Brazeau Formation (green). Red letters indicate locations from which specimens were recovered.

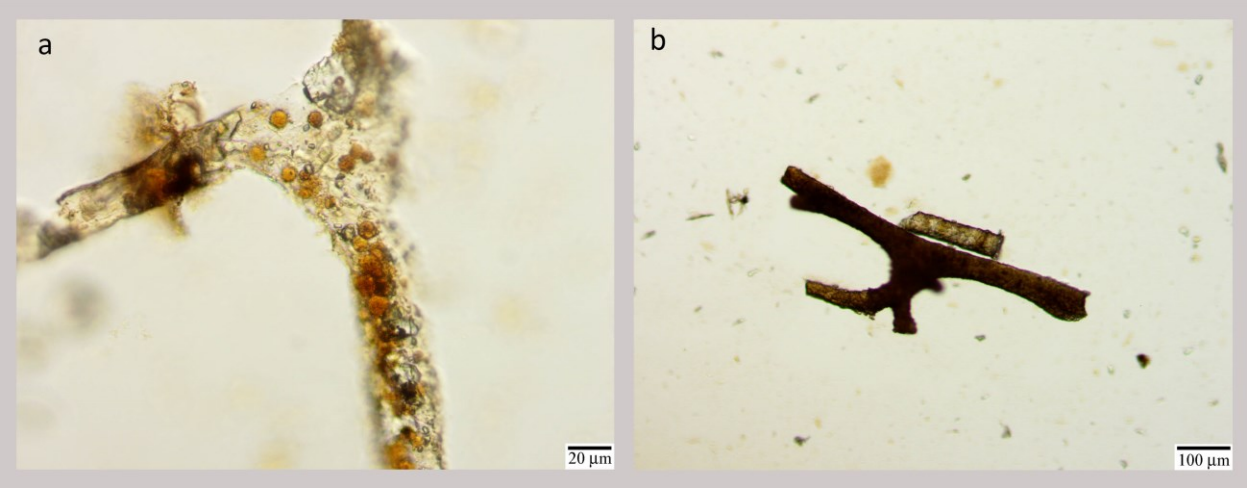

Figure 6-2. Select blood vessel-like structures. a) UALVP 60165, Hadrosauridae indet. from a femur. b) UALVP 60178, *Edmontosaurus regalis,* from a flat bone from a bonebed.

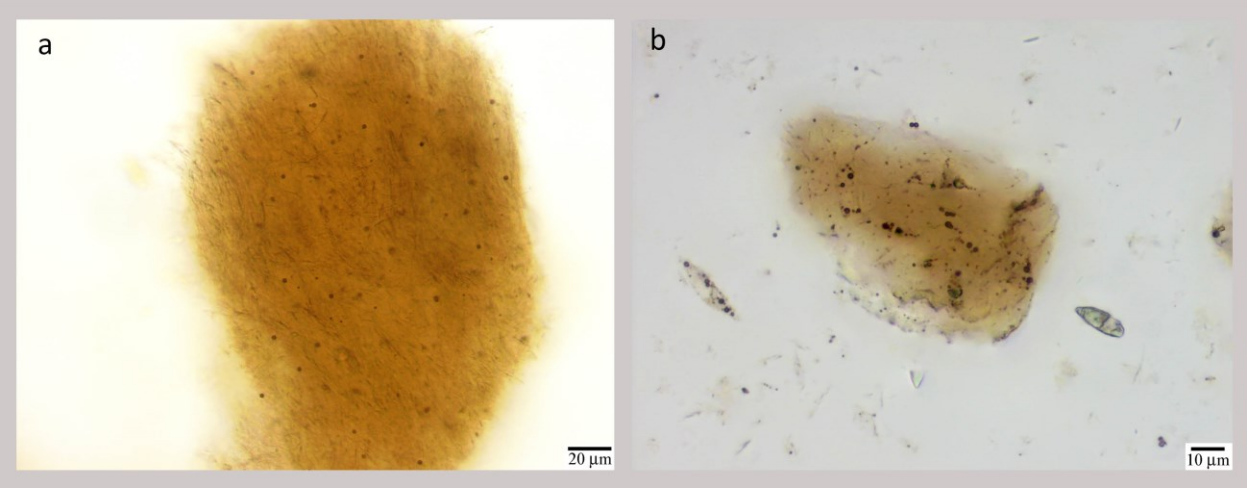

Figure 6-3. Extracellular organic matrix-like structures with osteocytes preserved within. a) UALVP 60165, Hadrosauridae indet. from a femur. b) UALVP 60166, Hadrosauridae indet. from a bone fragment.

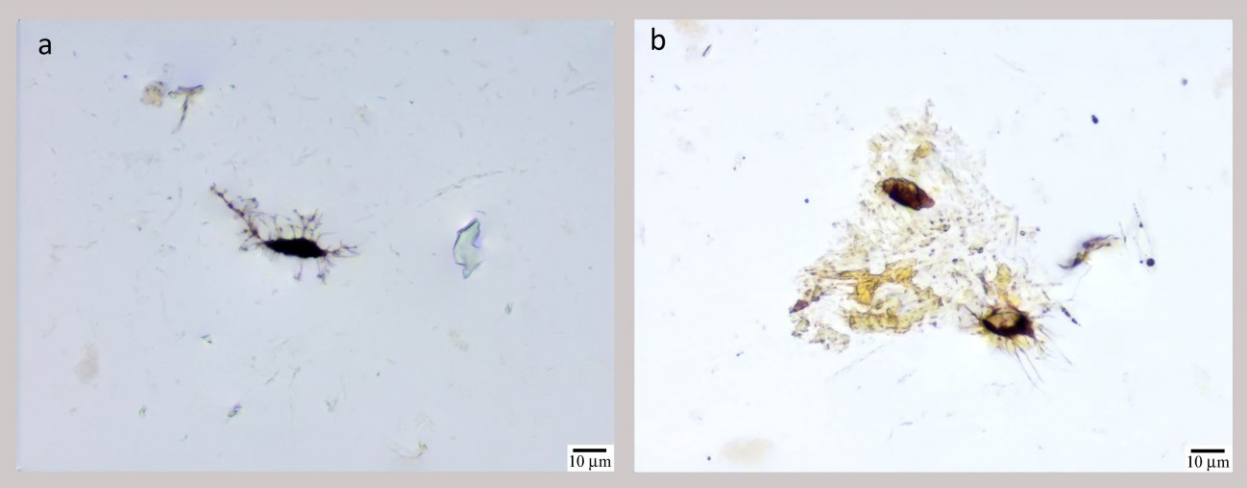

Figure 6-4. Select osteocyte-like structures. a) UALVP 60178 *Edmontosaurus regalis,* from a flat bone. b) UALVP 60165, Hadrosauridae indet. from a femur. Filipodia are observed are numerous and moderately well preserved.

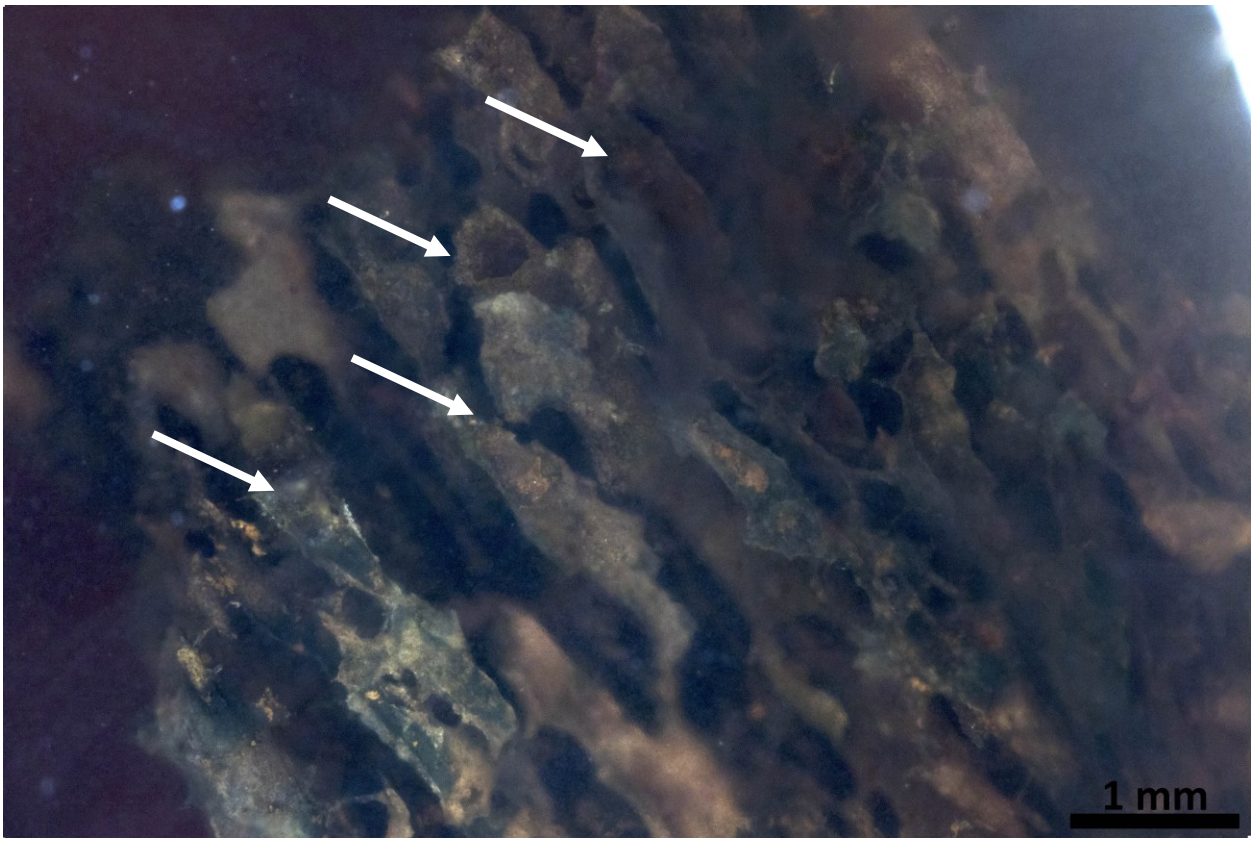

Figure 6-5. Vessel structures *in situ* within bone fragment exposed during dissolution of UALVP 60166. Image taken using Canon 7D Mk II and macro lens. Arrows point to ends of vessels.

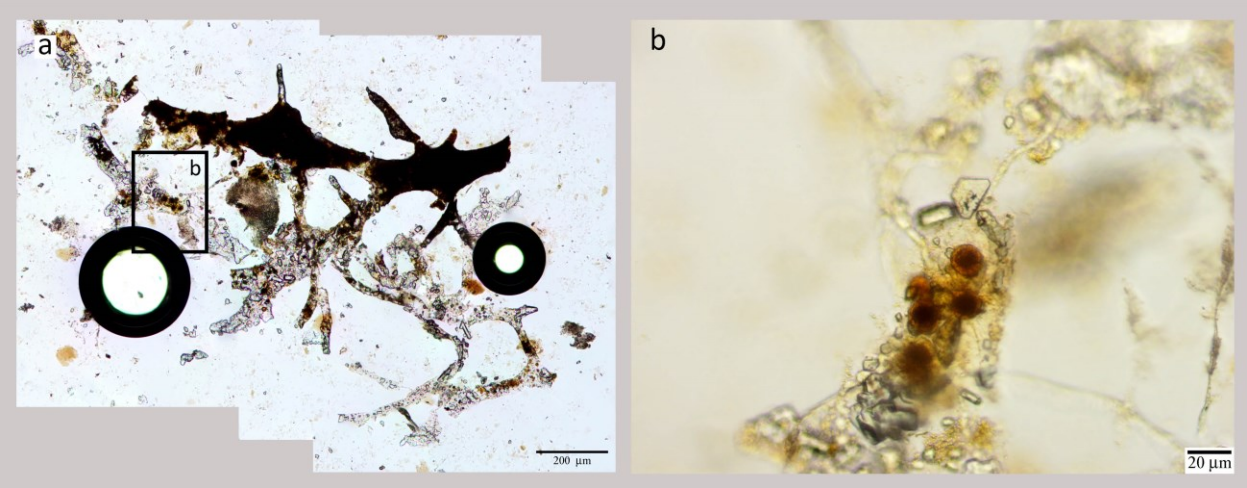

Figure 6-6. Vessels recovered from UALVP 60165. a) Three-dimensional vessel network (black circles are air bubbles beneath glass coverslip, bubbles formed after initial image capture of image “b”). b) enlarged area in “a” (rotated 90^{o}) showing detail of red blood cell-like structures contained within the lumen of the vessel structure. Note the darker coloured internal spherical structure within the RBC-like structure.

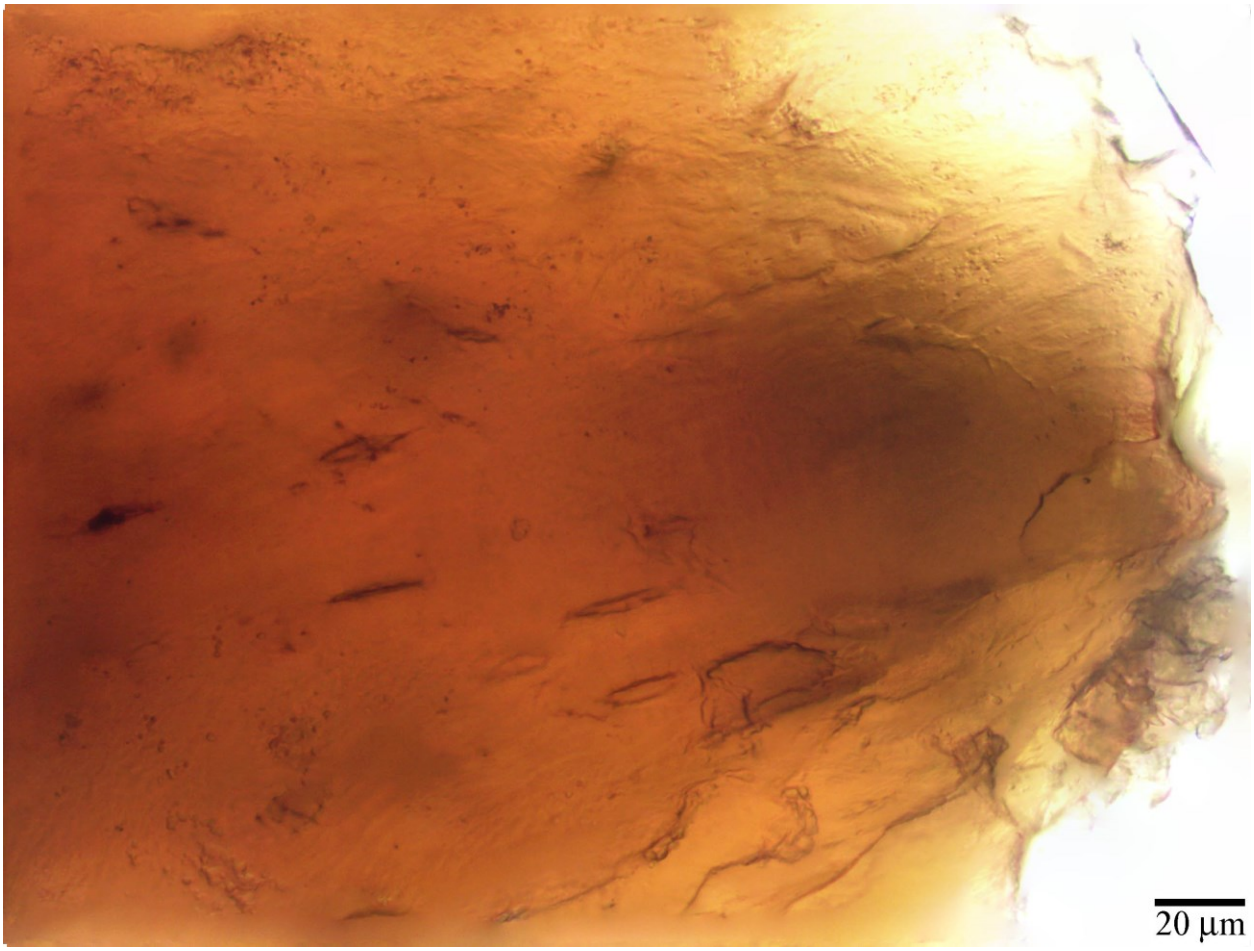

Figure 6-7. Vitrified bone fragment from UALVP 60164, recovered from a concretion formed by a freshwater stromatolite. No organics were recovered from this specimen. Note empty osteocyte lacunae.

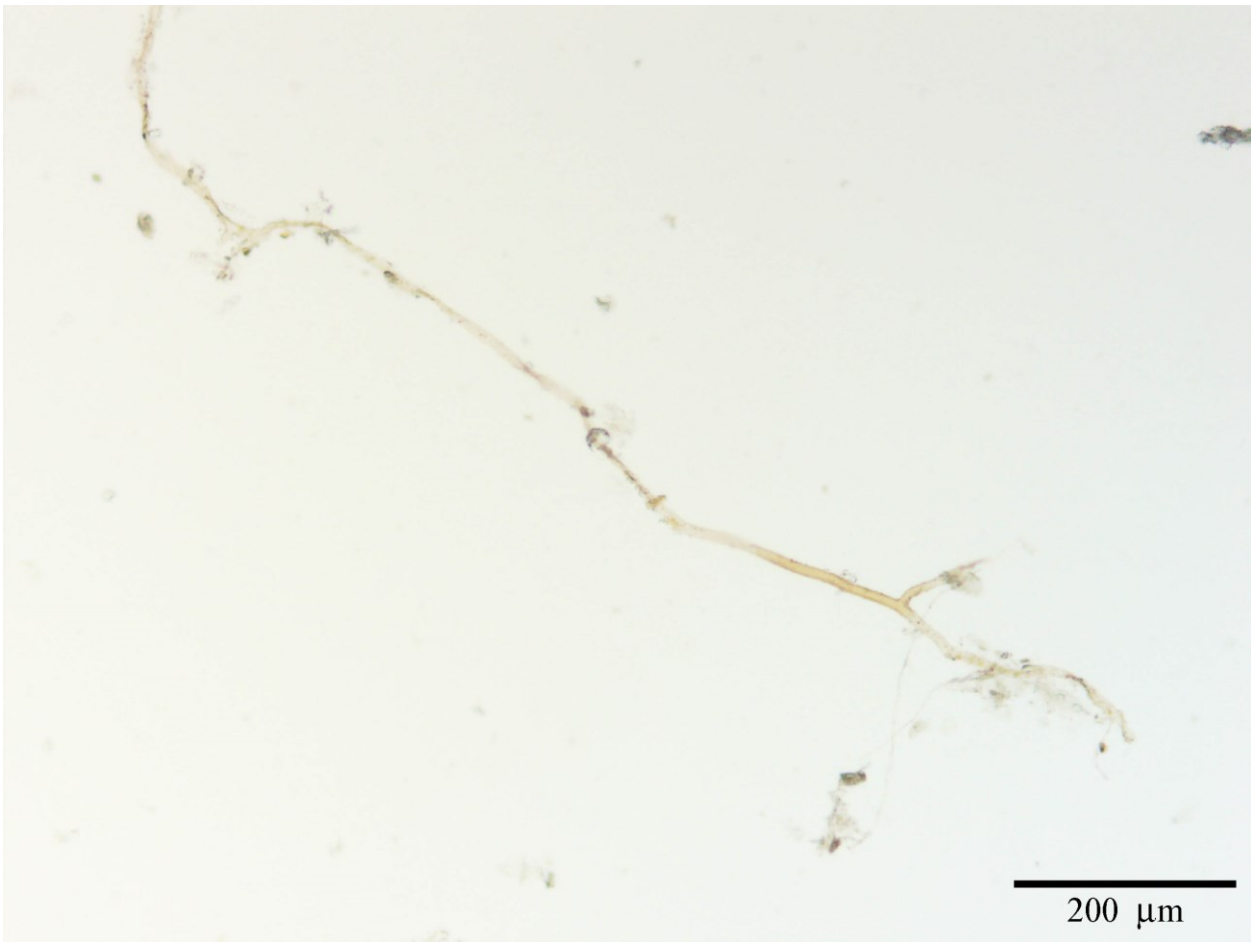

Figure 6-8. Fungal hyphae recovered from UALVP 60167, an unidentifiable, heavily weathered and powdery bone fragment. Note that the hyphae are none-septate.

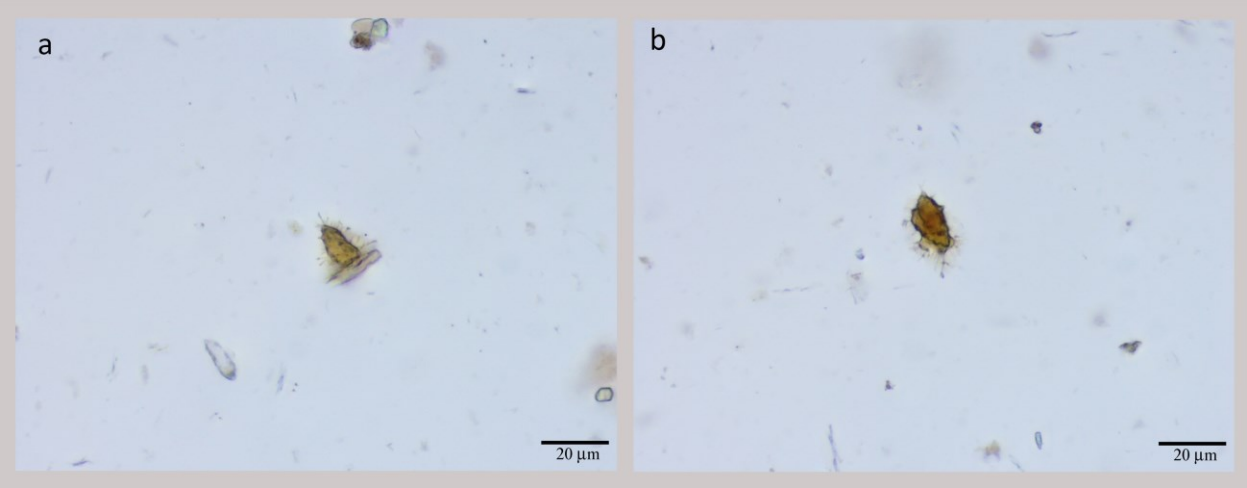

Figure 6-9. Osteocytes recovered from an associated hadrosaur skeleton, UALVP 58024. Note the majority of filipodia remain intact but are missing only the finest tips.

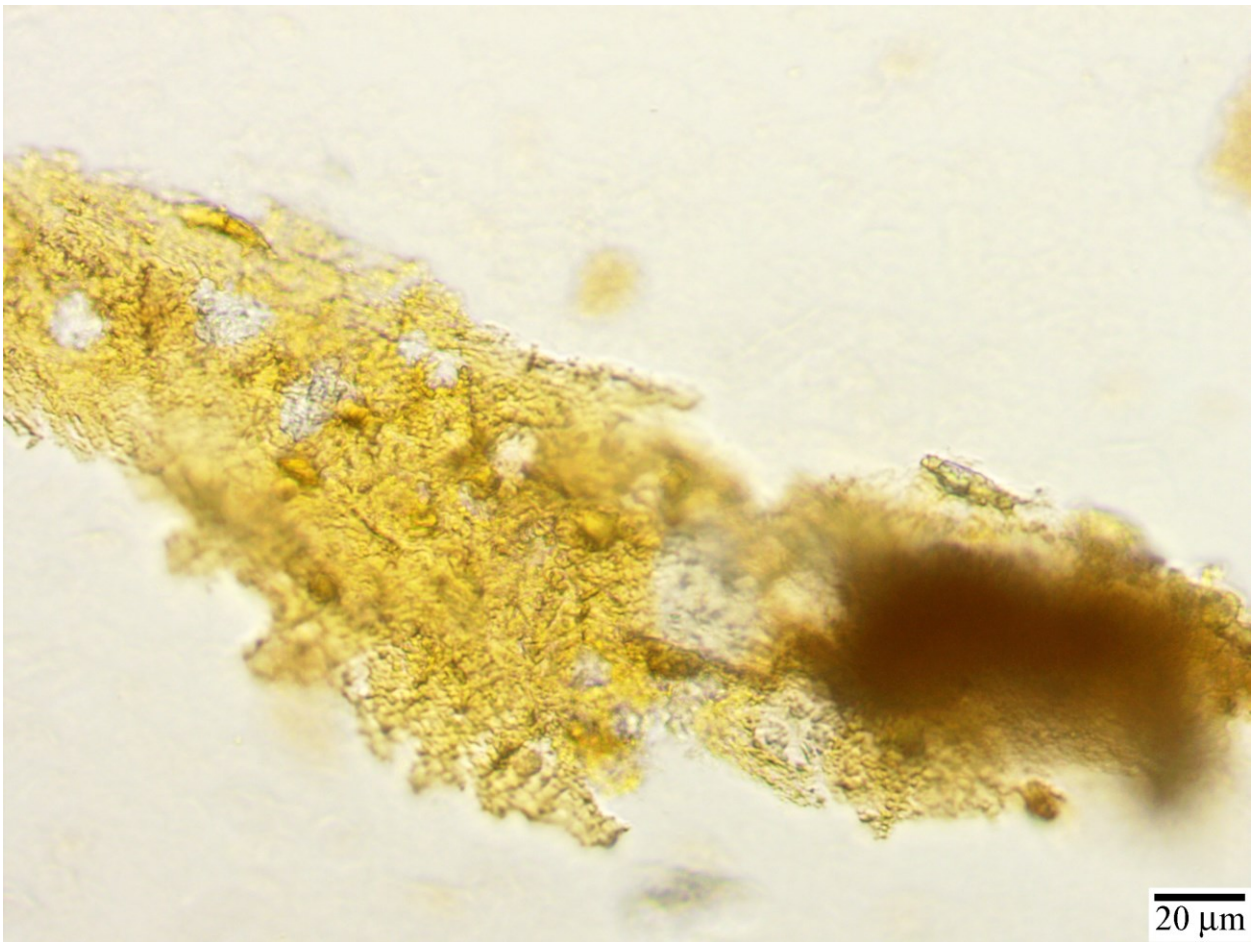

Figure 6-10. Extracellular Organic Matrix recovered from UALVP 60178. Note slight fibrous texture and significant yellow staining to the organics suggesting the cross linking of proteins.

Chapter 7: Preservation frequency of tissue-like structures in vertebrate remains from the Upper Campanian of Alberta: Upper Foremost Formation

7.1 INTRODUCTION

Research of original soft tissue structures in a palaeontological context has been a recent development in vertebrate palaeontology (Muyzer et al. 1992, Schweitzer et al. 1997, 2005b, 2009b, 2013, 2014, 2016a, Embery et al. 2000, Asara et al. 2007, Smith and Hayward 2010, San Antonio et al. 2011, Cleland et al. 2015, Saitta et al. 2017, 2018, Wiemann et al. 2018). Previous work conducted on a variety of bones from several upper Cretaceous formations suggested that original soft tissues are far more common than initially anticipated (Chapters 3, 4, 5, 6). Dissolution of bone from the Brazeau, Horseshoe Canyon, and Wapiti Formations indicates that alteration of the bioapatite into a vitrified form destroys tissue-like structures (Chapters 4, 5, 6), and that this may be related to geochemical influences in lacustrine or wetland palaeoenvironments (Chapter 6).

The Foremost Formation represents a series of small transgressive/regressive events centred around a shoreline, with both terrestrial and marine facies (Hathway et al. 2011, Thompson 2018). The upper Foremost represents the last small transgressive event prior to the regression series of the Oldman Formation. It is represented at the mouth of White Rock Coulee (South Saskatchewan River, Alberta) by two large sandstone units containing swaley cross-stratification separated by a six-metre-thick brown silty mudstone containing the foraminferan *Haplophragmoides* (Hathway et al. 2011). Swaley cross-stratification is formed between fair-weather and storm wave base in near shore environments (Hathway et al. 2011),

suggesting the sands of the Upper Foremost in the White Rock Coulee area are close to the shoreline. Furthermore, a series of micro vertebrate sites found in the lower of the two sand units in the Upper Foremost Formation yield shark teeth and marine reptile bones almost exclusively, which supports derivation from a marine environment. Bone fragments show a high degree of abrasive wear, supporting the development of these micro vertebrate sites in a near fair weather wave base environment by constant wave action. Each small micro vertebrate site (~30 cm wide) is separated laterally from the next (~50-60 cm) in a repeating pattern. This pattern suggests that the assemblages formed in the bottoms of troughs in wave formed dunes in an upper shoreface facies.

All but one of the vertebrate fossils used in this study were collected from the same series of micro vertebrate assemblages from the lower two upper sands from the Upper Foremost Formation at the mouth of White Rock Coulee in southern Alberta (Fig. 7-1). The single specimen not from these sites was collected from the middle of the brown silty mudstone that separates the two upper sands, and which has been interpreted as an interfingered coastal and marine setting. Based on bone density and depositional setting, it is inferred that all specimens are marine reptiles. Significant numbers of marine fossils (shark teeth, other fish teeth, etc.), and an identifiable partial elasmosaurid limb element, suggest that most of the bone fragments tested in this analysis likely belong to the Elasmosauridae. These specimens were sampled for this study based on the depositional setting. All other specimens sampled from Alberta formations originate from terrestrial environments that ranged from coastal floodplains to proximal fluvial environments (Chapters 3, 4, 5, 6). Trends observed in the terrestrial formations suggest that coastal floodplains are detrimental to the preservation of

delicate tissues such as osteocytes. Specimens from the upper shore face environments of the Upper Foremost Formation were sampled to investigate how deposition in a saltwater setting affects preservation of original tissues. Structures that were most commonly recovered and identified in the Foremost Formation study are vessel-like (Fig. 7-2), EOM (Fig, 7-3), or osteocyte-like (Fig. 7-4). Fungal hyphae fragments were also recovered from two specimens (Fig. 7-5). Two specimens also contained structures that resembled red blood cells.

7.2 MATERIALS AND METHODS

7.2.1 Specimen Selection

Specimens were collected with the intention of being dissolved for this study; specimens of possible importance were not sampled. Due to all but one specimen originating from sandstone, matrix type will not be a factor investigated in this study. This is also the case with degree of articulation, so the present investigation concerns the preservation potential of near shore marine environments in a general sense.

7.2.2 Dissolution of samples

Specimen treatment log sheets were kept as each sample was dissolved or as other treatments were performed (Appendix 7-1).

7.3 RESULTS

All ten specimens tested produced at least two of the three main forms of tissues of interest. Of the ten specimens, seven contained all three tissues of interest; EOM, osteocytes, and vessels. Two specimens preserve red blood cell-like structures, and two contained fungal

hyphae. Several specimens produced significant amounts of tissue, sufficient for $\delta^{13}C$ and $\delta^{15}N$ isotope analysis. Findings are summarized in Table 7-1.

7.3.1 Elasmosauridae indet**.** (Plesiosauria, UALVP 60168, fragment, sandstone, Fig. 7-1 "A")

UALVP 60168 is a bone fragment recovered from an upper shore face microsite. It was broken into three small pieces using wire snippers for dissolution. The specimen preserves all tissues of interest. Vessels are lightly stained with a globular appearance. Several vessel fragments contain red blood cell-like objects that are spherical with a darker centre. Small amounts of precipitated minerals are visible within the laminae (Fig. 7-6). EOM is moderately abundant and still retains a slightly fibrous texture (Fig. 7-6). Osteocytes are common (100s-1000s per 40 µL of spent EDTA), and regularly retain complete filipodia. Several clusters of associated osteocytes were preserved within collagen-like mats (Fig. 7-6). Fungal remains were also recovered from this specimen; they contain mineral crystals within the cellular spaces and have orange staining, which suggests these are original structures and not modern contamination (Fig. 7-5). Interestingly, there appears to be two different taxa of fungus represented. The first has a smooth external surface and is non-septate, similar to those recovered from bone from other formations in Alberta (Chapters 4,5,6). The second, although it seems to be non-septate, may be too small to make a proper interpretations; it possesses multiple short (half the diameter of the hyphae), robust spines (Fig. 7-5). The proper identification of these fungi is outside the scope of this research, but further research on them may assist in identifying the palaeoecosystem in which burial occurred.

7.3.2 Elasmosauridae indet**.** (Plesiosauria, UALVP 60169, fragment in sandstone (Fig. 7-1 "A")

UALVP 60169, a bone fragment from an upper shore face microsite preserved EOM and osteocytes, but no vessels. Osteocytes and EOM are remarkably abundant, and their preservation is astounding. Large clusters of osteocytes remain *in situ* within collagen matrix; filipodia are still in contact with those of neighbouring osteocytes, forming three dimensional clusters of cells (Fig. 7-7). Osteocytes that have become isolated or are in pairs show complete filipodia, with the fine tips still intact (Fig. 7-4), while several show darkened centres that are interpreted as representing the nucleus. EOM is generally observed surrounding clusters of osteocytes (Fig. 7-7).

7.3.3 Elasmosauridae indet**.** (Plesiosauria, UALVP 60170, fragment in sandstone (Fig. 7-1 "A")

UALVP 60170 is from an upper shore face, microvertebrate site. Three small bone samples were removed from it. The specimen preserves EOM and vessels, but no osteocytes were observed. Vessels are moderately well preserved and are heavily stained (Fig. 7-2). The surface of each, although intact, has a small degree of globular-like texture seen in other specimens. EOM is uncommon, but when observed, preserves fibrous textures.

7.3.4 Elasmosauridae indet**.** (Plesiosauria, UALVP 60171, fragment in sandstone (Fig. 7-1 "A")

UALVP 60171 is a bone fragment recovered from the upper shore face, micro vertebrate site that preserves all three forms of tissue structures of interest. Vessels are common and form three dimensional networks (Fig. 7-8). EOM is abundant with fibrous textures and contains large numbers of well-preserved osteocytes still *in situ* (Fig. 7-8). Osteocytes are abundant (1000's per 35 µL of spent EDTA solution) and typically retain their three-dimensional network with filipodia still contacting those of their neighbouring osteocytes (Fig. 7-8). Although not

common, several osteocytes possess nucleus-like structures. All tissues recovered from UALVP 60171 are only lightly stained orange-brown.

7.3.5 Elasmosauridae indet**.** (Plesiosauria, UALVP 60172 (WRC-2018-005), fragment from sandstone, Fig. 7-1 “B”)

UALVP 60172 is an isolated bone fragment recovered from the upper shore face, micro vertebrate site that produced all tissue structures of interest. EOM is preserved, although usually only found surrounding vessels in a thin layer and still retains a fibrous texture. Vessels are very common but show alteration into orange-brown colours and globular texture. Osteocytes are common, but are not found in large three-dimensional networks in the way they are in other specimens in this study; they also lack the finest tips of the filipodia.

7.3.6 Indet**.** (Unknown taxon, UALVP 60173, fragment from mudstone, Fig. 7-1 “C”)

UALVP 60173 is a fragment of unidentified bone that is the only specimen in this study originating from mudstone. This specimen was recovered from the brown silty mudstone between the two upper sand units in the Upper Foremost Formation. Large quantities of all three tissue types of interest were recovered. EOM is most common surrounding small clusters of osteocytes and retains a fibrous appearance. Osteocytes are very common (1000’s per 35 µL of spent EDTA solution) and are exceptionally well preserved with light to heavy staining (Fig. 7-9). Most of the osteocytes observed retain the finest tips of filipodia and are commonly linked with their neighbours, creating small clusters of three-dimensional networks. Most osteocyte bodies are round to sub-round (Fig. 7-9). One osteocyte-like object possesses a nucleus-like

structure in an expanded body and may represent an osteoblast in the process of transforming into an osteocyte (Fig. 7-9).

7.3.7 Elasmosauridae indet**.** (Plesiosauria, UALVP 60174, fragment from sandstone, Fig. 7-1 “B”)

UALVP 60174 is a bone fragment recovered from the upper shore face micro vertebrate site. It has produced all three major tissue structures of interest. EOM is generally uncommon and found in thin layers surrounding osteocytes (FIG. 7-10). Osteocytes are frequently found and are preserved in excellent condition. Lightly to moderately stained, osteocytes retain all filipodia for what is estimated to be nearly their entire lengths (Fig. 7-10). Several small clusters of osteocytes remain, although it is unclear if these clusters are in their original associations with their neighbours.

7.3.8 Elasmosauridae indet**.** (Plesiosauria, UALVP 60175, fragment, sandstone, Fig. 7-1 “A”)

UALVP 60175 is an unidentified fragment from the upper shore face micro vertebrate site. All three main tissue structure types of interest have been recovered from the sample, are abundant, and are found *in situ* regularly. Two separate three-dimensional fragments of tissue preserve vessel fragments surrounded by matrices of EOM containing intact networks of osteocytes (Fig. 7-11). Although the three-dimensional structure of the organic component of bone remains intact, the surfaces of all structures appear heavily modified into a globular-like appearance (Fig. 7-11). Despite the alteration to tissue surfaces, osteocytes retain the fine ends of the filipodia (Fig. 7-11).

7.3.9 Elasmosauridae indet**.** (Plesiosauria, UALVP 60176, fragment, sandstone, Fig. 7-1 “B”)

UALVP 60176 is an unidentified fragment from the upper shore face micro vertebrate site. EOM and vessels have been recovered from the sample, but not osteocytes. Also recovered were fragments of fungal hyphae and red blood cell-like structures within vessel lumina. All organic structures have similar degrees of staining, although the blood cell-like structures are darker and are a deeper red. EOM is uncommon, but that which is observed is fibrous in texture. Vessels are abundant and well preserved, although the surfaces are globular in appearance. The walls of the vessels are unique in having a peculiar crenulated structure (Fig. 7-2), which has not been seen in any other vessel structures recovered from formations from Alberta (Chapters 3, 4, 5, 6). The wavy appearance of these vessels may be the result of several factors. First, this specimen may not be from an elasmosaurid, and may be from some other large marine reptile such as a mosasaur, although this is unlikely. Second, if the animal had been a deep diver the wavy structure may be due to bone remodeling after damage from aerobullosis. Third, this texture may be the result of osteomyelitis, osteosarcoma, or some other disease of the bone itself.

7.3.10 Elasmosauridae indet**.** (Plesiosauria, UALVP 60177, fragment, sandstone, Fig. 7-1 “A”)

UALVP 60177 is a bone fragment from the micro vertebrate site that has produced all tissue structures of interest as well as red blood cell-like structures within vessels. Preservation of tissues is exceptional, with intact vessels being surrounded with EOM that appears slightly fibrous. Within the EOM surrounding vessels is a network of osteocytes, although not all osteocytes are well preserved. Several appear to have not been preserved whatsoever, leaving void lacunae. All tissues are moderately stained, and some alteration has occurred to the vessel walls to give the external surfaces a globular appearance. Most osteocytes retain filipodia,

although not to the degree of fine preservation that several other specimens have from the Foremost Formation. Mineral precipitation has occurred within vessels; however, mineral grain sizes are quite small, and do not appear to have affected tissues.

7.4 DISCUSSION

Specimens sampled for this research were collected with the specific intention for dissolution for the study of original tissue preservation. All specimens, except one, were collected from micro vertebrate accumulations concentrated within the troughs of dunes from an upper shore face facies in the Upper Foremost Formation at the mouth of White Rock Coulee in Prairie Coulees Natural Area (South Saskatchewan River), southern Alberta. Confirmation of the deposit being a near shore to upper shore face deposit comes from the large number of shark teeth, elasmosaurid teeth, sawfish teeth, and swaley cross-stratification found slightly below the micro vertebrate assemblages in stratigraphic section (Hathway et al. 2011). Fox (1974) described a single left tarsometatarsus from *Hesperornis cf. regalis* from the same sandstone horizons as the micro vertebrates collected for this study. Although Fox refers to these beds as being terrestrial in origin (Fox 1974), more recent work (Hathway et al. 2011, Thompson 2018) indicates these are marine and concludes the tarsometatarsus was not recovered from terrestrial deposits.

In general, the preservation of tissues recovered from the upper Foremost Formation near-shore marine deposits is exceptional. The tissues are found in an abundance not recovered from any other formation studied in Alberta to date (Chapters 3, 4, 5, 6). Quality of preservation resembles some previously published images (Schweitzer et al., 2005; Schweitzer,

2011). Tissues from the Foremost Formation retain a high degree of flexibility and do not show any form of the crystallization reported by Schweiter, (2011) or found in other Alberta specimens (Chapters 3, 4, 5, 6). Several specimens, however, do show signs of some alteration with globular-like surface textures. There can also be heavy orange-brown staining, which is hypothesized to be the result of protein cross-linking that forms N-heterocyclic polymers (Asara et al. 2007, Bertazzo et al. 2015, Wiemann et al. 2018).

Preservation rates are the highest reported from Alberta to date, with 100% of specimens preserving EOM, 90% preserving vessels, 80% preserving osteocytes, 20% preserving red blood cells, and 20% preserving fungal hyphae. The exceptional preservation of original tissues suggests further work into the preservational mode of the Foremost Formation should be undertaken. The flexibility of nearly all tissues, and the exquisite detail in the finest tips of osteocyte filipodia suggests that protein fragments may be present, which could provide the first molecular data for elasmosaurids. Many specimens preserved three-dimensional networks of osteocytes and collagen/elastin. Interestingly, the specimens sampled for this study must have been exposed to the surrounding marine environment for an extended period of time based on the significant amount of rounding and polishing exhibited. This suggests length of time exposed to the elements prior to final burial does not contribute to the likelihood of tissue preservation. A commonly proposed factor that influences the preservation of original tissues is the degree of anoxia (Schweitzer et al. 1997, Grellet-Tinner 2005, Schweitzer 2011), suggesting that anoxic environments inhibit bacterial growth that ultimately destroys organics. Based on sedimentological evidence of the dune structures from which the specimens were recovered, it appears that the specimens were buried in the upper shore face, a zone that is within the fair-

weather wave base. This constant turbulence and circulation of water, and proximity to the paleo shoreline, would suggest that the water in the area was well oxygenated. The elevated dissolved oxygen levels and the exceptional preservation of original tissues suggests that an anoxic environment does not have an effect on tissue preservation. Schweitzer (2011), proposed that sandstone may facilitate the drainage of the enzymes of decay. Regarding the specimens sampled herein, this factor may have an influence. However, because each specimen had clearly been weathering for an unspecified but probably long period of time prior to burial, any and all enzymes would have long been eliminated. Therefore, it is unknown in this case if the sandstone has any effect on the preservation of original tissues.

7.5 CONCLUSIONS

The extraordinarily high numbers of original tissues and the exquisite details that are preserved on structures such as osteocyte filipodia, indicate that the upper shore face facies of the upper Foremost Formation is a near perfect environment for preserving soft tissues. The depositional environment suggests that the time exposed to the environment prior to final burial does not play a major roll in tissue preservation, and neither do anoxic conditions. The sediments (sandstone) in this situation cannot be properly assessed for enzyme drainage because the length of exposure time for each specimen must have been highly variable. The degree of wear from wave action indicates long exposure to the elements in some cases. Based on swaley cross-stratification, high numbers of shark and fish remains, and dune structures, it is confirmed that these specimens originate from an upper shore face deposit. This suggests that

something about a near shore marine environment is beneficial to the preservation of original tissues. Further investigation and comparison between other formations and the fossil vertebrate preservation is still required. However, it is currently speculated that dissolved minerals or pH may play an important role in how original tissues persist in deep time.

Table 7-1. List of samples derived from specimens and types of soft-tissue preservations noted for each. I, Isolated; M, microvertebrate site. Abundance of tissue-like structures, X, rare; XX, common; XXX, abundant.

Taxon	Element	Specimen number	Vessels	EOM	Osteocytes	Fungal Hyphae	RBCs	Association
Plesiosauria								
Elasmosauridae indet.	Fragment	UALVP 60168	XXX	XX	XXX	X	X	M
Elasmosauridae indet.	Fragment	UALVP 60169	-	XXX	XXX	-	-	M
Elasmosauridae indet.	Fragment	UALVP 60170	XX	XX	-	-	-	M
Elasmosauridae indet.	Fragment	UALVP 60171	XXX	XXX	XXX	-	-	M
Elasmosauridae indet.	Fragment	UALVP 60172	XXX	X	XX	-	-	M
Elasmosauridae indet.	Fragment	UALVP 60174	XX	X	XX	-	-	M
Elasmosauridae indet.	Fragment	UALVP 60175	XXX	XXX	XXX	-	-	M
Elasmosauridae indet.	Fragment	UALVP 60176	XXX	XX	-	X	-	M
Elasmosauridae indet.	Fragment	UALVP 60177	XXX	XXX	XXX	-	X	M
Unknown								
Unidentifiable	Fragment	UALVP 60173	XXX	XXX	XXX	-	-	I

FIGURES

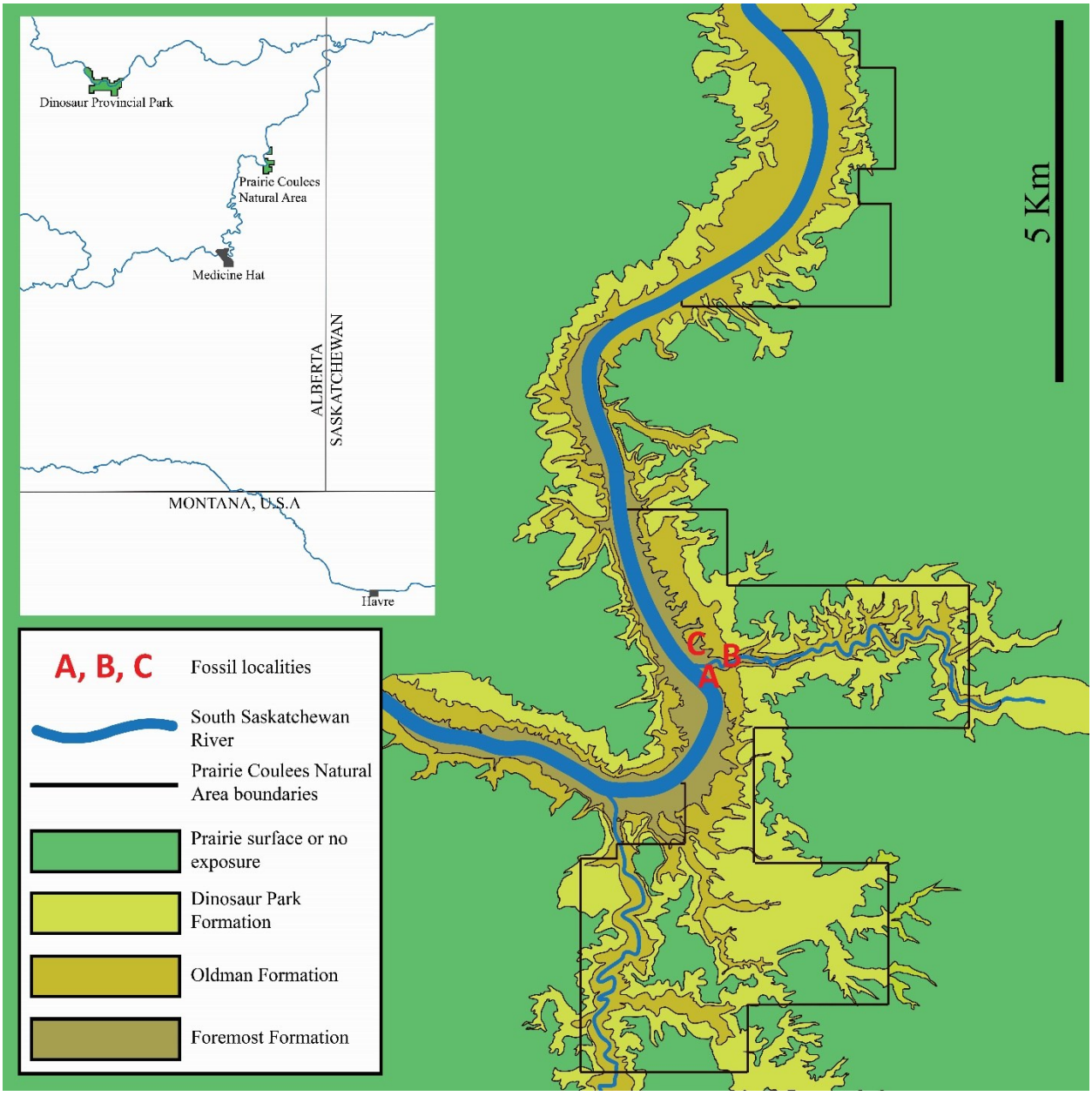

Figure 7-1. Map of southern-eastern Alberta and Prairie Coulees Natural area indicating the three localities from where the specimens studied here in came. See specimen descriptions for corresponding locations.

Figure 7-2. Select blood vessel-like structures. a) UALVP 60170, Elasmosauridae indet. from a bone fragment. b) UALVP 60176, Elasmosauridae indet. from a bone fragment.

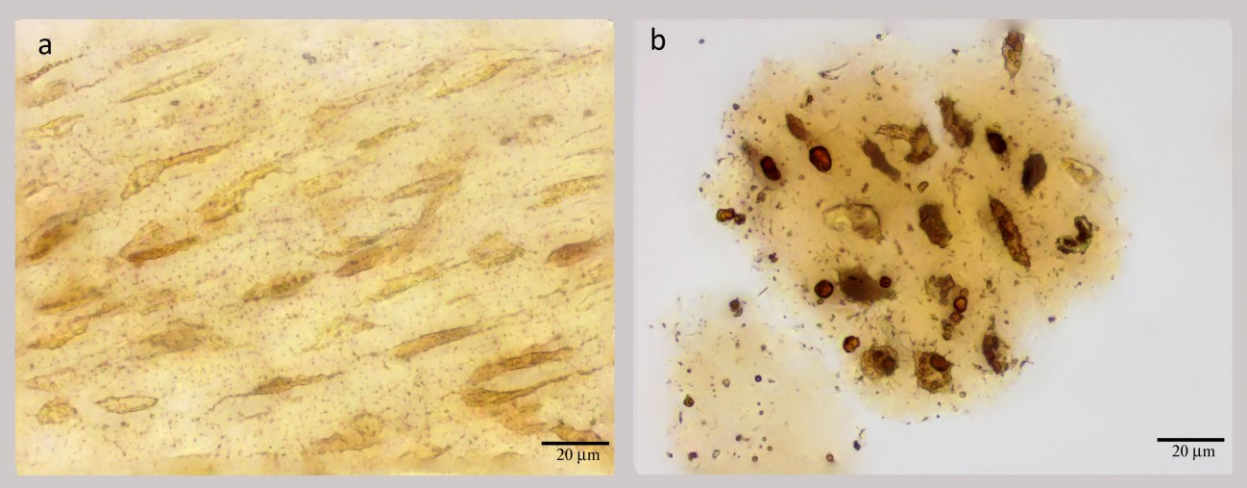

Figure 7-3. Extracellular organic matrix-like structures with osteocytes preserved within. a) UALVP 60171, Elasmosauridae indet. from a bone fragment. b) UALVP 60177 Elasmosauridae indet. from a bone fragment.

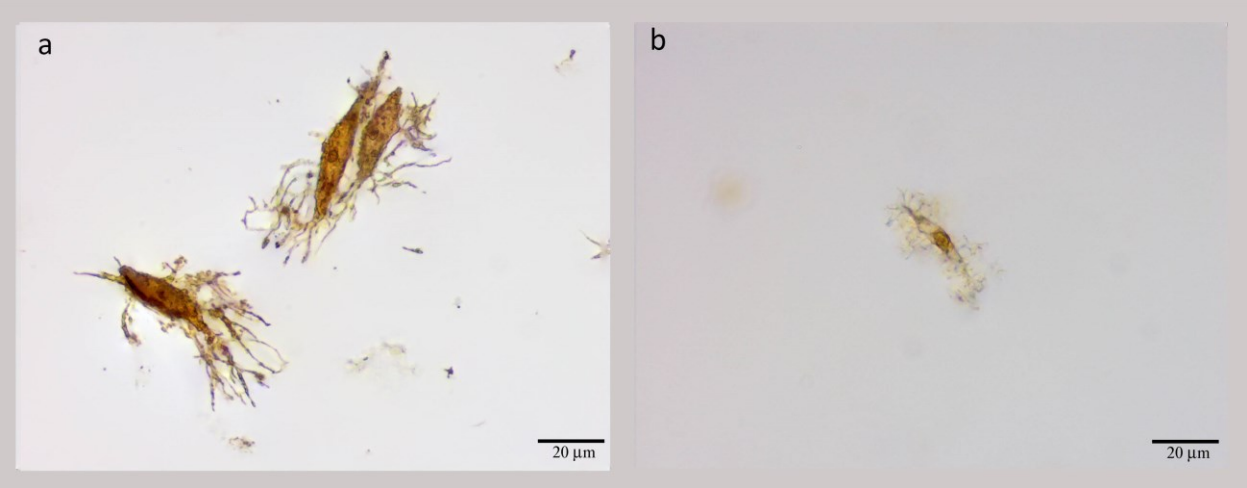

Figure 7-4. Select osteocyte-like structures. a) UALVP 60169, Elasmosauridae indet. from a bone fragment b) UALVP 60171, Elasmosauridae indet. from a bone fragment. Filipodia are observed are numerous with exceptional preserved.

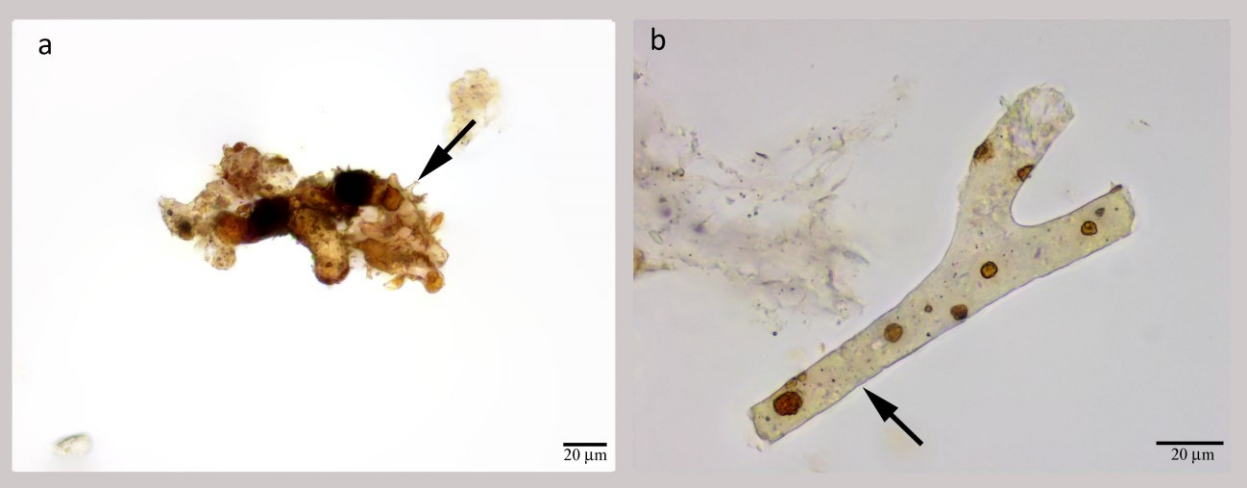

Figure 7-5. Preserved septate fungal hyphae recovered after dissolution. a) UALVP 60168 hyphal fragments with spines (arrow). b) UALVP 60176 with septate hyphal fragment with marked septum (arrow).

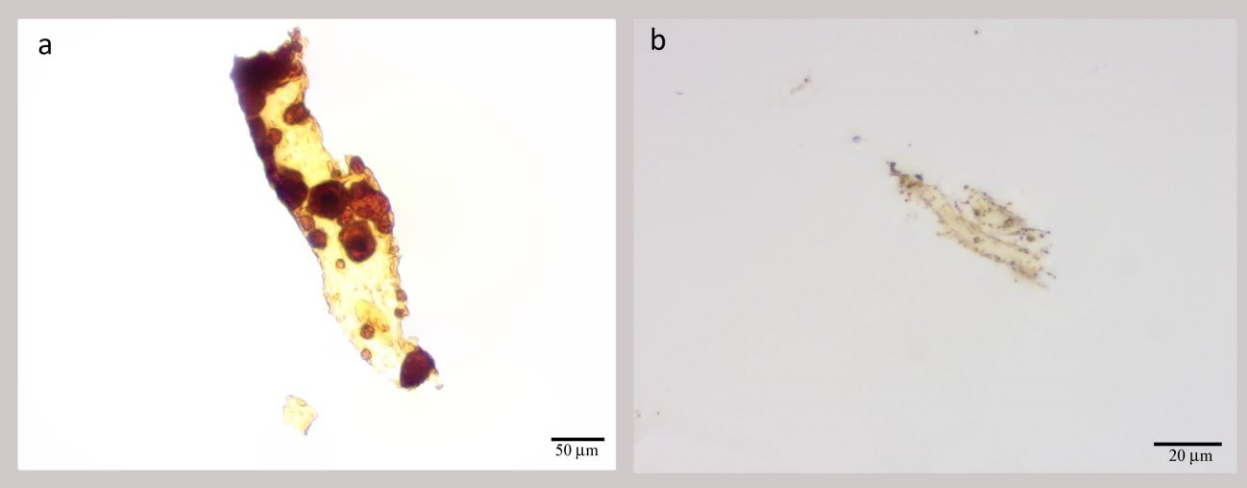

Figure 7-6. Tissues recovered from UALVP 60168. a) vessel fragment with red blood cell-like structures and small mineral grains within the lumen. b) osteocyte like structures exhibiting an elongated form with partly intact filipodia.

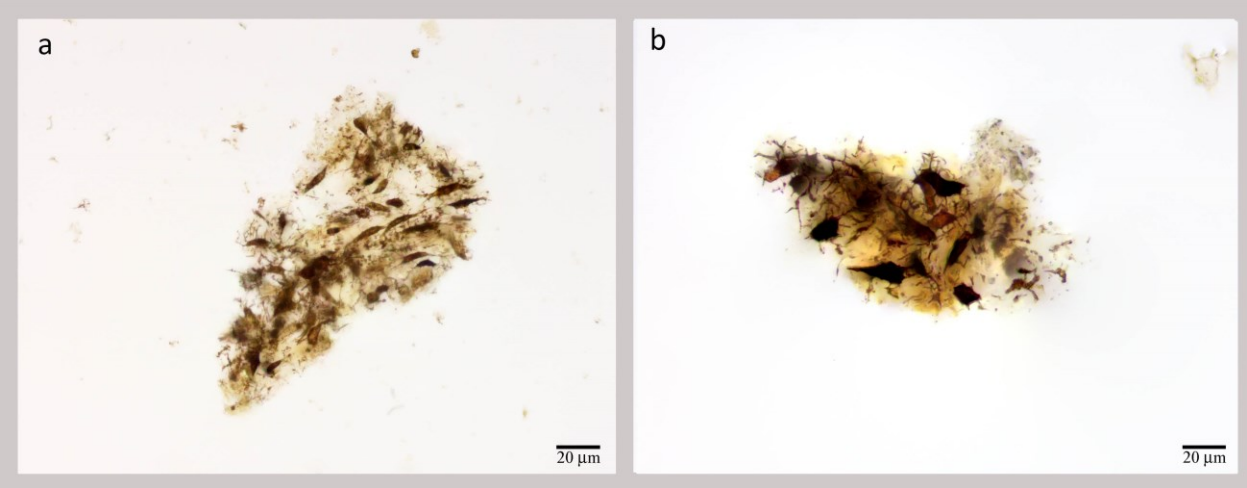

Figure 7-7. Organic material recovered from UALVP 60169. a) Osteocyte cluster with small amounts of fibrous EOM between each cell. b) Heavily stained osteocytes within a dense clump of EOM.

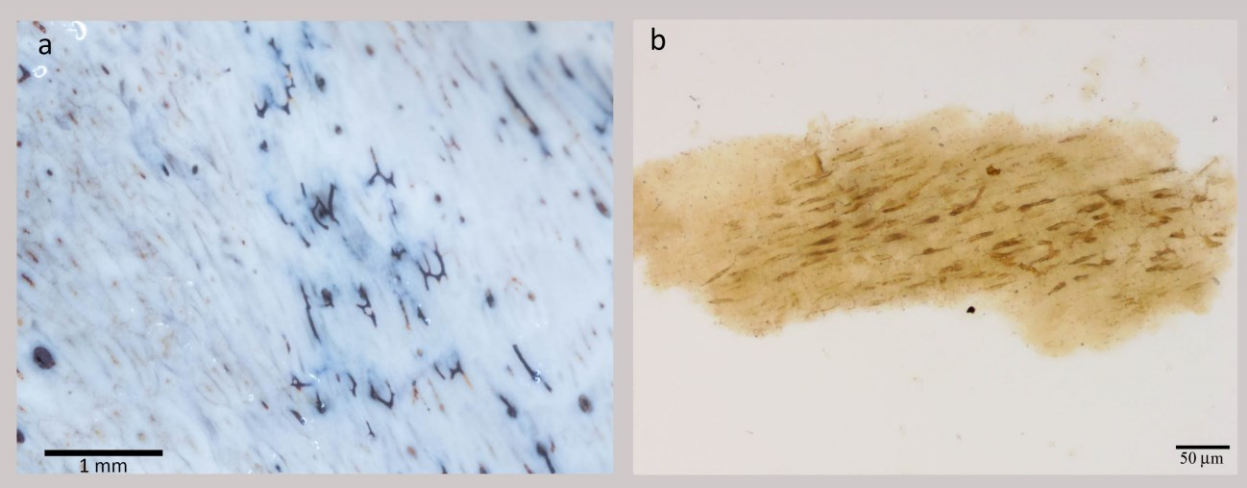

Figure 7-8. Recovered tissues from UALVP 60171. a) vessel network exposed during dissolution of bone fragment. b) cluster of osteocytes within an organic fibrous matrix.

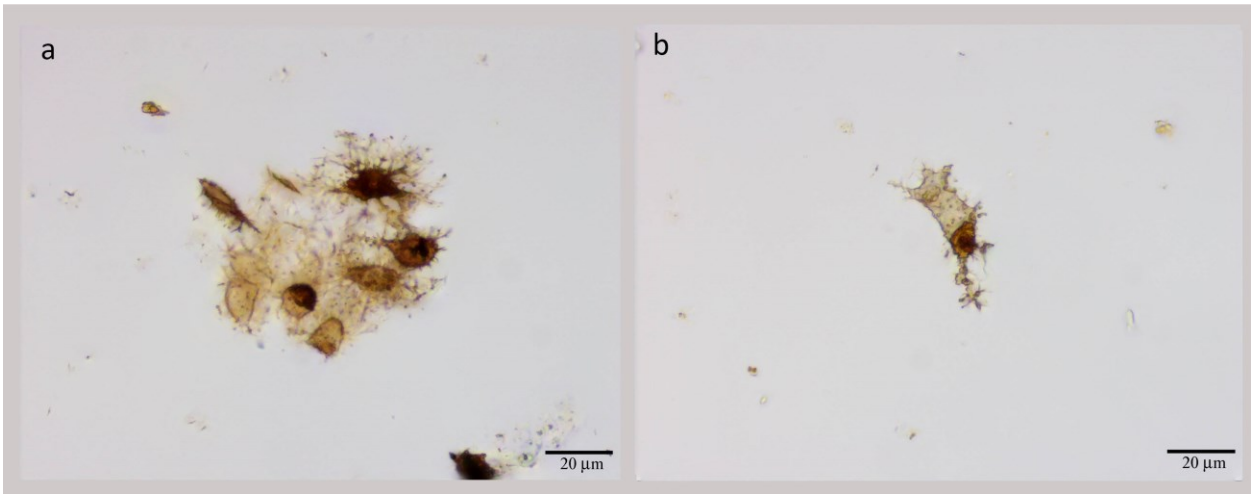

Figure 7-9. Osteocytes recovered from UALVP 60173. a) small cluster of subcircular osteocytes held together by EOM and filipodia. b) oddly shaped osteocyte structure that may represent an osteoblast during transformation into an osteocyte.

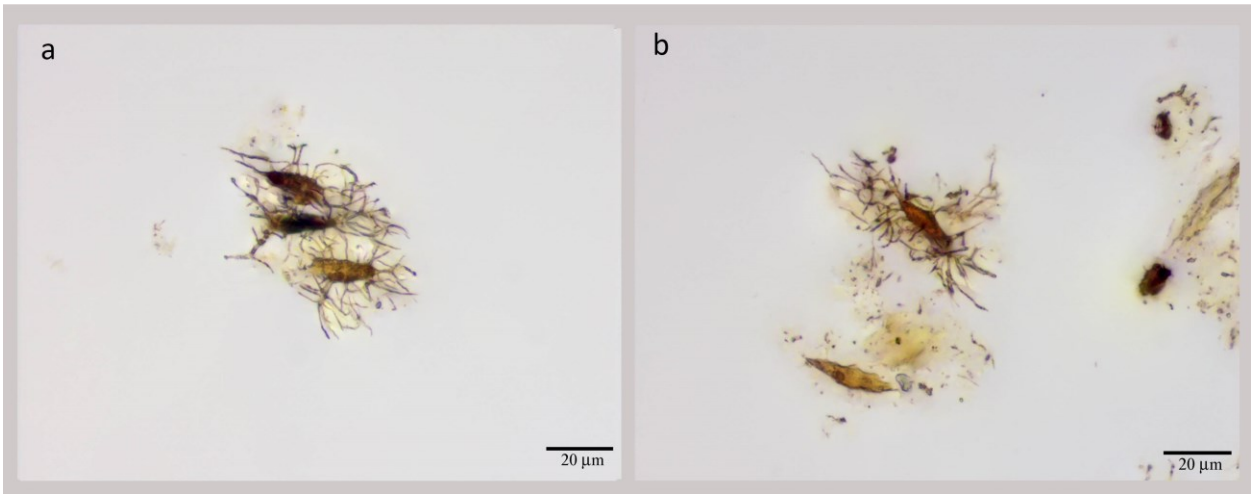

Figure 7-10. Osteocytes from UALVP 60174 showing detailed preservation of fine tips of the filipodia. Note small clumps of EOM in ‘b’.

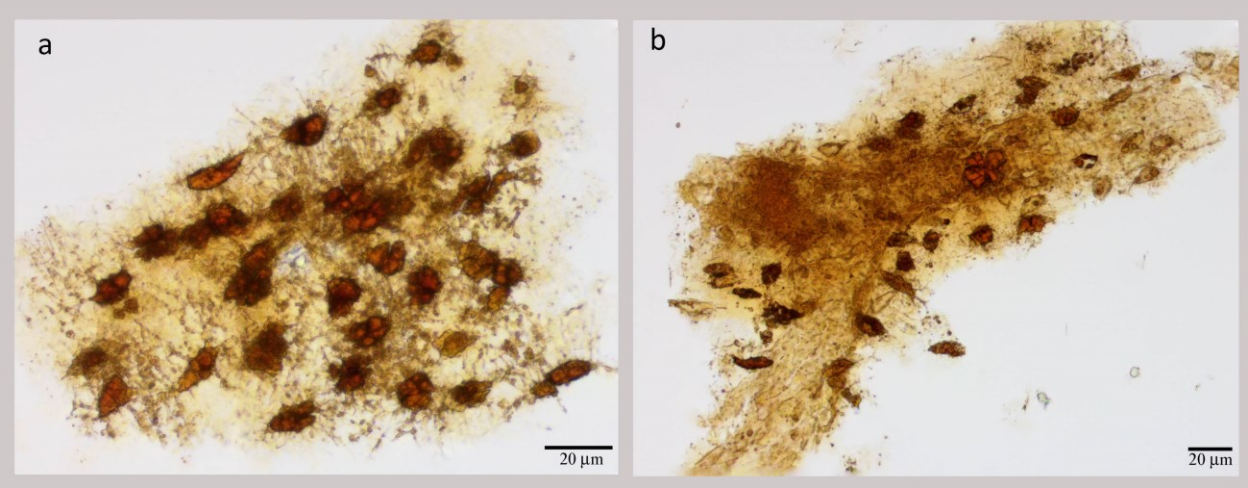

Figure 7-11. Tissues recovered from UALVP 60175. a) Osteocytes in situ within a collagen matrix. b) Vessel fragment surrounded by a collagen matrix with osteocytes still in situ.

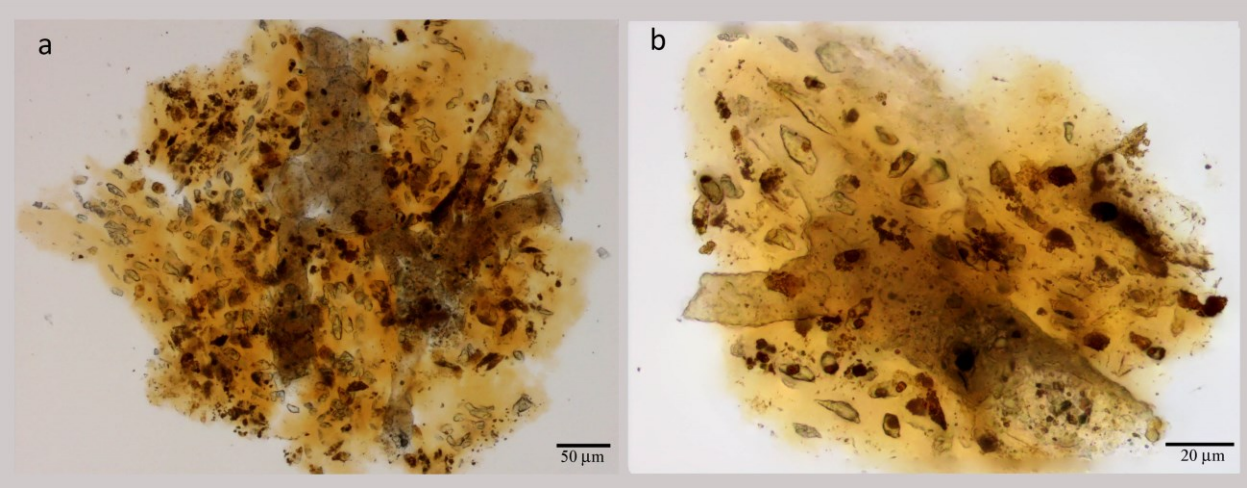

Figure 7-12. Tissues recovered from UALVP 60177. a) Multiple vessel fragments surrounded by EOM with osteocytes preserved within the collagen matrix. b) Vessel fragment surrounded by a collagen matrix with osteocytes still in situ. Note some lacunae preserve osteocytes while other do not.

Chapter 8: Analysis of tissue preservation variation in Alberta geological formations: A proposed mechanism for the preservation of original tissues in the geological record.

8.1 Results

Original organics have been recovered from fossil vertebrate bone from five Upper Cretaceous Alberta geological formations (Brazeau, Dinosaur Park, Foremost, Horseshoe Canyon, and Wapiti) in greater amounts as well as in better condition than anticipated. Although preservation of original tissues is common in all formations, the quantity of tissue preserved, and the overall quality of tissues vary between formations. Additionally, different types of tissue (blood vessels, collagen, and osteocytes) vary in preservation rates independently between formations. In all formations, vessels were most commonly preserved at relatively high rates, and collagen matrix is the second most common original organic preserved. In contrast, osteocyte preservation varied drastically between formations both in overall abundance as well as the quality of individual cells. Interestingly, several specimens show alteration of the bioapatite, which appears vitrified. Although most specimens do not show vitrification, those that do are in sediments that were laid down in still bodies of water (such as lakes, marshes, ponds or swamps). This suggests there are unidentified processes of fossilization that vary between different environments.

The transgressive/regressive sequences of the Western Interior Seaway that occurred in the upper Campanian, represented by the Bearpaw Formation, are complex, as are the associated changes with the depositional environments. Therefore, only generic interpretations

can be made regarding the depositional environments from which the bones were recovered. Presumptions are based on the overall general knowledge of the stratigraphic sequence for each formation, and on the palaeogeographic information established on the locations of known outcrops of upper shoreface, nearshore, or marine facies.

The uppermost Foremost Formation has been identified as marine upper shoreface based on swaley cross-stratification, decimetre scale dunes, microvertebrate assemblages, and foraminifera (Hathway et al. 2011, Cullen et al. 2016, Thompson 2018). In this instance, the preservational environment for specimens from the Upper Foremost Formation is well constrained because all but one specimen originate from the same horizon. Although the general environment is believed to be marine upper shoreface, microvertebrate sites contained remains of dinosaurs, turtles and other freshwater and terrestrial taxa, which indicates a terrestrial influence. This terrestrial influence is also noted for other microsites at equivalent positions within the Foremost Formation (Cullen et al. 2016).

The Dinosaur Park Formation represents a terrestrial, fluvial dominated, coastal plain (Eberth 2005). The formation formed under the influence of large deltaic lobes in the lower portion, which were replaced by large estuarine channels and brackish deposits higher in section as a major transgressive sequence occurred. As the transgression continued, the Dinosaur Park Formation was overlain by the Western Interior Seaway sediments of the Bearpaw Formation. Specimens studied for their tissue preservation rates and quality were all recovered from within the deltaic lobe portion of the formation. However, it is not exactly known how distant the coastline was from any given specimen. In addition to large channel

deposits, the formation also has sufficient numbers of palaeosol horizons, identified by large numbers of root traces in oxidized mudstones (Eberth 2005).

The Horseshoe Canyon Formation also represents a terrestrial, river dominated, coastal plane with overbank deposits. However, it is different from the Dinosaur Park Formation in that it contains multiple thick coal units (Eberth and Braman 2012, Eberth et al. 2013). Because the Horseshoe Canyon Formation is so thick and the sequence covers the last Bearpaw regression, there are multiple environmental changes. Specimens studied were stratigraphically limited to the Tolman Member (lowermost Maastrichtian). The Tolman Member is bounded by the final transgression of the Bearpaw Sea (Drumheller Marine Tongue) and the Carbon Member, and is noteworthy for its complete lack of coal units (Eberth and Braman 2012). Based on the sandy channel deposits, vitrisol mudstones, and the elevated angiosperm pollen, the Tolman Member is interpreted as a relatively dry environment compared to the other members of the Horseshoe Canyon Formation (Eberth and Braman 2012).

The Wapiti Formation is the alluvial wedge in the northernmost section of the Alberta upper Cretaceous foreland basin (Fanti and Catuneanu 2009). It is divided into five distinct stratigraphic units that represent several different depositional environments. Unit 1 is transitional between marine and fluvial facies; Units 2 and 3 are floodplain dominated deposits with massive channel-fill deposits at the base; Unit 3 is thought to represent the maximum flooding surface of the Western Interior Seaway; Unit 4 consists of major channel and floodplain deposits and is capped by the Red Willow Coal Zone (equivalent to the Drumheller Marine Tongue in the Horseshoe Canyon Formation); Unit 5 includes small channels, crevasse splays, and overbank deposits and is capped by the Cutbank Coal Zone (Fanti and Catuneanu

2009). All specimens used in the dissolution study were from Units 3 and 4. Due to the locations specimens were recovered from, it is presumed that the environment in which specimens were buried was a transitional area between the coastal plains (Tolman Member of the HCF) and an upland near-source fluvial environment (Brazeau Formation).

The Brazeau Formation represents a near source proximal pluvial alluvium sequence. It overlies the marine shales of the Wapiabi Formation on an erosional contact and is overlain by the Coalspur Formation. Thickening in the west to a maximum known thickness of ~1300 m, the Brazeau Formation spans ~13 Ma (~80-67 Mya). It is equivalent to the (from oldest to youngest) Foremost, Oldman, Dinosaur Park, Bearpaw, and Horseshoe Canyon Formations of the Alberta prairie region, and the Wapiti Formation in northern Alberta. Unfortunately, due to the lack of economic resources such as coal or gas, no vertebrate palaeontological papers and only a handful of geological papers have ever been published about the Brazeau Formation (Lang 1947, Gunther and Hills 1972, Jerzykiewicz 1985a, 1985b, 1997, Jerzykiewicz and Sweet 1988). Because of the lack of interest in the Brazeau Formation, volcanogenic sediments have only been sampled recently for U/Pb dating. The work is in progress, so it difficult to properly determine the stratigraphic/temporal levels of the specimens. Specimens used in the dissolution study (Chapter 6) were therefore placed stratigraphically based on local lithology, previously published geological maps, and unpublished (as of this writing) radiometric dates. Six of the eight specimens that were sampled for dissolution were recovered from a proximal near-source fluvial environment that represents a well drained upland environment. The other two are from a lowland environment and were recovered from lacustrine sediments. The lacustrine deposits were identified based on freshwater stromatolites growing on one specimen,

numerous freshwater bivalves, large amounts of organics, and algal traces that surround the second specimen. These lacustrine deposits are known to occur in the middle of the Brazeau Formation and are believed to be present during the maximum flooding event of the Western Interior Seaway (Jerzykiewicz 1985a, 1997, Jerzykiewicz and Sweet 1988).

Previous studies have proposed factors that may influence the preservation of original organics in vertebrate fossils. These include decay induced mineralization by bacteria (Allison 1988, Daniel and Chin 2010), molecular level interactions between bone minerals and organics (San Antonio et al. 2011), grain sizes of the surrounding rocks (Schweitzer 2011), haemoglobin iron binding to proteins to form crosslinking (Schweitzer et al. 2014), and N-heterocyclic polymerization of proteins in oxidative environments (Wiemann et al. 2018). Of these, only matrix grain size, and preservation in oxidative environments suggest a link to depositional environments. However, a specimen of the Jurassic ichthyosaur *Stenopterygius,* recovered from deep marine sediments of Holzmaden, Germany, preserves unmatched preservation of original tissues. Not only were bone tissues recovered, but original blubber, melanocytes, and skin cells were also found preserved intact (Lindgren et al. 2018). Because this specimen was recovered from a reducing environment that was supposedly unsuitable for tissue preservation (Wiemann et al. 2018), investigations into any environmental factors continue. By using data collected from the five upper Cretaceous Alberta formations studied, a hypothesis addressing the most suitable environmental conditions for preserving original organics can be formed. Three factors will be addressed herein; 1) type of surrounding matrix (sandstone vs mudstone), 2) degree of articulation (articulated/associated vs. isolated/bonebed), and 3) depositional environments.

The five formations that were studied provide a virtual transect across the Late Cretaceous Alberta landscape from the palaeo-foothills to the upper shoreface of the Western Interior Seaway. This transect provides five different depositional environments that could have an influence on preservation of original organics within buried bone (Fig. 8-1). These environments include; upland near-source fresh water (Brazeau), intermediate lowland (Wapiti), transgressive coastal plain (Dinosaur Park), regressive coastal plain (Tolman Member, Horseshoe Canyon Formation), and marine/brackish upper shoreface (upper Foremost).

8.1.1 Trends in original organic preservation in the Upper Cretaceous of Alberta

As noted, the Dinosaur Park Formation preservation is considered a base line for preservation rates and quality. The overall trend for organic preservation in specimens collected from the Dinosaur Park Formation is that vessels and extracellular organic matrix (EOM) are exceptionally common, whereas osteocytes are fleetingly rare (Chapter 3). Vessels are preserved in all specimens, apart from one: a *Panoplosaurus* osteoderm preserved in an iron rich cement sandstone nodule. EOM is preserved in all specimens, although in many specimens it is only recovered in small clumps of yellowed fibrous bundles (Chapter 3). Osteocytes are very rare and are only recovered from associated or articulated specimens. The overall appearance of tissue resembles that reported in previous studies (Schweitzer et al. 2005b, 2007b, 2014, Schweitzer 2011, Bertazzo et al. 2015). Most vessels have a brittle, crystalline appearance and tend to be moderately to heavily stained orange to orange-brown. Many specimens have at least some extent of three-dimensional anastomosing structure preserved, indicating significant portions of the vascular network persist (Chapter 3). This

network is extremely well preserved in several specimens such as UALVP 52613, an articulated juvenile *Chasmosaurus belli*. In this specimen, the entirety of the vascular network is preserved, not just fragments (Chapter 3). Despite the vast quantities of vascular network remaining, the majority of these structures have brittle crystalline-like appearance like those mentioned by Schweitzer et al. (2007). Recovered from UALVP 55804, the pelvis of *Latenivenatrix mcmasterae*, a vessel fragment preserved extraordinary details such as the endothelial cells, red blood cells, a potential basophil (type of white blood cell), and what appears to be the nuclear membrane for each of the aforementioned cell types (Chapter 3). None of the osteocytes recovered have complete filipodia, and usually only their bases remain (Chapter 3). This condition has been reported from other Upper Cretaceous dinosaur specimens (Schweitzer et al. 2007b). Minor recrystallization of the bioapatite bone matrix causes damage to the filipodia phospholipid bilayer but has been proposed to be the reason that only the bases remain intact (Chapters 3-7).

In comparison to original organics preserved in bone from the Dinosaur Park Formation, those recovered from the Horseshoe Canyon Formation show a very different pattern. The overall percent of specimens that retain organic preservation is much lower. Only 50% of the specimens sampled retained vessels, 40% retained EOM, and 30% retained osteocytes. Interestingly, two specimens preserved fungal hyphae, structures not observed in any of the Dinosaur Park Formation specimens (Chapter 4). In general, all cellular tissues recovered (vessels and osteocytes) are crystalline-like in appearance and brittle. Although vessels are recovered less frequently than in Dinosaur Park Formation specimens, if vessels are preserved in a specimen, they tend to be more complete three-dimensional anastomosing structures. A

good example is UALVP 60158, a partial ornithomimid rib. When dissolved, this rib fragment revealed the complete vascular network preserved in three dimensions with the EOM still intact around the vessels (Chapter 4). This is also seen in an isolated hadrosaurid metatarsal III (UALVP 60157), although to a slightly lesser extent. Furthermore, in contrast to specimens from the Dinosaur Park Formation, specimens that preserved osteocytes were not restricted to only articulated or associated skeletons as an isolated hadrosaur metatarsal III had two osteocytes recovered. As previously mentioned, osteocytes have a crystalline appearance, and similar to those recovered from specimens from the Dinosaur Park Formation, only retain the bases of filipodia. EOM is found in less abundance per specimen than the DPF but retains a fibrous appearance and is orange in colouration like that of the DPF and other reports (Schweitzer et al. 2005a, 2007a, Schweitzer 2011, Bertazzo et al. 2015, Wiemann et al. 2018). Two specimens were discovered that preserve fungal hyphae, both of which appear to be non-septate. However, the small sizes of the hyphal fragments make proper identification difficult (Chapter 4). Of note, two specimens (UALVP 59699, a champsosaur femur, and UALVP 60159, a juvenile hadrosaur maxilla) sampled from the Horseshoe Canyon Formation appear to have had the bioapatite portions of the bone altered into vitreous forms. This alteration cannot be recognized macroscopically but is easily identified when microscopic fragments are viewed under a light microscope (Chapter 4). The structure resembles small chips of man-made glass or obsidian with sharp transparent margins. Where all other dissolved bone retains visible bioapatite microcrystals that form a fibrous-like rough crystal lattice, the altered bone shows no sign of the original structure. These specimens do not preserve any identifiable organic matrix

and were both collected from mudstone, although the depositional setting (*i.e.* lacustrine, mud filled channel, overbank, palaeosol, etc.) is unknown.

Organic recovery from specimens from the Wapiti Formation had similar results to that of the Dinosaur Park Formation. However, the overall quality of tissues is much better. All specimens save for one preserved tissue in large quantities, although osteocytes are the least commonly preserved of the three tissue types. Vessels are preserved in all but one specimen, and are often in three-dimensional, anastomosing structures similar to that of the ornithomimid rib from the HCF. EOM is preserved in most specimens (~63%), and often preserves osteocytes surrounded by the fibre bundles (Chapter 5). Osteocytes vary in preservation quality, but on average are moderately well preserved. Filipodia preservation varies drastically. Most osteocytes preserve only the bases or partial filipodia. However, UALVP 57466 (unidentified bone fragment) produced osteocytes with the finest tips of osteocytes preserved. Several osteocytes recovered from UALVP 57466 were recovered still in contact with one another and were surrounded by a heavily brown-stained EOM. Similar to the Horseshoe Canyon Formation, fungal hyphae were recovered (Chapter 5). UALVP 57478 preserved large clusters of septate hyphae with clear perithecium-like structures that contained black objects resembling spores. Yellow staining of the structures, and the presence of precipitated minerals within the cellular spaces indicate these are fossil (rather than modern) hyphae. Also similar to specimens from the Horseshoe Canyon Formation, one specimen (UALVP 59554) possesses bioapatite that has been highly altered into a vitrified form (Chapter 5). Additionally, UALVP 59554 did not preserve any form of preserved tissues and was recovered from mudstone. Again, it is unknown what depositional environment this mudstone was deposited in.

Despite the poorly-known composition of the fauna from the Brazeau Formation of the central Alberta Foothills, several partial skeletons, isolated elements, and specimens from a bone bed were discovered and sampled for tissue extraction. Tissue preservation rates were very similar to those in the Wapiti Formation. Most specimens preserved vessels and EOM, and half of the specimens preserved osteocytes. It should be noted that the overall mineralization of bone from the Brazeau Formation is significantly higher than bone from any other formation in the study area. Cancellous bone can be completely infilled with precipitated siliceous minerals. Fortunately, the small pore spaces within the cortical bone are not as heavily mineralized, and therefore organics could be preserved. Vessels, like those recovered from specimens from other formations, are crystalline and brittle. Many vessel fragments are observed with high amounts of mineral precipitates thought to be an iron-based compound based on the inability of light to penetrate through the mineral (Chapter 6), and by how common hematite and pyrite are in preserved vessels. UALVP 60165 is an isolated hadrosaur femur (recovered from the base of a sandstone channel deposit) that contains multiple three-dimensional anastomosing vessel structures (Chapter 6). The vessel walls of these fragments are primarily clear and crystalline in appearance. Within the vessel lumen of UALVP 60165, reddish orange spherical structures matching the morphology of red blood cells are observed. In some portions of the vessels, there are so many red blood cell-like structures that these regions appear black until viewed with the highest brightness using a compound microscope. EOM is preserved in 75% of the specimens sampled. Most EOM is moderately well preserved, fibrous, and stained yellow like other EOM recovered from other Alberta formations (Chapters 3-5, 7). The preservation is also the same as those described in other previously published

studies (Schweitzer et al. 2005a, 2007a, Schweitzer 2011, Bertazzo et al. 2015, Wiemann et al. 2018). Many small bundles of EOM also contain intact osteocytes. Osteocytes vary in preservation from clear crystalline-like appearances to beautifully preserved cells with fully intact filipodia. The quality of osteocyte preservation exceeds those recovered from all other terrestrial deposits within the study area. In addition to animal tissues, one specimen possessed fragments of fungal hyphae. UALVP 60167, a poorly preserved unidentified fragment of bone that showed signs of pre-burial degradation (powdery consistency and water worn surfaces) contained non-septate fungal hyphae that are stained orange. As previously stated, the staining indicates that the hyphae are not recent in origin. In addition to the organics, two specimens from the Brazeau Formation that were sampled had bone that had become vitrified like those from the Horseshoe Canyon and Wapiti Formations. Similar to previously mentioned vitrified bone shards, the Brazeau Formation specimens exhibiting this recrystalized form of bone have no bioapatite fibrous-like micro-crystalline structure. Within slightly larger fragments of vitrified bone observed under a compound light microscope, empty osteocyte lacunae are observed. Just like the other specimens noted to have this vitrified form, both these specimens were recovered from mudstone. Fortunately, these mudstones are identifiable as lacustrine deposits based on algal mats, freshwater stromatolites, and large numbers of fresh water unionid clams (Chapter 6)

In contrast to the previous four formations, the Foremost Formation in southeast Alberta is interpreted as marine in origin (Hathway et al. 2011, Thompson 2018). This provides a means to test a significantly different depositional environment. Preservation of tissues in the upper shoreface environment was exceptional with every specimen preserving most types of

tissue (EOM – 100%, vessels – 90%, osteocytes – 80%). Two specimens also preserve red blood cell-like structures within the lumen of vessels. Preservation quality of vessels is similar to that of the other four formations, many being stained yellow orange with a crystalline or globular appearance (Chapter 7). Three-dimensional anastomosing vascular networks are present in the majority of specimens sampled, although because of the brittleness of the tissues the networks are easily damaged. Vessels recovered from one bone fragment (thought to be elasmosaur, UALVP 60176) have a peculiar morphology not observed in any other specimens researched in this or any other Alberta formation, nor in any previously published work (Schweitzer et al. 2005b, 2007b, Kaye et al. 2008, Schweitzer 2011, Bertazzo et al. 2015). Whereas all other vessels previously reported have generally straight and parallel walls, UALVP 60176 has highly irregular, undulating walls, resulting in a "tin-roof" appearance (Chapter 7, Fig. 7-2b). Although a thorough investigation into the cause of this appearance is out of the scope of this project, the following possible reasons may explain the odd vessel morphology: 1) This may be a phylogenetic signal, and may be an adaptation to increase surface area of vessel walls to increase O_2 and CO_2 transfer between blood cells and bone tissue. 2) The individual may have suffered from aerobullosis (decompression sickness). 3) The bone may have been impacted by an infection or disease (macroscopically, however, there does not appear to be any evidence for this). Further investigation into this, and other specimens from the upper Foremost Formation marine deposits should help elucidate this odd morphology. EOM from the upper Foremost Formation is preserved in relative abundance in all specimens sampled and exhibits yellow orange staining, and retains fibrous textures, like all other EOM previously recovered (Chapters 3-6). Osteocytes are generally preserved with exquisite details, including the

presence of the finest tips of their filipodia that remain quite flexible. The bodies of osteocytes vary in the degree of staining, both among sampled specimens and within the same specimen. This indicates very localized preservation of tissues during fossilization (Schweitzer et al. 2007b). Additionally, most osteocytes with transparent cellular membranes seem to have some form of cellular contents (Chapter 7, Fig. 7-10). It should be noted that two specimens recovered (UALVP 60175 and UALVP 60177), show unprecedented preservation of their original organic structures. Both these specimens retain vessel fragments retained within EOM matrices, which also continue to incorporate osteocytes in their original *in situ* positions (Chapter 7, Figures 7-11 and 7-12). For specimens sampled from Alberta, this quality of preservation has only been observed from the upper shoreface deposits from the upper Foremost Formation. In addition to the original organic tissues recovered, two specimens had fragments of fungal hyphae recovered from them (Chapter 7). The recovery of fungal hyphae, although unexpected from a marine environment, could be explained through two possible means; 1) Fungal hyphae are from marine taxa growing on/in the bone prior to deposition, or 2) These specimens are of terrestrial origin and were washed into the marine ecosystem and subsequently buried alongside marine faunal representatives. It should be noted that no bone recovered from the upper Foremost Formation exhibited the same vitrification of the bioapatite seen in the Brazeau, Horseshoe Canyon, or Wapiti Formations.

Specimens from the Dinosaur Park Formation showed no indication for vessel and EOM preservation preference between sediment type and degree of articulation. Osteocytes, however, were only recovered from articulated/associated skeletons (Chapter 3). Specimens from the Horseshoe Canyon Formation, however, indicate no preservational preference to

depositional matrix or the degree of articulation, including osteocytes. The only organics that appear to be associated with one factor are fungal hyphae that are only found in isolated specimens. Similarly, no tissue preservation preferences are observed within neither the Wapiti nor Brazeau Formations. However, in vitrified specimens from both formations – as well as the Horseshoe Canyon Formation – original organics were non-existent. Nine of ten specimens from the Foremost Formation were recovered from the same microsite horizon in the uppermost upper shoreface facies, whereas the tenth specimen was recovered from a brown silty mudstone believed to be an interfingering coastal and marine setting (Hathway et al. 2011, Cullen et al. 2016, Thompson 2018). Regardless of the differences in the depositional environments, the single specimen recovered from the mudstone did not show any differences in preservation or organic structures.

8.2 Discussion

Of the 55 specimens tested in this study (DPF =19, HCF = 10, WF = 8, BF = 8, FF, = 10), there was no correlation for vessels and EOM with the surrounding depositional matrix (Fig. 8-2) or with the degree of articulation (Fig. 8-3). Osteocytes do show a potential association with sandstone; however, this is most likely due to the low number of specimens obtained from mudstones (15 of 55). It is not considered a strong correlation, and therefore will not be discussed as significant. The only strong relationship suggested by inspection of data is between tissue type (primarily osteocytes) and the depositional environment (Fig. 8-4). In terrestrial environments, osteocytes tend to be more commonly preserved and significantly better

preserved in upland environments, and there are fewer, less well-preserved cells and cell structures as the depositional environments approach the coastline. Interestingly, the upper shoreface environment, even with its powerful wave influence, preserves osteocytes in abundance and with spectacular cellular details and flexibility (Fig. 8-5). This trend for osteocyte preservation suggests a very strong correlation towards depositional environments as a controlling factor in original organics persisting since deep time.

For nearly a century, fossilization has been proposed to occur in a simple model; death of the animal, decomposition and burial of the carcass, groundwater infiltrates the remaining hard parts (bones and teeth), minerals precipitate out and fill in open spaces or completely replace the bone (Paine 1937). Not until the late 1990's and early 2000's did this generalized model begin to be questioned. The difficulty with testing fossilization processes in modern systems is the length of time that mineralization is believed to occur. It is thought that maturation experiments can replicate the fossilization process. Such experiments generally are performed by placing specimens in some form of pressure vessel with sediment, increasing the pressure and temperature within the vessel for multiple days, then making observations of how specimens have been altered (Saitta et al. 2018). These experiments, however, usually increase both pressure and temperature so high that natural fossilization processes would never experience these values; in the case of (Saitta et al. 2018) the values can be associated with low grade metamorphism. Due to this lack of easily performed experiments, palaeontologists have not been able to understand how the fossilization process truly works. Because of this lack of knowledge, the understanding of how organics preserve in deep time is debated. These debates centre around hypotheses that mineralization is induced by bacterial decay (Allison

1988, Daniel and Chin 2010), that there are molecular level interactions of bone minerals and organics (San Antonio et al. 2011), that soft-tissue preservation is influenced by the surrounding matrix grain size (Schweitzer 2011), that there is haemoglobin iron binding to proteins to form crosslinking (Schweitzer et al. 2014), or that there is N-heterocyclic polymerization of proteins in oxidative environments (Wiemann et al. 2018). Due to the substantial percentage of specimens that preserved some form of original organics, this suggests that preservation of organics is not the exception, and that specimens without preserved organics is. For this reason, the question of "How do these tissues preserve?" should be reconsidered as "What ultimately destroys original organics during preservation?".

Other fields of study that commonly investigate preserved bones include archaeology, anthropology, forensics, and zooarchaeology. Fortunately, due to the relatively young nature of specimens studied by workers in these fields, the initial stages of bone fossilization have been studied in much greater detail (Arnaud et al. 1980, Gordon and Buikstra 1981, Schoeninger et al. 1989, Locock et al. 1992, Child 1995, Stephan 1997, Reiche et al. 2002, Trueman and Martill 2002, Turner-Walker and Syversen 2002, Collins et al. 2002, Fernández-Jalvo et al. 2002, Hedges 2002, Jans et al. 2002, Nord et al. 2005, Kars et al. 2005, Turner-Walker 2007, Manifold 2012, Keenan and Engel 2017). Advantages to studying more recent bone preservation is that it can be linked more readily with a vast variety of depositional environments, including bogs, deserts, forests, plains, marine shorelines, and rivers. For example, hot and dry environments are well known for preserving bones and tissues well, a fact that ancient Egyptians made use of in their religious practices. Despite the quality of preservation that desert regions can produce, if specimens are not buried by sands or artificial means, solar UV radiation quickly destroys the

collagen within the bone to produce cracking, flaking, and splintering of the cortex, and eventually the destruction of the element (Fernández-Jalvo et al. 2002). Similar processes can occur under other conditions, such as exposure to acidity, bacteria, moisture, roots and salinity (Gordon and Buikstra 1981, Child 1995, Stephan 1997, Fernández-Jalvo et al. 2002, Trueman and Martill 2002, Nord et al. 2005, Turner-Walker 2007, Manifold 2012).

Archaeological research recognises two main categories that influence bone preservation; 1) intrinsic factors – factors that directly relate to the life of the subject (age, body type and size, pathologies, bone porosity, and bone density), 2) extrinsic factors – factors that are external to the life of the subject (ground water, soil pH, temperature, flora (including roots and fungus) and fauna, human impact, and burial depth) (Manifold 2012). With regard to intrinsic factors, young individuals do not have fully ossified elements, and thus bones can be impacted by the environment more easily. This is the same case for the type of bone and its size (a long bone such as a femur compared with smaller, thinner elements like ribs). If bones have been impacted by disease, they also can be more porous and therefore more easily destroyed (Gordon and Buikstra 1981, Manifold 2012). Extrinsic factors, however, are the processes that ultimately degrade or destroy bone prior to recovery or preservation, and thus the factors that will have the greatest impact on long term preservation of bone.

The age of death of a specimen is important to consider, especially in a palaeontological context. Juveniles possess smaller and more porous bones that can be more easily damaged and can be transported across the landscape more easily. Adult bones are more robust than those of juveniles of the same species, and are less susceptible to being distributed or damaged by predation (Manifold 2012). These factors are likely the reason why articulated skeletons of

small bodied animals (<60 kg) are rare in the Upper Cretaceous formations of Alberta (Brown et al. 2013). Additionally, the extrinsic factor of consumption of small carcasses is of special concern in extinct ecosystems where predators such as *Daspletosaurus* and *Gorgosaurus* included individuals that reached multiple tonnes in mass. Adults, on the other hand are readily preserved, especially in the Dinosaur Park Formation, in a multitude of degrees of articulation, sediment types, and bone qualities.

Extrinsic factors are complex, especially those that tend to include anything pertaining to soil geochemistry (Manifold 2012). Research performed on human remains in Great Britain has noted that bone preservation varies considerably throughout the country, and not just from one soil type to the next, but also from one burial to the next. This has been attributed to the local geology in each region, although requires further investigation (Manifold 2012). In general, however, groundwater is considered to be the most influential factor in bone preservation. Three different hydrological interactions are thought to influence the way groundwater affects bone preservation and diagenesis – diffusion, hydraulic flow, and recharge (Hedges and Millard 1995). Diffusion refers to when water movement is limited in an environment (either waterlogged or where soils are not permanently saturated). Hydraulic flow is where bones are buried in environments where flow depends on volume of water influx (i.e. rainfall or seasonal influence). In recharge environments, bones go through wetting and drying cycles. In general, it is thought that bone buried in soil has higher survivability if it is within a diffusion environment (Hedges and Millard 1995, Manifold 2012). Although this may sound contrary to palaeontological evidence of specimens recovered from fluvial, lacustrine, and marine deposits, these factors refer to soils, suggesting this should only pertain to

palaeontological specimens recovered from palaeosols. Unfortunately, because no specimens studied herein were recovered from palaeosol facies, this will require future work to confirm.

The second most important factor (and arguably more important than soil groundwater because not all environments possess soil) that influences bone preservation in recent burials is surrounding pH (Manifold 2012). Because the main constituents of bone are organic (collagen) and mineral (hydroxyapatite), pH fluctuations can have a huge impact on preservation of either or both components (Gordon and Buikstra 1981, Locock et al. 1992, Stephan 1997, Jans et al. 2002, Nord et al. 2005, Turner-Walker 2007, Manifold 2012). These constituents will generally react differently to either acidic or alkaline pH ranges. Hydroxyapatite will readily dissolve in environments below pH 6 (Manifold 2012), whereas sediments with high alkalinity tend to destroy the organic components of bone (Fernández-Jalvo et al. 2002, Turner-Walker 2007). If pH is too low, hydroxyapatite will begin to deteriorate rapidly through natural dissolution of the carbonate component of the crystalline structure (Gordon and Buikstra 1981, Stephan 1997, Fernández-Jalvo et al. 2002, Nord et al. 2005, Manifold 2012). As a result, bone buried in slightly alkaline environments allow for the non-organic components of bone to preserve well, although exceptions have been noted when degrading organics surrounding the carcass produce organic acids that can etch the bone (Manifold 2012). Nicholson (1996) found that chalky environments (pH 7.5-8.9) from which skeletal remains were recovered were the most favourable for bone preservation. The buffering quality of chalky soil provides a more readily accessible source of calcium carbonate that can then neutralize any source of acidity that may be introduced into the soil. Although the Dinosaur Park Formation is generally completely devoid of preserved eggshell, bivalve and gastropod shell calcium carbonate buffering has also

been proposed to be what protects eggshell from dissolution in two known microvertebrate sites (Currie 1988, Tanke and Brett-Surman 2001). High alkaline conditions, however, negatively impact the organic protein components of bone (Collins et al. 2002, Nord et al. 2005), which in turn cause the mineral portions to become brittle, leading to degradation. The importance of balanced pH for preserving bone cannot be overstated; any fluctuations in the environmental conditions during the initial post burial stages of preservation can ultimately destroy one of the two main components (mineral or organic) of bone.

A major problem with the ideal pH of 7.5-8.9 for preserving bone is that this is also an ideal pH range for the growth of microbial colonies (Collins et al. 2002). For bacteria to have an impact on bone organics (collagen and osteocytes), the mineral phase of the bone must be compromised (Trueman and Martill 2002, Manifold 2012). This compromised state is required for two reasons; 1) collagen and osteocyte filipodia are too large to be directly engulfed by bacteria, and 2) the spaces in which collagen and osteocyte filipodia are held are too small for bacteria to access (Trueman and Martill 2002). For these reasons, bacteria must excrete enzymes to attack these structures. This, however, still requires previous damage to the bone because the spaces surrounding mineralized collagen are so small even ethanol cannot pass through them, let alone large enzymes (Trueman and Martill 2002). For enzymes to have access to these organics, the bone mineral phase must first be compromised by chemical etching to enlarge the collagen spaces for enzymatic attack. As discussed, pH must remain as near neutral as possible to not compromise the mineral phase. Several types of microbes – such as fungi, bacteria, and protozoa – can demineralize bone by slowly tunneling into it (Trueman and Martill 2002, Turner-Walker 2007). Most tunneling that has been reported is attributed to fungal

hyphae and is easily observed in histological thin sections (Fernández-Jalvo et al. 2002, Jans et al. 2002, Trueman and Martill 2002, Turner-Walker 2007). This tunneling provides potential access points for bacteria to begin degrading collagens and other organics that would usually be protected by bone minerals.

Due to the vast numbers of known human burial sites worldwide, the majority of research into bone preservation studies bone preserved in soils. In palaeontology, however, workers can specifically target different environments, such as marine environments. Unfortunately, research into human bone preserved in modern marine settings is difficult, and the unknown origins of human remains can be legally problematic (Mays 2008). For these reasons, very little work has investigated how human bone is preserved within marine settings (Arnaud et al. 1980, Mays 2008). The work that has been performed has shown that bone from marine environments preserves both the mineral and organic components very well, even after 2000 or more years (Arnaud et al. 1980, Mays 2008). Arnaud et al. (1980) discusses the preservation of the organic phase in seven human limb bones from two different shipwrecks (one in the Rade d'Agay, France, the other off Île Sainte-Marguerite, opposite Cannes, France) found in the Mediterranean. That work describes an interesting phenomenon within the hydroxyapatite, where new apatite of non-biological origin precipitates out of marine waters onto the ends of the biologically produced apatite crystals, causing an increase in density and hardness. In the same work the authors investigate the well-preserved organic phase, proposing that perhaps the salinity of the saltwater acts like the preservational process used in salting of meat. Arnaud et al. (1980), however, does acknowledge that if salt is the primary factor that preserves tissues in bone within marine settings, proteins would likely show some

form of denaturation, which was not detected in any samples. The preservation of organics in bone recovered from marine settings was also discussed by Mays (2008). In this work, the author suggests that low temperatures, low oxygen, and generally neutral pHs are the most reasonable factors that prevent the organics from being destroyed.

The complexity of how multiple factors interact to preserve the mineral and organic phases of bone continues to be researched within the archaeological field. However, it is generally understood that chemistry in the depositional environment surrounding the bone plays the most important role. If the pH is not within optimal values, either the mineral phase will dissolve, or the organic phase will degrade. Based on how the bone reacts to the surrounding environment, it may deteriorate enough for microbes to begin enzymatic attack. If enzymatic attack proceeds far enough, the organic phase will be compromised, leading to eventual destruction of bone. The pH has also been proposed to be the primary factor for preservation of bones buried in clay, gravel and sand (Brothwell 1972, Baxter 2004). Although surrounding pH levels of sand and gravels can vary, it has been noted that if these sediments are waterlogged, the preservation of bone can be quite good. Different clay types, however, have been noted to have varying pHs, and thus will preserve bone differently depending on their mineral compositions. Unfortunately, research into the preservation of modern bone in fluvial and lake deposits is severely lacking, providing only a general idea as to how these environments impact bone, however, it is likely pH also plays an important role.

As pH is the primary factor in the preservation of bone in the archaeological record, it is probably also the primary factor for long term survival of bone in the palaeontological record. During the deposition of the upper Foremost Formation, ocean water in the upper shoreface

facies was approximately pH 8-8.1 (Zeebe 2001), within the ideal range for preserving bone and their organics (Collins et al. 2002).

Although the exact pH ranges are not known for groundwater conditions in the other formations studied as part of this research, inferences can be drawn for each of them. The Dinosaur Park Formation, as previously mentioned, only preserves eggshell in microvertebrate sites that contain a high number of calcium carbonate invertebrate shells due to their buffering properties (Currie 1988, Tanke and Brett-Surman 2001), suggesting a slightly acidic environment. As plant matter decomposes, organic acids are formed and leach from the soil into bodies of water (David and Vance 1991). The Dinosaur Park Formation was derived from a coastal lowland and deltaic/estuarine dominated environment with major fluvial channels. In conjunction with the climatic conditions and the flora, both ground and flowing water would have been slightly acidic under most conditions. Additionally, slight dissolution of the mineral phase within the bone would have allowed access of bacterial enzymes to osteocyte filipodia, initiating degradation of the bone cells. Alternatively, as previously proposed (Chapter 3), a complex remineralization of the hydroxyapatite mineral phase, as observed in saline waters (Arnaud et al. 1980), may have damaged the phospholipid bilayer, initiating lysis of osteocytes. Like the Dinosaur Park Formation, eggshell recovered from the Horseshoe Canyon Formation is exceedingly rare (Funston and Currie 2018), and is thought to also be destroyed by acidic conditions during deposition (Ryan et al. 1998). Not surprisingly, the similarity in depositional environments between the Dinosaur Park and Horseshoe Canyon Formations shows similar preservation of original organics in specimens recovered from them. Unlike these previous two formations, the proximal, near source, upland Brazeau Formation represents a very different

type of environment. Although the Brazeau Formation has not been extensively studied like the Dinosaur Park Formation, valuable details that shed light on the water chemistry during the time of deposition have been noted. Jerzykiewicz and Sweet (1988) identify calcareous mudstone, carbonaceous shales and bentonites, freshwater limestones that contain stromatolites, and oncolytic structures. These structures form as a result of precipitation (biologically induced, or naturally induced) of calcium carbonate ($CaCO_3$) from saturated water, indicating that lakes and rivers represented within the Brazeau Formation were high in dissolved carbonates. This is supported by the geology of the region from which the water source originated during time of deposition. Fortunately, based on dates of thrust faults of the modern Main and Front Ranges of the Rocky Mountains, it is known that the water and sediment source for the Brazeau Formation within the regions studied had not been carried very far, and in some cases, less than 60 km (Chapter 9). As a thrust fault begins to form, rivers will cut through perpendicular to the fault sporadically along the front. As the thrust continues to build, those rivers will become confined to the initial valley. Thus, the dates for the Rocky Pass Thrust Fault (74.8 Mya) for example, confine the Athabasca River permanently at its current location through the main ranges and the western thrusts of the Front Ranges at this date (Pană and van der Pluijm 2014). The same process occurred with other major rivers (including the Bow, Brazeau, North Saskatchewan, and Smokey) exiting the mountains. Therefore, sediments deposited in the Brazeau Formation east of the modern Main Ranges may have only traveled short distances. Because these well-established rivers have been confined to their mountain valleys since the formation of the mountains defined their routes, it is argued they have been flowing over the same rock formations since the Late Cretaceous. Nearly all of

these rock formations at the source of the aforementioned rivers are Palaeozoic carbonate limestones (Pană and Elgr, 2013). As water flowed through the palaeo Rocky Mountains, it slowly dissolved carbonates from the rocks, which eventually precipitated back out in the Brazeau Formation lake sediments. This same process is continuing in the modern Athabasca and North Saskatchewan Rivers as they flow over the same rock formations, dissolving the carbonates and becoming slightly alkaline (Shaw et al. 1994, Tondu 2017). Recorded pH levels of the Athabasca River during the winter of 2015 in and just outside the Rocky Mountains were between pH 7.9-8.3 (Tondu 2017). It is assumed that pH levels would have been approximately equal during deposition of the Brazeau Formation. With the evidence that carbonates were precipitating out of the Brazeau Formation lakes, it is suggested that these water bodies had higher pH levels than the fluvial systems, likely due to concentration of carbonates through evaporation of lake water. All specimens sampled from the Brazeau Formation that contained original organic tissues were recovered from either fluvial systems or from a bonebed from an overbank deposit. The only specimens that did not preserve tissues originated from lacustrine deposits, which are identified by the presence of freshwater stromatolites and calcareous mudstones. Additionally, these two specimens were the only ones that were vitrified, which suggests non-biological precipitation of apatite into the voids between biologically formed apatite, the same process reported to occur in seawater (Arnaud et al. 1980). Intermediate between the upland and coastal plain environments is the Wapiti Formation, which would be expected to produce intermediate amounts and qualities of original organics within bone as decomposing plant matter began to neutralize the alkalinity in rivers. The results of bone dissolution from the Wapiti Formation are exactly as expected.

The general trend of tissue preservation in the Alberta Upper Cretaceous formations indicates that as distance of terrestrial burial increases in distance from the mountains, tissue preservation becomes poorer, both qualitatively and quantitatively. However, if the bones are buried in an upper shoreface environment, preservation quality is exquisite. Evidence of water conditions in each of the depositional environments can be used to infer the pH levels of the groundwater, lakes, and rivers., This provides some understanding of the chemistry of the water in the depositional environments. Fortunately, the anthropological and archaeological community has investigated the impact of the environments of burial and has shown that groundwater chemistry and the surrounding pH have the greatest impact on bone preservation. It is proposed that the Brazeau Formation alkalinity, the Wapiti Formation neutrality, the slight acidity of the Dinosaur Park and Horseshoe Canyon Formations, and the ideal alkalinity in the upper Foremost Formation, correlate well with their respective tissue preservations (Fig. 6). It can, therefore, be suggested that if both the mineral and organic phases of bones are not destroyed by the surrounding environments or microbes prior to permineralization, then soft tissues will persist into deep time. Although further investigation into different environments should be conducted and that further evidence of groundwater pH should be obtained for the formations studied, this work strongly supports the hypothesis that pH is the primary environmental factor that influences the preservation of organics in the palaeontological record. Ultimately, it is suggested that organics will survive in environments with pH ~7-8.5, only to be more easily destroyed the further pH deviates from this ideal.

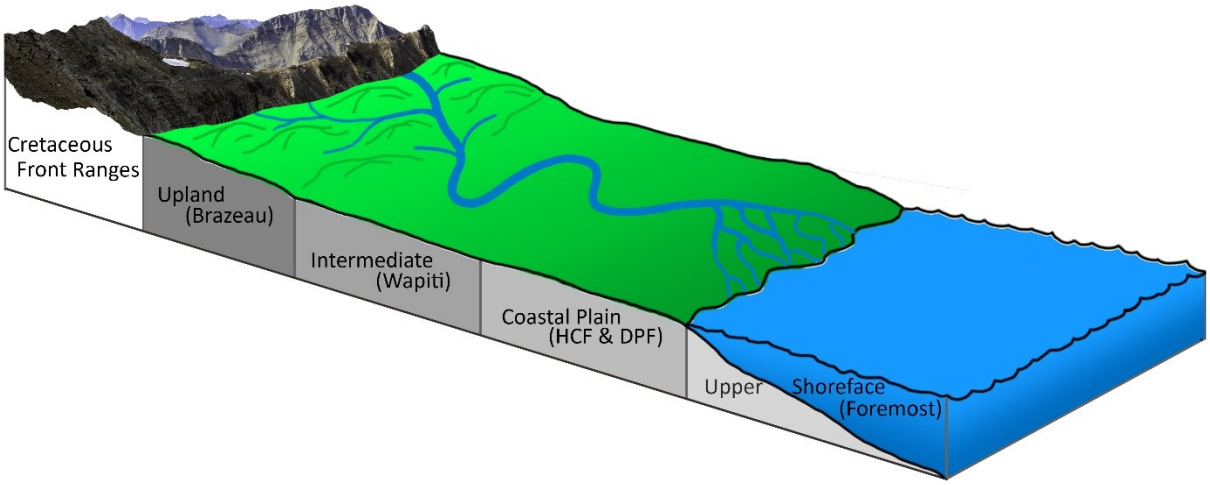

Figure 8-1. Illustrated virtual cross section of the five different formations and their depositional environment. Note that both the Horseshoe Canyon Formation (HCF) and the Dinosaur Park Formation (DPF) are coastal plains; however, the HCF (Tolman Member) is deposited during a regression, and the DPF is deposited during a transgression.

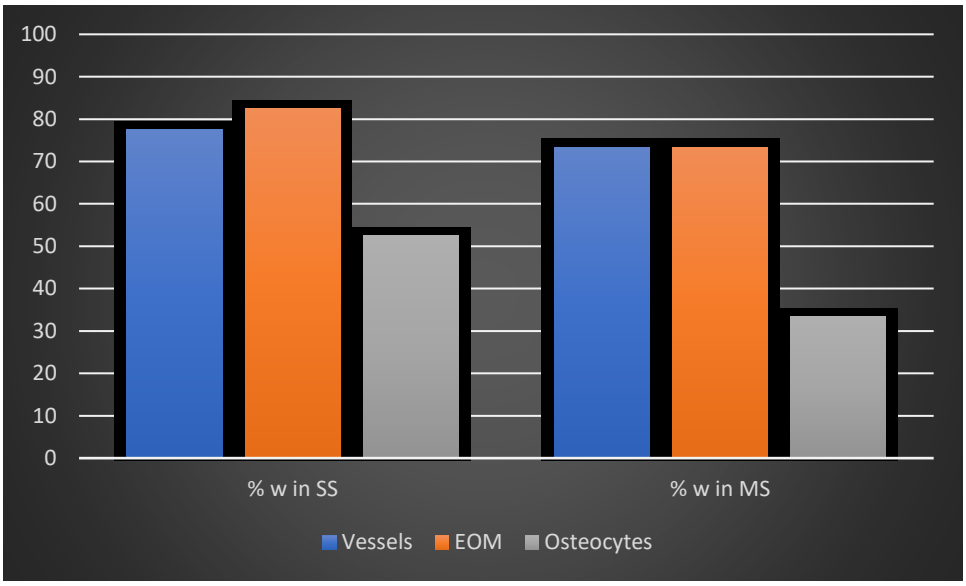

Figure 8-2. Total percentage of specimens tested that preserved each tissue of interest recovered from different depositional matrixes. Note there is no significant differences for vessels or EOM tissues, while osteocytes appear to be more readily preserved in specimens found in sandstone (this is likely sampling bias since only 15 or 55 specimens were recovered from mudstone, most of which originate from the DPF).

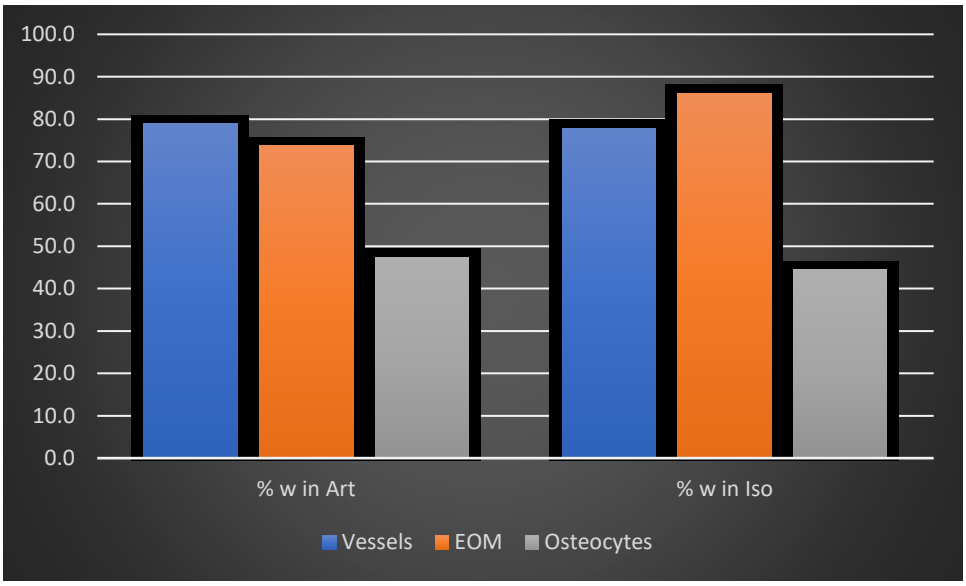

Figure 8-3. Total percentage of specimens tested that preserved each tissue of interest recovered from either articulated/associated skeletons or isolated/bonebed bones. Note there is no significant differences for any tissues.

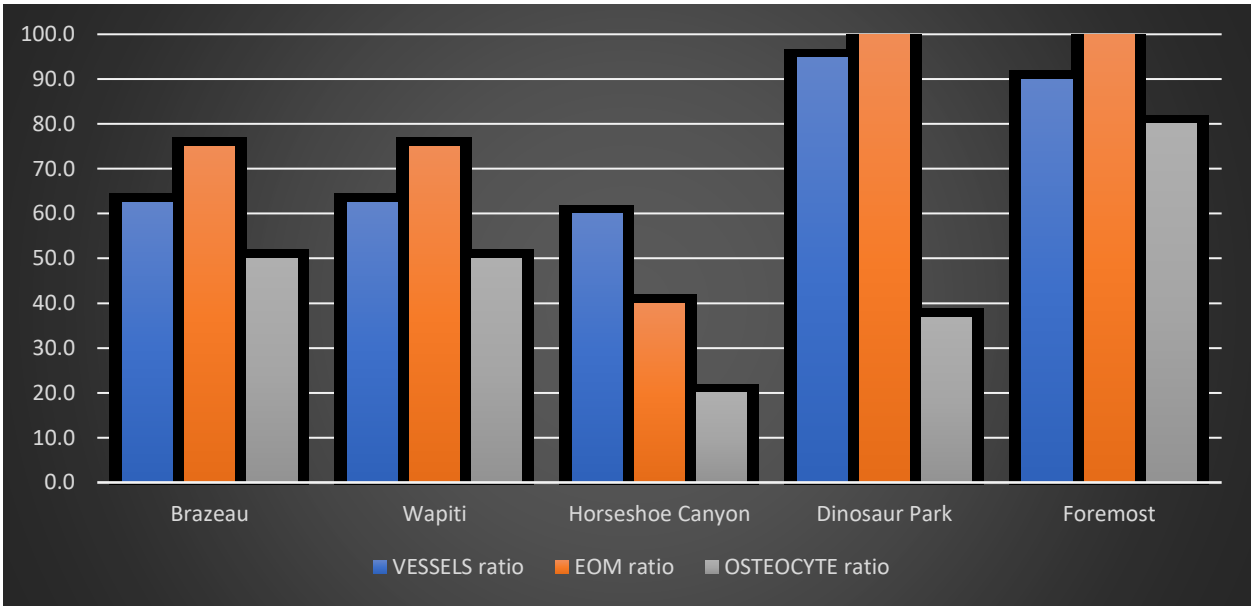

Figure 8-4. Percent of specimens from which each tissue type was recovered per formation in the study area. Formations ordered along virtual transect from more upland formations (left) to upper shoreface (right). Note that terrestrial environments generally preserve lower frequencies of original organic structures, but coastal environments preserve the lowest recoveries of osteocytes.

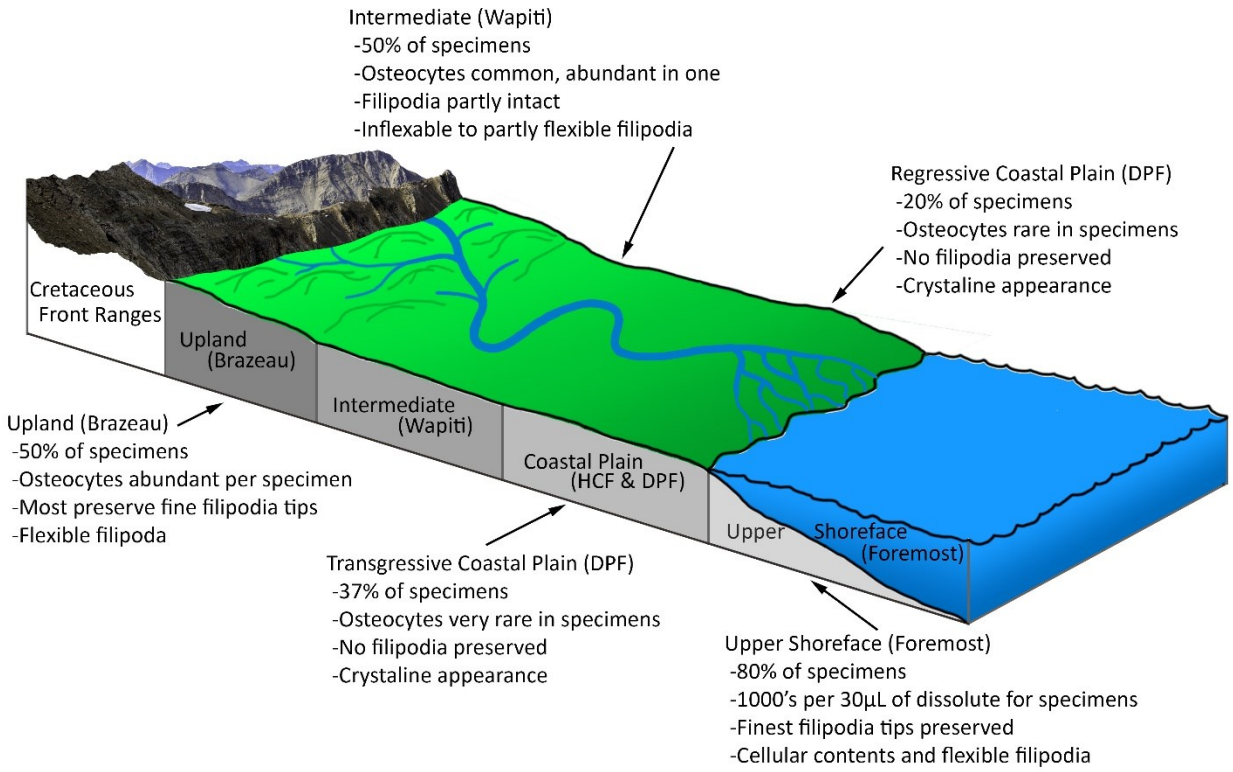

Figure 8.5. Summary of osteocyte rates and quality of preservation across the virtual transect of depositional environments from upland to upper shoreface. As terrestrial environments approach coastal plains from upland environments, osteocytes become less common and more poorly preserved. The upper shoreface of the upper Foremost Formation produced the best preservation for osteocytes in this study.

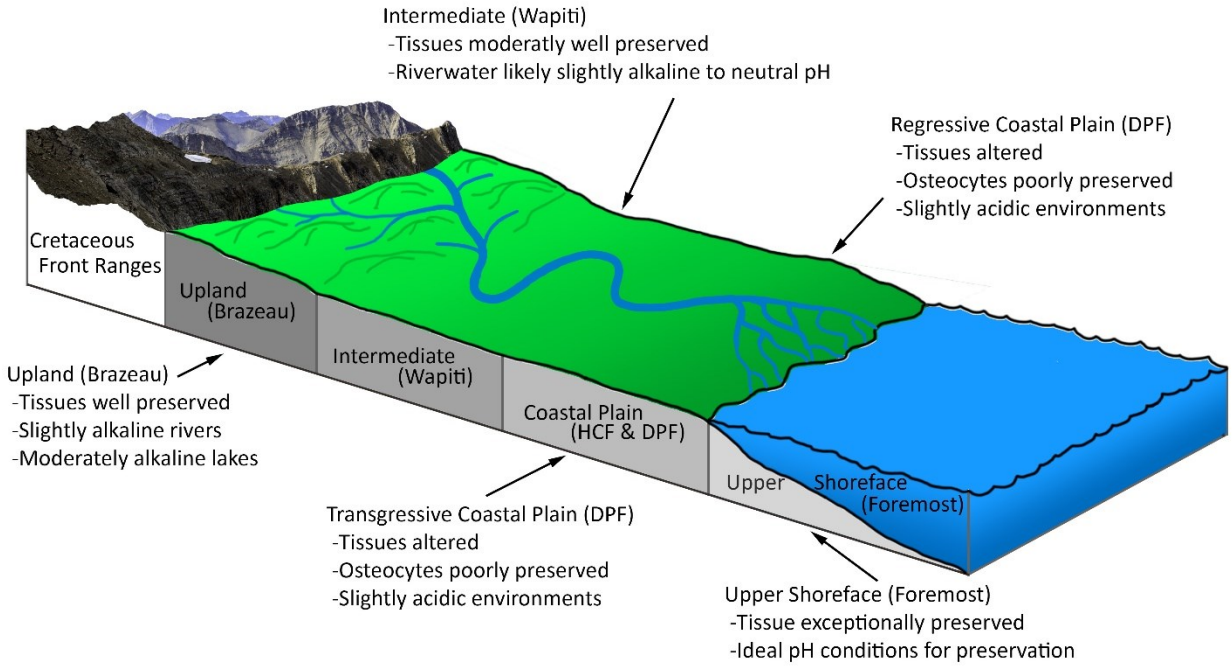

Figure 8-6. Summary of tissue preservation and the environmental pH conditions across the virtual transect of depositional environments from upland to upper shoreface. As terrestrial environments approach coastal plains from upland environments, pH decreases along with tissue preservation quality. The upper shoreface of the upper Foremost Formation produced the best tissue preservation and had pH closest to ideal.

Chapter 9: First description of vertebrate remains from the Brazeau Formation (Upper Cretaceous) of the Rocky Mountain Foothills, western Alberta.

9.1 Introduction

The Upper Cretaceous Brazeau Formation (early Campanian - early Maastrichtian) represents a regressive nearshore marine to proximal fluvial depositional environment with repeating channel sands, crevasse splays, floodplains, and paleosol deposits, with interbedded coal and tephra (Jerzykiewicz and McLean 1980). The Brazeau Formation is the Alberta Foothills equivalent to the Wapiti Formation in the Grande Prairie region. Additionally, it is temporally equivalent (from oldest to youngest formations) to the Foremost, Oldman, Dinosaur Park, Bearpaw, and the Horseshoe Canyon Formations in central Alberta (Jerzykiewicz and McLean 1980, Fanti and Catuneanu 2009). The Brazeau Formation conformably overlies the marine shales of the Wapiabi Formation (Coniacian-early Cenomanian) and underlies the terrestrial Coalspur Formation (Maastrichtian-Paleocene). Much of the formation underwent significant structural deformation during a series of Eocene thrust faulting events (Pană and van der Pluijm 2014). Previous work attempting to correlate the Brazeau Formation to others within Alberta relied heavily upon palynological collections. These correlations could only produce zones within the formation that could be placed as equivalents to other formations, not specific ages (Gunther and Hills 1972). Consequently, without radiometric dating it is difficult to determine precisely which stratigraphic levels outcrops in the formation represent.

In spite of the poor chronology and difficult stratigraphic correlation between outcrops, the Brazeau Formation represents a largely uninterrupted terrestrial sequence with no major unconformities, providing an opportunity to investigate terrestrial ecosystems and vertebrate diversity during the middle Campanian (Jerzykiewicz and McLean 1980). On the other hand, the marine Bearpaw Formation (middle Campanian) has more precise biostratigraphic dating control but lower likelihood of finding Campanian terrestrial vertebrate remains in central and eastern Alberta. Recovering vertebrate remains from the Brazeau Formation, however, is difficult due to forest cover and poor exposure. The limited exposures tend to be vertical cliff faces along swift moving mountain rivers and streams. Consequently, little exploration has been conducted for palaeontological resources. Prior to this study, the only reference to Brazeau Formation vertebrates was a tentative identification of "*Gorgosaurus"* teeth and a *"Corythosaurus*" "toe bone" (Lang 1947). These specimens were recovered from a presently unknown locale by R. C. Sibley, the local Entrance train station attendant, and sent to Barnum Brown at the American Museum of Natural History for identification (Appendix 9-1). Photos sent by R. C. Sibley to John Allen at the University of Alberta in the late 1940s (Fig. 9-1) show that several specimens were collected from a bonebed within a single mudstone layer. Several of the elements observed in the photographs indicate that the bonebed is dominated by large bodied, adult hadrosaurs.

During the fall of 2017 and the summer of 2018, a combined total of seven weeks was spent in the Brazeau Formation collecting geological samples and palaeontological specimens. In 2017, a rumoured bonebed in Entrance, Alberta (8.5 km west of Hinton) (Fig. 9-2) was investigated. Systematic excavation of the Bennett Bonebed, named after the landowner,

began in August 2018 and is scheduled to continue. The bonebed was originally exposed in the late 1970s during the construction of a driveway on the property, indicating that this is not the bonebed from which R. C. Sibley was collecting in the 1940s. Work in 2018 recovered 64 specimens from a quarter square metre, including a well preserved juvenile hadrosaur postorbital that can be identified as *Edmontosaurus regalis*. With such an abundance of specimens collected from such a small area, and the lack of vertebrate remains from the Brazeau Formation, the Bennett Bonebed could provide important information into Late Cretaceous palaeo-Rocky Mountain Foothill ecosystems. In addition, two tephra beds in close stratigraphic association to the bonebed were mapped and sampled for zircon U-Pb geochronology, yielding the first radiometric date for the Brazeau Formation.

9.2 Materials and Methods

9.2.1 Specimen imaging

Specimen photographs were taken using a Canon 7D Mark II with a Tamron 24-70 mm lens set to 70 mm with ISO 100, f/6.3, and 1/250 exposure time. Two Canon Speedlite 600EX flashes were set 180^{o} to each other to evenly illuminate the specimen. Three-dimensional models were created using FlexScan3D V 3.3.9.1 software with a Polyga HDI Advance R5X-Monochrome 3D Scanner and were manipulated in the ORS software Dragonfly 3.6. Figures were created using Adobe Photoshop CS6.

9.2.2 Tephra geochronology

Two tephra deposits were found ~16.5 m stratigraphically above the Bennett Bonebed (Fig. 9-3). The tephras are termed the Western Pacific Tephra (WPT) A and B. WPT-A is 10-20

cm thick and infills low-relief swales in underlying sandstone with a sharp lower contact. WPT-A has a sharp planar upper contact with an overlying 15-cm-thick organic-rich thinly bedded mud, which is in turn sharply overlain by the 10-20 cm-thick WPT-B. Both tephra beds extend laterally across at least ~20 m (bedding is dipping at ~40^{o} W so tephra is lost subsurface) at a relatively constant thickness. Large (~2 kg) samples were collected from each bed for zircon U-Pb geochronology, in order to constrain the timing of the eruption associated with the WPT-A and -B tephras.

Each sample was fluidized into a slurry in water and passed across a Wilfley table to concentrate dense minerals, similar to the method described by Söderlund and Johansson (2002). Between each sample great care was taken to clean the Wilfley table to reduce the risk of contamination. From the dense mineral concentrate ~50-100 zircons were hand picked to mount in epoxy. The grain mount was polished to expose the grain centres and regions suitable for analysis were identified from cathodoluminescence imaging.

U-Pb zircon data were collected using laser ablation multi collector inductively coupled mass spectrometry (LA-MC-ICPMS) at the Canadian Centre for Isotopic Microanalysis at the University of Alberta, Edmonton, Canada using procedures modified from Simonetti et al. (2005). The analytical setup consists of a New Wave UP-213 laser ablation system interfaced with a Nu Plasma MC-ICPMS equipped with three ion counters and 12 Faraday cups. We operated the laser at 4 Hz with a beam diameter of 30 µm which yielded a fluence of ~1-3 J/cm^2. Ablations were conducted in a He atmosphere at a flow rate of 1 L/min through the ablation cell. Output from the cell was joined to the output from a standard Nu Plasma desolvating nebulizer (DSN). On peak gas + acid blanks (30s) were measured prior to a set of

analyses. Data were collected statically consisting of 30 1s integrations. Before and after each set of analyses, zircon reference materials GJ1 (Jackson et al. 2004) and Plesovice (Sláma et al. 2008) were repeatedly analyzed, to monitor and correct for U-Pb fractionation, reproducibility, instrument drift, and to assess data quality. Mass bias for Pb isotopes was corrected by measuring $^{205}Tl/^{203}Tl$ from an aspirated Tl solution (NIST SRM 997) via the DSN-100 desolvating nebulizer using an exponential mass fractionation law and assuming a natural $^{205}Tl/^{203}Tl$ of 2.3871. All data were reduced offline using an Excel-based program. Unknowns were normalized to GJ1 as the primary reference; Plesovice was treated as an unknown to assess data quality and yielded a weighted average $^{206}Pb/^{238}U$ age of 338.3 ± 1.9 Ma (n=10, MSWD = 0.37), well within uncertainty of the age reported by Sláma et al. (2008). The uncertainties reported are a quadratic combination of the internal measurement precision and the overall reproducibility of the standards during an analytical session. The 2σ reproducibility for the standards is estimated to be ~1% for $^{207}Pb/^{206}Pb$ and 2% for $^{206}Pb/^{238}U$. The data are corrected for common Pb using a Tera-Wasserberg approach due to the difficulty of resolving transient contributions of ^{204}Hg present in the Ar gas from ^{204}Pb present in either the crystal and/or the acid + gas blank. Thus, reported ^{204}Pb values are for informational purposes only, but can be useful for identifying and rejecting samples that have obviously large amounts of common Pb.

Quoted ages for each tephra are the 2σ error-weighted mean of the youngest coherent population of $^{206}Pb/^{238}U$ zircon dates, calculated using the *weightedmean* function, without outlier detection, in the *IsoplotR* package within the R software environment (Vermeesch 2018).

9.3 Results

9.3.1 Description and comparison

UALVP 59617 is well preserved and represents a nearly complete postorbital from a juvenile (based on its small size), that is missing most of the jugal process and the most posterior centimetre of the squamosal process (Fig. 9-4). The overall appearance of the specimen is similar to the postorbitals of the holotype (CMN 2288) and paratype (CMN 2289) of *Edmontosaurus regalis* (Lambe 1920, Xing et al. 2017); it also shows slight similarities to the postorbital of *Edmontosaurus annectens* (Fig. 9-5). The anteriorly oriented frontal process is triangular with a frontal contact surface with two anteroposteriorly oriented grooves. Unfortunately, the ridge that forms the dorsal margin of the top groove is missing, so the complete depth is unknown. The lower, and much larger, groove extends the entire length of the frontal contact and forms approximately 80 percent the height of the contact surface. The anteromedial process is similar to those in CMN 2288 and CMN 2289 but differs slightly in that it hooks posteriorly. This is interpreted as a probable ontogenetic difference, as UALVP 59617 is from a juvenile individual. This process preserves a tripartite contact with three thin, tall, ridges for a limited contact surface with the parietal. The squamosal process, although missing the most distal portion, is a thin lateroventrally dipping bladelike structure that extends posteriorly with a slight medial deflection. The medial surface has a slightly rippled texture for the contact with the squamosal.

The main body of the postorbital is well preserved and possesses a large laterosphenoid facet, oriented medially and located directly ventral to the anteromedial process. The dorsolateral surface has a slight expansion due to the development of an enlarged postorbital

fossa along the orbit edge. The presence of the postorbital fossa is a diagnostic character for the genus *Edmontosaurus,* and the relatively enlarged size of the fossa is characteristic of *Edmontosaurus regalis* (Campione and Evans 2011, Xing et al. 2017). Although the well developed postorbital fossa is not present in the Alaskan hadrosaur *Ugrunaaluk kuukpikensis* (Mori et al. 2016), there is nevertheless a shallow fossa in this taxon. Other authors suggest that *Ugrunaaluk kuukpikensis* is synonymous with *Edmontosaurus regalis* (Xing et al. 2017). If this assessment is correct, it indicates that the postorbital pocket may develop to different degrees through ontogeny. The development of this postorbital pocket through ontogeny could explain the relative smaller size of the feature in UALVP 59617.

8.3.2 Geochronology

Zircon crystal morphology ranges from asicular to prismatic showing magmatic oscillatory zoning, with some grains exhibiting sector zoning. Grains with obvious inherited cores were not analyzed. The $^{206}Pb/^{238}U$ dates for WPT-A and WPT-B tephras are remarkably coherent. Of the 30 zircon grains analyzed from each sample, all 30 yielded a coherent age population for WPT-B and only three grains were rejected for WPT-A due to either high common Pb or dates that were markedly older than the youngest coherent population (Fig. 6; Table 1). Error-weighted means for zircon $^{206}Pb/^{238}U$ dates from WPT-A (69.9 ± 0.4 Ma; n=27/30, MSWD = 2.2) and WPT-B (69.9 ± 0.23Ma; n = 30/30, MSWD = 1.9) indicate that the timing of pre-eruption zircon crystallization is statistically indistinguishable between the two beds. Given that bonebed is only 16.5 m stratigraphically below the WPT, the zircon U-Pb dates for WPT-A and WPT-B tephra provide a close minimum age of ~70 Ma for the Bennett Bonebed, placing it in the lower Maastrichtian.

8.4 Discussion

The zircon $^{206}Pb/^{238}U$ dates for the WPT-A and WPT-B tephras are the first radiometric age constraints on the Brazeau Formation. The tephra beds at the Bennett Bonebed site yielded remarkably coherent distributions of zircon U-Pb dates with no modal groupings of dates prior to the Cretaceous (Table 9-1). The stratigraphic position of the Bennett Bonebed below the WPT beds indicates that the UALVP 59617 *Edmontosaurus* specimen must predate the eruption that deposited the WPT tephra beds. But because the bonebed is only 16.5 m stratigraphically below the WPT in a ~1300 m-thick formation, it is suggested that the zircon U-Pb dates for WPT-A and WPT-B tephra provide a close minimum age of ~70 Ma for the Bennett Bonebed, placing it into the early Maastrichtian. The zircon U-Pb dates represent close maxima for the age of the eruption that deposited WPT-A and WPT-B because they date the timing of pre-eruption zircon crystallization, although the magnitude of this offset is likely well within analytical uncertainty. Further research on sedimentation rates in the fluvial facies of the Brazeau Formation, and potentially high temporal precision zircon U-Pb dating by single grain thermal ionization mass spectrometry (e.g. Davies et al. 2014), are needed to refine the age constraints on the Bennett Bonebed that are provided by the WPT beds.

Edmontosaurus is a well known and widely distributed genus that has been recovered from Wyoming north to Alaska, from sediments spanning approximately 72.5-66 Ma (Lambe 1917, Campione and Evans 2011, Evans et al. 2015, Mori et al. 2016, Xing et al. 2017). *Edmontosaurus regalis* is common in Alberta, where it is most abundant in the Horseshoe

Canyon Formation (HCF) (Lambe 1917, Evans et al. 2015, Xing et al. 2017). The taxon is thought to be limited to the Horsethief Member of the HCF, with tentative remains from the Upper Drumheller Member, representing a potential temporal span of approximately 72.2 – 71 Ma (Eberth et al. 2013, Evans et al. 2015) within the HCF. A partial *Edmontosaurus regalis* with preserved skin impressions (UALVP 53722), recovered from the Wapiti Formation 2 m below a tephra deposit dated to 72.58 Ma (Bell et al. 2014), supports the possibility that *Edmontosaurus* is present in the Drumheller Member of the HCF (Eberth et al. 2013). With the addition of the Bennett Bonebed specimen, *Edmontosaurus regalis* is now recognized to span 72.58 – ~70 Ma, a total temporal range of at least 2.6 Myr.

The remains reported here are the first evidence for *Edmontosaurus regalis* from the Brazeau Formation, expanding the geographic range of the taxon into proximal fluvial environments. In comparison, UALVP 53722 from the Wapiti Formation (Unit 4) is associated with floodplain environments with several coal layers, suggesting a wetter, poorly drained environment (Fanti and Catuneanu 2009, Bell and Campione 2014). Additionally, the Horsethief Member of the HCF represents a warm, wet, and poorly drained environment in which *Edmontosaurus regalis* is the only known hadrosaur, suggesting a species well adapted to this type of ecosystem.

During the late Campanian, the Rundle orogenic pulse was occurring. Several thrust faults west of the Bennett Bonebed have been dated, providing a better understanding of paleogeography during the early Maastrichtian (Pană and van der Pluijm 2014). The closest of these dated faults is known as the Rocky Pass Thrust fault (74.8 Ma) (Fig. 9-2) and is presently exposed 37 km to the west. Based on geological cross sections from the Entrance area, the

palaeogeographical distance from the bonebed to the Rocky Pass Thrust is estimated to have been 55 km distant. This places the Bennett Bonebed specimens in close proximity to the palaeo-Rocky Mountains, suggesting that the animals preserved within were likely living in a more topographically diverse environment than existed on the coastal plains where the HCF was laid down. After a tectonic hiatus during the Late Maastrichtian and Paleocene, subsequent tectonic activity was initiated along the Rocky Mountain front during the Eocene McConnell orogeny (57.7-51.0 Ma). Further investigation into thrust faults in the front ranges of the Rocky Mountains could create more detailed palaeo-mountain location data, providing a better understanding of palaeotopography and environments.

The inferred ~70 Ma age (early Maastrichtian) for the Bennett Bonebed makes UALVP 59617 among the youngest identified *Edmontosaurus regalis* specimens currently known, tentatively by ~1 Ma. Prior to this study, *Edmontosaurus regalis* was thought to be restricted to the Late Campanian (Campione and Evans 2011). Additionally, the Bennett Bonebed is stratigraphically equivalent to the top of the Drumheller Marine Tongue in the lower Tolman Member of the HCF (Eberth et al. 2013). There are two known hadrosaur taxa from the HCF during this interval, *Hypacrosaurus altispinus* (Lambeosaurinae) and *Saurolophus osborni* (Hadrosaurinae). Eberth et al. (2013) provided evidence that hadrosaur taxa turnover events observed in the HCF occur during times of climatic change. They concluded that *Edmontosaurus regalis* preferred warm and wet environments and thus shifted its geographic range when the climate became cool and dry during times of climactic change. For example, the taxon is abundant in the Horsethief Member of the HCF, where palynology indicates warm and wet

environments. However, it is absent from stratigraphically higher members of the formation that have proxy evidence for cool and dry conditions.

The presence of *Edmontosaurus regalis* in the Brazeau Formation during the same cool, dry, climactic period in a topographically higher environment suggests that the taxon may have a wider ecological tolerance than previously assumed. Instead, it is possible that with the change in climate observed at the top of the Horsethief Member in the HCF, *Edmontosaurus regalis* was outcompeted by *Hypacrosaurus altispinus* and *Saurolophus osborni*, taxa that may have had stronger affinities for cool and dry coastal environments. The discovery of dinosaurs in the Brazeau Formation highlights new potential for research on environmental partitioning for other dinosaur taxa through the Campanian and early Maastrichtian of Alberta.

9.5 Conclusions

The identification and description of an *Edmontosaurus regalis* postorbital from the Bennett Bonebed represents the first identified taxon and the first described vertebrate remains from the Brazeau Formation. The postorbital is identified as *Edmontosaurus regalis* because it possesses a well-developed postorbital fossa, a feature that is presently only known in this species. Based on the small size, it appears to be from a subadult individual. Two tephra beds, the Western Pacific Tephra A and B, are 16.5 m above the Bennett Bonebed and date to ~70 Ma, suggesting the animal lived in the early Maastrichtian. This is the first report of *Edmontosaurus regalis* from the Maastrichtian, potentially extending the temporal distribution of the species by ~1 Ma. *Edmontosaurus regalis* therefore appears to have persisted for about 2.5 million years, which is within the range often talked about for vertebrate species (Uyeda et

al. 2011). This new specimen from the Bennett Bonebed, together with radiometric dating of stratigraphically associated tephra, suggests that *Edmontosaurus regalis* was coeval with *Hypacrosaurus* and *Saurolophus*, although their ecological preferences may have been different enough that their geographic ranges did not overlap.

Table 9-1. U-Pb isotope ratios and ages for WPT tephra zircons.

sample name	^{206}Pb (cps)	^{204}Pb (cps)	^{238}U/^{206}Pb	2 ?	^{207}Pb/^{206}Pb	2 ?	^{206}Pb*/^{238}U[b] f_{206}[a]	age (Ma)	2 ?
A-001	21923	33	93.25	1.68	0.0472	0.0008	1.000	68.8	1.24
A-003	22099	29	92.14	1.72	0.0469	0.0009	1.001	69.6	1.29
A-004	19977	19	92.39	1.74	0.0481	0.0014	0.999	69.3	1.30
A-005	34963	22	91.14	1.72	0.0474	0.0007	1.000	70.3	1.32
A-006	32240	19	91.87	1.77	0.0480	0.0007	0.999	69.7	1.33
A-007	30440	27	91.78	1.66	0.0504	0.0009	0.996	69.6	1.25
A-008	20768	31	91.96	1.61	0.0503	0.0009	0.996	69.5	1.21
A-009	38829	27	93.04	1.64	0.0479	0.0007	0.999	68.9	1.21
A-010	37257	19	89.05	1.77	0.0473	0.0007	1.000	72.0	1.43
A-011	15390	26	93.82	1.74	0.0475	0.0009	1.000	68.3	1.26
A-012	12155	25	92.42	1.76	0.0484	0.0010	0.999	69.3	1.31
A-013	41584	41	89.43	1.86	0.0477	0.0007	1.000	71.7	1.48
A-015	33384	26	91.00	1.81	0.0491	0.0010	0.998	70.3	1.39
A-016	13236	26	91.43	1.82	0.0474	0.0011	1.000	70.1	1.39
A-017	35196	59	87.69	1.55	0.0641	0.0036	0.979	71.6	1.26
A-018	40803	20	91.42	1.77	0.0494	0.0008	0.997	70.0	1.35
A-019	45639	6	92.36	1.73	0.0478	0.0007	0.999	69.4	1.29
A-020	22732	3	92.65	1.82	0.0478	0.0008	1.000	69.2	1.35
A-021	34830	14	89.26	1.90	0.0480	0.0009	0.999	71.8	1.52
A-022	29775	9	92.36	1.66	0.0494	0.0008	0.998	69.2	1.24
A-023	28292	17	90.30	1.98	0.0567	0.0041	0.988	70.2	1.53
A-024	42796	2	91.25	1.67	0.0479	0.0007	0.999	70.2	1.28
A-025	34003	43	90.80	1.65	0.0476	0.0007	1.000	70.6	1.27
A-027	40345	32	88.91	1.88	0.0469	0.0006	1.001	72.1	1.52
A-028	38627	48	91.17	1.74	0.0509	0.0013	0.996	70.0	1.33
A-029	23269	32	91.53	1.77	0.0486	0.0008	0.998	69.9	1.35
A-030	26150	25	92.88	1.84	0.0479	0.0007	0.999	69.0	1.36
B-001	25981	28	93.31	1.71	0.0484	0.0007	0.999	68.6	1.25
B-002	65103	30	92.44	1.71	0.0494	0.0008	0.997	69.2	1.27
B-003	175359	65	90.21	1.56	0.0501	0.0007	0.997	70.8	1.22
B-004	82064	42	91.50	1.62	0.0476	0.0006	1.000	70.1	1.23
B-005	19572	29	92.70	1.72	0.0475	0.0010	1.000	69.2	1.28
B-006	68540	33	91.65	1.60	0.0502	0.0012	0.996	69.7	1.21
B-007	26474	26	91.71	1.58	0.0487	0.0008	0.998	69.8	1.19
B-008	89008	34	91.57	1.69	0.0479	0.0006	0.999	70.0	1.28
B-009	56725	54	90.07	1.72	0.0483	0.0006	0.999	71.1	1.35
B-010	121444	92	91.43	1.65	0.0506	0.0006	0.996	69.8	1.25
B-011	70268	37	93.19	1.63	0.0479	0.0006	0.999	68.8	1.20
B-012	212011	48	89.36	1.62	0.0482	0.0005	0.999	71.7	1.29
B-013	276416	59	89.57	1.59	0.0486	0.0006	0.999	71.5	1.26
B-014	71039	36	91.39	1.63	0.0479	0.0007	0.999	70.1	1.24
B-015	59139	34	90.97	1.69	0.0476	0.0006	1.000	70.5	1.30
B-016	48972	49	90.40	1.54	0.0481	0.0007	0.999	70.9	1.20
B-017	50836	61	90.85	1.57	0.0492	0.0009	0.998	70.4	1.21
B-018	54844	49	89.22	1.71	0.0482	0.0006	0.999	71.8	1.37
B-019	73146	55	92.31	1.70	0.0489	0.0007	0.998	69.3	1.27
B-020	137948	72	90.84	1.65	0.0494	0.0007	0.997	70.4	1.27
B-021	54582	53	92.02	1.76	0.0504	0.0010	0.996	69.4	1.32
B-022	58878	65	91.26	1.58	0.0518	0.0008	0.994	69.9	1.20
B-023	94485	57	92.46	1.55	0.0489	0.0005	0.998	69.2	1.15
B-024	17239	32	93.06	1.63	0.0475	0.0010	1.000	68.9	1.20
B-025	26765	46	90.85	1.50	0.0495	0.0009	0.997	70.4	1.15
B-026	78758	53	92.12	1.60	0.0481	0.0006	0.999	69.5	1.20
B-027	70331	39	91.55	1.54	0.0477	0.0006	1.000	70.0	1.17
B-028	73966	46	92.58	1.59	0.0478	0.0006	1.000	69.2	1.19
B-029	64305	65	92.18	1.62	0.0484	0.0006	0.999	69.5	1.21
B-030	33392	97	91.45	1.67	0.0628	0.0025	0.981	68.8	1.25

[a] f_{206} is the fraction of radiogenic Pb defined by the equation f_{206} =(7/6c -7/6m)/(7/6c-7/6rad), where7/6c is common ^{207}Pb/^{206}Pb at time t estimated from Stacey Kramers Pb evolution model, 7/6m is the measured ^{207}Pb/^{206}Pb, and 7/6rad is radiogenic ^{207}Pb/^{206}Pb at time t. In this case the radiogenic and common Pb at 70 Ma is 0.04747 and 0.8401 respectively.

[b] Radiogenic ^{206}Pb/^{238}U age.

FIGURES

Figure 9-1. Photographs sent from R. C. Sibley to John Allan of material collected in the 1940s along the abandoned Western Pacific Railway. The current location of the specimens is not known. a) Horizon from which specimens were collected (white arrows marked by Sibley on original photographs). Note wooden railway ties at base of exposure. b) Proximal hadrosaur humerus (left) and anterior portion of hadrosaur ilium missing preacetabular process (right). c) Large tibia (left) and large fibula (right). d) Variety of tyrannosaur teeth and a large hadrosaur pedal ungual (far right).

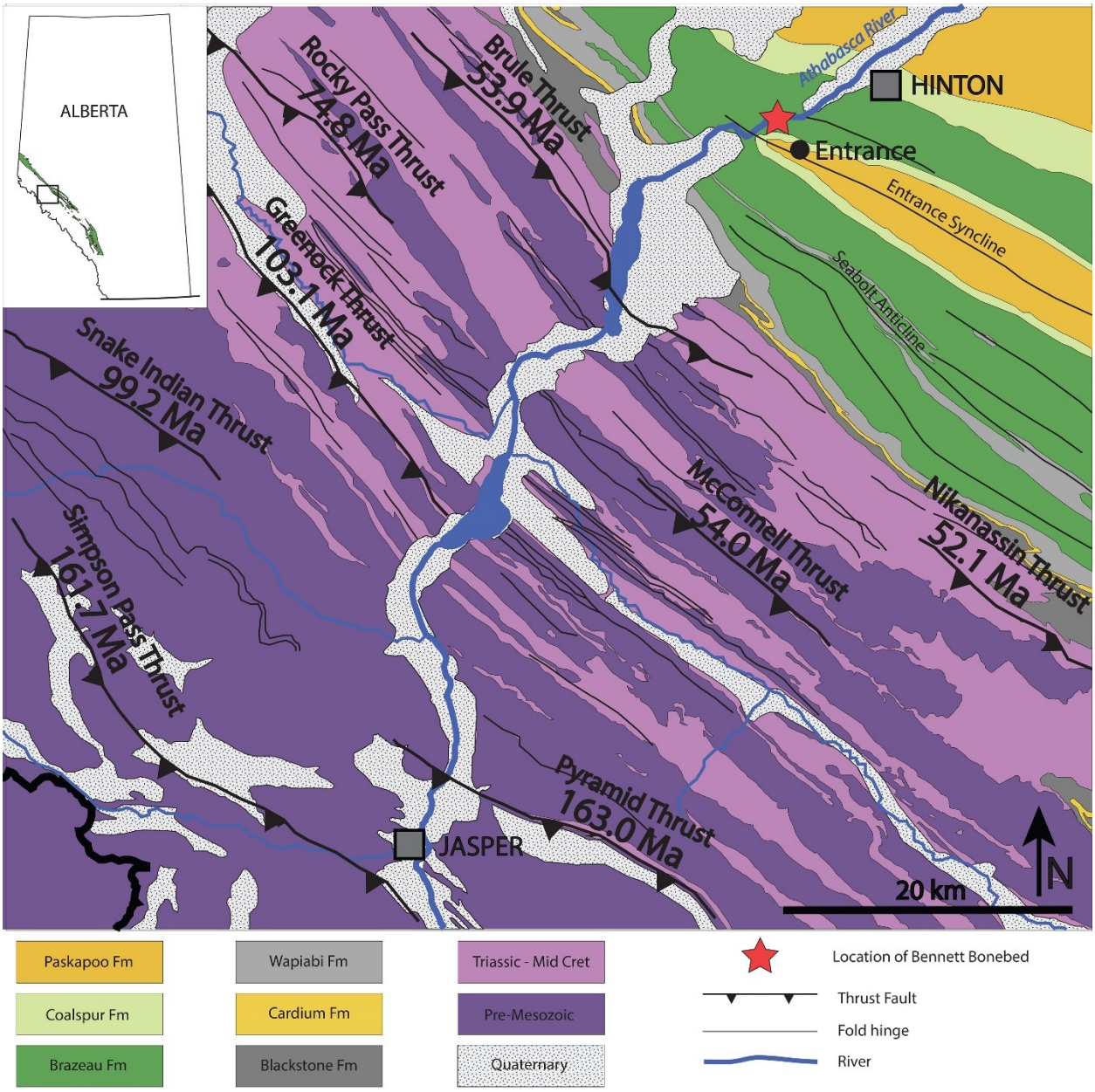

Figure 9-2. Geological map of the area surrounding the Bennett Bonebed showing formations and geological structures. Dates are the approximate ages of corresponding thrust faults (Pană and van der Pluijm 2014). Modified from Alberta Geological Survey Map 560.

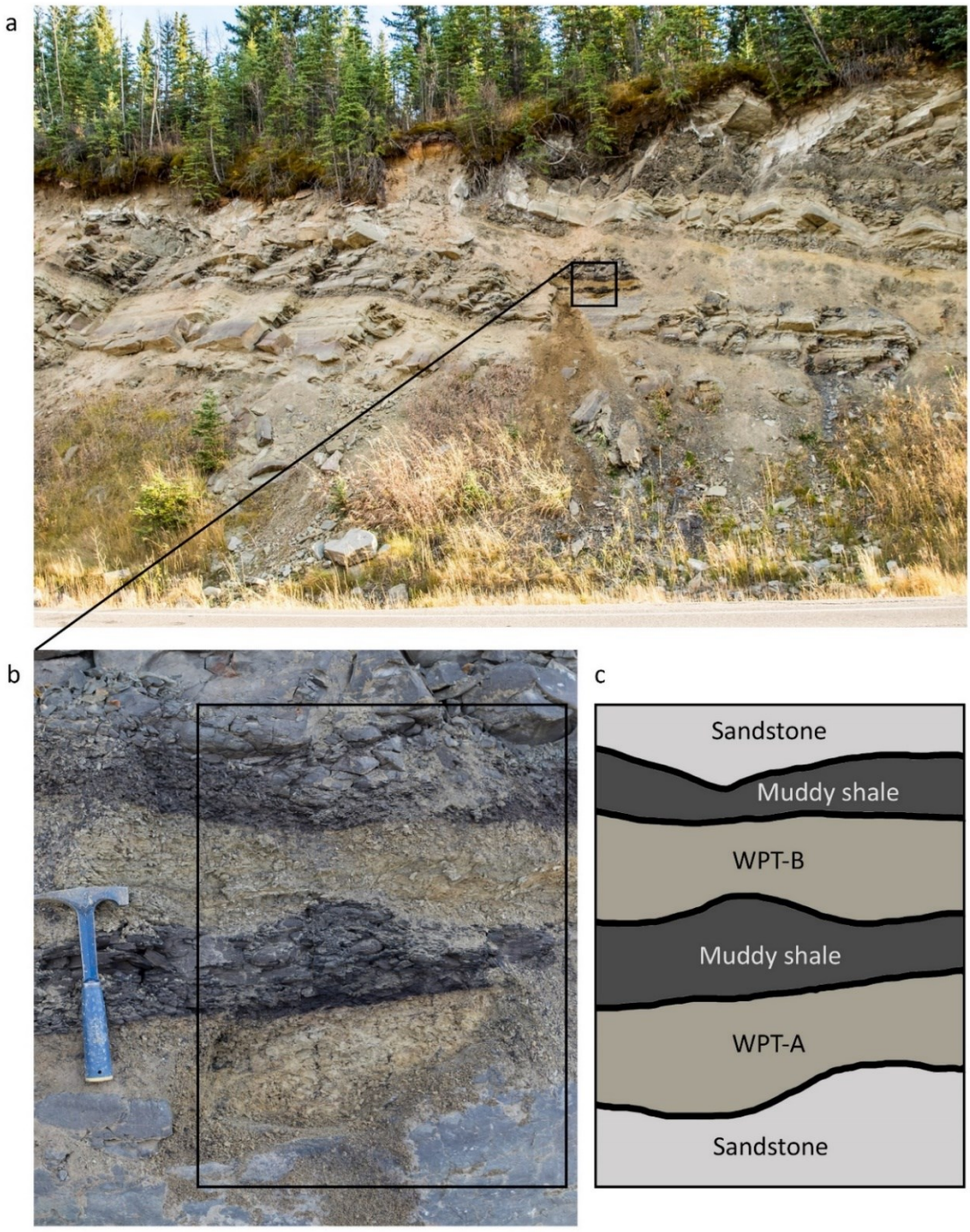

Figure 9-3. Western Pacific Tephra site and stratigraphy. a) Road cut exposure along Alberta Highway 40 showing location of the WPT in context with surrounding stratigraphy. b) Enlarged portion in “a” showing WPT-A and -B. c) Graphical illustration of outlined portion in “b”. Hammer as scale is 30 cm in length.

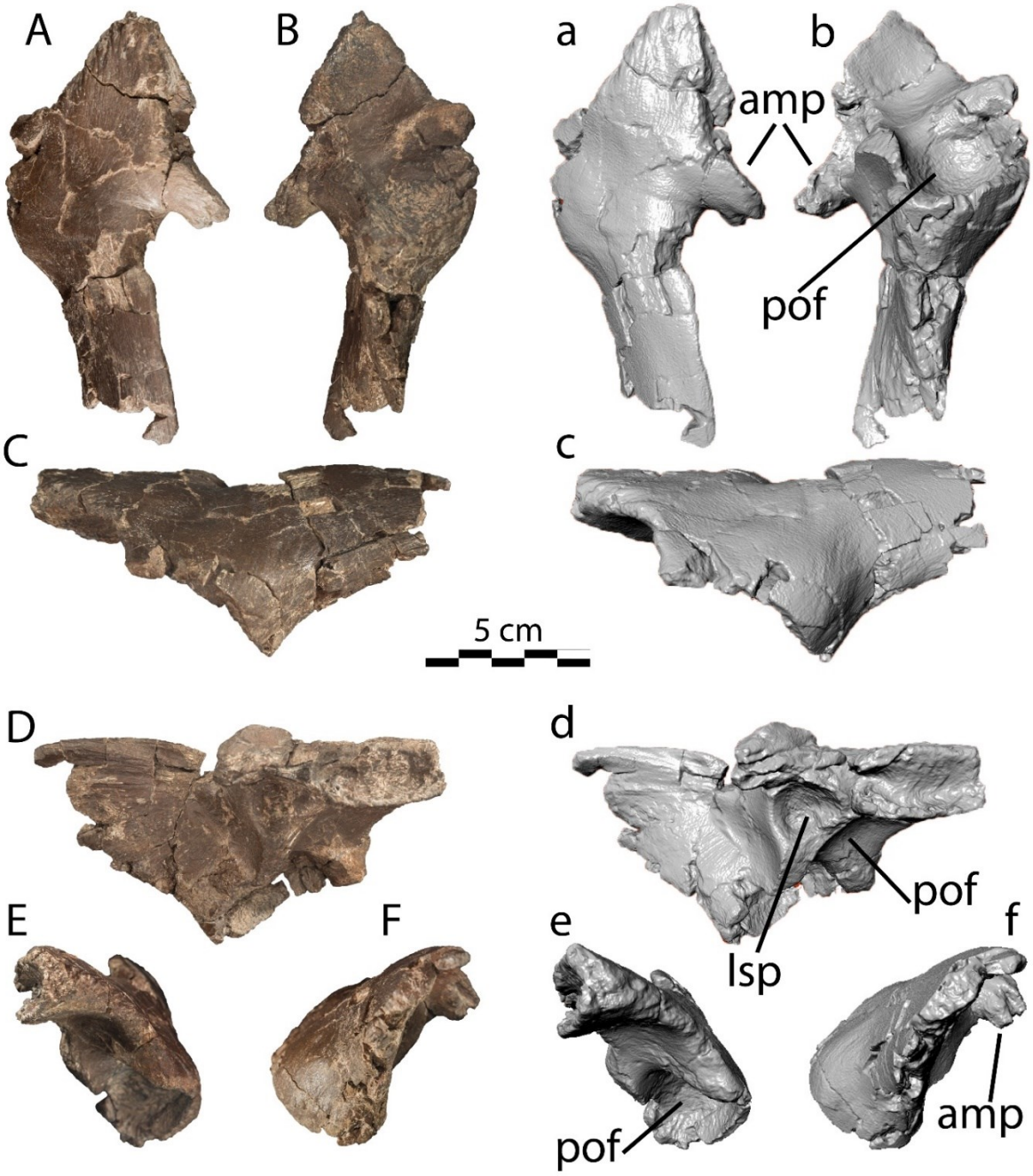

Figure 9-4. UALVP 59617. Corresponding letters represent the same view. Capital letters are photographs and lower-case letters are 3D models. A) Dorsal view. B) Ventral view. C) Lateral view. D) Medial view. E) Anterior view. F) Posterior view. Abbreviations: amp, anteromedial process; lsp, laterosphenoid sulcus; pof, postorbital fossa.

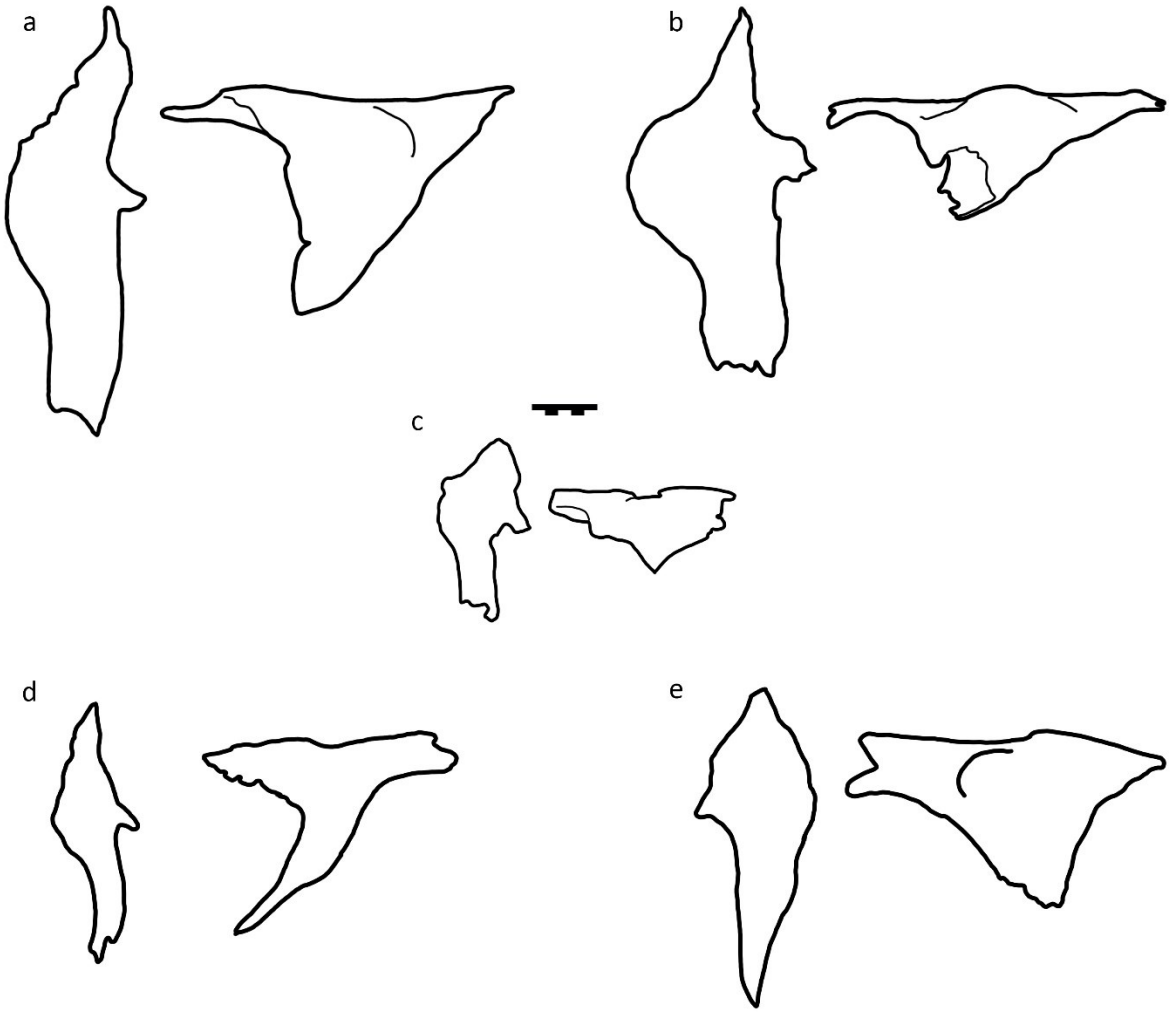

Figure 9-5. Postorbital outlines of *Edmontosaurus*. a, *E. regalis* (holotype, CMN 2288) left postorbital in dorsal (left) and lateral (right) views. b, *E. regalis* (paratype, CMN 2289) left postorbital in dorsal (left) and lateral (right) views. c, *E. regalis* (UALVP 59617) left postorbital in dorsal (left) and lateral (right) views. d, *E. annectens* (CMN 8509) left postorbital in dorsal (left) and lateral (right) views. e, *E. annectens* (ROM 64076) right postorbital in dorsal (left) and lateral (right) views. Scale bar is 5 cm.

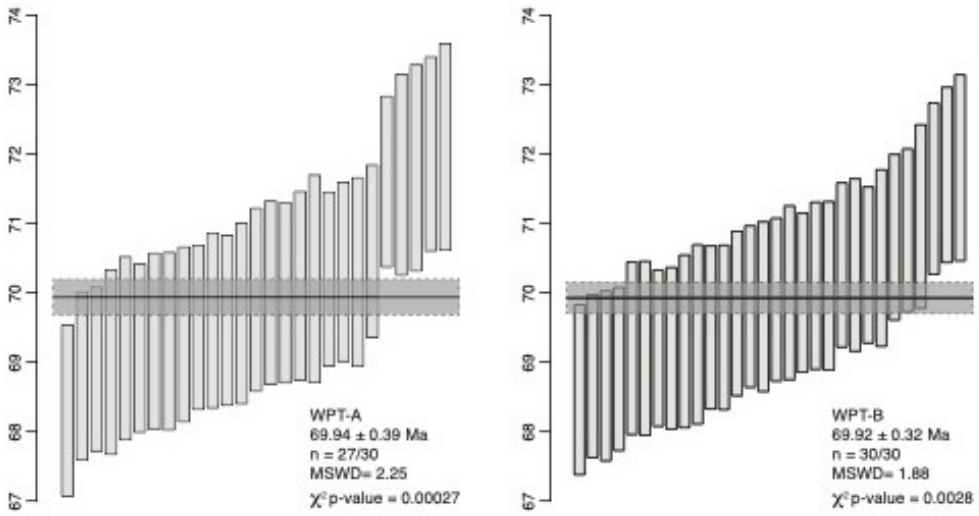

Figure 9-6. Weighted mean $^{206}Pb/^{238}U$ zircon dates for WPT-A and WPT-B. Vertical bars are the 2σ age ranges for individual zircon dates (Table 1). The horizontal line and horizontal bar with dashed outline mark the error-weighted mean and 2σ confidence interval for the plotted zircon dates.

CONCLUSIONS

Preservational rates of tissues in Upper Cretaceous formations from Alberta are greater than expected, and the quality of tissue structures vary significantly. Although each formation had specimens that produced tissues, a trend towards lower quality of tissues in coastal plains is observed. Therefore, an understanding of the depositional environment is required to formulate a hypothesis that can explain why tissues persist into deep time.

Original organic tissues were identified in the feathered *Ornithomimus edmontonicus* specimen UALVP 52531 in the form of feathers. After further investigation into these feathers, evidence that fragments, if not near complete portions, of α-keratin, β-keratin, and other whole feather proteins remain intact. Eumelanin within melanosome microbodies support the proposal that original organic compounds have been preserved within the feathers. By identifying keratin proteins and eumelanin within the feathers, there is sufficient support to suggest that microstructures observed in SEM images are original keratinous microstructural components of the feather. *Ornithomimus* feather cortex is formed by multiple layers of keratin like that of modern bird feathers. Also like modern avian feathers, melanosomes are deposited in layers between the keratin layers. Internal pith structures present the same morphology as modern pith, including each of the types of keratin fibres, pores, and how pith cells are attached to one another and to the cortex. This indicates that medullary pith within feathers is a basal character and evolved long before the evolution of flight in a phylogenetic context. Because of this insight, it can be concluded that pith was exapted for the stresses on feathers during flight, and that the original function of pith is still unknown, although it is possible it was for higher insulating capacity or to strengthen a quill like structure.

The identification of original organics in *Ornithomimus* feathers suggested that other organic tissues may be recoverable from within bone fragments from the Upper Cretaceous formations of Alberta. Vertebrate specimens from the Brazeau, Dinosaur Park, Foremost, Horseshoe Canyon, and Wapiti Formations were sampled for dissolution in EDTA. Tissues recovered ranged from poorly preserved, crystalline-like, fragments, to completely three dimensional, flexible, networks of vessels with EOM and osteocytes. A trend is apparent when preservation rates and qualities of tissues are compared between each of the five formations. The upland Brazeau Formation environments, which were close to the water source for the fluvial systems, provided well preserved tissues and osteocyte filipodia that remained fully intact. The Dinosaur Park and Horseshoe Canyon Formations, which were coastal plain environments, mainly preserved crystalline vessels, and rarely osteocytes. Osteocytes that were recovered from bone preserved in these two formations were cell bodies only and appeared as crystalline structures. Tissues recovered from the Wapiti Formation, an intermediate depositional environment between upland and coastal systems present intermediate preservational quality between the Brazeau and Dinosaur Park Formations. The Foremost Formation, an upper shoreface environment, produced exquisitely preserved tissues, including fully three dimensional *in situ* organic phases of bone (vessels surrounded by EOM with osteocytes still connected with one another in the EOM). When the paleo environments of the formations are considered, a change in pH of groundwater follows a trend to change from slightly alkaline in upland environments, to slightly acidic in coastal plain environments. Paleo oceanic pH has been determined to be approximately pH 8.0 – 8.1, near perfect for tissue survival in the archaeological record (Gordon and Buikstra 1981, Baxter 2004, Manifold 2012).

Although specific research into the groundwater conditions during deposition of the five formations of interest have has not been done, freshwater limestones in the Brazeau Formation, and bivalve and gastropod shell buffering at dinosaur eggshell sites in the Dinosaur Park Formation, give clues to environmental pH. It is suggested that a slight alkaline environment in the Brazeau Formation prevented bone dissolution and stabilized organic components for preservation into deep time. Whereas, a slightly acidic environment in the DPF and HCF environments dissolved just enough hydroxy apatite of the canaliculi of the osteocyte filipodia to provide access for bacteria and their digestive enzymes to destroy the tissues. This is supported by the preservational qualities in the Foremost Formation. Due to the near perfect pH of late Cretaceous oceans for both the mineral and organic phases of bone, tissues were unmatched in quality within this study.

Although further investigation into ancient environments with different pH levels during deposition is required to verify the results found as part of this thesis, the trend observed does suggest that initial environmental conditions plays a major role. Because the most important extrinsic factor for immediate preservation of bone is the pH of the surrounding environment, it suggests that this is also the main factor for preservation of tissues into deep time.

LITERATURE CITED

Allison, P.A. 1988. The role of anoxia in the decay and mineralization of proteinaceous macro-fossils. Paleobiology, **2**: 139–154. doi:10.1017/S009483730001188X.

Arnaud, G., Arnaud, S., Ascenzi, A., Bonucci, E., and Graziani, G. 1980. On the problem of the preservation of human bone in sea-water. The international Journal of Nautical Archaeology and Underwater Exploration, **9**: 53–65. doi:10.1016/S0047-2484(78)80091-8.

Asara, J.M., Schweitzer, M.H., Freimark, L.M., Phillips, M., and Cantley, L.C. 2007. Protein Sequences from Mastodon and Tyrannosaurus Rex Revealed by Mass Spectrometry. Science, **316**: 280–285.

Baxter, K. 2004. Extrinsic factors that effect the preservation of bone. The Nebraska Anthropologist, **19**: 38–45.

Bell, P.R., and Campione, N.E. 2014. Taphonomy of the Danek Bonebed: a monodominant Edmontosaurus (Hadrosauridae) bonebed from the Horseshoe Canyon Formation, Alberta. Canadian Journal of Earth Sciences, **51**: 992–1006. doi:10.1139/cjes-2014-0062.

Bell, P.R., Fanti, F., Currie, P.J., and Arbour, V.M. 2014. A mummified duck-billed dinosaur with a soft-tissue cock's comb. Current Biology, **24**: 70–75. doi:10.1016/j.cub.2013.11.008.

Benson, R.B.J., Campione, N.E., Carrano, M.T., Mannion, P.D., Sullivan, C., Upchurch, P., and Evans, D.C. 2014. Rates of Dinosaur Body Mass Evolution Indicate 170 Million Years of Sustained Ecological Innovation on the Avian Stem Lineage. PLoS Biology, **12**. doi:10.1371/journal.pbio.1001853.

Bertazzo, S., Maidment, S.C.R., Kallepitis, C., Fearn, S., Stevens, M.M., and Xie, H.N. 2015. Fibres and cellular structures preserved in 75-million-year-old dinosaur specimens. Nature Communications, **6**: 1–8. Nature Publishing Group. doi:10.1038/ncomms8352.

Brothwell, D.R. 1972. Digging Up Bones: The Excavation, Treatment and Study of Human Skeletal Remains. *In* 2nd edition. British Museum of Natural History, London.

Brown, C.M., Evans, D.C., Campione, N.E., O'Brien, L.J., and Eberth, D.A. 2013. Evidence for taphonomic size bias in the Dinosaur Park Formation (Campanian, Alberta), a model Mesozoic terrestrial alluvial-paralic system. Palaeogeography, Palaeoclimatology, Palaeoecology, **372**: 108–122. Elsevier B.V. doi:10.1016/j.palaeo.2012.06.027.

Brush, A.H. 2000. Evolving a protofeather and feather diversity. American Zoology, **40**: 631–639.

Buckland, W. 1824. Notice of the Megalosaurus or great fossil lizard of Stonesfield. Transactions of the Geological Scociety, **1**: 390–396.

Campione, N.E., and Evans, D.C. 2011. Cranial growth and variation in edmontosaurs (Dinosauria: Hadrosauridae): Implications for latest Cretaceous megaherbivore diversity in North America. PLoS ONE, **6**. doi:10.1371/journal.pone.0025186.

Campione, N.E., Evans, D.C., Brown, C.M., and Carrano, M.T. 2014. Body mass estimation in non-avian bipeds using a theoretical conversion to quadruped stylopodial proportions. Methods in Ecology and Evolution,: n/a-n/a. doi:10.1111/2041-210X.12226.

Chen, P.J., Dong, Z.M., and Zhen, S.N. 1998. An exceptionally well-preserved theropod dinosaur

from the Yixian Formation of China. Nature, **391**: 147–152. doi:10.1038/34356.

Child, A.M. 1995. Microbial Taphonomy of Archaeological Bone. Studies in Conservation, **40**: 19–30.

Cleland, T.P., Schroeter, E.R., Zamdborg, L., Zheng, W., Lee, J.E., Tran, J.C., Bern, M., Duncan, M.B., Lebleu, V.S., Ahlf, D.R., Thomas, P.M., Kalluri, R., Kelleher, N.L., and Schweitzer, M.H. 2015. Mass Spectrometry and Antibody-Based Characterization of Blood Vessels from Brachylophosaurus canadensis. Journal of Proteome Research, **14**: 5252–5262. doi:10.1021/acs.jproteome.5b00675.

Collins, M.J., Hiller, J., Smith, C.I., Roberts, J.P., Prigodich, R. V, Wess, T.J., and Millard, A.R. 2002. The survival of organic matter in bone: A review. Archaeometry, **3**: 383–394.

Cullen, T.M., Fanti, F., Capobianco, C., Ryan, M.J., and Evans, D.C. 2016. A vertebrate microsite from a marine-terrestrial transition in the Foremost Formation (Campanian) of Alberta, Canada, and the use of faunal assemblage data as a paleoenvironmental indicator. Palaeogeography, Palaeoclimatology, Palaeoecology, **444**: 101–114. Elsevier B.V. doi:10.1016/j.palaeo.2015.12.015.

Currie, P.J. 1988. The discovery of dinosaur eggs at Devil's Coulee. Alberta, **1**: 3–10. doi:10.1017/CBO9781107415324.004.

Currie, P.J., and Chen, P. 2001. Anatomy of Sinosauropteryx prima from Liaoning, northeastern China. Canadian Journal of Earth Sciences, **38**: 1705–1727. doi:10.1139/cjes-38-12-1705.

Currie, P.J., Holmes, R.B., Ryan, M.J., and Coy, C. 2016. A juvenile chasmosaurine ceratopsid

(Dinosauria, Ornithischia) from the Dinosaur Park Formation, Alberta, Canada. Journal of Vertebrate Paleontology, **36**. doi:10.1080/02724634.2015.1048348.

Daniel, J.C., and Chin, K. 2010. The Role of Bacterially Mediated Precipitation in the Permineralization of Bone. Palaios, **25**: 507–516. doi:10.2110/palo.2009.p09-120r.

David, M.B., and Vance, G.F. 1991. Chemical Character and Origin of Organic Acids in Streams and Seepage Lakes of Central Maine. Biogeochemistry, **12**: 17–41.

Davies, J.H.F.L., Wotzlaw, J.-F., Wolfe, A.P., Heaman, L.M., and Arbour, V. 2014. Assessing the age of the Late Cretaceous Danek Bonebed with U–Pb geochronology. Canadian Journal of Earth Sciences, **51**: 982–986. doi:10.1139/cjes-2014-0136.

Eberth, D.A. 2005. The Geology. *In* Dinosaur Provincial Park: A spectacular ancient ecosystem revealed. *Edited by* P.J. Currie and E.B. Koppelhus. Indiana University Press, Bloomington, Indiana. pp. 54–82.

Eberth, D.A., and Braman, D.R. 2012. A revised stratigraphy and depositional history for the Horseshoe Canyon Formation (Upper Cretaceous), southern Alberta plains. Canadian Journal of Earth Sciences, **49**: 1053–1086. doi:10.1139/e2012-035.

Eberth, D.A., Evans, D.C., Brinkman, D.B., Therrien, F., Tanke, D.H., and Russell, L.S. 2013. Dinosaur biostratigraphy of the Edmonton Group (Upper Cretaceous), Alberta, Canada: evidence for climate influence. Canadian Journal of Earth Sciences, **50**: 701–726. doi:10.1139/cjes-2012-0185.

Embery, G., Milner, A., Waddington, R.J., Hall, R.C., Langley, M.S., and Milan, A.M. 2000. The

isolation and detection of non-collagenous proteins from the compact bone of the dinosaur Iguanodon. Connective Tissue Research, **41**: 249–259. doi:10.3109/03008200009005293.

Evans, D.C., Eberth, D.A., and Ryan, M.J. 2015. Hadrosaurid (Edmontosaurus) bonebeds from the Horseshoe Canyon Formation (Horsethief Member) at Drumheller, Alberta, Canada: geology, preliminary taphonomy, and significance. Canadian Journal of Earth Sciences, **52**: 642–654. doi:10.1139/cjes-2014-0184.

Fanti, F., Bell, P.R., and Sissons, R.L. 2013. A diverse, high-latitude ichnofauna from the Late Cretaceous Wapiti Formation, Alberta, Canada. Cretaceous Research, **41**: 256–269. Elsevier Ltd. doi:10.1016/j.cretres.2012.12.010.

Fanti, F., and Catuneanu, O. 2009. Stratigraphy of the Upper Cretaceous Wapiti Formation, west-central Alberta, Canada. Canadian Journal of Earth Sciences, **46**: 263–286. doi:10.1139/E09-020.

Fernández-Jalvo, Y., Sánchez-Chillón, B., Andrews, P., Fernández-López, S., and Martínez, L.A. 2002. Morphological taphonomic transformations of fossil bones in continental environments, and repercussions on their chemical composition. Archaeometry, **44**: 353–361. doi:10.1111/1475-4754.t01-1-00068.

Field, D.J., D'Alba, L., Vinther, J., Webb, S.M., Gearty, W., and Shawkey, M.D. 2013. Melanin Concentration Gradients in Modern and Fossil Feathers. PLoS ONE, **8**. doi:10.1371/journal.pone.0059451.

Fox, R.C. 1974. A Middle Campanian, Nonmarine Occurrence of the Cretaceous Toothed Bird Hesperornis Marsh. Canadian Journal of Earth Sciences, **11**: 1335–1338. doi:10.1139/e74-127.

Funston, G.F., and Currie, P.J. 2018. The first record of dinosaur eggshell from the Horseshoe Canyon Formation (Maastrichtian) of Alberta, Canada. Canadian Journal of Earth Sciences, **441**: 436–441.

Gordon, C.C., and Buikstra, J.E. 1981. Soil pH, bone preservation, and sampling bias from mortuary sites. American Antiquity, **28**: 566–571. doi:10.1017/S0021937100024837.

Grellet-Tinner, G. 2005. Membrana testacea of titanosaurid dinosaur eggs from Auca Mahuevo (Argentina): Implications for exceptional preservation of soft tissue in Lagerstätten. Journal of Vertebrate Paleontology, **25**: 99–106. doi:10.1671/0272-4634(2005)025[0099:MTOTDE]2.0.CO;2.

Gunther, P.R., and Hills, L. V. 1972. Megaspores and other palynomorphs of the Brazeau Formation (Upper Cretaceous), Nordegg area, Alberta. Geoscience and Man, **4**: 29–48. doi:10.1080/00721395.1972.9989717.

Gurley, L.R., Valdez, J.G., Spall, W.D., Smith, B.F., and Gillette, D.D. 1991. Proteins in the fossil bone of the dinosaur, Seismosaurus. Journal of protein chemistry, **10**: 75–90. doi:10.1007/BF01024658.

Hathway, B., Banks, C.., and Hay, D.. 2011. Measured Outcrop Section T17-R3W4-01 of the Foremost, Oldman and Dinosaur Park Formations. Edmonton, Alberta, Canada. Available

from www.ags.gov.ab.ca.

Hedges, R.E.M. 2002. Bone diagenesis: An overview of processes. Archaeometry, **3**: 319–328. doi:10.1111/1475-4754.00064.

Hedges, R.E.M., and Millard, A.R. 1995. Bones and Groundwater: Towards the Modelling of Diagenetic Processes. Journal of Archaeological Science, **22**: 155–164. doi:10.1006/jasc.1995.0017.

Jackson, S.E., Pearson, N.J., Griffin, W.L., and Belousova, E.A. 2004. The application of laser ablation-inductively coupled plasma-mass spectrometry to in situ U-Pb zircon geochronology. Chemical Geology, **211**: 47–69. doi:10.1016/j.chemgeo.2004.06.017.

Jans, M.M.E., Kars, H., Nielsen-Marsh, C.M., Smith, C.I., Nord, A.G., Arthur, P., and Earl, N. 2002. In situ preservation of archaeological bone: A histological study within a multidisciplinary approach. Archaeometry, **44**: 343–352. doi:10.1111/1475-4754.t01-1-00067.

Jarvis, E.D., Mirabab, S., Aberer, A.J., Zhang, G., Li, C., Li, Q., Li, B., Larkin, D.M., Lee, C., Storz, J.F., Antunes, A., Greenwold, M.J., Meredith, R.W., Odeen, A., Cui, J., Zhou, Q., Xu, L., Pan, H., Wang, Z., Jin, L., Zhang, P., Hu, H., Yang, W., Hu, J., Xiao, J., Yang, Z., Liu, Y., Xie, Q., Yu, H., Lian, J., Wen, P., Zhang, F., Li, H., Zeng, Y., Xiong, Z., Liu, S., Zhou, L., Huang, Z., An, N., Wang, J., Zheng, Q., Xiong, Y., Wang, G., Wang, B., Wang, J., Fan, Y., da Fonseca, R.R., Alfaro-Nunez, A., Schubert, M., Orlando, L., Mourier, T., Howard, J.T., Ganapathy, G., Pfenning, A., Whitney, O., Rivas, M. V., Hara, E., Smith, J., Farre, M., Narayan, J., Slavov, G., Romanov, M.N., Borges, R., Machado, J.P., Khan, I., Springer, M.S., Gatesy, J., Hoffmann, F.G., Opazo, J.C., Hastad, O., Sawyer, R.H., Kim, H., Kim, K.-W., Kim, H.J., Cho, S., Li, N.,

Huang, Y., Bruford, M.W., Zhan, X., Dixon, A., Bertelsen, M.F., Derryberry, E., Warren, W., Wilson, R.K., Li, S., Ray, D.A., Green, R.E., O'Brien, S.J., Griffin, D., Johnson, W.E., Haussler, D., Ryder, O.A., Willerslev, E., Graves, G.R., Alstrom, P., Fjeldsa, J., Mindell, D.P., Edwards, S. V., Braun, E.L., Rahbek, C., Burt, D.W., Houde, P., Zhang, Y., Yang, H., Wang, J., Gilbert, M.T.P., Wang, J., Ye, C., Liang, S., Yan, Z., Zepeda, M.L., Campos, P.F., Velazquez, A.M. V., Samaniego, J.A., Avila-Arcos, M., Martin, M.D., Barnett, R., Ribeiro, A.M., Mello, C. V, Lovell, P. V, Almeida, D., Maldonado, E., Pereira, J., Sunagar, K., Philip, S., Dominguez-Bello, M.G., Bunce, M., Lambert, D., Brumfield, R.T., Sheldon, F.H., Holmes, E.C., Gardner, P.P., Steeves, T.E., Stadler, P.F., Burge, S.W., Lyons, E., Smith, J., McCarthy, F., Pitel, F., Rhoads, D., and Froman, D.P. 2014. Comparative genomics reveals insights into avian genome evolution and adaptation. Science, **346**: 1311–1320. doi:10.1126/science.1251385.

Jerzykiewicz, T. 1985a. Stratigraphy of the Saunders Group in the central Alberta Foothills - a progress report. *In* Current Research, Part B, Paper 85-1. Geological Survey of Canada. pp. 247–258.

Jerzykiewicz, T. 1985b. Techtonically deformed pebbles in the Brazeau and Paskapoo Formation, central Alberta foothills, Canada. Sedimentary Geology, **42**: 159–180.

Jerzykiewicz, T. 1997. Stratigraphic framework of the Uppermost Cretaceous to Paleocene strata of the Alberta basin. Geological Survey of Canada Bulletin, **510**: 1–121.

Jerzykiewicz, T., and McLean, J.R. 1980. Lithostratigraphical and sedimentological framework of coal-bearing Upper Cretaceous and Lower Tertiary strata, Coal Valley area, central Alberta foothills. Geological Survey of Canada Paper, **79**–**12**: 1–47.

Jerzykiewicz, T., and Sweet, A.R. 1988. Sedimentological and palynological evidence of regional climatic changes in the Campanian to Paleocene sediments of the Rocky Mountain Foothills , Canada. **59**: 29–76.

Ji, Q., and Ji, S. 1996. On the Discovery of the earliest fossil bird in China (Sinosauropteryx gen. nov.) and the origin of birds. Chinese Geology, **233**: 30–33.

Kars, H., Ullén, I., Tronner, K., and Kars, E. 2005. Deterioration of archaeological bone - a statistical approach. Journal of Nordic Archaeological Science, **86**: 77–86.

Kaye, T.G., Gaugler, G., and Sawlowicz, Z. 2008. Dinosaurian soft tissues interpreted as bacterial biofilms. PLoS ONE, **3**: 1–7. doi:10.1371/journal.pone.0002808.

Keenan, S.W., and Engel, A.S. 2017. Early diagenesis and recrystallization of bone. Geochimica et Cosmochimica Acta, **196**: 209–223. Elsevier Ltd. doi:10.1016/j.gca.2016.09.033.

Knight, T.K., Bingham, P.S., Lewis, R.D., and Savrda, C.E. 2011. Feathers of the Ingersoll Shale, Eutaw Formation (Upper Cretaceous), Eastern Alabama: the Largest Collection of Feathers From North American Mesozoic Rocks. Palaios, **26**: 364–376. doi:10.2110/palo.2010.p10-091r.

Lambe, L.M. 1917. A new genus and species of crestless hadrosaur from the Edmonton Formation of Alberta. The Ottawa Naturalist, **31**: 65–73. doi:10.4039/Ent50387a-11.

Lambe, L.M. 1920. The hadrosaur Edmontosaurus from the Upper Cretaceous of Alberta. Memoirs of the Canada Department of Mines, Geological Survey, **120**: 1–79.

Lang, A.H. 1947. Brule and Entrance map-areas, Alberta. Canadian Department of Mines and

Resources Geological Survey Memoir, **2479**: 1–65.

Langston, W. 1959. Alberta and Fossil Vertebrates. *In* Nineth Annual Field Conference: Moose Mountain-Drumheller. pp. 8–19.

Lee, Y.-C., Chiang, C.-C., Huang, P.-Y., Chung, C.-Y., Huang, T.D., Wang, C.-C., Chen, C.-I., Chang, R.-S., Liao, C.-H., and Reisz, R.R. 2017. Evidence of preserved collagen in an Early Jurassic sauropodomorph dinosaur revealed by synchrotron FTIR microspectroscopy. Nature Communications, **8**: 14220. Nature Publishing Group. doi:10.1038/ncomms14220.

Li, Q., Gao, K.-Q., Meng, Q., Clarke, J.A., Shawkey, M.D., D'Alba, L., Pei, R., Ellison, M., Norell, M.A., and Vinther, J. 2012. Reconstruction of Microraptor and the Evolution of Iridescent Plumage. Science (New York, N.Y.), **335**: 1215–1220.

Li, Q., Gao, K.Q., Vintner, J., Shawkey, M.D., Clarke, J.A., D'Alba, L., Meng, Q., Briggs, D.E.G., and Prum, R.O. 2010. Plumage color patterns of an extinct dinosaur. Science, **327**: 1369–1372. doi:10.1126/science.1186290.

Lindgren, J., Sjövall, P., Carney, R.M., Cincotta, A., Uvdal, P., Hutcheson, S.W., Gustafsson, O., Lefèvre, U., Escuillié, F., Heimdal, J., Engdahl, A., Gren, J.A., Kear, B.P., Wakamatsu, K., Yans, J., and Godefroit, P. 2015. Molecular composition and ultrastructure of Jurassic paravian feathers. Scientific Reports, **5**: 1–13. Nature Publishing Group. doi:10.1038/srep13520.

Lindgren, J., Sjövall, P., Thiel, V., Zheng, W., Ito, S., Wakamatsu, K., Hauff, R., Kear, B.P., Engdahl, A., Alwmark, C., Eriksson, M.E., Jarenmark, M., Sachs, S., Ahlberg, P.E., Marone, F.,

Kuriyama, T., Gustafsson, O., Malmberg, P., Thomen, A., Rodríguez-Meizoso, I., Uvdal, P., Ojika, M., and Schweitzer, M.H. 2018. Soft-tissue evidence for homeothermy and crypsis in a Jurassic ichthyosaur. Nature, **564**: 359–365. Springer US. doi:10.1038/s41586-018-0775-x.

Lindgren, J., Uvdal, P., Sjövall, P., Nilsson, D.E., Engdahl, A., Schultz, B.P., and Thiel, V. 2012. Molecular preservation of the pigment melanin in fossil melanosomes. Nature Communications, **3**. doi:10.1038/ncomms1819.

Lingham-Soliar, T., and Murugan, N. 2013. A New Helical Crossed-Fibre Structure of β-Keratin in Flight Feathers and Its Biomechanical Implications. PLoS ONE, **8**. doi:10.1371/journal.pone.0065849.

Locock, M., Currie, C.K., and Gray, S. 1992. Chemical changes in buried animal bone: Data from a postmedieval assemblage. International Journal of Osteoarchaeology, **2**: 297–304. doi:10.1002/oa.1390020405.

Lucas, A.M., and Stettenheim, P.R. 1972. Avian Anatomy: Integument Part I. United States Department of Agriculture, Washington D.C.

Manifold, B. 2012. Intrinsic and extrinsic factors involved in the preservation of non-adult skeletal remains in archaeology and forensic science. Bulletin of the International Association for Paleodontology, **6**: 51–69. Available from http://hrcak.srce.hr/95443.

Mays, S. 2008. Human remains in marine archaeology. Environmental Archaeology, **13**: 123–133. doi:10.1179/174963108X343245.

McGowan, C. 1983. The Successful Dragons: A Natural History of Extinct Reptiles. Samuel Stevens and Company, Toronto, Ontario, Canada.

McGraw, K.J. 2006a. Mechanics of Carotinoid-Based Coloration. *In* Bird Coloration, vol I, Mechanisms and Measurments. *Edited by* G.E. Hill and K.J. McGraw. Harvard University Press, Cambridge, Massachusetts, USA. pp. 177–242.

McGraw, K.J. 2006b. Mechanics of Melanin-Based Coloration. *In* Bird Coloration, vol I, Mechanisms and Measurments. *Edited by* G.E. Hill and K.J. McGraw. Harvard University Press, Cambridge, Massachusetts, USA. pp. 243–294.

McGraw, K.J. 2006c. Mechanics of Uncommon Colors: Pterins, Porphyrins, and Psittacofulvins. *In* Bird Coloration, vol I, Mechanisms and Measurments. *Edited by* G.E. Hill and K.J. McGraw. Harvard University Press, Cambridge, Massachusetts, USA. pp. 354–398.

McKellar, R.C., Chatterton, B.D.E., Wolfe, A.P., and Currie, P.J. 2011. A Diverse Assemblage of Late Cretaceous Dinosaur and Bird Feathers from Canadian Amber. Science, **333**: 1619–1622. doi:10.1126/science.1203344.

Miller, M.F., and Wyckoff, R.W.G. 1968. Proteins in Dinosaur Bones. Proceedings of the National Academy of Sciences, **60**: 176–178.

Mori, H., Drunkenmiller, P.S., and Erickson, G.M. 2016. A new Arctic hadrosaurid from the Prince Creek Formation (Lower Maastrichtian) of northern Alaska. Acta Palaeontologica Polonica, **61**: 15–32. doi:10.4202/app.00233.2015.

Morlon, H., Parsons, T.L., and Plotkin, J.B. 2011. Reconciling molecular phylogenies with the

fossil record. Proceedings of the National Academy of Sciences of the United States of America, **108**: 16327–32. doi:10.1073/pnas.1102543108.

Moyer, A.E., Zheng, W., Johnson, E.A., Lamanna, M.C., Li, D.Q., Lacovara, K.J., and Schweitzer, M.H. 2014. Melanosomes or microbes: Testing an alternative hypothesis for the origin of microbodies in fossil feathers. Scientific Reports, **4**: 1–9. doi:10.1038/srep04233.

Muyzer, G., Sandberg, P., Knapen, M.H.J., Vermeer, C., Collins, M., and Westbroek, P. 1992. Preservation of the bone protein osteocalcin in dinosaurs. Geology, **20**: 871–874. doi:10.1130/0091-7613(1992)020<0871:POTBPO>2.3.CO.

Nicholson, R.A. 1996. Bone degradation, burial medium and species representation: Debunking the myths, an experiment-based approach. Journal of Archaeological Science, **23**: 513–533. doi:10.1006/jasc.1996.0049.

Nord, A.G., Tronner, K., Mattsson, E., and Borg, G.C. 2005. Environmental Threats to Buried Archaeological Remains. Royal Swedish Academy of Sciences, **34**: 256–262.

Owen, R. 1862. On the Archeopteryx of Von Meyer, with a Description of the Fossil Remains of a Long- Tailed Species, from the Lithographic Stone of Solenhofen. Philosophical Transactions of the Royal Society of London, **153**: 33–47.

Paine, G. 1937. Fossilization of bone. American Journal of Science, **34**: 148–157.

Pana, D.I., and Elgr, R. 2013. Geology of the Alberta Rocky Mountains and Foothills, Energy Resources Conservation Board, ERCB/AGS Map 560.

Pană, D.I., and van der Pluijm, B.A. 2014. Orogenic pulses in the Alberta Rocky Mountains:

Radiometric dating of major faults and comparison with the regional tectono-stratigraphic record. Bulletin of the Geological Society of America, **127**: 480–502. doi:10.1130/B31069.1.

Pawlicki, R., Korbel, A., and Kubiak, H. 1966. Cells, collagen fibrils and vessels in dinosaur bone. Nature, **211**: 655–657. doi:10.1038/211655a0.

Perrichot, V., Marion, L., Néraudeau, D., Vullo, R., and Tafforeau, P. 2008. The early evolution of feathers: fossil evidence from Cretaceous amber of France. Proceedings of the Royal Society B: Biological Sciences, **275**: 1197–1202. doi:10.1098/rspb.2008.0003.

Peterson, J.E., Lenczewski, M.E., and Scherer, R.P. 2010. Influence of microbial biofilms on the preservation of primary soft tissue in fossil and extant archosaurs. PLoS ONE, **5**. doi:10.1371/journal.pone.0013334.

Prum, R.O. 1999. Development and evolutionary origin of feathers. Journal of Experimental Zoology, **285**: 291–306. doi:10.1002/(SICI)1097-010X(19991215)285:4<291::AID-JEZ1>3.0.CO;2-9.

Prum, R.O. 2006. Anatomy, Physics, and Evolution of Structural Colors. *In* Bird Coloration, vol I, Mechanisms and Measurments. *Edited by* G.E. Hill and K.J. McGraw. Harvard University Press, Cambridge, Massachusetts, USA. pp. 295–353.

Prum, R.O., and Brush, A.H. 2002. The evolutionary and diversification of feathers. The Quarterly Review of Biology, **77**: 261–295.

Qiang, J., Currie, P.J., Norell, M.A., and Shu-An, J. 1998. Two feathered dinosaurs from northeastern china. Nature, **393**: 753–761. doi:10.1038/31635.

Rauhut, O.W.M., Foth, C., Tischlinger, H., and Norell, M.A. 2012. Exceptionally preserved juvenile megalosauroid theropod dinosaur with filamentous integument from the Late Jurassic of Germany. Proceedings of the National Academy of Sciences, **109**: 11746–11751. doi:10.1073/pnas.1203238109.

Reiche, I., Vignaud, C., and Menu, M. 2002. The crystallinity of ancient bone and dentine: New insights by transmission electron microscopy. Archaeometry, **44**: 447–459. doi:10.1111/1475-4754.00077.

Reisz, R.R., Huang, T.D., Roberts, E.M., Peng, S., Sullivan, C., Stein, K., Leblanc, A.R.H., Shieh, D., Chang, R., Chiang, C., Yang, C., and Zhong, S. 2013. Embryology of Early Jurassic dinosaur from China with evidence of preserved organic remains. Nature, **496**: 210–214. doi:10.1038/nature11978.

Ryan, M.J., Currie, P.J., Gardner, J.D., Vickaryous, M.K., and Lavigne, J.M. 1998. Baby hadrosaurid material associated with and unusually high abundance of Troodon teeth from the Horseshoe Canyon Formation, Upper Cretaceous. Gaia, **133**: 123–133.

Ryan, M.J., Evans, D.C., Currie, P.J., and Loewen, M.A. 2014. A new chasmosaurine from northern Laramidia expands frill disparity in ceratopsid dinosaurs. Naturwissenschaften, **101**: 505–512. doi:10.1007/s00114-014-1183-1.

Saitta, E.T., Fletcher, I., Martin, P., Pittman, M., Kaye, T.G., True, L.D., Norell, M.A., Abbott, G.D., Summons, R.E., Penkman, K., and Vinther, J. 2018. Preservation of feather fibers from the Late Cretaceous dinosaur Shuvuuia deserti raises concern about immunohistochemical analyses on fossils. Organic Geochemistry, **125**: 142–151. Elsevier Ltd.

doi:10.1016/j.orggeochem.2018.09.008.

Saitta, E.T., Rogers, C., Brooker, R.A., Abbott, G.D., Kumar, S., O'Reilly, S.S., Donohoe, P., Dutta, S., Summons, R.E., and Vinther, J. 2017. Low fossilization potential of keratin protein revealed by experimental taphonomy. Palaeontology, **60**: 547–556. doi:10.1111/pala.12299.

San Antonio, J.D., Schweitzer, M.H., Jensen, S.T., Kalluri, R., Buckley, M., and Orgel, J.P.R.O. 2011. Dinosaur peptides suggest mechanisms of protein survival. PLoS ONE, **6**. doi:10.1371/journal.pone.0020381.

Sato, H., Murray, A.M., Vernygora, O., and Currie, P.J. 2018. A rare, articulated sturgeon (Chondrostei: Acipenseriformes) from the Upper Cretaceous of Dinosaur Provincial Park, Alberta, Canada. Journal of Vertebrate Paleontology, **0**: 1–15. Taylor & Francis. doi:10.1080/02724634.2018.1488137.

Schoeninger, M.J., Moore, K.M., Murray, M.L., and Kingston, J.D. 1989. Detection of bone preservation in archaeological and fossil samples. Applied Geochemistry, **4**: 281–292. doi:10.1016/0883-2927(89)90030-9.

Schroeter, E.R., Dehart, C.J., Cleland, T.P., Zheng, W., Thomas, P.M., Kelleher, N.L., Bern, M., and Schweitzer, M.H. 2017. Expansion for the *Brachylophosaurus canadensis* Collagen I Sequence and Additional Evidence of the Preservation of Cretaceous Protein. Journal of Proteome Research, **16**: 920–932. doi:10.1021/acs.jproteome.6b00873.

Schweitzer, M.H. 2011. Soft Tissue Preservation in Terrestrial Mesozoic Vertebrates. Annual

Review of Earth and Planetary Sciences, Vol 39, **39**: 187–216. doi:10.1146/annurev-earth-040610-133502.

Schweitzer, M.H., Chiappe, L., Garrido, A.., Lowenstein, J.., and Pincus, S.. 2005a. Molecular preservation in Late Cretaceous sauropod dinosaur eggshells. Proceedings of the Royal Society B: Biological Sciences, **272**: 775–784. doi:10.1098/rspb.2004.2876.

Schweitzer, M.H., Marshall, M., Carron, K., Bohle, D.S., Busse, S.C., Arnold, E. V, Barnard, D., Horner, J.R., and Starkey, J.R. 1997. Heme compounds in dinosaur trabecular bone. Proceedings of the National Academy of Sciences, **94**: 6291–6296. doi:10.1073/pnas.94.12.6291.

Schweitzer, M.H., Moyer, A.E., and Zheng, W. 2016a. Testing the hypothesis of biofilm as a source for soft tissue and cell-like structures preserved in dinosaur bone. PLoS ONE, **11**: 1–19. doi:10.1371/journal.pone.0150238.

Schweitzer, M.H., Suo, Z., Avci, R., Asara, J.M., Allen, M. a, Arce, F.T., and Horner, J.R. 2007a. Analyses of soft tissue from Tyrannosaurus rex suggest the presence of protein. Science, **316**: 277–280. doi:10.1126/science.1138709.

Schweitzer, M.H., Watt, J.A., Avci, R., Knapp, L., Chiappe, L., Norell, M., and Marshall, M. 1999. Beta-keratin specific immunological reactivity in feather-like structures of the cretaceous alvarezsaurid, Shuvuuia deserti. Journal of Experimental Zoology, **285**: 146–157. doi:10.1002/(SICI)1097-010X(19990815)285:2<146::AID-JEZ7>3.0.CO;2-A.

Schweitzer, M.H., Wittmeyer, J.L., and Horner, J.R. 2007b. Soft tissue and cellular preservation

in vertebrate skeletal elements from the Cretaceous to the present. Proceedings. Biological sciences / The Royal Society, **274**: 183–97. doi:10.1098/rspb.2006.3705.

Schweitzer, M.H., Wittmeyer, J.L., Horner, J.R., Jan, K., Science, S., Series, N., Gut, T., Tube, I., and Niiio-like, E. 2005b. Soft-Tissue Vessels and Cellular Preservation in Tyrannosaurus rex. Science, **307**: 1952–1955.

Schweitzer, M.H., Zheng, W., Cleland, T.P., and Bern, M. 2013. Molecular analyses of dinosaur osteocytes support the presence of endogenous molecules. Bone, **52**: 414–423. Elsevier Inc. doi:10.1016/j.bone.2012.10.010.

Schweitzer, M.H., Zheng, W., Cleland, T.P., Goodwin, M.B., Boatman, E., Theil, E., Marcus, M.A., and Fakra, S.C. 2014. A role for iron and oxygen chemistry in preserving soft tissues, cells and molecules from deep time. Proceedings of the Royal Society B, **281**: 20132741. doi:10.1098/rspb.2013.2741.

Schweitzer, M.H., Zheng, W., Organ, C.L., Avci, R., Suo, Z., Freimark, L.M., Lebleu, V.S., Duncan, M.B., Vander Heiden, M.G., Neveu, J.M., Lane, W.S., Cottrell, J.S., Horner, J.R., Cantley, L.C., Kalluri, R., and Asara, J.M. 2009a. Biomolecular characterization and protein sequences of the Campanian hadrosaur B. canadensis. Science, **324**: 626–31. doi:10.1126/science.1165069.

Schweitzer, M.H., Zheng, W., Organ, C.L., Avci, R., Suo, Z., Freimark, L.M., Lebleu, V.S., Duncan, M.B., Vander Heiden, M.G., Neveu, J.M., Lane, W.S., Cottrell, J.S., Horner, J.R., Cantley, L.C., Kalluri, R., and Asara, J.M. 2009b. Biomolecular characterization and protein sequences of the Campanian hadrosaur Brachylophosaurus canadensis. Science, **324**: 626–

629.

Schweitzer, M.H., Zheng, W., Zanno, L., Werning, S., and Sugiyama, T. 2016b. Chemistry supports the identification of gender-specific reproductive tissue in Tyrannosaurus rex. Scientific Reports, **6**: 1–10. Nature Publishing Group. doi:10.1038/srep23099.

Shaw, R.D., Mitchell, P.A., and Anderson, A.M. 1994. Water quality of the North Saskatchewan River in Alberta.

Simonetti, A., Heaman, L.M., Hartlaub, R.P., Creaser, R.A., MacHattie, T.G., and Böhm, C. 2005. U-Pb zircon dating by laser ablation-MC-ICP-MS using a new multiple ion counting Faraday collector array. Journal of Analytical Atomic Spectrometry, **20**: 677–686. doi:10.1039/b504465k.

Sláma, J., Košler, J., Condon, D.J., Crowley, J.L., Gerdes, A., Hanchar, J.M., Horstwood, M.S.A., Morris, G.A., Nasdala, L., Norberg, N., Schaltegger, U., Schoene, B., Tubrett, M.N., and Whitehouse, M.J. 2008. Plešovice zircon - A new natural reference material for U-Pb and Hf isotopic microanalysis. Chemical Geology, **249**: 1–35. doi:10.1016/j.chemgeo.2007.11.005.

Smith, D.L., and Hayward, J.L. 2010. Bacterial Decomposition of Avian Eggshell: a Taphonomic Experiment. Palaios, **25**: 318–326. doi:10.2110/palo.2009.p09-115r.

Söderlund, U., and Johansson, L. 2002. A simple way to extract baddeleyite (ZrO_2). Geochemistry, Geophysics, Geosystems, **3**: 1 of 7–7 7. doi:10.1029/2001GC000212.

Stephan, E. 1997. Patterns of chemical change in fossil bones and various states of bone

preservation associated with soil conditions. Anthropozoologica, **25**–**26**: 173–180.

Tanke, D.H., and Brett-Surman, M.K. 2001. Evidence of Hatchling and Nestling-Size Hadrosaurs (Reptilia:Ornithischia) from Dinosaur Provincial Park (Dinosaur Park Formation: Campanian), Alberta, Canada. *In* Mesozoic Vertebrate Life. *Edited by* D.H. Tanke, K. Carpenter, and M.W. Skrepnick. Indiana University Press, Bloomington, Indiana. pp. 206–218.

Thiel, V., and Sjövall, P. 2011. Using Time-of-Flight Secondary Ion Mass Spectrometry to Study Biomarkers. Annual Review of Earth and Planetary Sciences, **39**: 125–156. doi:10.1146/annurev-earth-040610-133525.

Thomas, D.B., Nascimbene, P.C., Dove, C.J., Grimaldi, D.A., and James, H.F. 2014. Seeking carotenoid pigments in amber-preserved fossil feathers. Scientific Reports, **4**. doi:10.1038/srep05226.

Thompson, M.G.W. 2018. A Multidisciplinary Palaeoenvironmental Reconstruction of the Campanian Foremost Formation of Southern Alberta. Carlton University. Available from https://curve.carleton.ca/3c11d8cf-52ea-40d9-b484-409615aa2e28.

Tondu, J.M.E. 2017. Longitudinal water quality patterns in the Athabasca River: Winter synoptic survey (2015). Alberta Environment and Parks.

Trueman, C.N., and Martill, D.M. 2002. The long-term survival of bone: the role of bioerosion. Archaeometry, **44**: 371–382.

Turner-Walker, G. 2007. The Chemical and Microbial Degradation of Bones and Teeth. *In*

Advances in Human Palaeopathology. *Edited by* R. Phinhasi and S. Mays. John Wiley & Sons, Ltd. pp. 3–29. doi:10.1002/9780470724187.ch1.

Turner-Walker, G., and Syversen, U. 2002. Quantifying histological changes in archaeological bones using BSE-SEM image analysis. Archaeometry, **44**: 461–468. doi:10.1111/1475-4754.t01-1-00078.

Uyeda, J.C., Hansen, T.F., Arnold, S.J., and Pienaar, J. 2011. The million-year wait for macroevolutionary bursts. Proceedings of the National Academy of Sciences, **108**: 15908–15913. doi:10.5061/dryad.7d580.

van der Reest, A.J., and Currie, P.J. 2017. Troodontids (Theropoda) from the Dinosaur Park Formation , Alberta , with a description of a unique new taxon : implications for deinonychosaur diversity in North America. Canadian Journal of Earth Sciences, **935**: 919–935. doi:10.1139/cjes-2017-0031.

van der Reest, A.J., Wolfe, A.P., and Currie, P.J. 2016. A densely feathered ornithomimid (Dinosauria: Theropoda) from the Upper Cretaceous Dinosaur Park Formation, Alberta, Canada. Cretaceous Research, **62**: 90–94. Elsevier Ltd. doi:10.1016/j.cretres.2016.01.005.

Vellis, P.K. 2011. Preface. *In* Cell Biology Research Progress Series: Basophil Granulocytes. *Edited by* P.K. Vellis. Nova Science Publishers, Inc., New York, New York, USA. pp. ix–xiii.

Vermeesch, P. 2018. IsoplotR: A free and open toolbox for geochronology. Geoscience Frontiers, **9**: 1479–1493. Elsevier Ltd. doi:10.1016/j.gsf.2018.04.001.

Wang, B., Yang, W., McKittrick, J., and Meyers, M.A. 2016. Keratin: Structure, mechanical

properties, occurrence in biological organisms, and efforts at bioinspiration. Progress in Materials Science, **76**: 229–318. Elsevier Ltd. doi:10.1016/j.pmatsci.2015.06.001.

Wiemann, J., Fabbri, M., Yang, T.-R., Stein, K., Sander, P.M., Norell, M.A., and Briggs, D.E.G. 2018. Fossilization transforms vertebrate hard tissue proteins into N-heterocyclic polymers. Nature Communications, **9**: 4741. Springer US. doi:10.1038/s41467-018-07013-3.

Xing, H., Mallon, J.C., and Currie, M.L. 2017. Supplementary cranial description of the types of Edmontosaurus regalis (Ornithischia: Hadrosauridae), with comments on the phylogenetics and biogeography of Hadrosaurinae. *In* PLoS ONE. doi:10.1371/journal.pone.0175253.

Xu, X., and Guo, Y. 2009. The origin and early evolution of feathers: insights from recent paleontological and neontological data. Vertebrata PalAsiatica, **10**: 311–329. Available from http://scholar.google.com/scholar?hl=en&btnG=Search&q=intitle:The+Origin+and+Early+Evolution+of+Feathers:+Insights+From+Recent+Paleontological+and+Neontological+Data#0.

Xu, X., Norell, M.A., Kuang, X., Wang, X., Zhou, Q., and Jia, C. 2004. Basal tyrannosauroids from China and evidence for protofeathers in tyrannosauroids. Nature, **431**: 680–684. doi:10.1029/2001JD001278.

Xu, X., Tang, Z., and Wang, X. 1999. A therizinosauroid dinosaur with integumentary structures from China. Nature, **399**: 350–354.

Xu, X., Zhou, Z.H., and Prum, R.O. 2001. Branched integumental structures in Sinornithosaurus and the origin of feathers. Nature, **410**: 200–204. doi:10.1038/35065589.

Zeebe, R.E. 2001. Seawater pH and isotopic paleotemperatures of Cretaceous oceans. Palaeogeography, Palaeoclimatology, Palaeoecology, **170**: 49–57.

Zelenitsky, D.K., Therrien, F., Erickson, G.M., Christopher, L., Kobayashi, Y., Eberth, D.A., and Hadfield, F. 2012. Feathered Non-Avian Dinosaurs from North America Provide Insight into Wing Origins. Science, **338**: 510–514.

Zhang, F., Zhonghe, Z., and Dyke, G. 2006. Feathers and 'feather-like' integumentary structures in Liaoning birds and dinosaurs. Geological Journal, **41**: 395–404. doi:10.1002/gj.

Zheng, X.T., You, H.L., Xu, X., and Dong, Z.M. 2009. An Early Cretaceous heterodontosaurid dinosaur with filamentous integumentary structures. Nature, **458**: 333–336. doi:10.1038/nature07856.

APPENDICES

APPENDIX 2-1: Extant avian specimens sampled for comparison to fossil feather structure.

Figure A2-1. UAMZ 1062, female *Branta canadensis parvipes* (Lesser Canada Goose). a, ventral view. b, dorsal view indicating where feathers were sampled from. c, remex, indicating where (f) is from. d, rectrix, indicating where (g) is from. e, contour, indicating where (h) is from.

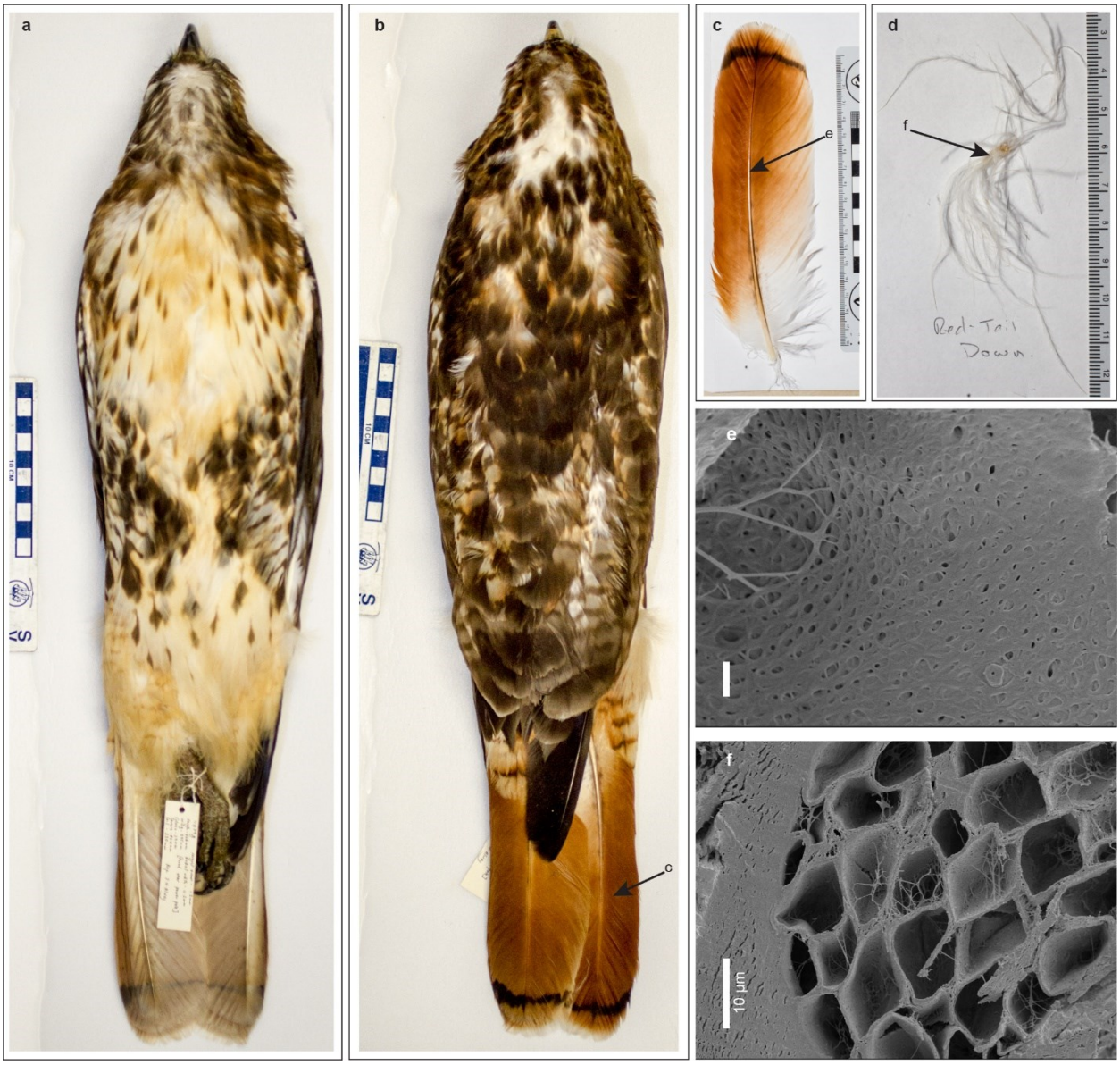

Figure A2-2. UAMZ 5436, female *Buteo jamaicensis* (Red Tailed Hawk). a, ventral view. b, dorsal view indicating locations of feathers sampled. c, rectrix showing location of (e). d, down showing location of (f).

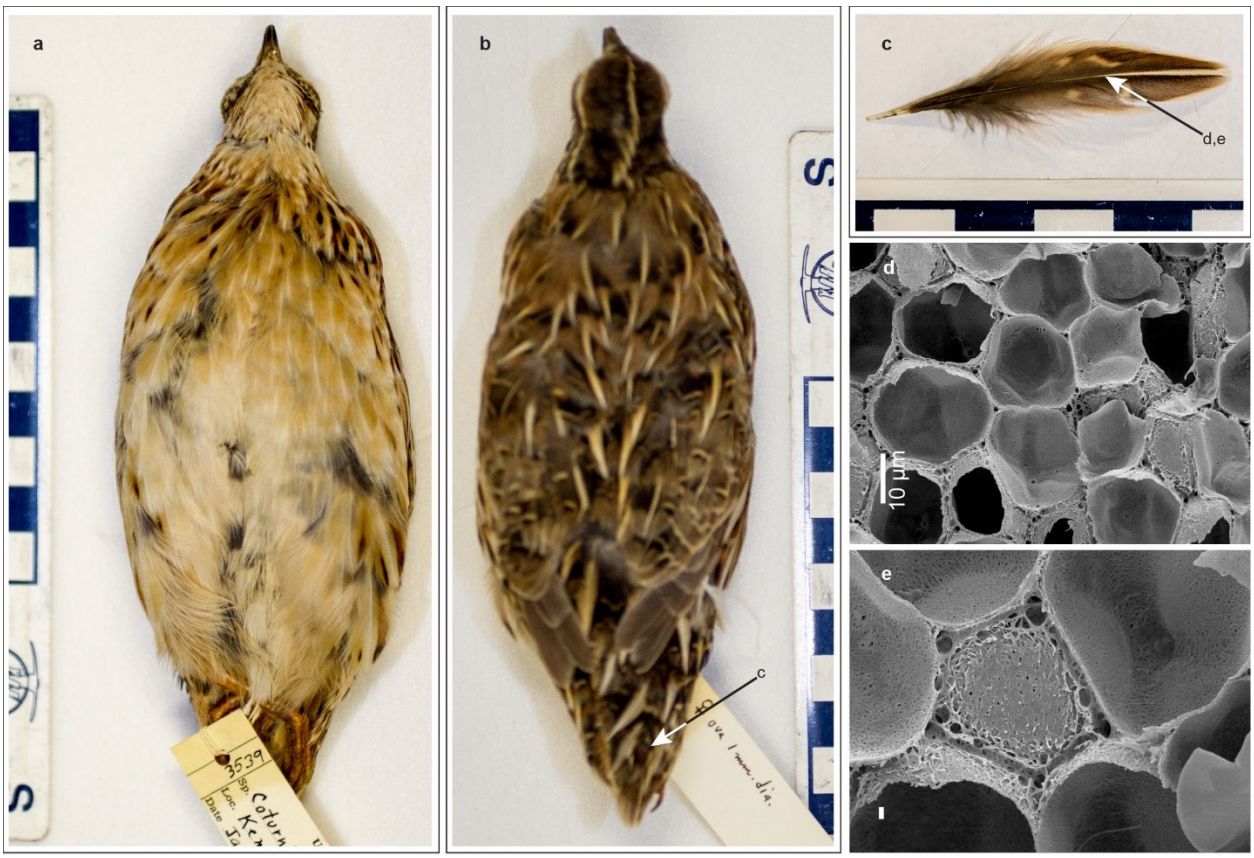

Figure A2-3. UAMZ 3539, female *Coturnix coturnix* (Common Quail). a, ventral view. b, dorsal view showing location of feather specimen. c, rectrix indicating location of (d) and (e).

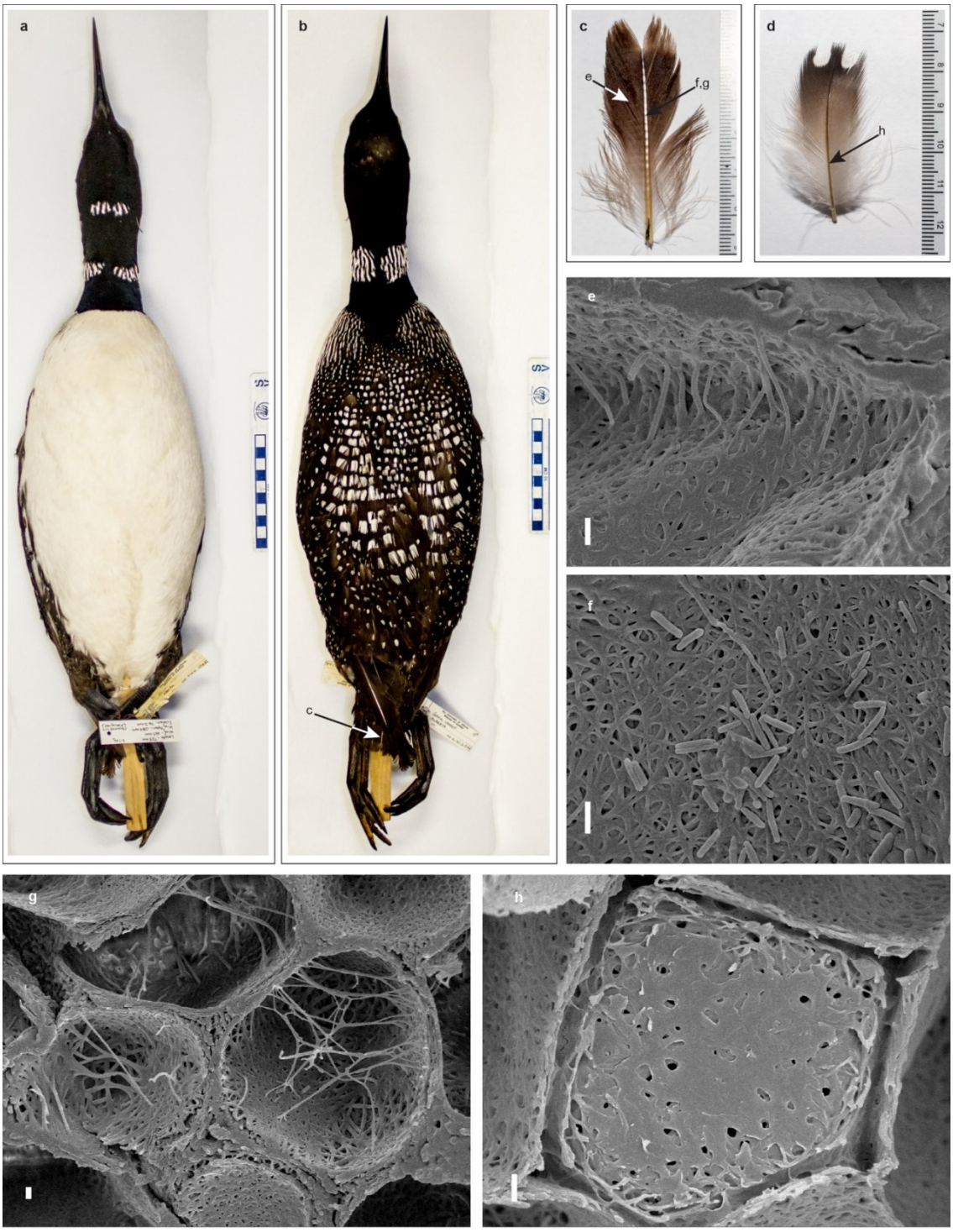

Figure A2-4. UAMZ 5293, male *Gavia immure* (Great Northern Loon). a, ventral view. b, dorsal view indicating location of feather specimens studied. c, rectrix showing location of (e), (f), and (g). d, contour showing location of (h).

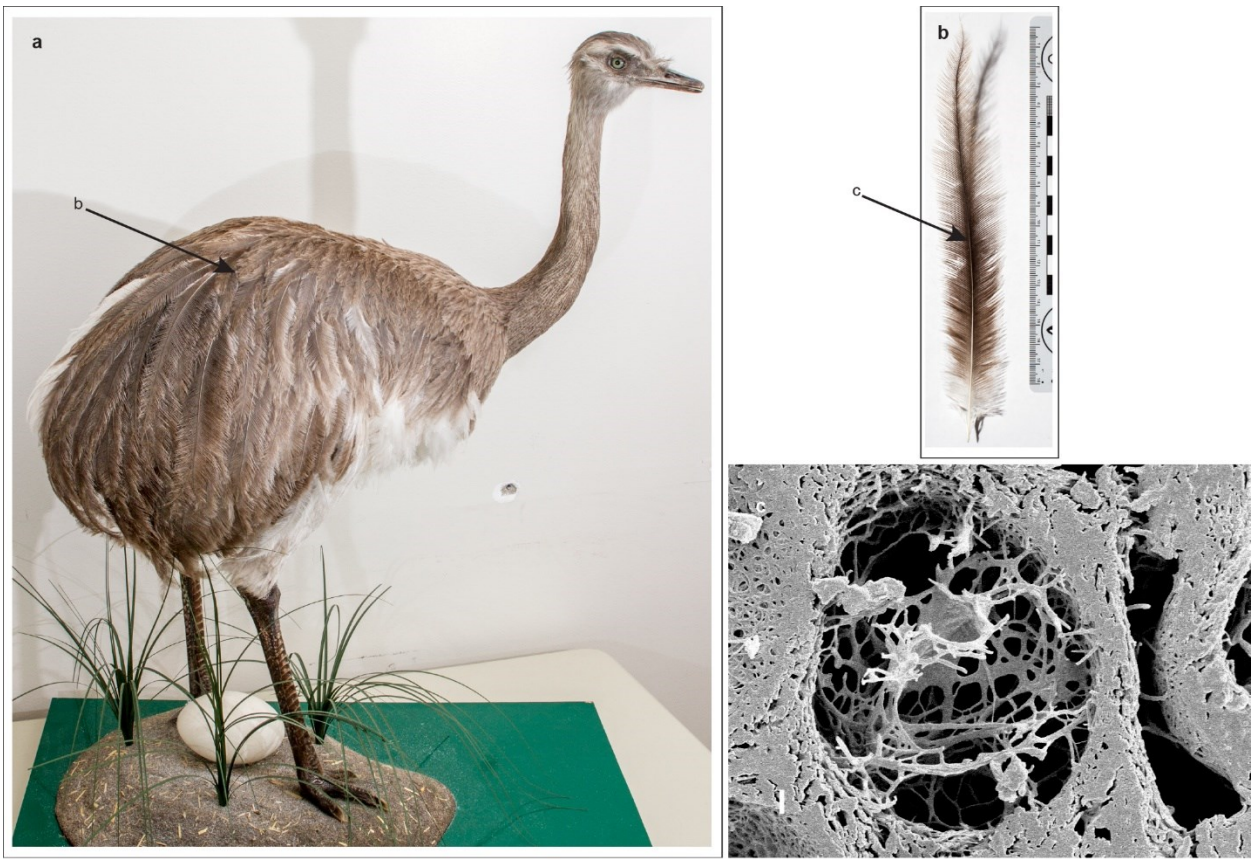

Figure A2-5. UALVP unaccessioned specimen, unknown sex, *Rhea pennata* (Darwin's Rhea). a, lateral view showing location of feather sampled. b, contour feather showing location of (c).

APPENDIX 3-1: Lab treatment forms for bone samples from the Dinosaur Park Formation.

Forms organized in the same order as Table 3-1.

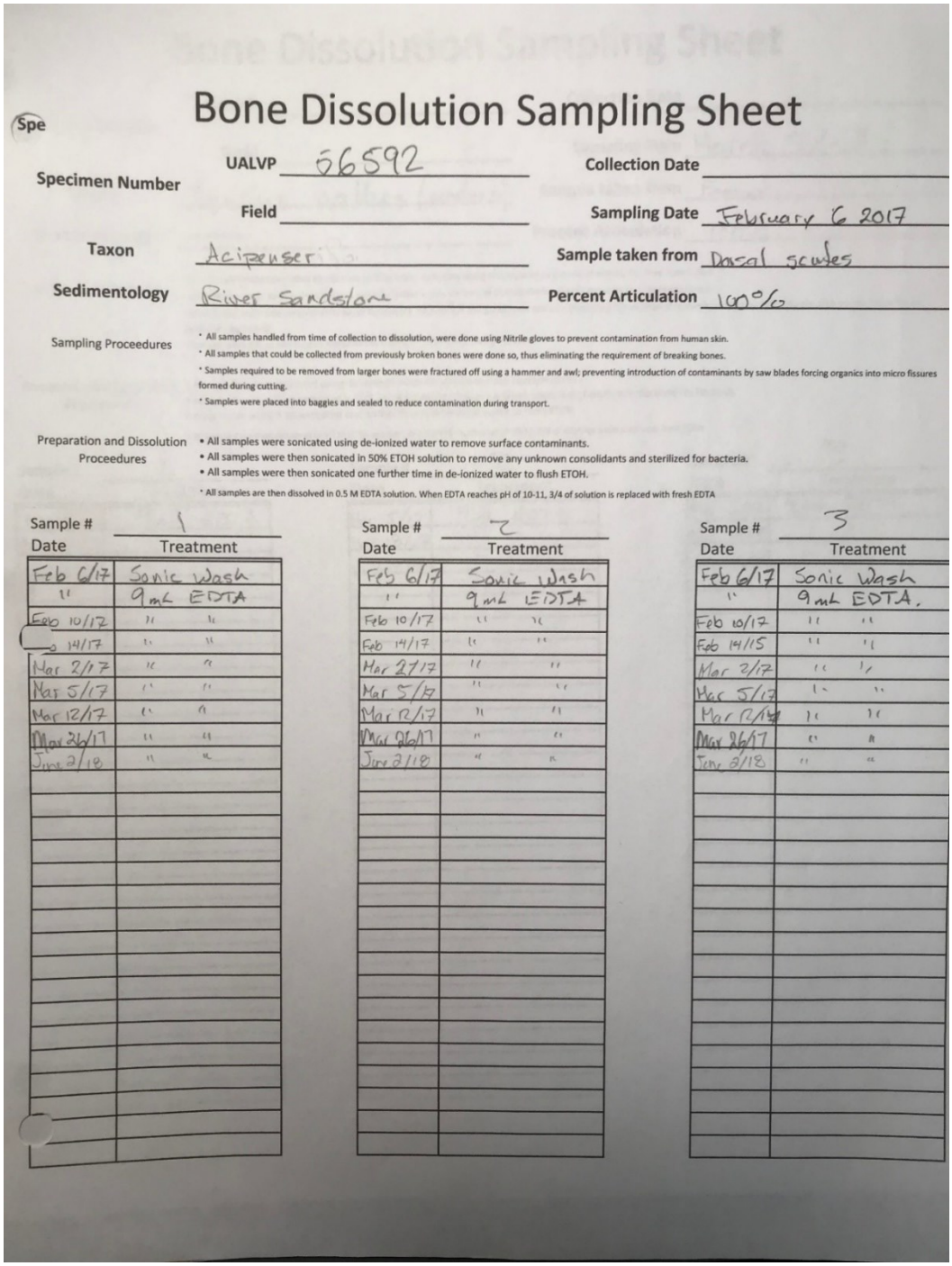

Bone Dissolution Sampling Sheet

Spe

Specimen Number UALVP 56592 **Collection Date** _____

Field _____ **Sampling Date** February 6 2017

Taxon Acipenser **Sample taken from** Dorsal scutes

Sedimentology River Sandstone **Percent Articulation** 100%

Sampling Proceedures

- All samples handled from time of collection to dissolution, were done using Nitrile gloves to prevent contamination from human skin.
- All samples that could be collected from previously broken bones were done so, thus eliminating the requirement of breaking bones.
- Samples required to be removed from larger bones were fractured off using a hammer and awl; preventing introduction of contaminants by saw blades forcing organics into micro fissures formed during cutting.
- Samples were placed into baggies and sealed to reduce contamination during transport.

Preparation and Dissolution Proceedures

- All samples were sonicated using de-ionized water to remove surface contaminants.
- All samples were then sonicated in 50% ETOH solution to remove any unknown consolidants and sterilized for bacteria.
- All samples were then sonicated one further time in de-ionized water to flush ETOH.
- All samples are then dissolved in 0.5 M EDTA solution. When EDTA reaches pH of 10-11, 3/4 of solution is replaced with fresh EDTA

Sample # 1

Date	Treatment
Feb 6/17	Sonic Wash
"	9mL EDTA
Feb 10/17	" "
Feb 14/17	" "
Mar 2/17	" "
Mar 5/17	" "
Mar 12/17	" "
Mar 26/17	" "
June 2/18	" "

Sample # 2

Date	Treatment
Feb 6/17	Sonic Wash
"	9mL EDTA
Feb 10/17	" "
Feb 14/17	" "
Mar 27/17	" "
Mar 5/17	" "
Mar 12/17	" "
Mar 26/17	" "
June 2/18	" "

Sample # 3

Date	Treatment
Feb 6/17	Sonic Wash
"	9mL EDTA.
Feb 10/17	" "
Feb 14/15	" "
Mar 2/17	" "
Mar 5/17	" "
Mar 12/17	" "
Mar 26/17	" "
June 2/18	" "

Bone Dissolution Sampling Sheet

Specimen Number UALVP 59613 **Collection Date** _____

Field _____ **Sampling Date** January 24 2017

Taxon Basilemys **Sample taken from** ungual phalanx

Sedimentology Mudstone **Percent Articulation** isolated in microsite

Sampling Proceedures

- All samples handled from time of collection to dissolution, were done using Nitrile gloves to prevent contamination from human skin.
- All samples that could be collected from previously broken bones were done so, thus eliminating the requirement of breaking bones.
- Samples required to be removed from larger bones were fractured off using a hammer and awl; preventing introduction of contaminants by saw blades forcing organics into micro fissures formed during cutting.
- Samples were placed into baggies and sealed to reduce contamination during transport.

Preparation and Dissolution Proceedures

- All samples were sonicated using de-ionized water to remove surface contaminants.
- All samples were then sonicated in 50% ETOH solution to remove any unknown consolidants and sterilized for bacteria.
- All samples were then sonicated one further time in de-ionized water to flush ETOH.
- All samples are then dissolved in 0.5 M EDTA solution. When EDTA reaches pH of 10-11, 3/4 of solution is replaced with fresh EDTA

Sample # 1

Date	Treatment
Jan 24/17	Sonic Wash
"	9 mL EDTA.
Jan 26/17	6 mL EDTA
Jan 28/17	9mL EDTA
Feb 3/17	9mL EDTA
Feb 6/17	9mL EDTA
Feb 10/17	" "
Feb 14/17	" "
Feb 22/17	" "
Mar 18/17	" "
May 2/18	" "
May 30/18	" "
June 22/18	" "

Sample # 2

Date	Treatment
Jan 24/17	Sonic Wash
"	9 mL EDTA
Jan 26/17	6 mL EDTA
Jan 28/17	9mL EDTA
Feb 3/17	9mL EDTA
Feb 6/17	9mL EDTA
Feb 10/17	" "
Feb 14/17	" "
Feb 22/17	" "
Mar 18/17	" "
May 2/18	" "
May 30/18	" "
June 22/18	" "

Sample # 3

Date	Treatment
Jan 24/17	Sonic Wash
"	9 mL EDTA
Jan 26/17	6mL EDTA.
Jan 28/17	9mL EDTA
Feb 3/17	9mL EDTA
Feb 6/17	9mL EDTA
Feb 10/17	" "
Feb 14/17	" "
Feb 22/17	" "
Mar 18/17	" "
May 2/18	" "
May 30/18	" "
June 22/18	" "

Bone Dissolution Sampling Sheet

Specimen Number UALVP 59615 **Collection Date** _____

Field _____ **Sampling Date** January 24/2017

Taxon Crocodilia **Sample taken from** Osteoderm (whole)

Sedimentology mud stone **Percent Articulation** Isolated in microsite

Sampling Proceedures

- All samples handled from time of collection to dissolution, were done using Nitrile gloves to prevent contamination from human skin.
- All samples that could be collected from previously broken bones were done so, thus eliminating the requirement of breaking bones.
- Samples required to be removed from larger bones were fractured off using a hammer and awl; preventing introduction of contaminants by saw blades forcing organics into micro fissures formed during cutting.
- Samples were placed into baggies and sealed to reduce contamination during transport.

Preparation and Dissolution Proceedures

- All samples were sonicated using de-ionized water to remove surface contaminants.
- All samples were then sonicated in 50% ETOH solution to remove any unknown consolidants and sterilized for bacteria.
- All samples were then sonicated one further time in de-ionized water to flush ETOH.
- All samples are then dissolved in 0.5 M EDTA solution. When EDTA reaches pH of 10-11, 3/4 of solution is replaced with fresh EDTA

Sample # 1

Date	Treatment
Jan 24/17	sonic wash
"	9mL EDTA
Jan 29/17	6mL EDTA
Feb 3/17	9mL EDTA
Feb 10/17	9mL EDTA
Feb 16/17	" "
Mar 2/17	" "
Mar 18/17	" "
May 8/18	" "
June 2/18	" "
July 24/18	" "

Sample # _____

Date	Treatment

Sample # _____

Date	Treatment

Bone Dissolution Sampling Sheet

Specimen Number UALVP 59618

Field

Taxon Leidyosuchus

Sedimentology Mudstone shale

Collection Date

Sampling Date January 24 2017

Sample taken from Cranial and dentary

Percent Articulation Articulated skull in microsite.

Sampling Proceedures

- All samples handled from time of collection to dissolution, were done using Nitrile gloves to prevent contamination from human skin.
- All samples that could be collected from previously broken bones were done so, thus eliminating the requirement of breaking bones.
- Samples required to be removed from larger bones were fractured off using a hammer and awl; preventing introduction of contaminants by saw blades forcing organics into micro fissures formed during cutting.
- Samples were placed into baggies and sealed to reduce contamination during transport.

Preparation and Dissolution Proceedures

- All samples were sonicated using de-ionized water to remove surface contaminants.
- All samples were then sonicated in 50% ETOH solution to remove any unknown consolidants and sterilized for bacteria.
- All samples were then sonicated one further time in de-ionized water to flush ETOH.
- All samples are then dissolved in 0.5 M EDTA solution. When EDTA reaches pH of 10-11, 3/4 of solution is replaced with fresh EDTA

Sample # 1

Date	Treatment
Jan 24/17	Sonic wash
"	9mL EDTA
Jan 26/17	6mL EDTA
Jan 28/17	9mL EDTA
Feb 3/17	9mL EDTA
Feb 10/17	" "
Feb 16/17	" "
Feb 27/17	" "
Mar 18/17	" "
April 8/18	" "
May 2/18	" "
May 30/18	" "
June 22/18	" "

Sample # 2

Date	Treatment
Jan 24/17	Sonic wash
"	9mL EDTA
Jan 26/17	6mL EDTA
Jan 28/17	9mL EDTA
Feb 3/17	9mL EDTA
Feb 10/17	" "
Feb 16/17	" "
Feb 27/17	" "
Mar 18/17	" "
Apr 8/18	" "
May 2/18	" "
May 30/18	" "
June 22/18	" "

Sample # 3

Date	Treatment
Jan 24/17	Sonic Wash
"	9mL EDTA
Jan 26/17	6mL EDTA
Jan 28/17	9mL EDTA
Feb 8/17	9mL EDTA
Feb 10/17	" "
Feb 16/17	" "
Feb 27/17	" "
Mar 18/17	" "
Apr 8/18	" "
May 2/18	" "
May 30/18	" "
June 22/18	" "

Bone Dissolution Sampling Sheet

Specimen Number UALVP 56607 **Collection Date** ?

Field _____ **Sampling Date** January 24 2017

Taxon Ankylosaurid **Sample taken from** Skull Roof.

Sedimentology Sand concretion **Percent Articulation** Isolated

Sampling Proceedures

- All samples handled from time of collection to dissolution, were done using Nitrile gloves to prevent contamination from human skin.
- All samples that could be collected from previously broken bones were done so, thus eliminating the requirement of breaking bones.
- Samples required to be removed from larger bones were fractured off using a hammer and awl; preventing introduction of contaminants by saw blades forcing organics into micro fissures formed during cutting.
- Samples were placed into baggies and sealed to reduce contamination during transport.

Preparation and Dissolution Proceedures

- All samples were sonicated using de-ionized water to remove surface contaminants.
- All samples were then sonicated in 50% ETOH solution to remove any unknown consolidants and sterilized for bacteria.
- All samples were then sonicated one further time in de-ionized water to flush ETOH.
- All samples are then dissolved in 0.5 M EDTA solution. When EDTA reaches pH of 10-11, 3/4 of solution is replaced with fresh EDTA

Sample # 1

Date	Treatment
Jan 24/17	Sonic Wash
Jan 24/17	9mL EDTA
Jan 29/17	9mL EDTA
Feb 1/17	9mL EDTA
Feb 6/17	9mL EDTA
Feb 10/17	" "
Feb 14/17	" "
Feb 20/17	" "
Mar 5/17	" "
Mar 11/17	" "
Mar 26/17	" "
May 2/18	" "
June 2/18	" "
June 16/18	" "

Sample # 2

Date	Treatment
Jan 24/17	Sonic Wash
"	9mL EDTA
Jan 29/17	9mL EDTA
Feb 1/17	9mL EDTA
Feb 6/17	9mL EDTA
Feb 10/17	" "
Feb 14/17	" "
Feb 20/17	" "
Mar 5/17	" "
Mar 11/17	" "
Mar 26/17	" "
May 2/18	" "
June 2/18	" "
June 16/18	" "

Sample # 3

Date	Treatment
Jan 24/17	Sonic Wash
"	9mL EDTA
Jan 29/17	9mL EDTA
Feb 1/17	9mL EDTA
Feb 6/17	9mL EDTA
Feb 10/17	" "
Feb 14/17	" "
Feb 20/17	" "
Mar 5/17	" "
Mar 11/17	" "
Mar 26/17	" "
May 2/18	" "
June 2/18	" "
June 16/18	" "

Bone Dissolution Sampling Sheet

Specimen Number UALVP 12 **Collection Date** _____

Field _____ **Sampling Date** _____

Taxon Panoplosaurus **Sample taken from** Cranial Bone

Sedimentology Iron rich sand nodule **Percent Articulation** Associated cranial and osteoderms.

Sampling Proceedures

- All samples handled from time of collection to dissolution, were done using Nitrile gloves to prevent contamination from human skin.
- All samples that could be collected from previously broken bones were done so, thus eliminating the requirement of breaking bones.
- Samples required to be removed from larger bones were fractured off using a hammer and awl; preventing introduction of contaminants by saw blades forcing organics into micro fissures formed during cutting.
- Samples were placed into baggies and sealed to reduce contamination during transport.

Preparation and Dissolution Proceedures

- All samples were sonicated using de-ionized water to remove surface contaminants.
- All samples were then sonicated in 50% ETOH solution to remove any unknown consolidants and sterilized for bacteria.
- All samples were then sonicated one further time in de-ionized water to flush ETOH.
- All samples are then dissolved in 0.5 M EDTA solution. When EDTA reaches pH of 10-11, 3/4 of solution is replaced with fresh EDTA

Sample # 1

Date	Treatment
Jan 24/17	sonic wash
"	9mL EDTA
Jan 29/17	6mL EDTA
Feb 3/17	9mL EDTA
Feb 10/17	" "
Feb 16/17	" "
Mar 2/17	" "
Mar 18/17	" "
May 8/18	" "
June 2/18	" "
July 24/18	" "

Sample # 2

Date	Treatment
Jan 24/17	sonic wash
"	9mL EDTA
Jan 29/17	6mL EDTA
Feb 3/17	9mL EDTA
Feb 10/17	" "
Feb 16/17	" "
Mar 2/17	" "
Mar 18/17	" "
May 8/18	" "
June 2/18	" "
July 24/18	" "

Sample # 3

Date	Treatment
Jan 24/17	sonic wash
"	9mL EDTA
Jan 29/17	6mL EDTA
Feb 3/17	9mL EDTA
Feb 10/17	" "
Feb 16/17	" "
Mar 2/17	" "
Mar 18/17	" "
May 8/18	" "
June 2/18	" "
July 24/18	" "

Bone Dissolution Sampling Sheet

Specimen Number UALVP 54559 **Collection Date** _____

Field _____ **Sampling Date** January 24/17

Taxon Mercuriceratops gemini **Sample taken from** Cranial wash float

Sedimentology Sandstone **Percent Articulation** Associated

Sampling Proceedures

- All samples handled from time of collection to dissolution, were done using Nitrile gloves to prevent contamination from human skin.
- All samples that could be collected from previously broken bones were done so, thus eliminating the requirement of breaking bones.
- Samples required to be removed from larger bones were fractured off using a hammer and awl; preventing introduction of contaminants by saw blades forcing organics into micro fissures formed during cutting.
- Samples were placed into baggies and sealed to reduce contamination during transport.

Preparation and Dissolution Proceedures

- All samples were sonicated using de-ionized water to remove surface contaminants.
- All samples were then sonicated in 50% ETOH solution to remove any unknown consolidants and sterilized for bacteria.
- All samples were then sonicated one further time in de-ionized water to flush ETOH.
- All samples are then dissolved in 0.5 M EDTA solution. When EDTA reaches pH of 10-11, 3/4 of solution is replaced with fresh EDTA

Sample # 1

Date	Treatment
Jan 24/17	Sonic Wash
"	9 mL EDTA
Jan 29/17	6 mL EDTA
Feb 3/17	6 mL EDTA
Feb 10/17	9 mL "
Feb 16/17	" "
Feb 21/17	" "
Mar 5/17	" "
Mar 12/17	" "
Mar 25/17	" "
May 2/18	" "
June 2/18	" "
June 22/18	" "

Sample # 2

Date	Treatment
Jan 24/17	Sonic Wash
"	9 mL EDTA
Jan 29/17	6 mL EDTA
Feb 3/17	6 mL EDTA
Feb 10/17	9 mL "
Feb 16/17	" "
Feb 21/17	" "
Mar 5/17	" "
Mar 12/17	" "
Mar 25/17	" "
May 2/18	" "
June 2/18	" "
June 22/18	" "

Sample # 3

Date	Treatment
Jan 24/17	Sonic wash
"	9 mL EDTA
Jan 29/17	6 mL EDTA
Feb 3/17	6 mL EDTA
Feb 10/17	9 mL "
Feb 16/17	" "
Feb 21/17	" "
Mar 5/17	" "
Mar 12/17	" "
Mar 18/17	" "
May 2/18	" "
June 2/18	" "
June 22/18	" "

Bone Dissolution Sampling Sheet

Specimen Number UALVP 52613 **Collection Date** _____

Field _____ **Sampling Date** January 24 2017.

Taxon Chasmosaurus belli **Sample taken from** Cranial Bone Fragments

Sedimentology Sandstone. **Percent Articulation** 100% articulated.

Sampling Proceedures

- All samples handled from time of collection to dissolution, were done using Nitrile gloves to prevent contamination from human skin.
- All samples that could be collected from previously broken bones were done so, thus eliminating the requirement of breaking bones.
- Samples required to be removed from larger bones were fractured off using a hammer and awl; preventing introduction of contaminants by saw blades forcing organics into micro fissures formed during cutting.
- Samples were placed into baggies and sealed to reduce contamination during transport.

Preparation and Dissolution Proceedures

- All samples were sonicated using de-ionized water to remove surface contaminants.
- All samples were then sonicated in 50% ETOH solution to remove any unknown consolidants and sterilized for bacteria.
- All samples were then sonicated one further time in de-ionized water to flush ETOH.
- All samples are then dissolved in 0.5 M EDTA solution. When EDTA reaches pH of 10-11, 3/4 of solution is replaced with fresh EDTA

Sample # 1

Date	Treatment
Jan 24/17	Sonic wash
"	9mL EDTA
Jan 29/17	6 mL EDTA
Feb 3/17	9mL EDTA
Feb 10/17	" "
Feb 14/17	" "
Mar 2/17	" "
Mar 11/17	" "
Mar 18/17	" "
Mar 25/17	" " 0.05M
May 3/18	" " 0.5 M
May 30/18	" "
June 29/18	" "
July 17/18	" "

Sample # 2

Date	Treatment
Jan 24/17	Sonic wash
"	9mL EDTA
Jan 29/17	6mL EDTA
Feb 3/17	9mL EDTA
Feb 10/17	" "
Feb 14/17	" "
Mar 2/17	" "
Mar 11/17	" "
Mar 18/17	" "
Mar 25/17	" " 0.05M
May 3/18	" " 0.5M
May 30/18	" "
June 29/18	" "
July 17/18	" "

Sample # 3

Date	Treatment
Jan 24/17	Sonic wash
"	9mL EDTA.
Jan 29/17	6mL EDTA
Feb 3/17	9mL EDTA
Feb 10/17	" "
Feb 14/17	" "
Mar 2/17	" "
Mar 11/17	" "
Mar 18/17	" "
Mar 25/17	" " 0.05M
May 3/18	" " 0.5 M
May 30/18	" "
June 29/18	" "
July 17/18	" "

Bone Dissolution Sampling Sheet

Specimen Number UALVP 55926 **Collection Date** _____

Field _____ **Sampling Date** January 24/17

Taxon "Vagaceratops" Chasmosaurine **Sample taken from** Tibia

Sedimentology mudstone **Percent Articulation** Articulated/Associated

Sampling Proceedures

- All samples handled from time of collection to dissolution, were done using Nitrile gloves to prevent contamination from human skin.
- All samples that could be collected from previously broken bones were done so, thus eliminating the requirement of breaking bones.
- Samples required to be removed from larger bones were fractured off using a hammer and awl; preventing introduction of contaminants by saw blades forcing organics into micro fissures formed during cutting.
- Samples were placed into baggies and sealed to reduce contamination during transport.

Preparation and Dissolution Proceedures

- All samples were sonicated using de-ionized water to remove surface contaminants.
- All samples were then sonicated in 50% ETOH solution to remove any unknown consolidants and sterilized for bacteria.
- All samples were then sonicated one further time in de-ionized water to flush ETOH.
- All samples are then dissolved in 0.5 M EDTA solution. When EDTA reaches pH of 10-11, 3/4 of solution is replaced with fresh EDTA

Sample # 1

Date	Treatment
Jan 24/17	Sonic Wash
"	9mL EDTA
Jan 29/17	6mL EDTA
Feb 3/17	9mL EDTA
Feb 10/17	" "
Feb 14/17	" "
Mar 2/17	" "
Mar 11/17	" "
Mar 18/17	" "
Mar 25/17	9mL 0.05 M
May 2/18	" 0.5 M EDTA
May 30/18	" "
June 29/18	" "
July 17/18	" "

Sample # 2

Date	Treatment
Jan 24/17	Sonic Wash
"	9mL. EDTA
Jan 29/17	6 mL EDTA
Feb 3/17	9mL EDTA
Feb 10/17	" "
Feb 14/17	" "
Mar 2/17	" "
Mar 11/17	" "
Mar 18/17	" "
Mar 25/17	0.05 M 9mL
May 2/18	0.5M EDTA "
May 30/18	" "
June 29/18	" "
July 17/18	" "

Sample # 3

Date	Treatment
Jan 24/17	Sonic Wash
"	9 mL EDTA.
Jan 29/17	6 mL EDTA
Feb 3/17	9mL EDTA
Feb 10/17	" "
Feb 14/17	" "
Mar 2/17	" "
Mar 6/17	Removed from EDTA
	Placed into DI water
Mar 11/17	Taken out of water
	to dry
Mar 16/17	Micro CT.
Mar 20	Embedded for Histo

Bone Dissolution Sampling Sheet

Specimen Number UALVP 55794 **Collection Date** _____

Field _____ **Sampling Date** January 24/17

Taxon Centrosaurus apertus **Sample taken from** Cranial fragment.

Sedimentology Sandstone river channel **Percent Articulation** Articulated.

Sampling Proceedures

- All samples handled from time of collection to dissolution, were done using Nitrile gloves to prevent contamination from human skin.
- All samples that could be collected from previously broken bones were done so, thus eliminating the requirement of breaking bones.
- Samples required to be removed from larger bones were fractured off using a hammer and awl; preventing introduction of contaminants by saw blades forcing organics into micro fissures formed during cutting.
- Samples were placed into baggies and sealed to reduce contamination during transport.

Preparation and Dissolution Proceedures

- All samples were sonicated using de-ionized water to remove surface contaminants.
- All samples were then sonicated in 50% ETOH solution to remove any unknown consolidants and sterilized for bacteria.
- All samples were then sonicated one further time in de-ionized water to flush ETOH.
- All samples are then dissolved in 0.5 M EDTA solution. When EDTA reaches pH of 10-11, 3/4 of solution is replaced with fresh EDTA

Sample # 1

Date	Treatment
Jan 24/17	Sonic wash
"	9 mL EDTA.
Jan 29/17	6 mL EDTA
Feb 3/17	9 mL EDTA
Feb 6/17	9 mL EDTA
Feb 10/17	" "
Feb 14/17	" "
Feb 22/17	" "
Mar 12/17	" "
Mar 18/17	" "
May 2/18	" "
May 30/18	" "
June 22/18	" "

Sample # 2

Date	Treatment
Jan 24/17	Sonic wash
"	9 mL EDTA
Jan 29/17	6 mL EDTA
Feb 3/17	9 mL EDTA
Feb 6/17	9 mL EDTA
Feb 10/17	" "
Feb 14/17	" "
Feb 22/17	" "
Mar 12/17	" "
Mar 18/17	" "
May 2/18	" "
May 30/18	" "
June 22/18	" "

Sample # 3

Date	Treatment
Jan 24/17	Sonic Wash
"	9 mL EDTA
Jan 29/17	6 mL EDTA
Feb 3/17	9 mL EDTA
Feb 6/17	9 mL EDTA
Feb 10/17	" "
Feb 14/17	" "
Feb 22/17	" "
Mar 12/17	" "
Mar 18/17	" "
May 2/18	" "
May 30/18	" "
June 22/18	" "

Bone Dissolution Sampling Sheet

Specimen Number UALVP 52612 **Collection Date** _____

Field _____ **Sampling Date** January 24 2017

Taxon Styracosaurus albertensis **Sample taken from** Cranial Roof

Sedimentology Sandstone to fine grained rind. **Percent Articulation** Articulated / Associated

Sampling Proceedures

- All samples handled from time of collection to dissolution, were done using Nitrile gloves to prevent contamination from human skin.
- All samples that could be collected from previously broken bones were done so, thus eliminating the requirement of breaking bones.
- Samples required to be removed from larger bones were fractured off using a hammer and awl; preventing introduction of contaminants by saw blades forcing organics into micro fissures formed during cutting.
- Samples were placed into baggies and sealed to reduce contamination during transport.

Preparation and Dissolution Proceedures

- All samples were sonicated using de-ionized water to remove surface contaminants.
- All samples were then sonicated in 50% ETOH solution to remove any unknown consolidants and sterilized for bacteria.
- All samples were then sonicated one further time in de-ionized water to flush ETOH.
- All samples are then dissolved in 0.5 M EDTA solution. When EDTA reaches pH of 10-11, 3/4 of solution is replaced with fresh EDTA

Sample # 1

Date	Treatment
Jan 24/17	sonic wash
"	9mL EDTA
Jan 29/17	9mL EDTA
Feb 2/17	9mL EDTA
Feb 6/17	9mL EDTA
Feb 10/17	" "
Feb 14/17	" "
Mar 2/17	" "
Mar 12/17	" "
May 8/18	" "
June 2/18	" "
July 24/18	" "

Sample # 2

Date	Treatment
Jan 24/17	sonic wash
"	9mL EDTA
Jan 29/17	9mL EDTA
Feb 2/17	9mL EDTA
Feb 6/17	9mL EDTA
Feb 10/17	" "
Feb 14/17	" "
Mar 2/17	" "
Mar 12/17	" "
May 8/18	" "
June 2/18	" "
July 24/18	" "

Sample # 3

Date	Treatment
Jan 24/17	Sonic wash
"	9mL EDTA
Jan 29/17	9mL EDTA
Feb 2/17	9mL EDTA
Feb 6/17	9mL EDTA
Feb 10/17	" "
Feb 14/17	" "
Mar 2/17	" "
Mar 12/17	" "
May 8/18	" "
June 2/18	" "
July 24/18	" "

Bone Dissolution Sampling Sheet

Specimen Number UALVP 55900 **Collection Date** _____

Field _____ **Sampling Date** January 31 2017

Taxon Styracosaurus **Sample taken from** Humerus

Sedimentology Channel lag sandstone. **Percent Articulation** 100%

Sampling Proceedures

- All samples handled from time of collection to dissolution, were done using Nitrile gloves to prevent contamination from human skin.
- All samples that could be collected from previously broken bones were done so, thus eliminating the requirement of breaking bones.
- Samples required to be removed from larger bones were fractured off using a hammer and awl; preventing introduction of contaminants by saw blades forcing organics into micro fissures formed during cutting.
- Samples were placed into baggies and sealed to reduce contamination during transport.

Preparation and Dissolution Proceedures

- All samples were sonicated using de-ionized water to remove surface contaminants.
- All samples were then sonicated in 50% ETOH solution to remove any unknown consolidants and sterilized for bacteria.
- All samples were then sonicated one further time in de-ionized water to flush ETOH.
- All samples are then dissolved in 0.5 M EDTA solution. When EDTA reaches pH of 10-11, 3/4 of solution is replaced with fresh EDTA

Sample # 1

Date	Treatment
Jan 31/17	Sonic Wash
"	9mL EDTA
Feb 3/17	9mL EDTA
Feb 6/17	9mL EDTA
Feb 10/17	" "
Feb 14/17	" "
Feb 16/17	" "
Mar 2/17	" "
Mar 18/17	" "
Mar 26/17	" "
May 8/18	" "
June 2/18	" "

Sample # 2

Date	Treatment
Jan 31/17	S.W.
"	9mL EDTA
Feb 3/17	9mL EDTA
Feb 6/17	9mL EDTA
Feb 10/17	" "
Feb 14/17	" "
Feb 16/17	" "
Mar 2/17	" "
Mar 18/17	" "
Mar 26/17	" "
May 8/18	" "
June 2/18	" "

Sample # 3

Date	Treatment
Jan 31/17	S.W.
"	9 mL EDTA
Feb 3/17	9mL EDTA
Feb 6/17	9mL EDTA
Feb 10/17	" "
Feb 14/17	" "
Feb 16/17	" "
Mar 2/17	" "
Mar 18/17	" "
Mar 26/17	" "
May 8/18	" "
June 2/18	" "

Bone Dissolution Sampling Sheet

Specimen Number UALVP 55900 **Collection Date** _____

Field _____ **Sampling Date** January 24/2017

Taxon Styracosaurus **Sample taken from** Scapula

Sedimentology Sandstone channel lag. **Percent Articulation** 100%

Sampling Proceedures

- All samples handled from time of collection to dissolution, were done using Nitrile gloves to prevent contamination from human skin.
- All samples that could be collected from previously broken bones were done so, thus eliminating the requirement of breaking bones.
- Samples required to be removed from larger bones were fractured off using a hammer and awl; preventing introduction of contaminants by saw blades forcing organics into micro fissures formed during cutting.
- Samples were placed into baggies and sealed to reduce contamination during transport.

Preparation and Dissolution Proceedures

- All samples were sonicated using de-ionized water to remove surface contaminants.
- All samples were then sonicated in 50% ETOH solution to remove any unknown consolidants and sterilized for bacteria.
- All samples were then sonicated one further time in de-ionized water to flush ETOH.
- All samples are then dissolved in 0.5 M EDTA solution. When EDTA reaches pH of 10-11, 3/4 of solution is replaced with fresh EDTA

Sample # 1

Date	Treatment
Jan 24/17	sonic wash
"	9mL EDTA
Jan 29/17	9mL EDTA
Feb 2/17	9mL EDTA
Feb 6/17	9mL EDTA
Feb 10/17	" "
Feb 10/17	" "
Mar 2/17	" "
Mar 12/17	" "
May 8/18	" "
June 2/18	" "
July 24/18	" "

Sample # 2

Date	Treatment
Jan 24/17	Sonic wash
"	9mL EDTA
Jan 29/17	9mL EDTA
Feb 2/17	9mL EDTA
Feb 6/17	9mL EDTA
Feb 10/17	" "
Feb 14/17	" "
Mar 2/17	" "
Mar 12/17	" "
May 8/18	" "
June 2/18	" "
July 24/18	" "

Sample # 3

Date	Treatment
Jan 24/17	Sonic wash
"	9mL EDTA
Jan 29/17	9mL EDTA
Feb 2/17	9mL EDTA
Feb 6/17	9mL EDTA
Feb 10/17	" "
Feb 14/17	" "
Mar 2/17	" "
Mar 12/17	" "
May 8/18	" "
June 2/18	" "
July 24/18	" "

Bone Dissolution Sampling Sheet

Specimen Number UALVP 59614 **Collection Date** _____

Field _____ **Sampling Date** January 24 2017

Taxon Hadrosauridae **Sample taken from** caudal vert

Sedimentology mudstone **Percent Articulation** isolated in microsite

Sampling Proceedures

- All samples handled from time of collection to dissolution, were done using Nitrile gloves to prevent contamination from human skin.
- All samples that could be collected from previously broken bones were done so, thus eliminating the requirement of breaking bones.
- Samples required to be removed from larger bones were fractured off using a hammer and awl; preventing introduction of contaminants by saw blades forcing organics into micro fissures formed during cutting.
- Samples were placed into baggies and sealed to reduce contamination during transport.

Preparation and Dissolution Proceedures

- All samples were sonicated using de-ionized water to remove surface contaminants.
- All samples were then sonicated in 50% ETOH solution to remove any unknown consolidants and sterilized for bacteria.
- All samples were then sonicated one further time in de-ionized water to flush ETOH.
- All samples are then dissolved in 0.5 M EDTA solution. When EDTA reaches pH of 10-11, 3/4 of solution is replaced with fresh EDTA

Sample # 1

Date	Treatment
Jan 24/17	Sonic Wash
"	9mL EDTA
Jan 26/17	6mL EDTA
Jan 28/17	9mL EDTA
Feb 3/17	9mL EDTA
Feb 6/17	9mL EDTA
Feb 10/17	" "
Feb 14/17	" "
Mar 2/17	" "
Mar 18/17	" "
May 2/18	" "
May 30/18	" "
July 17/18	3mL "

Sample # 2

Date	Treatment
Jan 24/17	Sonic Wash
"	9mL EDTA
Jan 26/17	6mL EDTA
Jan 28/17	9mL EDTA
Feb 3/17	9mL EDTA
Feb 6/17	9mL EDTA
Feb 10/17	" "
Feb 14/17	" "
Mar 2/17	" "
Mar 18/17	" "
May 2/18	" "
May 30/18	" "
July 17/18	3mL "

Sample # 3

Date	Treatment
Jan 24/17	Sonic Wash
"	9mL EDTA
Jan 26/17	6mL EDTA
Jan 28/17	9mL EDTA
Feb 3/17	9mL EDTA
Feb 6/17	9mL EDTA
Feb 10/17	" "
Feb 14/17	" "
Mar 2/17	" "
Mar 18/17	" "
May 2/18	" "
May 30/18	" "
July 17/18	3mL "

Bone Dissolution Sampling Sheet

Specimen Number UALVP 35880 **Collection Date** _____

Field _____ **Sampling Date** January 24 2017

Taxon Procamarahphus maximus **Sample taken from** Tendon

Sedimentology River sandstone **Percent Articulation** 100%

Sampling Proceedures

- All samples handled from time of collection to dissolution, were done using Nitrile gloves to prevent contamination from human skin.
- All samples that could be collected from previously broken bones were done so, thus eliminating the requirement of breaking bones.
- Samples required to be removed from larger bones were fractured off using a hammer and awl; preventing introduction of contaminants by saw blades forcing organics into micro fissures formed during cutting.
- Samples were placed into baggies and sealed to reduce contamination during transport.

Preparation and Dissolution Proceedures

- All samples were sonicated using de-ionized water to remove surface contaminants.
- All samples were then sonicated in 50% ETOH solution to remove any unknown consolidants and sterilized for bacteria.
- All samples were then sonicated one further time in de-ionized water to flush ETOH.
- All samples are then dissolved in 0.5 M EDTA solution. When EDTA reaches pH of 10-11, 3/4 of solution is replaced with fresh EDTA

Sample # 1

Date	Treatment
Jan 24/17	Sonic wash
"	9mL EDTA
Jan 28/17	9mL EDTA
Feb 3/17	9mL EDTA
Feb 6/17	9mL EDTA
Feb 10/17	" "
Feb 14/17	" "
Mar 2/17	" "
Mar 18/17	" "
May 2/18	" "
May 30/18	" "
July 17/18	" "

Sample # 2

Date	Treatment
Jan 24/17	Sonic wash
"	9mL EDTA
Jan 28/17	9mL EDTA
Feb 3/17	9mL EDTA
Feb 6/17	9mL EDTA
Feb 10/17	" "
Feb 14/17	" "
Mar 2/17	" "
Mar 18/17	" "
May 2/18	" "
May 30/18	" "
July 17/18	" "

Sample # 3

Date	Treatment
Jan 24/17	Sonic wash
"	9mL EDTA
Jan 28/17	9mL EDTA
Feb 3/17	9mL EDTA
Feb 6/17	9mL EDTA
Feb 10/17	" "
Feb 14/17	" "
Mar 2/17	" "
Mar 18/17	" "
May 2/18	" "
May 30/18	" "
July 17/18	" "

Bone Dissolution Sampling Sheet

Specimen Number UALVP 55980 **Collection Date** _____

Field _____ **Sampling Date** January 31 2017

Taxon Prosaurolophus **Sample taken from** Radius

Sedimentology River sandstone **Percent Articulation** 100%

Sampling Proceedures

- All samples handled from time of collection to dissolution, were done using Nitrile gloves to prevent contamination from human skin.
- All samples that could be collected from previously broken bones were done so, thus eliminating the requirement of breaking bones.
- Samples required to be removed from larger bones were fractured off using a hammer and awl; preventing introduction of contaminants by saw blades forcing organics into micro fissures formed during cutting.
- Samples were placed into baggies and sealed to reduce contamination during transport.

Preparation and Dissolution Proceedures

- All samples were sonicated using de-ionized water to remove surface contaminants.
- All samples were then sonicated in 50% ETOH solution to remove any unknown consolidants and sterilized for bacteria.
- All samples were then sonicated one further time in de-ionized water to flush ETOH.
- All samples are then dissolved in 0.5 M EDTA solution. When EDTA reaches pH of 10-11, 3/4 of solution is replaced with fresh EDTA

Sample # 1

Date	Treatment
Jan 31/17	Sonic Wash
"	9mL EDTA
Feb 3/17	9mL EDTA
Feb 6/17	9mL EDTA
Feb 10/17	" "
Feb 14/17	" "
Feb 16/17	" "
Mar 2/17	" "
Mar 18/17	" "
Mar 26/17	" "
May 8/18	" "
June 2/18	" "

Sample # 2

Date	Treatment
Jan 31/17	S. W.
"	9mL EDTA
Feb 3/17	9mL EDTA
Feb 6/17	9mL EDTA
Feb 10/17	" "
Feb 14/17	" "
Feb 16/17	" "
Mar 2/17	" "
Mar 18/17	" "
Mar 26/17	" "
May 8/18	" "
June 2/18	" "

Sample # 3

Date	Treatment
Jan 31/17	S. W.
"	9mL EDTA.
Feb 3/17	9mL EDTA
Feb 6/17	9mL EDTA
Feb 10/17	" "
Feb 14/17	" "
Feb 16/17	" "
Mar 2/17	" "
Mar 18/17	" "
Mar 26/17	" "
May 8/18	" "
June 2/18	" "

Bone Dissolution Sampling Sheet

Specimen Number UALVP 10 — **Collection Date** 1920's

Field — **Sampling Date** January 24/17

Taxon Gorgosaurus libratus — **Sample taken from** right pubic shaft.

Sedimentology Sand with concretions — **Percent Articulation** Tightly associated.

Sampling Proceedures

- All samples handled from time of collection to dissolution, were done using Nitrile gloves to prevent contamination from human skin.
- All samples that could be collected from previously broken bones were done so, thus eliminating the requirement of breaking bones.
- Samples required to be removed from larger bones were fractured off using a hammer and awl; preventing introduction of contaminants by saw blades forcing organics into micro fissures formed during cutting.
- Samples were placed into baggies and sealed to reduce contamination during transport.

Preparation and Dissolution Proceedures

- All samples were sonicated using de-ionized water to remove surface contaminants.
- All samples were then sonicated in 50% ETOH solution to remove any unknown consolidants and sterilized for bacteria.
- All samples were then sonicated one further time in de-ionized water to flush ETOH.
- All samples are then dissolved in 0.5 M EDTA solution. When EDTA reaches pH of 10-11, 3/4 of solution is replaced with fresh EDTA

Sample # 1

Date	Treatment
Jan 24/17	Sonic Wash
"	9mL EDTA
Jan 29/17	6 mL EDTA
Feb 3/17	6 mL EDTA
Feb 10/17	9mL EDTA
Feb 16/17	" "
Feb 21/17	" "
Mar 5/17	" "
Mar 12/17	" "
Mar 25/17	" "
May 2/18	" "
June 2/18	" "
June 22/18	" "

Sample # 2

Date	Treatment
Jan 24/17	Sonic Wash
"	9 mL EDTA
Jan 29/17	6 mL EDTA
Feb 3/17	6 mL EDTA
Feb 10/17	9 mL "
Feb 16/17	" "
Feb 21/17	" "
Mar 5/17	" "
Mar 12/17	" "
Mar 25/17	" "
May 2/18	" "
June 2/18	" "
June 22/18	" "

Sample # 3

Date	Treatment
Jan 24/17	Sonic wash
"	9mL EDTA.
Jan 29/17	6mL EDTA
Feb 3/17	6mL EDTA
Feb 10/17	9 mL "
Feb 16/17	" "
Feb 21/17	" "
Mar 5/17	" "
Mar 12/17	" "
Mar 18/17	" "
May 2/18	" "
June 2/18	" "
June 22/18	" "

Bone Dissolution Sampling Sheet

Specimen Number UALVP 49500 — **Collection Date** _____

Field _____ — **Sampling Date** January 24 2017

Taxon Gorgosaurus libratus — **Sample taken from** long bone float

Sedimentology muddy sand stone — **Percent Articulation** tightly associated

Sampling Proceedures

- All samples handled from time of collection to dissolution, were done using Nitrile gloves to prevent contamination from human skin.
- All samples that could be collected from previously broken bones were done so, thus eliminating the requirement of breaking bones.
- Samples required to be removed from larger bones were fractured off using a hammer and awl; preventing introduction of contaminants by saw blades forcing organics into micro fissures formed during cutting.
- Samples were placed into baggies and sealed to reduce contamination during transport.

Preparation and Dissolution Proceedures

- All samples were sonicated using de-ionized water to remove surface contaminants.
- All samples were then sonicated in 50% ETOH solution to remove any unknown consolidants and sterilized for bacteria.
- All samples were then sonicated one further time in de-ionized water to flush ETOH.
- All samples are then dissolved in 0.5 M EDTA solution. When EDTA reaches pH of 10-11, 3/4 of solution is replaced with fresh EDTA

Sample # 1

Date	Treatment
Jan 24/17	Sonic wash
"	9 mL EDTA
Jan 29/17	9mL EDTA
Feb 1/17	9mL EDTA
Feb 6/17	9mL EDTA
Feb 10/17	" "
Feb 14/17	" "
Feb 21/17	" "
Mar 12/17	" "
Mar 25/17	" "
Mar 27/17	" "
May 2/18	" "
June 2/18	" "
June 22/18	" "

Sample # 2

Date	Treatment
Jan 24/17	Sonic wash
"	9mL EDTA
Jan 29/17	9mL EDTA
Feb 1/17	9mL EDTA
Feb 6/17	9mL EDTA
Feb 10/17	" "
Feb 14/17	" "
Feb 21/17	" "
Mar 12/17	" "
Mar 25/17	" "
Mar 27/17	" "
May 2/18	" "
June 2/18	" "
June 22/18	" "

Sample # 3

Date	Treatment
Jan 24/17	Sonic Wash
"	9 mL EDTA
Jan 29/17	9mL EDTA
Feb 1/17	9mL EDTA
Feb 6/17	9mL EDTA
Feb 10/17	" "
Feb 14/17	" "
Feb 21/17	" "
Mar 12/17	" "
Mar 25/17	" "
Mar 27/17	" "
May 2/18	" "
June 2/18	" "
June 22/18	" "

Bone Dissolution Sampling Sheet

Specimen Number UALVP 52531 **Collection Date** 2009

Field _____ **Sampling Date** January 24/2017

Taxon Ornithomimus edmontonicus **Sample taken from** pedal phalanx

Sedimentology Iron rich sandstone **Percent Articulation** 100%

Sampling Proceedures

- All samples handled from time of collection to dissolution, were done using Nitrile gloves to prevent contamination from human skin.
- All samples that could be collected from previously broken bones were done so, thus eliminating the requirement of breaking bones.
- Samples required to be removed from larger bones were fractured off using a hammer and awl; preventing introduction of contaminants by saw blades forcing organics into micro fissures formed during cutting.
- Samples were placed into baggies and sealed to reduce contamination during transport.

Preparation and Dissolution Proceedures

- All samples were sonicated using de-ionized water to remove surface contaminants.
- All samples were then sonicated in 50% ETOH solution to remove any unknown consolidants and sterilized for bacteria.
- All samples were then sonicated one further time in de-ionized water to flush ETOH.
- All samples are then dissolved in 0.5 M EDTA solution. When EDTA reaches pH of 10-11, 3/4 of solution is replaced with fresh EDTA

Sample # 1

Date	Treatment
Jan 26/17	9mL EDTA
Feb 3/17	9mL EDTA
Feb 10/17	" "
Feb 16/17	" "
Mar 2/17	" "
Mar 12/17	" "
Mar 26/17	" "
May 8/18	" "
June 2/18	" "

Sample # 2

Date	Treatment
Jan 26/17	9mL EDTA
Feb 3/17	9mL EDTA
Feb 10/17	" "
Feb 16/17	" "
Mar 2/17	" "
Mar 12/17	" "
Mar 26/17	" "
May 8/18	" "
June 2/18	" "

Sample # 3

Date	Treatment
Jan 26/17	9mL EDTA.
Feb 3/17	9mL EDTA
Feb 10/17	" "
Feb 16/17	" "
Mar 2/17	" "
Mar 12/17	" "
Mar 26/17	" "
May 8/18	" "
June 2/18	" "

Bone Dissolution Sampling Sheet

Specimen Number UALVP 55800 **Collection Date** Sept 2014

Field _____ **Sampling Date** January 26 2017

Taxon Sauroniftholestes langstoni **Sample taken from** caudal vert

Sedimentology Iron rich sandstone **Percent Articulation** 100%

Sampling Proceedures

- All samples handled from time of collection to dissolution, were done using Nitrile gloves to prevent contamination from human skin.
- All samples that could be collected from previously broken bones were done so, thus eliminating the requirement of breaking bones.
- Samples required to be removed from larger bones were fractured off using a hammer and awl; preventing introduction of contaminants by saw blades forcing organics into micro fissures formed during cutting.
- Samples were placed into baggies and sealed to reduce contamination during transport.

Preparation and Dissolution Proceedures

- All samples were sonicated using de-ionized water to remove surface contaminants.
- All samples were then sonicated in 50% ETOH solution to remove any unknown consolidants and sterilized for bacteria.
- All samples were then sonicated one further time in de-ionized water to flush ETOH.
- All samples are then dissolved in 0.5 M EDTA solution. When EDTA reaches pH of 10-11, 3/4 of solution is replaced with fresh EDTA

Sample # 1

Date	Treatment
Jan 26/17	Sonic wash
"	9mL EDTA
Feb 3/17	9mL EDTA
Feb 10/17	" "
Feb 16/17	" "
Mar 2/17	" "
Mar 12/17	" "
Mar 26/17	" "
May 2/18	" "
June 2/18	" "

Sample # 2

Date	Treatment
Jan 26/17	sonic wash
"	9mL EDTA
Feb 3/17	9mL EDTA
Feb 10/17	" "
Feb 16/17	" "
Mar 2/17	~~Mar~~ " "
Mar 12/17	" "
Mar 26/17	" "
May 2/18	" "
June 2/18	" "

Sample # 3

Date	Treatment
Jan 26/17	sonic wash
"	9mL EDTA
Feb 3/17	9mL EDTA
Feb 10/17	" "
Feb 16/17	" "
Mar 2/17	" "
Mar 12/17	" "
Mar 26/17	" "
May 2/18	" "
June 2/18	" "

Bone Dissolution Sampling Sheet

Specimen Number UALVP 55804

Collection Date _____

Field _____

Sampling Date January 24 2017

Taxon Latenivenator. memasterae

Sample taken from left ilium

Sedimentology Sandstone

Percent Articulation disarticulated

Sampling Proceedures

- All samples handled from time of collection to dissolution, were done using Nitrile gloves to prevent contamination from human skin.
- All samples that could be collected from previously broken bones were done so, thus eliminating the requirement of breaking bones.
- Samples required to be removed from larger bones were fractured off using a hammer and awl; preventing introduction of contaminants by saw blades forcing organics into micro fissures formed during cutting.
- Samples were placed into baggies and sealed to reduce contamination during transport.

Preparation and Dissolution Proceedures

- All samples were sonicated using de-ionized water to remove surface contaminants.
- All samples were then sonicated in 50% ETOH solution to remove any unknown consolidants and sterilized for bacteria.
- All samples were then sonicated one further time in de-ionized water to flush ETOH.
- All samples are then dissolved in 0.5 M EDTA solution. When EDTA reaches pH of 10-11, 3/4 of solution is replaced with fresh EDTA

Sample # 1

Date	Treatment
Jan 24/17	Sonic Wash
"	9mL EDTA
Jan 29/17	9mL EDTA
Feb 1/17	9mL EDTA
Feb 6/17	9mL EDTA
Feb 10/17	" "
Feb 14/17	" "
Feb 21/17	" "
Mar 12/17	" "
Mar 25/17	" "
Mar 27/17	" "
May 2/18	" "
June 2/18	" "
June 22/18	" "

Sample # 2

Date	Treatment
Jan 24/17	Sonic Wash
"	9mL EDTA
Jan 29/17	9mL EDTA
Feb 1/17	9mL EDTA
Feb 6/17	9mL EDTA
Feb 10/17	" "
Feb 14/17	" "
Feb 21/17	" "
Mar 12/17	" "
Mar 25/17	" "
Mar 27/17	" "
May 2/18	" "
June 2/18	" "
June 22/18	" "

Sample # 3

Date	Treatment
Jan 24/17	Sonic wash
"	9mL EDTA
Jan 29/17	9mL EDTA
Feb 1/17	9mL EDTA
Feb 6/17	9mL EDTA
Feb 10/17	" "
Feb 14/17	" "
Feb 21/17	" "
Mar 12/17	" "
Mar 25/17	" "
Mar 26/17	" "
May 2/18	" "
June 2/18	" "
June 22/18	" "

APPENDIX 4-1: Lab treatment forms for bone samples from the Horseshoe Canyon Formation.
Forms organized in the same order as Table 4-1.

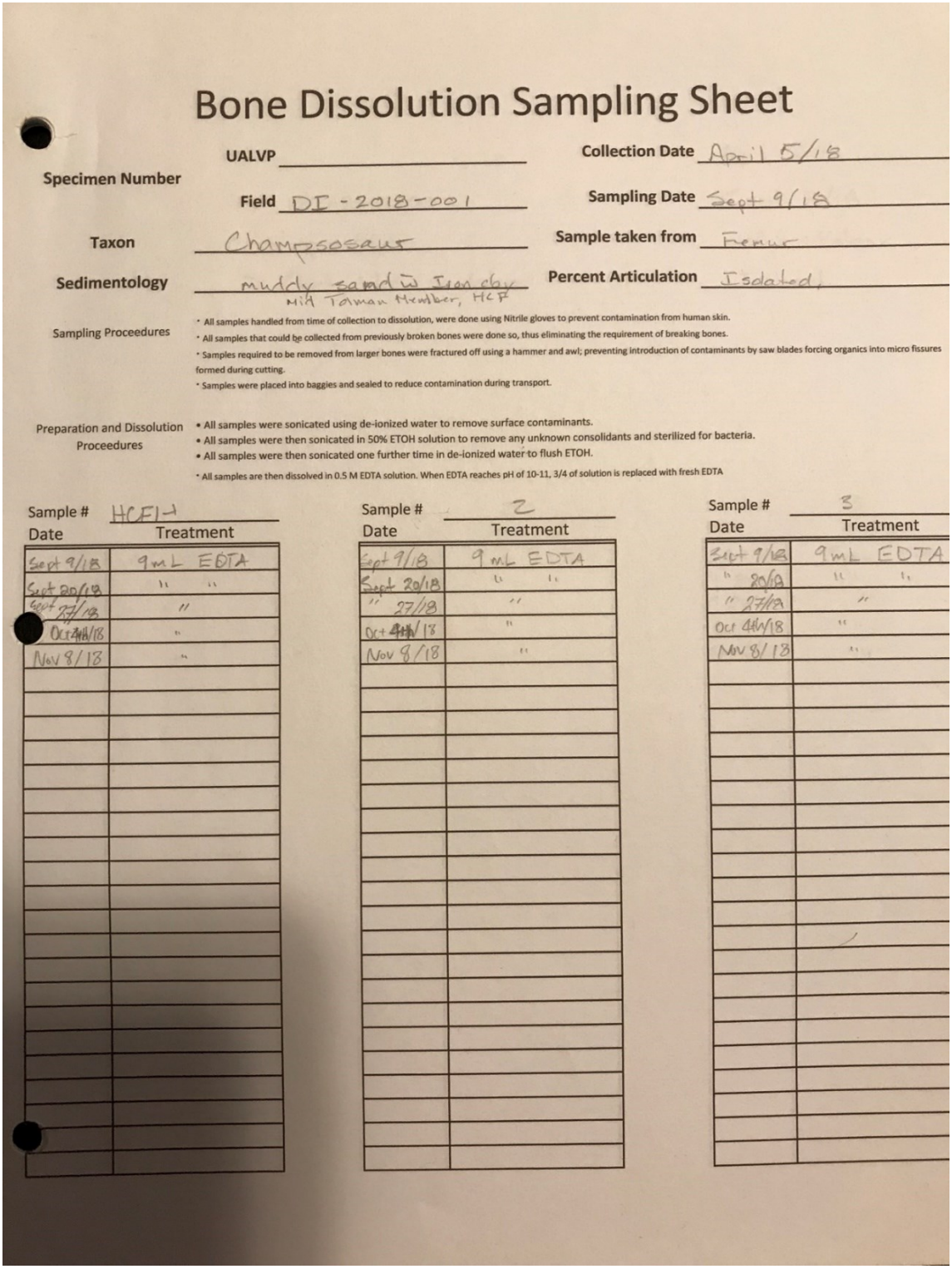

Bone Dissolution Sampling Sheet

Specimen Number

UALVP _____ Collection Date April 5/18

Field DI-2018-001 Sampling Date Sept 9/18

Taxon Champsosaurus Sample taken from Femur

Sedimentology muddy sand w Iron clay Mid Tolman Member, HCF Percent Articulation Isolated

Sampling Proceedures

- All samples handled from time of collection to dissolution, were done using Nitrile gloves to prevent contamination from human skin.
- All samples that could be collected from previously broken bones were done so, thus eliminating the requirement of breaking bones.
- Samples required to be removed from larger bones were fractured off using a hammer and awl; preventing introduction of contaminants by saw blades forcing organics into micro fissures formed during cutting.
- Samples were placed into baggies and sealed to reduce contamination during transport.

Preparation and Dissolution Proceedures

- All samples were sonicated using de-ionized water to remove surface contaminants.
- All samples were then sonicated in 50% ETOH solution to remove any unknown consolidants and sterilized for bacteria.
- All samples were then sonicated one further time in de-ionized water to flush ETOH.
- All samples are then dissolved in 0.5 M EDTA solution. When EDTA reaches pH of 10-11, 3/4 of solution is replaced with fresh EDTA

Sample # HCF1-1

Date	Treatment
Sept 9/18	9mL EDTA
Sept 20/18	" "
Sept 27/18	"
Oct 4th/18	"
Nov 8/18	"

Sample # 2

Date	Treatment
Sept 9/18	9mL EDTA
Sept 20/18	" "
" 27/18	"
Oct 4th/18	"
Nov 8/18	"

Sample # 3

Date	Treatment
Sept 9/18	9mL EDTA
" 20/18	" "
" 27/18	"
Oct 4th/18	"
Nov 8/18	"

Bone Dissolution Sampling Sheet

Specimen Number

UALVP _____ **Collection Date** April 6/18

Field DE-2018-002 **Sampling Date** Sept 9/18

Taxon Ceratopsidae **Sample taken from** pedal phalanx

Sedimentology ? flint, likely sandstone **Percent Articulation** Isolated

Sampling Proceedures

- All samples handled from time of collection to dissolution, were done using Nitrile gloves to prevent contamination from human skin.
- All samples that could be collected from previously broken bones were done so, thus eliminating the requirement of breaking bones.
- Samples required to be removed from larger bones were fractured off using a hammer and awl; preventing introduction of contaminants by saw blades forcing organics into micro fissures formed during cutting.
- Samples were placed into baggies and sealed to reduce contamination during transport.

Preparation and Dissolution Proceedures

- All samples were sonicated using de-ionized water to remove surface contaminants.
- All samples were then sonicated in 50% ETOH solution to remove any unknown consolidants and sterilized for bacteria.
- All samples were then sonicated one further time in de-ionized water to flush ETOH.
- All samples are then dissolved in 0.5 M EDTA solution. When EDTA reaches pH of 10-11, 3/4 of solution is replaced with fresh EDTA

Sample # 1

Date	Treatment
Sept 9/18	9 mL EDTA
Sept 20/18	" "
" 27/18	"
Oct 4th/18	"
Nov 8/18	"

Sample # 2

Date	Treatment
Sept 9/18	9 mL EDTA
" 20/18	" "
" 27/18	"
Oct 4th/18	"
Nov 8/18	"

Sample # 3

Date	Treatment
Sept 9/18	9 mL EDTA
" 20/18	" "
" 27/18	"
Oct 4th/18	"
Nov 8/18	"

Bone Dissolution Sampling Sheet

Specimen Number

UALVP _____

Field DI - 2018-003

Taxon Hadrosauridae

Sedimentology Muddy sandstone

Collection Date April 5/18

Sampling Date Sept 9/18

Sample taken from manual phalanx

Percent Articulation Isolated

Sampling Proceedures

- All samples handled from time of collection to dissolution, were done using Nitrile gloves to prevent contamination from human skin.
- All samples that could be collected from previously broken bones were done so, thus eliminating the requirement of breaking bones.
- Samples required to be removed from larger bones were fractured off using a hammer and awl; preventing introduction of contaminants by saw blades forcing organics into micro fissures formed during cutting.
- Samples were placed into baggies and sealed to reduce contamination during transport.

Preparation and Dissolution Proceedures

- All samples were sonicated using de-ionized water to remove surface contaminants.
- All samples were then sonicated in 50% ETOH solution to remove any unknown consolidants and sterilized for bacteria.
- All samples were then sonicated one further time in de-ionized water to flush ETOH.
- All samples are then dissolved in 0.5 M EDTA solution. When EDTA reaches pH of 10-11, 3/4 of solution is replaced with fresh EDTA

Sample # 1

Date	Treatment
Sept 9/18	9mL EDTA
Sept 25/18	"
" 27/18	"
Oct 4/18	"
Nov 8/18	"

Sample # 2

Date	Treatment
Sept 9/18	9mL EDTA
" 20/18	"
" 27/18	"
Oct 4th/18	"
Nov 8/18	"

Sample # 3

Date	Treatment
Sept 9/18	9mL EDTA
" 20/18	"
" 27/18	"
Oct 4th/18	"
Nov 8/18	"

Bone Dissolution Sampling Sheet

Specimen Number

UALVP _____ **Collection Date** May 17, 18

Field DI-2018-004 **Sampling Date** Sept 9/18

Taxon Hadrosauridae - Juvenile **Sample taken from** Ilium

Sedimentology Sandstone **Percent Articulation** Associated

Sampling Proceedures

- All samples handled from time of collection to dissolution, were done using Nitrile gloves to prevent contamination from human skin.
- All samples that could be collected from previously broken bones were done so, thus eliminating the requirement of breaking bones.
- Samples required to be removed from larger bones were fractured off using a hammer and awl; preventing introduction of contaminants by saw blades forcing organics into micro fissures formed during cutting.
- Samples were placed into baggies and sealed to reduce contamination during transport.

Preparation and Dissolution Proceedures

- All samples were sonicated using de-ionized water to remove surface contaminants.
- All samples were then sonicated in 50% ETOH solution to remove any unknown consolidants and sterilized for bacteria.
- All samples were then sonicated one further time in de-ionized water to flush ETOH.
- All samples are then dissolved in 0.5 M EDTA solution. When EDTA reaches pH of 10-11, 3/4 of solution is replaced with fresh EDTA

Sample # 1

Date	Treatment
Sept 9/18	9 mL EDTA
" 20/18	"
" 27/18	"
Oct 4/18	"
Nov 8/18	"

Sample # 2

Date	Treatment
Sept 9/18	9 mL EDTA
Sept 20/18	"
" 27/18	"
Oct 4th/18	"
Nov 8/18	"

Sample # 3

Date	Treatment
Sept 9/18	9 mL EDTA
" 20/18	"
" 27/18	"
Oct 4th/18	"
Nov 8/18	"

Bone Dissolution Sampling Sheet

Specimen Number UALVP _____ **Collection Date** May 14/18

Field DI-2018-005 **Sampling Date** Sept 9/18

Taxon Juv. Hadrosauridae **Sample taken from** Humerus

Sedimentology Mudstone **Percent Articulation** Associated

Sampling Proceedures

* All samples handled from time of collection to dissolution, were done using Nitrile gloves to prevent contamination from human skin.
* All samples that could be collected from previously broken bones were done so, thus eliminating the requirement of breaking bones.
* Samples required to be removed from larger bones were fractured off using a hammer and awl; preventing introduction of contaminants by saw blades forcing organics into micro fissures formed during cutting.
* Samples were placed into baggies and sealed to reduce contamination during transport.

Preparation and Dissolution Proceedures

- All samples were sonicated using de-ionized water to remove surface contaminants.
- All samples were then sonicated in 50% ETOH solution to remove any unknown consolidants and sterilized for bacteria.
- All samples were then sonicated one further time in de-ionized water to flush ETOH.

* All samples are then dissolved in 0.5 M EDTA solution. When EDTA reaches pH of 10-11, 3/4 of solution is replaced with fresh EDTA

Sample # 1

Date	Treatment
Sept 9/18	9 mL EDTA
" 20/18	"
" 27/18	"
Oct 4th/18	"
Nov 8/18	"

Sample # 2

Date	Treatment
Sept 9/18	9 mL EDTA
" 20/18	"
" 27/18	"
Oct 4th/18	"
Nov 8/18	"

Sample # 3

Date	Treatment
Sept 9/18	9 mL EDTA
" 20/18	"
" 27/18	"
Oct 4/18	"
Nov 8/18	"

Bone Dissolution Sampling Sheet

Specimen Number

UALVP _____ Collection Date May 19/18

Field DI-2018-6 Sampling Date Sept 9/18

Taxon Hadrosauridae Sample taken from Metatarsal III

Sedimentology Muddy sand. Percent Articulation Isolated

Sampling Proceedures

- All samples handled from time of collection to dissolution, were done using Nitrile gloves to prevent contamination from human skin.
- All samples that could be collected from previously broken bones were done so, thus eliminating the requirement of breaking bones.
- Samples required to be removed from larger bones were fractured off using a hammer and awl; preventing introduction of contaminants by saw blades forcing organics into micro fissures formed during cutting.
- Samples were placed into baggies and sealed to reduce contamination during transport.

Preparation and Dissolution Proceedures

- All samples were sonicated using de-ionized water to remove surface contaminants.
- All samples were then sonicated in 50% ETOH solution to remove any unknown consolidants and sterilized for bacteria.
- All samples were then sonicated one further time in de-ionized water to flush ETOH.
- All samples are then dissolved in 0.5 M EDTA solution. When EDTA reaches pH of 10-11, 3/4 of solution is replaced with fresh EDTA

Sample # 1

Date	Treatment
Sept 9/18	9mL EDTA
" 20/18	"
" 27/18	"
Oct 4/18	"
Nov 8/18	"

Sample # 2

Date	Treatment
Sept 9/18	9 mL EDTA
" 20/18	"
" 27/18	"
Oct 4/18	"
Nov 8/18	"

Sample # 3

Date	Treatment
Sept 9/18	9mL EDTA
Sept 20/18	"
Sept 27/18	"
Oct 4/18	"
Nov 8/18	"

Bone Dissolution Sampling Sheet

Specimen Number

UALVP _____ **Collection Date** May 15 - 2018

Field DT - 2018:8 **Sampling Date** Sept 10/18

Taxon Hadrosauridae **Sample taken from** Maxilla

Sedimentology Sandstone **Percent Articulation** Isolated

Sampling Proceedures

- All samples handled from time of collection to dissolution, were done using Nitrile gloves to prevent contamination from human skin.
- All samples that could be collected from previously broken bones were done so, thus eliminating the requirement of breaking bones.
- Samples required to be removed from larger bones were fractured off using a hammer and awl; preventing introduction of contaminants by saw blades forcing organics into micro fissures formed during cutting.
- Samples were placed into baggies and sealed to reduce contamination during transport.

Preparation and Dissolution Proceedures

- All samples were sonicated using de-ionized water to remove surface contaminants.
- All samples were then sonicated in 50% ETOH solution to remove any unknown consolidants and sterilized for bacteria.
- All samples were then sonicated one further time in de-ionized water to flush ETOH.
- All samples are then dissolved in 0.5 M EDTA solution. When EDTA reaches pH of 10-11, 3/4 of solution is replaced with fresh EDTA

Sample # 1

Date	Treatment
Sept 10/18	9mL EDTA
" 20/18	"
" 27/18	"
Oct 4/18	"
Nov 8/18	"

Sample # 2

Date	Treatment
Sept 10/18	9mL EDTA
" 20/18	"
" 27/18	"
Oct 4/18	"
Nov 8/18	"

Sample # 3

Date	Treatment
Sept 10/18	9mL EDTA
" 20/18	"
" 27/18	"
Oct 4/18	"
Nov 8/18	"

Bone Dissolution Sampling Sheet

Specimen Number

UALVP _____ **Collection Date** April 5 2018

Field DI-2018-90 **Sampling Date** Sept 10/18

Taxon Hadrosauridae **Sample taken from** Rib

Sedimentology Sandstone **Percent Articulation** Isolated.

Sampling Proceedures

- All samples handled from time of collection to dissolution, were done using Nitrile gloves to prevent contamination from human skin.
- All samples that could be collected from previously broken bones were done so, thus eliminating the requirement of breaking bones.
- Samples required to be removed from larger bones were fractured off using a hammer and awl; preventing introduction of contaminants by saw blades forcing organics into micro fissures formed during cutting.
- Samples were placed into baggies and sealed to reduce contamination during transport.

Preparation and Dissolution Proceedures

- All samples were sonicated using de-ionized water to remove surface contaminants.
- All samples were then sonicated in 50% ETOH solution to remove any unknown consolidants and sterilized for bacteria.
- All samples were then sonicated one further time in de-ionized water to flush ETOH.
- All samples are then dissolved in 0.5 M EDTA solution. When EDTA reaches pH of 10-11, 3/4 of solution is replaced with fresh EDTA

Sample # 1

Date	Treatment
Sept 10/18	9 mL EDTA
" 20/18	"
" 27/18	"
Oct 4/18	"
Nov 8/18	"

Sample # 2

Date	Treatment
Sept 10/18	9mL EDTA
Sept 20/18	"
" 27/18	"
Oct 4/18	"
Nov 8/18	"

Sample # 3

Date	Treatment
Sept 10/18	9mL EDTA
" 20/18	"
" 27/18	"
Oct 4/18	"
Nov 8/18	"

Bone Dissolution Sampling Sheet

Specimen Number

UALVP _____ **Collection Date** April 25/18

Field DI-2018-9 **Sampling Date** Sept 10/18

Taxon Hypacrosaurus **Sample taken from** Neural Spine

Sedimentology Sandstone w Fe nodules **Percent Articulation** Associated skeleton

Sampling Proceedures

- All samples handled from time of collection to dissolution, were done using Nitrile gloves to prevent contamination from human skin.
- All samples that could be collected from previously broken bones were done so, thus eliminating the requirement of breaking bones.
- Samples required to be removed from larger bones were fractured off using a hammer and awl; preventing introduction of contaminants by saw blades forcing organics into micro fissures formed during cutting.
- Samples were placed into baggies and sealed to reduce contamination during transport.

Preparation and Dissolution Proceedures

- All samples were sonicated using de-ionized water to remove surface contaminants.
- All samples were then sonicated in 50% ETOH solution to remove any unknown consolidants and sterilized for bacteria.
- All samples were then sonicated one further time in de-ionized water to flush ETOH.
- All samples are then dissolved in 0.5 M EDTA solution. When EDTA reaches pH of 10-11, 3/4 of solution is replaced with fresh EDTA

Sample # 1

Date	Treatment
Sept 10/18	9mL EDTA
" 20/18	"
" 27/18	"
Oct 4/18	"
Nov 8/18	"

Sample # 2

Date	Treatment
Sept 10/18	9mL EDTA
" 20/18	"
" 27/18	"
Oct 4/18	"
Nov 8/18	"

Sample # 3

Date	Treatment
Sept 10/18	9mL EDTA
" 20/18	"
" 27/18	"
Oct 4/18	"
Nov 8/18	"

Bone Dissolution Sampling Sheet

Specimen Number

UALVP _____ **Collection Date** May 18, 2018

Field DI-2018-7 **Sampling Date** Sept. 10/18

Taxon Ornithomimidae **Sample taken from** Rib

Sedimentology Sandstone **Percent Articulation** Bonebed.

Sampling Proceedures

- All samples handled from time of collection to dissolution, were done using Nitrile gloves to prevent contamination from human skin.
- All samples that could be collected from previously broken bones were done so, thus eliminating the requirement of breaking bones.
- Samples required to be removed from larger bones were fractured off using a hammer and awl; preventing introduction of contaminants by saw blades forcing organics into micro fissures formed during cutting.
- Samples were placed into baggies and sealed to reduce contamination during transport.

Preparation and Dissolution Proceedures

- All samples were sonicated using de-ionized water to remove surface contaminants.
- All samples were then sonicated in 50% ETOH solution to remove any unknown consolidants and sterilized for bacteria.
- All samples were then sonicated one further time in de-ionized water to flush ETOH.
- All samples are then dissolved in 0.5 M EDTA solution. When EDTA reaches pH of 10-11, 3/4 of solution is replaced with fresh EDTA

Sample # 1

Date	Treatment
Sept 10/18	9 mL EDTA
" 20/18	"
" 27/18	"
Oct 4/18	"
Nov 8/18	"

Sample # 2

Date	Treatment
Sept 10/18	9 mL EDTA
" 20/18	"
" 27/18	"
Oct 4/18	"
Nov 8/18	"

Sample # 3

Date	Treatment
Sept 10/18	9 mL EDTA
" 20/18	"
" 27/18	"
Oct 4/18	"
Nov 8/18	"

APPENDIX 5-1: Lab treatment forms for bone samples from the Wapiti Formation. Forms organized in the same order as Table 5-1.

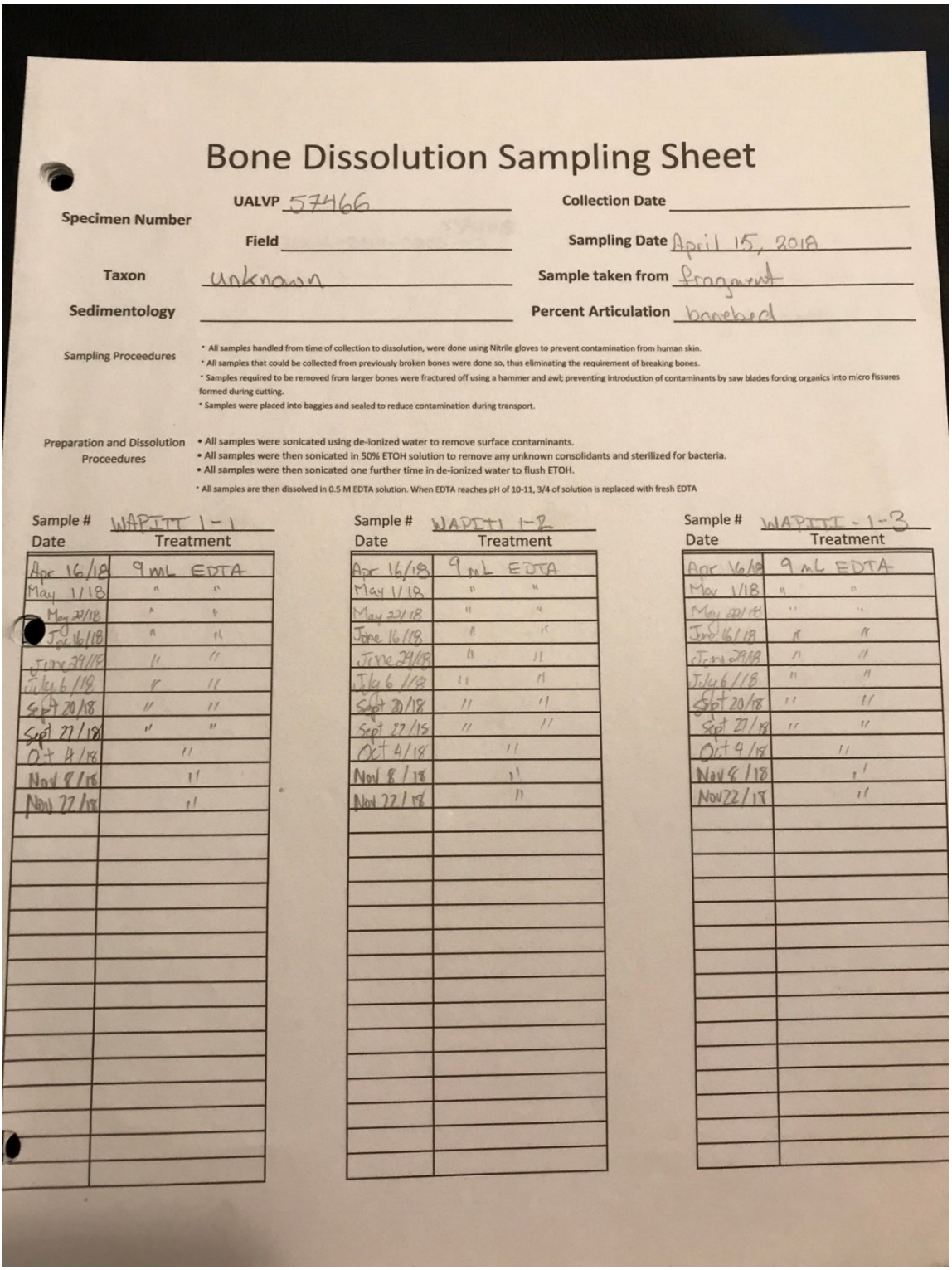

Bone Dissolution Sampling Sheet

Specimen Number UALVP 57466 **Collection Date** _____

Field _____ **Sampling Date** April 15, 2018

Taxon unknown **Sample taken from** fragment

Sedimentology _____ **Percent Articulation** bonebed

Sampling Proceedures

- All samples handled from time of collection to dissolution, were done using Nitrile gloves to prevent contamination from human skin.
- All samples that could be collected from previously broken bones were done so, thus eliminating the requirement of breaking bones.
- Samples required to be removed from larger bones were fractured off using a hammer and awl; preventing introduction of contaminants by saw blades forcing organics into micro fissures formed during cutting.
- Samples were placed into baggies and sealed to reduce contamination during transport.

Preparation and Dissolution Proceedures

- All samples were sonicated using de-ionized water to remove surface contaminants.
- All samples were then sonicated in 50% ETOH solution to remove any unknown consolidants and sterilized for bacteria.
- All samples were then sonicated one further time in de-ionized water to flush ETOH.
- All samples are then dissolved in 0.5 M EDTA solution. When EDTA reaches pH of 10-11, 3/4 of solution is replaced with fresh EDTA

Sample # WAPITI 1-1

Date	Treatment
Apr 16/18	9 mL EDTA
May 1/18	"
May 22/18	"
Jun 16/18	"
June 29/18	"
July 6/18	"
Sept 20/18	"
Sept 27/18	"
Oct 4/18	"
Nov 8/18	"
Nov 22/18	"

Sample # WAPITI 1-2

Date	Treatment
Apr 16/18	9 mL EDTA
May 1/18	"
May 22/18	"
June 16/18	"
June 29/18	"
July 6/18	"
Sept 20/18	"
Sept 27/18	"
Oct 4/18	"
Nov 8/18	"
Nov 22/18	"

Sample # WAPITI - 1-3

Date	Treatment
Apr 16/18	9 mL EDTA
May 1/18	"
May 22/18	"
June 16/18	"
June 29/18	"
July 6/18	"
Sept 20/18	"
Sept 27/18	"
Oct 4/18	"
Nov 8/18	"
Nov 22/18	"

Bone Dissolution Sampling Sheet

Specimen Number

UALVP _____ Collection Date _____

NADP H. 07. 30-07

Field 57466 Sampling Date _____

Taxon _____ Sample taken from _____

Sedimentology _____ Percent Articulation _____

Sampling Proceedures

- All samples handled from time of collection to dissolution, were done using Nitrile gloves to prevent contamination from human skin.
- All samples that could be collected from previously broken bones were done so, thus eliminating the requirement of breaking bones.
- Samples required to be removed from larger bones were fractured off using a hammer and awl; preventing introduction of contaminants by saw blades forcing organics into micro fissures formed during cutting.
- Samples were placed into baggies and sealed to reduce contamination during transport.

Preparation and Dissolution Proceedures

- All samples were sonicated using de-ionized water to remove surface contaminants.
- All samples were then sonicated in 50% ETOH solution to remove any unknown consolidants and sterilized for bacteria.
- All samples were then sonicated one further time in de-ionized water to flush ETOH.
- All samples are then dissolved in 0.5 M EDTA solution. When EDTA reaches pH of 10-11, 3/4 of solution is replaced with fresh EDTA

Sample # A

Date	Treatment
Nov 22	9mL 0.5M EDTA

Sample # B

Date	Treatment
Nov 22	9mL 0.5M EDTA

Sample # C

Date	Treatment
Nov 22	9mL 0.5M EDTA

Bone Dissolution Sampling Sheet

Specimen Number UALVP 57478
Field NADP-2014-0805-02

Collection Date _____

Sampling Date April 17, 2018

Taxon unknown

Sample taken from fragment (rib)

Sedimentology _____

Percent Articulation frog bonebed.

Sampling Proceedures

- All samples handled from time of collection to dissolution, were done using Nitrile gloves to prevent contamination from human skin.
- All samples that could be collected from previously broken bones were done so, thus eliminating the requirement of breaking bones.
- Samples required to be removed from larger bones were fractured off using a hammer and awl; preventing introduction of contaminants by saw blades forcing organics into micro fissures formed during cutting.
- Samples were placed into baggies and sealed to reduce contamination during transport.

Preparation and Dissolution Proceedures

- All samples were sonicated using de-ionized water to remove surface contaminants.
- All samples were then sonicated in 50% ETOH solution to remove any unknown consolidants and sterilized for bacteria.
- All samples were then sonicated one further time in de-ionized water to flush ETOH.
- All samples are then dissolved in 0.5 M EDTA solution. When EDTA reaches pH of 10-11, 3/4 of solution is replaced with fresh EDTA

Sample # WAPITI 1-4

Date	Treatment	
Apr 16/18	9 mL EDTA	
May 1/18	"	"
May 22/18	"	"
June 16/18	"	"
June 29/18	"	"
July 6/18	"	"
Sept 20/18	"	"
Sept 27/18	"	"
Oct 4/18		"
Nov 8/18		"
Nov 22/18		"

Sample # WAPITI 1-5

Date	Treatment	
Apr 16/18	9mL EDTA	
May 1/18	"	"
May 22/18	"	"
June 16/18	"	"
June 29/18	"	"
July 6/18	"	"
Sept 20/18	"	"
Sept 27/18	"	"
Oct 4/18		"
Nov 8/18		"
Nov 22/18		"

Sample # WAPITI 1-6

Date	Treatment	
Apr 16/18	9mL EDTA	
May 1/18	"	"
May 22/18	"	"
June 16/18	"	"
June 29/18	"	"
July 6/18	"	"
Sept 20/18	"	"
Sept 27/18	"	"
Oct 4/18		"
Nov 8/18		"
Nov 22/18		"

Bone Dissolution Sampling Sheet

Specimen Number UALVP 57-428

Field NADR-2016-0712-05

Taxon unknown

Sedimentology

Collection Date

Sampling Date April 15, 2018

Sample taken from rib frag

Percent Articulation bonebed

Sampling Proceedures

- All samples handled from time of collection to dissolution, were done using Nitrile gloves to prevent contamination from human skin.
- All samples that could be collected from previously broken bones were done so, thus eliminating the requirement of breaking bones.
- Samples required to be removed from larger bones were fractured off using a hammer and awl; preventing introduction of contaminants by saw blades forcing organics into micro fissures formed during cutting.
- Samples were placed into baggies and sealed to reduce contamination during transport.

Preparation and Dissolution Proceedures

- All samples were sonicated using de-ionized water to remove surface contaminants.
- All samples were then sonicated in 50% ETOH solution to remove any unknown consolidants and sterilized for bacteria.
- All samples were then sonicated one further time in de-ionized water to flush ETOH.
- All samples are then dissolved in 0.5 M EDTA solution. When EDTA reaches pH of 10-11, 3/4 of solution is replaced with fresh EDTA

Sample # WAPITI 2-1

Date	Treatment
Apr 16/18	9mL EDTA
May 1/18	" "
May 22/18	" "
June 16/18	" "
June 29/18	" "
July 6/18	" "
July 17/18	" "
Sept 20/18	" "
Sept 27/18	" "
Oct 4/18	"
Nov 8/18	"
Nov 22/18	"

Sample # WAPITI 2-2

Date	Treatment
Apr 16/18	9mL EDTA
May 1/18	" "
May 22/18	" "
June 16/18	" "
June 29/18	" "
July 6/18	" "
July 17/18	" "
Sept 20/18	" "
Sept 27/18	" "
Oct 4/18	"
Nov 8/18	"
Nov 22/18	"

Sample # WAPITI - 2-3

Date	Treatment
Apr 16/18	9mL EDTA
May 1/18	" "
May 22/18	" "
June 16/18	" "
June 29/18	" "
July 6/18	" "
July 17/18	" "
Sept 20/18	" "
Sept 27/18	" "
Oct 4/18	"
Nov 8/18	"
Nov 22/18	"

Bone Dissolution Sampling Sheet

Specimen Number UALVP 57506

Field NADP2015-20721-10 "LEFT"

Collection Date _____

Sampling Date April 15, 2018

Taxon unknown

Sample taken from fragment

Sedimentology _____

Percent Articulation bonbed.

Sampling Proceedures

- All samples handled from time of collection to dissolution, were done using Nitrile gloves to prevent contamination from human skin.
- All samples that could be collected from previously broken bones were done so, thus eliminating the requirement of breaking bones.
- Samples required to be removed from larger bones were fractured off using a hammer and awl; preventing introduction of contaminants by saw blades forcing organics into micro fissures formed during cutting.
- Samples were placed into baggies and sealed to reduce contamination during transport.

Preparation and Dissolution Proceedures

- All samples were sonicated using de-ionized water to remove surface contaminants.
- All samples were then sonicated in 50% ETOH solution to remove any unknown consolidants and sterilized for bacteria.
- All samples were then sonicated one further time in de-ionized water to flush ETOH.
- All samples are then dissolved in 0.5 M EDTA solution. When EDTA reaches pH of 10-11, 3/4 of solution is replaced with fresh EDTA

Sample # WAPITI 2-4

Date	Treatment
Apr 16/18	9mL EDTA
May 1/18	" "
May 22/18	" "
June 16/18	" "
June 29/18	" "
July 6/18	" "
July 17/18	" "
Sept 20/18	" "
Sept 27/18	" "
Oct 4/18	"
Nov 8/18	"
Nov 22/18	"

Sample # WAPITI 2-5

Date	Treatment
Apr 16/18	9mL EDTA
May 1/18	" "
May 22/18	" "
June 16/18	" "
June 29/18	" "
July 6/18	" "
July 17/18	" "
Sept 20/18	" "
Sept 27/18	" "
Oct 4/18	"
Nov 8/18	"
Nov 22/18	"

Sample # WAPITI 2-6

Date	Treatment
Apr 16/18	9mL EDTA
May 1/18	" "
May 22/18	" "
June 16/18	" "
June 29/18	" "
July 6/18	" "
July 17/18	" "
Sept 20/18	" "
Sept 27/18	" "
Oct 4/18	"
Nov 8/18	"
Nov 22/18	"

Bone Dissolution Sampling Sheet

Specimen Number

UALVP _____ **Collection Date** _____

Field CU13-01-05 57523 **Sampling Date** Sept 20/18

Taxon unknown **Sample taken from** ?

Sedimentology Sandstone **Percent Articulation** Isolated fragment

Sampling Proceedures

- All samples handled from time of collection to dissolution, were done using Nitrile gloves to prevent contamination from human skin.
- All samples that could be collected from previously broken bones were done so, thus eliminating the requirement of breaking bones.
- Samples required to be removed from larger bones were fractured off using a hammer and awl; preventing introduction of contaminants by saw blades forcing organics into micro fissures formed during cutting.
- Samples were placed into baggies and sealed to reduce contamination during transport.

Preparation and Dissolution Proceedures

- All samples were sonicated using de-ionized water to remove surface contaminants.
- All samples were then sonicated in 50% ETOH solution to remove any unknown consolidants and sterilized for bacteria.
- All samples were then sonicated one further time in de-ionized water to flush ETOH.
- All samples are then dissolved in 0.5 M EDTA solution. When EDTA reaches pH of 10-11, 3/4 of solution is replaced with fresh EDTA

Sample # WF3-1

Date	Treatment
Sept 20/18	9mL EDTA
Sept 27/18	" "
Oct 4/18	"
Nov 8/18	"
Nov 22/18	"

Sample # WF3-2

Date	Treatment
Sept 20/18	9mL EDTA
Sept 27/18	" "
Oct 4/18	"
Nov 8/18	"
Nov 22/18	"

Sample # WF3-3

Date	Treatment
Sept 20/18	9mL EDTA
Sept 27/18	" "
Oct 4/18	"
Nov 8/18	"
Nov 22/18	"

Bone Dissolution Sampling Sheet

Specimen Number

UALVP [redacted] Collection Date Aug 6 2014

Field NADP-2014.0806.07 57449 Sampling Date Sept 20 2018

Taxon unknown Sample taken from ?

Sedimentology sandstone Percent Articulation microsite

Sampling Proceedures

- All samples handled from time of collection to dissolution, were done using Nitrile gloves to prevent contamination from human skin.
- All samples that could be collected from previously broken bones were done so, thus eliminating the requirement of breaking bones.
- Samples required to be removed from larger bones were fractured off using a hammer and awl; preventing introduction of contaminants by saw blades forcing organics into micro fissures formed during cutting.
- Samples were placed into baggies and sealed to reduce contamination during transport.

Preparation and Dissolution Proceedures

- All samples were sonicated using de-ionized water to remove surface contaminants.
- All samples were then sonicated in 50% ETOH solution to remove any unknown consolidants and sterilized for bacteria.
- All samples were then sonicated one further time in de-ionized water to flush ETOH.
- All samples are then dissolved in 0.5 M EDTA solution. When EDTA reaches pH of 10-11, 3/4 of solution is replaced with fresh EDTA

Sample # WF #3 4

Date	Treatment
Sept 20/18	9mL EDTA
Sept 27/18	" "
Oct 4/18	"
Nov 8/18	"
Nov 22/18	"

Sample # WF3 5

Date	Treatment
Sept 20/18	9mL EDTA
Sept 27/18	" "
Oct 4/18	"
Nov 8/18	"
Nov 22/18	"

Sample # WF3 6

Date	Treatment
Sept 20/18	9mL EDTA
Sept 27/18	" "
Oct 4/18	"
Nov 8/18	"
Nov 22/18	"

Bone Dissolution Sampling Sheet

Specimen Number

UALVP _____ Collection Date _____

Field Red Willow Edmonton 69554 Sampling Date _____

Taxon _____ Sample taken from _____

Sedimentology Sandstone. Percent Articulation _____

Sampling Proceedures

- All samples handled from time of collection to dissolution, were done using Nitrile gloves to prevent contamination from human skin.
- All samples that could be collected from previously broken bones were done so, thus eliminating the requirement of breaking bones.
- Samples required to be removed from larger bones were fractured off using a hammer and awl; preventing introduction of contaminants by saw blades forcing organics into micro fissures formed during cutting.
- Samples were placed into baggies and sealed to reduce contamination during transport.

Preparation and Dissolution Proceedures

- All samples were sonicated using de-ionized water to remove surface contaminants.
- All samples were then sonicated in 50% ETOH solution to remove any unknown consolidants and sterilized for bacteria.
- All samples were then sonicated one further time in de-ionized water to flush ETOH.
- All samples are then dissolved in 0.5 M EDTA solution. When EDTA reaches pH of 10-11, 3/4 of solution is replaced with fresh EDTA

Sample # A

Date	Treatment
Nov 22	9mL 0.5M EDTA

Sample # B

Date	Treatment
Nov 22	0.5M EDTA 9mL

Sample # C

Date	Treatment
Nov 22	0.5M EDTA 9mL

APPENDIX 6-1: Lab treatment forms for bone samples from the Brazeau Formation. Forms organized in the same order as Table 6-1.

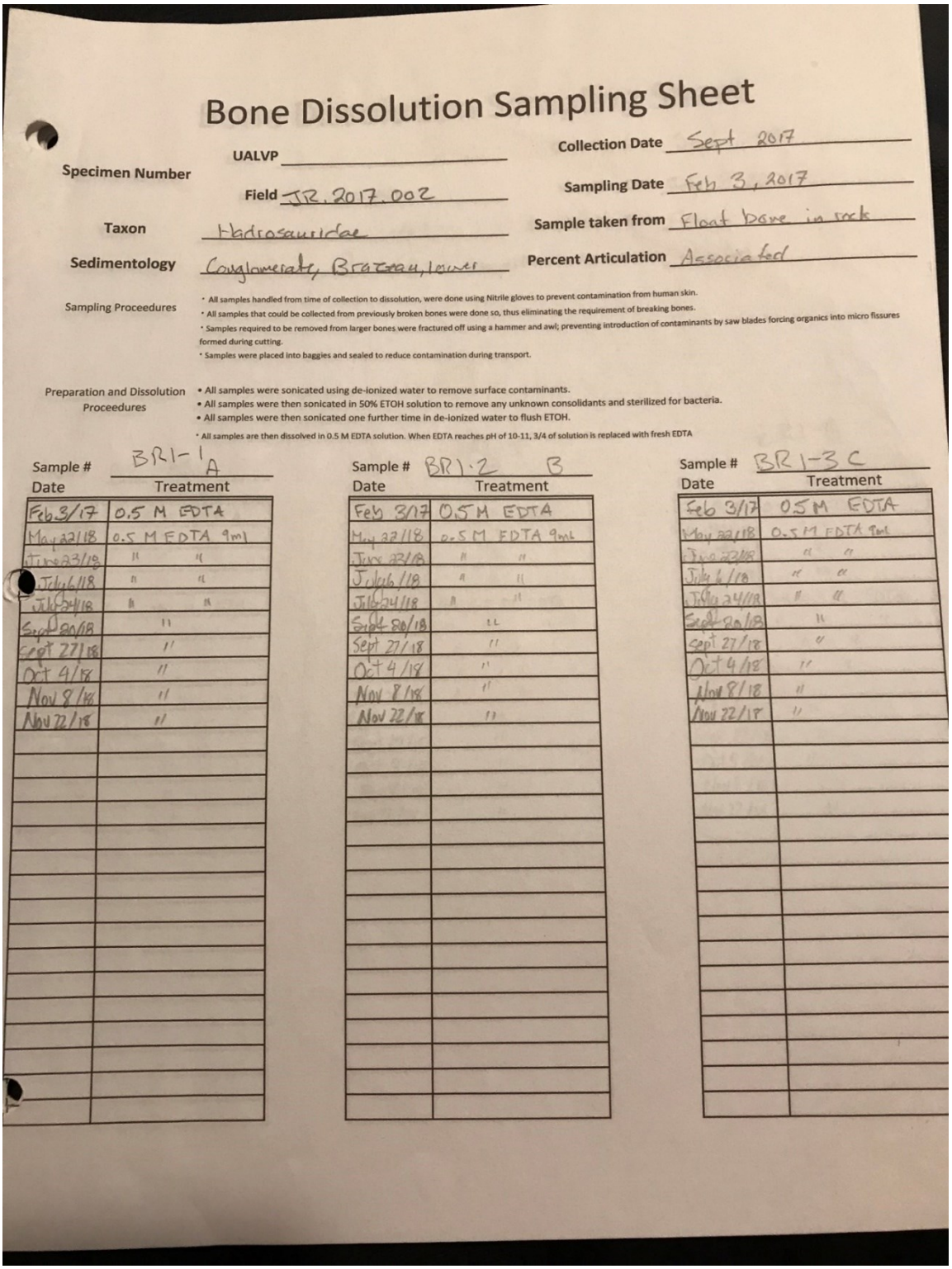

Bone Dissolution Sampling Sheet

Specimen Number

UALVP _____

Field JR.2017.002

Taxon Hadrosauridae

Sedimentology Conglomerate, Brazeau, lower

Collection Date Sept 2017

Sampling Date Feb 3, 2017

Sample taken from Float bone in rock

Percent Articulation Associated

Sampling Proceedures

- All samples handled from time of collection to dissolution, were done using Nitrile gloves to prevent contamination from human skin.
- All samples that could be collected from previously broken bones were done so, thus eliminating the requirement of breaking bones.
- Samples required to be removed from larger bones were fractured off using a hammer and awl; preventing introduction of contaminants by saw blades forcing organics into micro fissures formed during cutting.
- Samples were placed into baggies and sealed to reduce contamination during transport.

Preparation and Dissolution Proceedures

- All samples were sonicated using de-ionized water to remove surface contaminants.
- All samples were then sonicated in 50% ETOH solution to remove any unknown consolidants and sterilized for bacteria.
- All samples were then sonicated one further time in de-ionized water to flush ETOH.
- All samples are then dissolved in 0.5 M EDTA solution. When EDTA reaches pH of 10-11, 3/4 of solution is replaced with fresh EDTA

Sample # BR1-1 A

Date	Treatment
Feb 3/17	0.5 M EDTA
May 22/18	0.5 M EDTA 9ml
June 23/18	" "
July 6/18	" "
July 24/18	" "
Sept 20/18	"
Sept 27/18	"
Oct 4/18	"
Nov 8/18	"
Nov 22/18	"

Sample # BR1-2 B

Date	Treatment
Feb 3/17	0.5M EDTA
May 22/18	0.5 M EDTA 9mL
June 23/18	" "
July 6/18	" "
July 24/18	" "
Sept 20/18	"
Sept 27/18	"
Oct 4/18	"
Nov 8/18	"
Nov 22/18	"

Sample # BR1-3 C

Date	Treatment
Feb 3/17	0.5M EDTA
May 22/18	0.5 M EDTA 9mL
June 23/18	" "
July 6/18	" "
July 24/18	" "
Sept 20/18	"
Sept 27/18	"
Oct 4/18	"
Nov 8/18	"
Nov 22/18	"

Bone Dissolution Sampling Sheet

Specimen Number UALVP _____ **Collection Date** Sept 2017

Field JR-2017.001 **Sampling Date** Feb 3, 2017

Taxon Hadrosauridae indet **Sample taken from** Femur

Sedimentology Sandstone, Brazeau, Lower **Percent Articulation** isolated

Sampling Proceedures

- All samples handled from time of collection to dissolution, were done using Nitrile gloves to prevent contamination from human skin.
- All samples that could be collected from previously broken bones were done so, thus eliminating the requirement of breaking bones.
- Samples required to be removed from larger bones were fractured off using a hammer and awl; preventing introduction of contaminants by saw blades forcing organics into micro fissures formed during cutting.
- Samples were placed into baggies and sealed to reduce contamination during transport.

Preparation and Dissolution Proceedures

- All samples were sonicated using de-ionized water to remove surface contaminants.
- All samples were then sonicated in 50% ETOH solution to remove any unknown consolidants and sterilized for bacteria.
- All samples were then sonicated one further time in de-ionized water to flush ETOH.
- All samples are then dissolved in 0.5 M EDTA solution. When EDTA reaches pH of 10-11, 3/4 of solution is replaced with fresh EDTA

Sample # BR 1-4 A

Date	Treatment
Feb 3/18	0.5 M EDTA
" 20/18	"
Mar 5/18	"
" 20/18	"
May 22/18	9mL 0.5 M EDTA
June 16/18	" " "
June 23/18	" "
July 6/18	" "
July 24/18	" "
Sept 20/18	"
Sept 27/18	"
Oct 4/18	"
Nov 8/18	"
Nov 22/18	"

Sample # BR1-5 B

Date	Treatment
Feb 3/18	0.5 M EDTA
" 20/18	"
Mar 5/18	"
" 20/18	"
May 22/18	9mL 0.5 M EDTA
June 16/18	" " "
June 23/18	" "
July 6/18	" "
July 24/18	" "
Sept 20/18	"
Sept 27/18	"
Oct 4/18	"
Nov 8/18	"
Nov 22/18	"

Sample # BR1-6 C

Date	Treatment
Feb 3/18	0.5 M EDTA
" 20/18	"
Mar 5/18	"
" 20/18	"
May 22/18	9mL 0.5 M EDTA
June 16/18	" " "
June 23/18	" "
July 6/18	" "
July 24/18	" "
Sept 20/18	"
Sept 27/18	"
Oct 4/18	"
Nov 8/18	"
Nov 22/18	"

Bone Dissolution Sampling Sheet

Specimen Number UALVP _____ **Collection Date** Aug/18

Field Algoasaur **Sampling Date** Oct 2018

Taxon Hadrosauridae **Sample taken from** transverse process

Sedimentology Sandy mud? **Percent Articulation** isolated

Sampling Proceedures

- All samples handled from time of collection to dissolution, were done using Nitrile gloves to prevent contamination from human skin.
- All samples that could be collected from previously broken bones were done so, thus eliminating the requirement of breaking bones.
- Samples required to be removed from larger bones were fractured off using a hammer and awl; preventing introduction of contaminants by saw blades forcing organics into micro fissures formed during cutting.
- Samples were placed into baggies and sealed to reduce contamination during transport.

Preparation and Dissolution Proceedures

- All samples were sonicated using de-ionized water to remove surface contaminants.
- All samples were then sonicated in 50% ETOH solution to remove any unknown consolidants and sterilized for bacteria.
- All samples were then sonicated one further time in de-ionized water to flush ETOH.
- All samples are then dissolved in 0.5 M EDTA solution. When EDTA reaches pH of 10-11, 3/4 of solution is replaced with fresh EDTA

Sample # A

Date	Treatment
Oct 4/18	0.5M EDTA 9ml
Nov 8/18	"
Nov 22/18	"

Sample # B

Date	Treatment
Oct 4/18	0.5M EDTA 9ml
Nov 8/18	"
Nov 22/18	"

Sample # C

Date	Treatment
Oct 4/18	0.5M EDTA 9ml
Nov 8/18	"
Nov 22/18	"

Bone Dissolution Sampling Sheet

Specimen Number UALVP _____ **Collection Date** Aug 2018

Field Macleod River Chunk **Sampling Date** Aug 2018

Taxon Unknown **Sample taken from** ?

Sedimentology Sandstone **Percent Articulation** Isolated - rotten b/c bassal.

Sampling Proceedures

- All samples handled from time of collection to dissolution, were done using Nitrile gloves to prevent contamination from human skin.
- All samples that could be collected from previously broken bones were done so, thus eliminating the requirement of breaking bones.
- Samples required to be removed from larger bones were fractured off using a hammer and awl; preventing introduction of contaminants by saw blades forcing organics into micro fissures formed during cutting.
- Samples were placed into baggies and sealed to reduce contamination during transport.

Preparation and Dissolution Proceedures

- All samples were sonicated using de-ionized water to remove surface contaminants.
- All samples were then sonicated in 50% ETOH solution to remove any unknown consolidants and sterilized for bacteria.
- All samples were then sonicated one further time in de-ionized water to flush ETOH.
- All samples are then dissolved in 0.5 M EDTA solution. When EDTA reaches pH of 10-11, 3/4 of solution is replaced with fresh EDTA

Sample # A

Date	Treatment
Oct 4/18	0.5M EDTA 9ml
Nov 8/18	"
Nov 22/18	"

Sample # B

Date	Treatment
Oct 4/18	0.5M EDTA 9ml
Nov. 8/18	"
Nov 22/18	"

Sample # C

Date	Treatment
Oct 4/18	0.5M EDTA 9ml
Nov 8/18	"
Nov 22/18	"

Bone Dissolution Sampling Sheet

Specimen Number

UALVP _____ **Collection Date** Aug 2018

Field SR 2018- **Sampling Date** Oct 2018

Taxon Hadrosaur **Sample taken from** caudal vert

Sedimentology Sandstone **Percent Articulation** isolated

Sampling Proceedures

- All samples handled from time of collection to dissolution, were done using Nitrile gloves to prevent contamination from human skin.
- All samples that could be collected from previously broken bones were done so, thus eliminating the requirement of breaking bones.
- Samples required to be removed from larger bones were fractured off using a hammer and awl; preventing introduction of contaminants by saw blades forcing organics into micro fissures formed during cutting.
- Samples were placed into baggies and sealed to reduce contamination during transport.

Preparation and Dissolution Proceedures

- All samples were sonicated using de-ionized water to remove surface contaminants.
- All samples were then sonicated in 50% ETOH solution to remove any unknown consolidants and sterilized for bacteria.
- All samples were then sonicated one further time in de-ionized water to flush ETOH.
- All samples are then dissolved in 0.5 M EDTA solution. When EDTA reaches pH of 10-11, 3/4 of solution is replaced with fresh EDTA

Sample # A

Date	Treatment
Oct 4/18	0.5M EDTA 9ml
Nov 8/18	"
Nov 22/18	"

Sample # B

Date	Treatment
Oct 4/18	0.5M EDTA 9ml
Nov 8/18	"
Nov 22/18	"

Sample # C

Date	Treatment
Oct 4/18	0.5M EDTA 9ml
Nov 8/18	"
Nov 22/18	"

Bone Dissolution Sampling Sheet

Specimen Number

UALVP _____ **Collection Date** Sept 2017

Field EDT. 2017.002 **Sampling Date** Feb 3, 2017

Taxon Hadrosauridae **Sample taken from** float

Sedimentology mudstone, Brazeau, 71 mya. **Percent Articulation** associated

Sampling Proceedures

- All samples handled from time of collection to dissolution, were done using Nitrile gloves to prevent contamination from human skin.
- All samples that could be collected from previously broken bones were done so, thus eliminating the requirement of breaking bones.
- Samples required to be removed from larger bones were fractured off using a hammer and awl; preventing introduction of contaminants by saw blades forcing organics into micro fissures formed during cutting.
- Samples were placed into baggies and sealed to reduce contamination during transport.

Preparation and Dissolution Proceedures

- All samples were sonicated using de-ionized water to remove surface contaminants.
- All samples were then sonicated in 50% ETOH solution to remove any unknown consolidants and sterilized for bacteria.
- All samples were then sonicated one further time in de-ionized water to flush ETOH.
- All samples are then dissolved in 0.5 M EDTA solution. When EDTA reaches pH of 10-11, 3/4 of solution is replaced with fresh EDTA

Sample # A BR2-4

Date	Treatment	
Feb 3/18	0.5 M EDTA	
Feb 20/18	"	
Mar 5/18	"	
" 20/18	"	
May 22/18	"	9mL
June 23/18	"	"
July 6/18	"	"
July 30/18	"	"
Sept 20/18	"	"
Sept 27/18	"	"
Oct 4/18	"	
Nov 8/18	"	
Nov 22/18	"	

Sample # B BR2-5

Date	Treatment	
Feb 3/18	0.5 M EDTA	
Feb 20/18	"	
Mar 5/18	"	
" 20/18	"	
May 22/18	"	9ml
June 23/18	"	"
July 6/18	"	"
July 30/18	"	"
Sept 20/18	"	"
Sept 27/18	"	"
Oct 4/18	"	
Nov 8/18	"	
Nov 22/18	"	

Sample # BR2-6 C

Date	Treatment	
Feb 3/18	0.5 M EDTA	
" 20/18	"	
Mar 5/18	"	
" 20/18	"	
May 22/18	"	9mL
June 23/18	"	"
July 6/18	"	"
July 30/18	"	"
Sept 20/18	"	"
Sept 27/18	"	"
Oct 4/18	"	
Nov 8/18	"	
Nov 22/18	"	

Bone Dissolution Sampling Sheet

Specimen Number

UALVP _____ **Collection Date** Aug 2017

Field EJT.2017.001 **Sampling Date** Feb 3, 2017

Taxon Hadrosauridae indet **Sample taken from** float bone

Sedimentology mudstone, Brazeau, 70. Mya **Percent Articulation** Bonebed

Sampling Proceedures

- All samples handled from time of collection to dissolution, were done using Nitrile gloves to prevent contamination from human skin.
- All samples that could be collected from previously broken bones were done so, thus eliminating the requirement of breaking bones.
- Samples required to be removed from larger bones were fractured off using a hammer and awl; preventing introduction of contaminants by saw blades forcing organics into micro fissures formed during cutting.
- Samples were placed into baggies and sealed to reduce contamination during transport.

Preparation and Dissolution Proceedures

- All samples were sonicated using de-ionized water to remove surface contaminants.
- All samples were then sonicated in 50% ETOH solution to remove any unknown consolidants and sterilized for bacteria.
- All samples were then sonicated one further time in de-ionized water to flush ETOH.
- All samples are then dissolved in 0.5 M EDTA solution. When EDTA reaches pH of 10-11, 3/4 of solution is replaced with fresh EDTA

Sample # A BRZ-1

Date	Treatment	
Feb 3/18	0.5 M EDTA	
Feb 20/18	"	"
Mar 5/18	"	"
" 20/18	"	"
May 22/18	"	9mL
June 23/18	"	"
July 6/18	"	"
July 30/18	"	"
Sept 20/18	"	"
Sept 27/18	"	"
Oct 4/18	"	
Nov 8/18	"	
Nov 22/18	"	

Sample # B BRZ-2

Date	Treatment	
Feb 3/18	0.5 M EDTA	
Feb 20/18	"	
Mar 5/18	"	
" 20/18	"	
May 22/18	"	9mL
June 23/18	"	"
July 6/18	"	"
July 30/18	"	"
Sept 20/18	"	"
Sept 27/18	"	"
Oct 4/18	"	
Nov 8/18	"	
Nov 22/18	"	

Sample # C BRZ-3

Date	Treatment	
Feb 3/18	0.5M EDTA	
Feb 20/18	"	
Mar 5/18	"	
" 20/18	"	
May 22/18	"	9mL
June 23/18	"	"
July 6/18	"	"
July 30/18	"	"
Sept 20/18	"	"
Sept 27/18	"	"
Oct 4/18	"	
Nov 8/18	"	
Nov 22/18	"	

Bone Dissolution Sampling Sheet

Specimen Number

UALVP _____ **Collection Date** Aug 2018

Field Drowned Hadro **Sampling Date** Oct 2018

Taxon Hadrosauridae **Sample taken from** surface float

Sedimentology Mudstone **Percent Articulation** Associated

Sampling Proceedures

- All samples handled from time of collection to dissolution, were done using Nitrile gloves to prevent contamination from human skin.
- All samples that could be collected from previously broken bones were done so, thus eliminating the requirement of breaking bones.
- Samples required to be removed from larger bones were fractured off using a hammer and awl; preventing introduction of contaminants by saw blades forcing organics into micro fissures formed during cutting.
- Samples were placed into baggies and sealed to reduce contamination during transport.

Preparation and Dissolution Proceedures

- All samples were sonicated using de-ionized water to remove surface contaminants.
- All samples were then sonicated in 50% ETOH solution to remove any unknown consolidants and sterilized for bacteria.
- All samples were then sonicated one further time in de-ionized water to flush ETOH.
- All samples are then dissolved in 0.5 M EDTA solution. When EDTA reaches pH of 10-11, 3/4 of solution is replaced with fresh EDTA

Sample # A

Date	Treatment
Oct 4/18	0.5M EDTA 9ml
Nov 8/18	"
Nov 22/18	"

Sample # B

Date	Treatment
Oct 4/18	0.5M EDTA 9ml
Nov 8/18	"
Nov 22/18	"

Sample # C

Date	Treatment
Oct 4/18	0.5M EDTA 9ml
Nov 8/18	"
Nov 22/18	"

APPENDIX 7-1: Lab treatment forms for bone samples from the Foremost Formation. Forms organized in the same order as Table 7-1.

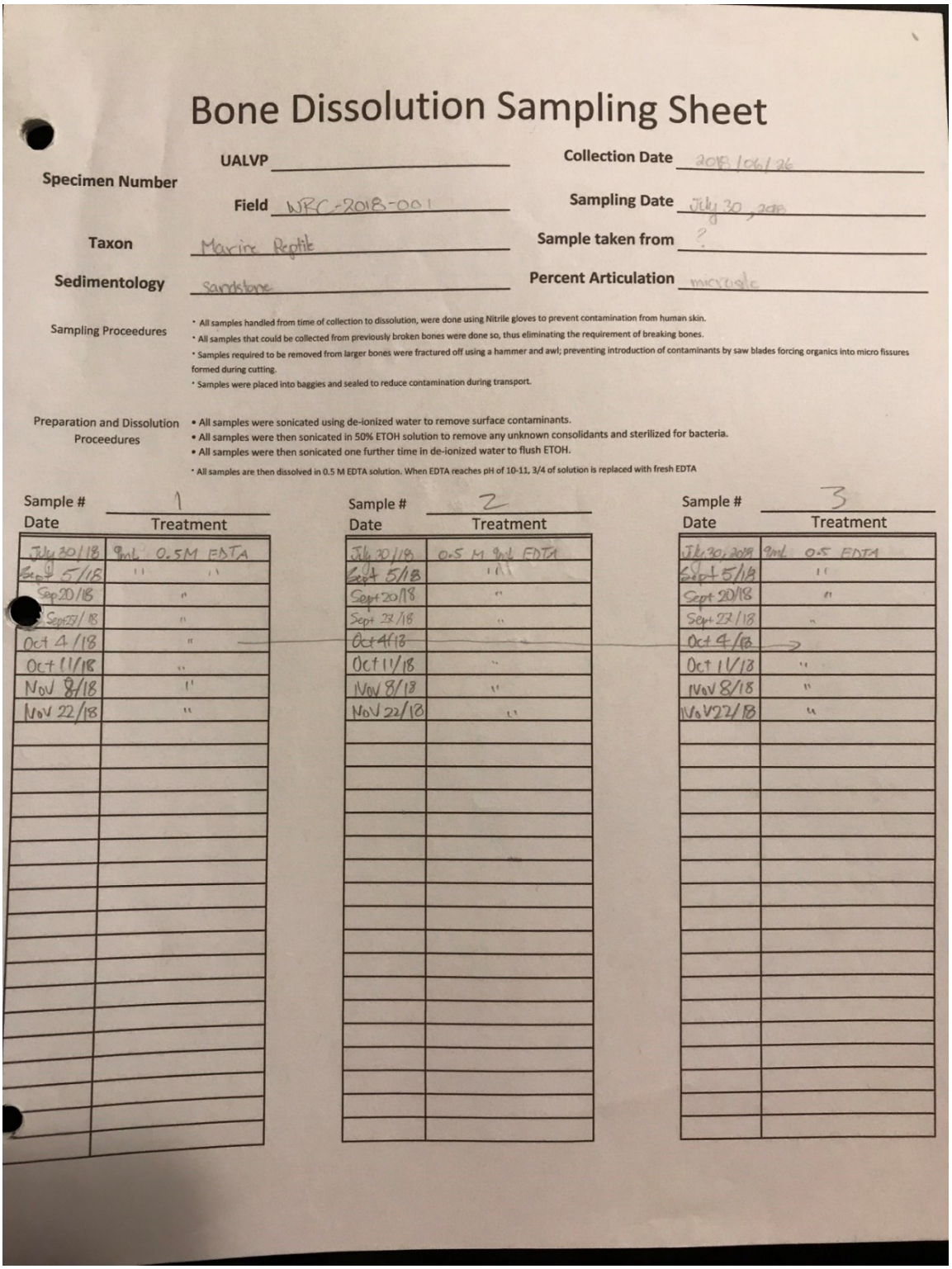

Bone Dissolution Sampling Sheet

Specimen Number UALVP _____ Collection Date 2018/06/26

Field WRC-2018-001 Sampling Date July 30, 2018

Taxon Marine Reptile Sample taken from ?

Sedimentology Sandstone Percent Articulation micrograle

Sampling Proceedures

- All samples handled from time of collection to dissolution, were done using Nitrile gloves to prevent contamination from human skin.
- All samples that could be collected from previously broken bones were done so, thus eliminating the requirement of breaking bones.
- Samples required to be removed from larger bones were fractured off using a hammer and awl; preventing introduction of contaminants by saw blades forcing organics into micro fissures formed during cutting.
- Samples were placed into baggies and sealed to reduce contamination during transport.

Preparation and Dissolution Proceedures

- All samples were sonicated using de-ionized water to remove surface contaminants.
- All samples were then sonicated in 50% ETOH solution to remove any unknown consolidants and sterilized for bacteria.
- All samples were then sonicated one further time in de-ionized water to flush ETOH.
- All samples are then dissolved in 0.5 M EDTA solution. When EDTA reaches pH of 10-11, 3/4 of solution is replaced with fresh EDTA

Sample # 1

Date	Treatment
July 30/18	9mL 0.5M EDTA
Sept 5/18	" "
Sep 20/18	"
Sept 27/18	"
Oct 4/18	"
Oct 11/18	"
Nov 8/18	"
Nov 22/18	"

Sample # 2

Date	Treatment
July 30/18	0.5 M 9mL EDTA
Sept 5/18	"
Sept 20/18	"
Sept 27/18	"
Oct 4/18	
Oct 11/18	"
Nov 8/18	"
Nov 22/18	"

Sample # 3

Date	Treatment
July 30, 2018	9mL 0.5 EDTA
Sept 5/18	"
Sept 20/18	"
Sept 27/18	"
Oct 4/18	→
Oct 11/18	"
Nov 8/18	"
Nov 22/18	"

Bone Dissolution Sampling Sheet

Specimen Number

UALVP _____

Field WRC-2018-007

Taxon Marine Reptile

Sedimentology Sandstone

Collection Date 2018/06/30

Sampling Date July 30, 2018

Sample taken from _____

Percent Articulation Isolate

Sampling Proceedures

- All samples handled from time of collection to dissolution, were done using Nitrile gloves to prevent contamination from human skin.
- All samples that could be collected from previously broken bones were done so, thus eliminating the requirement of breaking bones.
- Samples required to be removed from larger bones were fractured off using a hammer and awl; preventing introduction of contaminants by saw blades forcing organics into micro fissures formed during cutting.
- Samples were placed into baggies and sealed to reduce contamination during transport.

Preparation and Dissolution Proceedures

- All samples were sonicated using de-ionized water to remove surface contaminants.
- All samples were then sonicated in 50% ETOH solution to remove any unknown consolidants and sterilized for bacteria.
- All samples were then sonicated one further time in de-ionized water to flush ETOH.
- All samples are then dissolved in 0.5 M EDTA solution. When EDTA reaches pH of 10-11, 3/4 of solution is replaced with fresh EDTA

Sample # 1

Date	Treatment
July 30/18	9ml 0.5 M EDTA
Sept 5/18	"
Sept 20/18	"
Sept 27/18	"
Oct 4/18	"
Oct 11/18	"
Nov 8/18	"
Nov 22/18	"

Sample # 2

Date	Treatment
July 30/2018	9ml 0.5 M EDTA
Sept 5/18	"
Sept 20/18	"
Sept 27/18	"
Oct 4/18	"
Oct 11/18	"
Nov 8/18	"
Nov 22/18	"

Sample # 3

Date	Treatment
July 30/18	9ml 0.5 M EDTA
Sept 5/18	"
Sept 20/18	"
Sept 27/18	"
Oct 4/18	"
Oct 11/18	"
Nov 8/18	"
Nov 22/18	"

Bone Dissolution Sampling Sheet

Specimen Number

UALVP _____ **Collection Date** 2018/06/26

Field WRC-2018-003 **Sampling Date** July 30 2018

Taxon Marine Reptile **Sample taken from** rib?

Sedimentology sandstone **Percent Articulation** Miscrate

Sampling Proceedures

- All samples handled from time of collection to dissolution, were done using Nitrile gloves to prevent contamination from human skin.
- All samples that could be collected from previously broken bones were done so, thus eliminating the requirement of breaking bones.
- Samples required to be removed from larger bones were fractured off using a hammer and awl; preventing introduction of contaminants by saw blades forcing organics into micro fissures formed during cutting.
- Samples were placed into baggies and sealed to reduce contamination during transport.

Preparation and Dissolution Proceedures

- All samples were sonicated using de-ionized water to remove surface contaminants.
- All samples were then sonicated in 50% ETOH solution to remove any unknown consolidants and sterilized for bacteria.
- All samples were then sonicated one further time in de-ionized water to flush ETOH.
- All samples are then dissolved in 0.5 M EDTA solution. When EDTA reaches pH of 10-11, 3/4 of solution is replaced with fresh EDTA

Sample # 1

Date	Treatment
July 30/18	9ml EDTA 0.5M
Sept 5/18	"
Sept 20/18	"
Sept 27/18	"
Oct 4/18	"
Oct 11/18	"
Nov 8/18	"
Nov 22/18	"

Sample # 2

Date	Treatment
July 30/18	9ml 0.5M EDTA
Sept 5/18	"
Sept 20/18	"
Sept 27/18	"
Oct 4/18	"
Oct 11/18	"
Nov 8/18	"
Nov 22/18	"

Sample # 3

Date	Treatment
July 30/18	9ml 0.5M EDTA
Sept 5/18	"
Sept 20/18	"
Sept 27/18	"
Oct 4/18	"
Oct 11/18	"
Nov 8/18	"
Nov 22/18	"

Bone Dissolution Sampling Sheet

Specimen Number

UALVP _____ Collection Date 2018/ 06/ 26

Field UVRC-2018-004 Sampling Date July 30, 2018

Taxon Reptilia (Crocodilia) Sample taken from _____

Sedimentology sandstone Percent Articulation micro stic

Sampling Proceedures

- All samples handled from time of collection to dissolution, were done using Nitrile gloves to prevent contamination from human skin.
- All samples that could be collected from previously broken bones were done so, thus eliminating the requirement of breaking bones.
- Samples required to be removed from larger bones were fractured off using a hammer and awl; preventing introduction of contaminants by saw blades forcing organics into micro fissures formed during cutting.
- Samples were placed into baggies and sealed to reduce contamination during transport.

Preparation and Dissolution Proceedures

- All samples were sonicated using de-ionized water to remove surface contaminants.
- All samples were then sonicated in 50% ETOH solution to remove any unknown consolidants and sterilized for bacteria.
- All samples were then sonicated one further time in de-ionized water to flush ETOH.
- All samples are then dissolved in 0.5 M EDTA solution. When EDTA reaches pH of 10-11, 3/4 of solution is replaced with fresh EDTA

Sample # _____

Date	Treatment
July 20/18	9ml 0.5M EDTA
Sept 5/18	"
Sept 20/18	"
Sept 27/18	"
Oct 4/18	"
Oct 11/18	"
Nov 8/18	"
Nov 22/18	"

Sample # _____

Date	Treatment
July 30/18	9ml 0.5 M EDTA
Sept 5/18	"
Sept 20/18	"
Sept 27/18	"
Oct 4/18	"
Oct 11/18	"
Nov 8/18	"
Nov 22/8	"

Sample # _____

Date	Treatment
July 20/18	9ml 0.5 M EDTA
Sept 5/18	"
Sept 20/18	"
Sept 27/18	"
Oct 4/18	"
Oct 11/18	"
Nov 8/18	"
Nov 22/18	"

Bone Dissolution Sampling Sheet

Specimen Number UALVP _____ **Collection Date** June 20, 2018

Field WRC-2018-005 **Sampling Date** Sept 5, 2018

Taxon Marine Reptile **Sample taken from** Limb bone

Sedimentology Sandstone **Percent Articulation** Microsite

Sampling Proceedures

* All samples handled from time of collection to dissolution, were done using Nitrile gloves to prevent contamination from human skin.
* All samples that could be collected from previously broken bones were done so, thus eliminating the requirement of breaking bones.
* Samples required to be removed from larger bones were fractured off using a hammer and awl; preventing introduction of contaminants by saw blades forcing organics into micro fissures formed during cutting.
* Samples were placed into baggies and sealed to reduce contamination during transport.

Preparation and Dissolution Proceedures

- All samples were sonicated using de-ionized water to remove surface contaminants.
- All samples were then sonicated in 50% ETOH solution to remove any unknown consolidants and sterilized for bacteria.
- All samples were then sonicated one further time in de-ionized water to flush ETOH.

* All samples are then dissolved in 0.5 M EDTA solution. When EDTA reaches pH of 10-11, 3/4 of solution is replaced with fresh EDTA

Sample # 1

Date	Treatment
Sept 5/18	9 mL EDTA
Sept 20/18	"
Sept 27/18	"
Oct 4/18	"
Oct 11/18	"
Nov 8/18	"
Nov 22/18	"

Sample # 2

Date	Treatment
Sept 5/18	9 mL EDTA
Sept 20/18	"
Sept 27/18	"
Oct 4/18	"
Oct 11/18	"
Nov 8/18	"
Nov 22/18	"

Sample # 3

Date	Treatment
Sept 5/18	9 mL EDTA
Sept 20/18	"
Sept 27/18	"
Oct 4/18	"
Oct 11/18	"
Nov 8/18	"
Nov 22/18	"

Bone Dissolution Sampling Sheet

Specimen Number UALVP _____ **Collection Date** July 30, 2018

Field WRC-2018-7 **Sampling Date** Sept 9, 2018

Taxon Marine Reptile? **Sample taken from** Sternal?

Sedimentology Sandstone **Percent Articulation** Microsite

Sampling Proceedures

- All samples handled from time of collection to dissolution, were done using Nitrile gloves to prevent contamination from human skin.
- All samples that could be collected from previously broken bones were done so, thus eliminating the requirement of breaking bones.
- Samples required to be removed from larger bones were fractured off using a hammer and awl; preventing introduction of contaminants by saw blades forcing organics into micro fissures formed during cutting.
- Samples were placed into baggies and sealed to reduce contamination during transport.

Preparation and Dissolution Proceedures

- All samples were sonicated using de-ionized water to remove surface contaminants.
- All samples were then sonicated in 50% ETOH solution to remove any unknown consolidants and sterilized for bacteria.
- All samples were then sonicated one further time in de-ionized water to flush ETOH.
- All samples are then dissolved in 0.5 M EDTA solution. When EDTA reaches pH of 10-11, 3/4 of solution is replaced with fresh EDTA

Sample # 1

Date	Treatment
Sept 9/18	9mL EDTA
Sept 20/18	"
Sept 27/18	"
Oct 4/18	"
Oct 11/18	"
Nov 8/18	"
Nov 22/18	"

Sample # 2

Date	Treatment
Sept 9/18	9mL EDTA
Sept 20/18	"
Sept 27/18	"
Oct 4/18	"
Oct 11/18	"
Nov 8/18	"
Nov 22/18	"

Sample # 3

Date	Treatment
Sept 9/18	9 mL EDTA
Sept 20/18	"
Sept 27/18	"
Oct 4/18	"
Oct 11/18	"
Nov 8/18	"
Nov 22/18	"

Bone Dissolution Sampling Sheet

Specimen Number UALVP _____ **Collection Date** June 30/18

Field WRC-2018-8 **Sampling Date** Sept 9/18

Taxon Marine Reptile **Sample taken from** unknown

Sedimentology Sandstone **Percent Articulation** microsite

Sampling Proceedures

- All samples handled from time of collection to dissolution, were done using Nitrile gloves to prevent contamination from human skin.
- All samples that could be collected from previously broken bones were done so, thus eliminating the requirement of breaking bones.
- Samples required to be removed from larger bones were fractured off using a hammer and awl; preventing introduction of contaminants by saw blades forcing organics into micro fissures formed during cutting.
- Samples were placed into baggies and sealed to reduce contamination during transport.

Preparation and Dissolution Proceedures

- All samples were sonicated using de-ionized water to remove surface contaminants.
- All samples were then sonicated in 50% ETOH solution to remove any unknown consolidants and sterilized for bacteria.
- All samples were then sonicated one further time in de-ionized water to flush ETOH.
- All samples are then dissolved in 0.5 M EDTA solution. When EDTA reaches pH of 10-11, 3/4 of solution is replaced with fresh EDTA

Sample # 1

Date	Treatment
Sept 9/18	9mL EDTA
Sept 20/18	"
Sept 22/18	"
Oct 4/18	"
Oct 11/18	"
Nov 8/18	"
Nov 22/18	"

Sample # 2

Date	Treatment
Sept 9/18	9mL EDTA
Sept 20/18	"
Sept 22/18	"
Oct 4/18	"
Oct 11/18	"
Nov 8/18	"
Nov 22/18	"

Sample # 3

Date	Treatment
Sept 9/18	9mL EDTA
Sept 20/18	"
Sept 22/18	"
Oct 4/18	"
Oct 11/18	"
Nov 8/18	"
Nov 22/18	"

Bone Dissolution Sampling Sheet

Specimen Number UALVP _____ **Collection Date** June 30/18

Field NJRL-2018-9 **Sampling Date** Sept 9/18

Taxon Marine Reptile **Sample taken from** unknown

Sedimentology Sandstone **Percent Articulation** microsite

Sampling Proceedures

- All samples handled from time of collection to dissolution, were done using Nitrile gloves to prevent contamination from human skin.
- All samples that could be collected from previously broken bones were done so, thus eliminating the requirement of breaking bones.
- Samples required to be removed from larger bones were fractured off using a hammer and awl; preventing introduction of contaminants by saw blades forcing organics into micro fissures formed during cutting.
- Samples were placed into baggies and sealed to reduce contamination during transport.

Preparation and Dissolution Proceedures

- All samples were sonicated using de-ionized water to remove surface contaminants.
- All samples were then sonicated in 50% ETOH solution to remove any unknown consolidants and sterilized for bacteria.
- All samples were then sonicated one further time in de-ionized water to flush ETOH.
- All samples are then dissolved in 0.5 M EDTA solution. When EDTA reaches pH of 10-11, 3/4 of solution is replaced with fresh EDTA

Sample # 1

Date	Treatment
Sept 9/18	9 mL EDTA
Sept 20/18	"
Sept 27/18	"
Oct 4/18	
Oct 11/18	"
Nov 8/18	"
Nov 22/18	"

Sample # 2

Date	Treatment
Sept 9/18	9 mL EDTA
Sept 20/18	"
Sept 27/18	"
Oct 4/18	"
Oct 11/18	"
Nov 8/18	"
Nov 22/18	"

Sample # 3

Date	Treatment
Sept 9/18	9 mL EDTA
Sept 20/18	"
Sept 27/18	"
Oct 4/18	"
Oct 11/18	"
Nov 8/18	"
Nov 22/18	"

Bone Dissolution Sampling Sheet

Specimen Number UALVP _____ Collection Date June 30/18

Field WBC-2018-010 Sampling Date Sept 9/18

Taxon Marine Reptile Sample taken from unknown

Sedimentology Sandstone Percent Articulation microsite

Sampling Proceedures

- All samples handled from time of collection to dissolution, were done using Nitrile gloves to prevent contamination from human skin.
- All samples that could be collected from previously broken bones were done so, thus eliminating the requirement of breaking bones.
- Samples required to be removed from larger bones were fractured off using a hammer and awl; preventing introduction of contaminants by saw blades forcing organics into micro fissures formed during cutting.
- Samples were placed into baggies and sealed to reduce contamination during transport.

Preparation and Dissolution Proceedures

- All samples were sonicated using de-ionized water to remove surface contaminants.
- All samples were then sonicated in 50% ETOH solution to remove any unknown consolidants and sterilized for bacteria.
- All samples were then sonicated one further time in de-ionized water to flush ETOH.
- All samples are then dissolved in 0.5 M EDTA solution. When EDTA reaches pH of 10-11, 3/4 of solution is replaced with fresh EDTA

Sample # 1

Date	Treatment
Sept 9/18	9mL EDTA
Sept 20/18	"
Sept 27/18	"
Oct 4/18	"
Oct 11/18	"
Nov 9/18	"
Nov 22/18	"

Sample # 2

Date	Treatment
Sept 9/18	9mL EDTA
Sept 20/18	"
Sept 27/18	"
Oct 4/18	"
Oct 11/18	"
Nov 8/18	"
Nov 22/18	"

Sample # 3

Date	Treatment
Sept 9/18	9mL EDTA
Sept 20/18	"
Sept 27/18	"
Oct 4/18	"
Oct 11/18	"
Nov 8/18	"
Nov 22/18	"

APPENDIX 9-1: Copies of letters send from Barnum Brown to R.C. Sibley.

C
O
P
Y

September the nineteenth
Nineteen hundred and forty-one

Mr. R. C. Sibley
Entrance
Alberta.

Dear Mr. Sibley:-

Mrs. Davison came to the Museum last Tuesday bringing the tooth and some fossil leaves from her ranch and your letter.

The tooth is in all probability Gorgosaurus, one of the large Belly River Cretaceous carnivorous dinosaurs. This type of dinosaur, as you may know, had teeth of large and small sizes according to the position in the mouth but quite similar in form and character.

From your description I am convinced that this is wash accumulation and that you cannot expect more than isolated or fragmentary bones no matter how much you may dig. Two or three feet beyond the surface exposure is as much as one is justified in digging under such conditions. Better look elsewhere in exposures of the same formation for there must be more exposures of the same formation along rivers or stream courses in that area where you may find connected parts of skeletons.

I should very much like to see the other specimens especially any teeth, no matter how small or fragmentary, if they differ in form from the one sent. Also different bones having articular ends. Ribs cannot be identified. Such an accumulation gives us a good idea of the age and indicates that somewhere in that region you will be rewarded by a worth while specimen.

When convenient send me any specimens by express collect and I will return them if you wish or record them in our collection as a gift from you and at the end of the year an official recognition will be sent from the Trustees.

Dinosaur tracks have been found farther north on Peace River but these are the farthest north bones.

I sincerely hope that you may be rewarded by other discoveries and shall look forward to further letters. Thanking you for your courtesy, I am,

Very sincerely,

(Signed) Barnum Brown

BB:RM

C
O
P
Y

October the second
Nineteen hundred and forty-one

Mr. R. C. Sibley
Entrance,
Alberta.

Dear Mr. Sibley:-

Miss Gertrude Jasper came to the Museum on September 30th and brought the bones, teeth and photographs, which you so very kindly sent by her. I have compared the toe bone carefully with our Red Deer River specimens, also the photographs of the tibia and fibula and I am quite convinced that the hoof and the tibia and fibula belong to a Trachodon or duck-bill dinosaur - Corythosaurus (casuarius?). The hoof is a right lateral hind toe. The other U-shaped bone sent is a spinous process of probably a duck-bill dinosaur and may well be this same genus and species; also, one of the photographs showing three bones and another showing two of these bones on a box are the upper end of a humerus or fore-arm bone of a duck-bill dinosaur, and the front end of an illium or hip bone. The third bone in the two pictures lying next to a door I cannot make out clearly so am not able to designate what it may be.

Under separate cover I am sending you some pamphlets on the dinosaurs, many of which are those found in the Belly River formation on the Red Deer River.

The curved serrated teeth are those of a carnivorous dinosaur, presumably Gorgosaurus libratus, and the very tiny curved serrated tooth may be an undescribed carnivorous dinosaur because the point is much more curved than is found in the large Gorgosaurus-like genera. The fragmentary tooth which you had separated from the others is one of the duck-bill dinosaurs but as the edge of the tooth is smooth I am of the opinion that it is not Corythosaurus. You must remember that in a mixed quarry of this sort there may be the remains of a good many of different kinds of dinosaurs collected in one place.

I will keep the specimens here until I hear from you as to their disposition. We would like very much to have the bones that you have found and to receive and diagnose any others that you discover, but I am sorry to say that we could not offer any money for them. Scattered specimens of this sort can not be put on exhibition but they are of interest to scientists who are studying the different groups and the major part of material of this sort is in our study collection for just that purpose.

The stomach stones were also of considerable interest to me as they show a high degree of polish similar to those we have found in the lower Cretaceous beds of Montana.

I took the liberty of telling Miss Jasper to keep one of those stones as a souvenir.

There were also two other specimens of interest - one is the seed of a plant, probably one of the palmettos, the other is a fresh-water shell. Later if we can determine the genus and species I will let you know.

Thanking you for your courtesy in letting me examine the specimens and hoping to again hear from you shortly, I am,

Very sincerely yours,

(Signed) Barnum Brown

BB:RM